TECHNISCHE UNIVERSITÄT MÜNCHEN

TUM School of Engineering and Design

Automated Condition Monitoring for Industrial Robot Gears

Corbinian Ernst Nentwich

Vollständiger Abdruck der von der TUM School of Engineering and Design der Technischen Universität München zur Erlangung des akademischen Grades eines Doktors der Ingenieurwissenschaften (Dr.-Ing.) genehmigten Dissertation.

Vorsitz:	Prof. Dr.-Ing. Wolfram Volk
Prüfer*innen der Dissertation:	1. Prof. Dr.-Ing. Rüdiger Daub
	2. Prof. Dr. ir. Daniel J. Rixen

Die Dissertation wurde am 26.09.2022 bei der Technischen Universität München eingereicht und durch die TUM School of Engineering and Design am 23.01.2023 angenommen.

Preface

In times of global challenges, such as climate change, the transformation of mobility, and an ongoing demographic change, production engineering is crucial for the sustainable advancement of our industrial society. The impact of manufacturing companies on the environment and society is highly dependent on the equipment and resources employed, the production processes applied, and the established manufacturing organization. The company's full potential for corporate success can only be taken advantage of by optimizing the interaction between humans, operational structures, and technologies. The greatest attention must be paid to becoming as resource-saving, efficient, and resilient as possible to operate flexibly in the volatile production environment.

Remaining competitive while balancing the varying and often conflicting priorities of sustainability, complexity, cost, time, and quality requires constant thought, adaptation, and the development of new manufacturing structures. Thus, there is an essential need to reduce the complexity of products, manufacturing processes, and systems. Yet, at the same time, it is also vital to gain a better understanding and command of these aspects.

The research activities at the Institute for Machine Tools and Industrial Management (iwb) aim to continuously improve product development and manufacturing planning systems, manufacturing processes, and production facilities. A company's organizational, manufacturing, and work structures, as well as the underlying systems for order processing, are developed under strict consideration of employee-related requirements and sustainability issues. However, the use of computer-aided and artificial intelligence-based methods and the necessary increasing degree of automation must not lead to inflexible and rigid work organization structures. Thus, questions concerning the optimal integration of ecological and social aspects in all planning and development processes are of utmost importance.

The volumes published in this book series reflect and report the results from the research conducted at iwb. Research areas covered span from the design and development of manufacturing systems to the application of technologies in manufacturing and assembly. The management and operation of manufacturing systems, quality assurance, availability, and autonomy are overarching topics affecting all areas of our research. In this series, the latest results and insights from our application-oriented research are published, and it is intended to improve knowledge transfer between academia and a wide industrial sector.

Rüdiger Daub Gunther Reinhart Michael Zäh

Acknowledgment

This dissertation was written while I was working as a research associate at the Institute for Machine Tools and Industrial Management (*iwb*) at the Technical University of Munich.

I would like to express my gratitude to Professor Rüdiger Daub, Professor Gunther Reinhart and Professor Michael Zäh for accepting me at the *iwb* and giving me the opportunity to write my dissertation there. The critical discussions with you have provided me with many ideas that are inherent in this document.

I would also like to thank the *iwb* family, especially my research group Assembly Technologies and Robotics: Fabian for his trust to invite me to the iwb as a trainee, Till for the KIVI project, which is the foundation of this thesis, and Daria for the freedom to work independently. Yi for your perspective from outside. Max, Jonas and Michi for the valuable comments on this dissertation and finally Dani and Sebastian, you were always a reason to drive to Garching.

Special thanks to my family and Hannah. You bring me the peace of mind that it took to do this job.

München, April 2022 *Corbinian Nentwich*

Abstract

Condition monitoring has the potential to increase the operating time and availability of industrial robot gears. In this dissertation, a reference architecture for such a condition-monitoring system is designed and evaluated based on different datasets of accelerated wear tests. The reference architecture allows the automated detection of different defects of industrial robot gearboxes and has the potential to make the development process of a condition-monitoring system for industrial robot gearboxes more efficient.

Condition Monitoring besitzt das Potential die Lebensdauer und Verfügbarkeit von Industrierobotergetrieben zu erhöhen. Im Rahmen dieser Dissertation wird eine Referenzarchitektur für ein solches Condition-Monitoring-System entworfen und anhand von verschiedenen Datensätzen von beschleunigten Verschleißtests evaluiert. Die Referenzarchitektur ermöglicht die automatisierte Detektion von unterschiedlichen Schäden bei Industrierobotergetrieben und besitzt so das Potential den Entwicklungsprozess eines Condition-Monitoring-Systems für Industrierobotergetriebe effizienter zu gestalten.

Table of Content

List of Abbreviations

AUC	Area under the curve
CM	Condition monitoring
CMS	Condition-monitoring system
HI	Health indicator
IR	Industrial robot
ISO	International Organization for Standardization
LOF	Local outlier factor
LSTM	Long short-term memory neural network
ML	Machine learning
RA	Reference architecture
RMS	Root mean square
ROC	Receiver operator characteristic
RV	Rotate vector
SCARA	Selective compliance assembly robot arm
STFT	Short-time Fourier transform

List of Symbols

A	Data point
α	Error level
B	Data point that is a i-nearest neighbor of data point A
B_d	Diameter of the bearing
$BPFI$	Ball passing frequency at inner ring
$C_{CM,Robot}$	Yearly costs per robot in a condition-monitoring scenario
C_{dep}	Depreciation costs of a robot
$C_{dep,CMs}$	Depreciation costs of a condition monitoring system
$C_{downtime}$	Downtime costs
$C_{running}$	Running costs of a condition-monitoring system
$C_{prev,Robot}$	Yearly costs per robot in a preventive maintenance scenario
c_t	Current state of cell
D_P	Pitch diameter
δ	Dirac operator
e	Allowed error
FN	False Negative
FP	False Positive
FPR	False positive rate
$f_{sampling}$	Required sampling rate in Hz
$f(X)$	Function with input vector X
i	Number of the i-nearest neighbor
i-distance(A)	Distance to the i-nearest neighbor from data point A
K	Sampling frequency
k	Frequency in Hz
$LOF_i(A)$	Local outlier factor
$lrd_i(A)$	Local reachability density
m	Time step of window function
m_{max}	Maximum multiple of gear input speed
N	Number of samples of a signal
N_b	Number of roller elements

$N_k(A)$	Set of k-th neighbors of data point A
$N(0,1)$	Normal distribution with mean 0 and standard deviation 1
n	Timestep
n_{harm}	Number of considered harmonics
$n_{robot\ gear}$	Transmission rate of robot gear
ω_{robot}	Rotational speed of robot in 1/s
P	Probability
p	P-value
R	Window length
R^2	R² measure
S	Radial speed in 1/s
S_{cs}	Maximal occurrence value of a sign
s	Maximum step back
$spec(t,\ k)_{avg,ref}$	Average spectrogram of reference measurements
$spec(t,\ k)_{meas}$	Spectrogram of a measurement
$spec(t,\ k)_{std,ref}$	Standard deviation spectrogram of reference measurements
σ	Standard deviation
T	Length of measurement in samples
TP	True Positive
TPR	True positive rate
θ	Contact angle
w	Window function
X_k	Fourier transformed signal at frequenc y k
$X_m(t,\ k)$	Short time fourier transform at time step t and frequency k
$\ddot{X}$	Probability distribution
x	Sample value
$\bar{x}$	Mean
x_n	Signal value at time step n
$\overline{x_n}$	Mean of time series
$\widehat{x_n}$	Estimated value of a fitted function at time step n
$x(n)$	Signal function
y	Dependent variable

Z_{cs}	Test statistic
Z_{score}	Z-Score
$Z(t,\ k)$	Z-score-matrix
$z_{1-\frac{\alpha}{2}}$	Z-value for error level α

1 Introduction

“Solving climate change would be the most amazing thing humanity has ever done” (JUSTIN ROWLATT 2021).

This quote from Bill Gates shows on the one hand, the great potential our civilization could unleash in the coming decades; on the other hand, it emphasizes the challenges that society has faced. Transforming energy systems, mobility behavior, or the way goods are produced are only some aspects of this globally needed change (BUNDESMINISTERIUM FÜR UMWELT, NATURSCHUTZ UND NUKLEARE SICHERHEI 2019). In the manufacturing sector, the reduction of energy consumption, the circular economy, and the increased lifetime of assets are enablers for this transformation (CADEZ & CZERNY 2016).

1.1 Motivation

The prolongation of the useful lifetimes of machines can be based on suitable maintenance strategies. With the advent of Industrie 4.0 – the fourth industrial revolution – technologies such as machine connectivity, fast processing of large datasets, and artificial intelligence to support decisions, condition monitoring (CM) strategies allow the triggering of maintenance actions based on the machine state shortly before failure (DALENOGARE ET AL. 2018). Hence, the premature exchange of an asset based on a predetermined maintenance schedule can be avoided, and the lifetime of the asset can be increased.

As well as these long-term benefits, condition monitoring also increases the availability of assets by avoiding unexpected downtimes due to failures (DIN DEUTSCHES INSTITUT FÜR NORMUNG E. V 2018). Such unexpected downtimes are caused, for example, by the faults of industrial robots (IRs), the workhorses of high-wage countries such as Germany. More precisely, gear faults usually lead to the replacement of the robot in a production line (NENTWICH & REINHART 2021c). Hence, the design of a CM system for these components would have the potential to improve the productivity and lifetime of these assets.

However, the design of such systems is often hindered by the lack of the necessary data, expert knowledge, or a business case (MULDERS & HAARMAN 2018). Additionally, the growing number of published CM approaches increases the potential solution space for the CM system. In Chapter 3, it is pointed out that many of these publications do not meet industry requirements. These approaches require data from defective robots that are difficult to acquire. Moreover, they do not consider the transient velocities and temperature fluctuations of robot gears. Since the development of a CM system for IR gears cannot be based on existing approaches,

the implementation of such a system is an iterative and time-consuming process, which reduces the profitability of the system. A reduction of time and effort is needed, to improve this situation.

1.2 Objective

Given the situation described in Section 1.1, the objective of this dissertation is as follows:

To increase the efficiency in the development process of condition-monitoring systems for industrial robot gears.

In this context, efficiency relates to reducing timely efforts – and hence cost – within the development process compared to a reference scenario. The definition of the condition-monitoring system (CMS) development process is given in Section 2.2.2. To achieve this objective, two main approaches to increase efficiency are considered. Firstly, iterations within the development process shall be reduced. Secondly, the time for data acquisition required for a successful operation of the CM system shall be decreased. The two levers are realized by designing a CM reference architecture (RA) for IR gears. A RA is a template for developing a particular solution (ISO/IEC 2021).This architecture requires little data and is particularly designed for the characteristics of robot operations, such as gear temperature fluctuations and transient velocities. The components of the architecture can be used directly in the development process and thus reduce iterations and the time for data acquisition.

1.3 Methods and Structure of the Dissertation

To achieve the objective of this work, this dissertation follows the design research methodology (BLESSING & CHAKRABARTI 2009), which also defines the structure of this work. The objective of this methodology is to improve the rigor of research projects and therefore increase the applicability of research outcomes to practice (BLESSING & CHAKRABARTI 2009, p. 9). In general, a design research methodology project consists of four steps. First, from a global motivation, a research gap is identified. Second, a descriptive study is performed to gain a comprehensive understanding of the research problem by means of literature analysis, experiments, or data analysis. Third, a solution model is built based on the findings of the descriptive study in a prescriptive study. Fourth, another descriptive study is performed to validate the outcome of the prescriptive study (BLESSING & CHAKRABARTI 2009, p. 15 - 17).

In this dissertation, the general topic is presented in Chapter 1, and the most relevant fundamentals of this work are introduced in Chapter 2 as part of the research clarification. The state

of the art is summarized and critically discussed in Chapter 3 as part of the first descriptive study. The publications related to this dissertation are then presented in Chapter 4. They focus on the different aspects of the CM RA for IR gears and consist of prescriptive and descriptive elements. They can therefore be classified as part of the prescriptive or the second descriptive study. Hence, the overall approach can be classified as a research project of type 6, as described in BLESSING & CHAKRABARTI (2009, p. 33). This type of project consists of a review-based research clarification and first descriptive study and a comprehensive prescriptive and second descriptive study. The contribution of this dissertation is discussed in Chapter 5, and a summary and outlook are given in Chapter 6. The structure of the dissertation and the classification of its modules in the different processes are summarized in Figure 1.

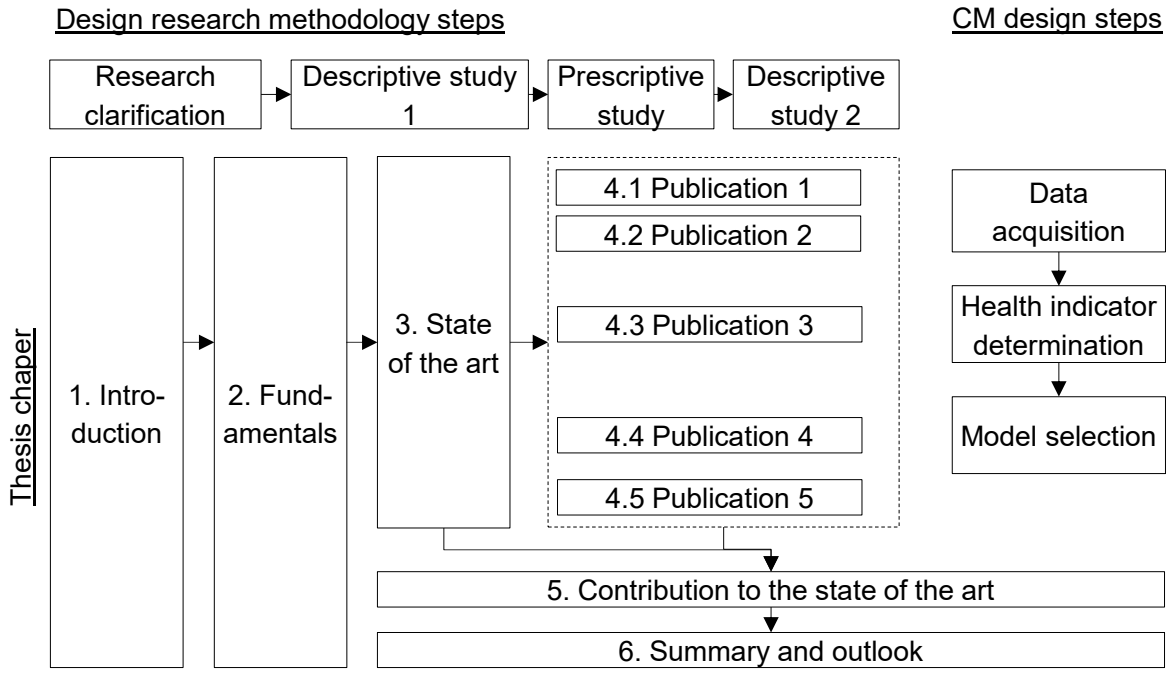

Figure 1: Structure of the dissertation

2 Fundamentals

This chapter provides the basic theoretical concepts upon which this dissertation is based. It discusses IRs in Section 2.1. As these systems deteriorate over time, Section 2.2 focuses on maintenance. The topic of machine learning is covered in Section 2.3, since it is of importance for the maintenance strategy considered in this work. Next, two relevant types of machine learning models, trend- and anomaly-detection models, are discussed in Sections 2.4 and 2.5.

2.1 Industrial Robots

According to DIN EN ISO 10218-1, IRs are automatically controlled, freely programmable, multi-purpose manipulators that can be programmed in three or more axes and which are used in mobile or stationary automation technologies (DEUTSCHES INSTITUT FÜR NORMUNG E. V 2012). Within this dissertation, only six-axis articulated robots with a payload over 200 kg are considered, as these robots have long exchange times in the case of a gear failure due to their dimensions and weight.

2.1.1 Structure and Working Principle

Six-axis articulated robots consist of six axes that are connected in series by rotational joints to enable movements within a spherical working space. An example of the structure of a six-axis articulated robot is shown on the left side of Figure 2. Each joint consists of an electric motor that enables the movement of the axis by transmitting torque via a gear. The motors, which are mostly brushless direct current motors, are controlled by the robot controller, which plans the robot movements according to the user commands or robot programs (SICILIANO & KHATIB 2008, p. 79 - 82). These movements, if not defined otherwise, are usually characterized by steep acceleration and deceleration ramps and phases of stationary velocity. To cope with these characteristics and with other requirements such as low space requirements and transmission ratios, mostly cycloidal drives are used in the robot payload class over 200 kg (PHAM & AHN 2018). These gears, also known as rotate vector (RV) reducers, transmit the motor's torque in two stages. The motor pinion drives three planetary wheels. Their shafts are mounted eccentrically in two cycloidal discs. The movement of the cycloidal discs enables the robot axis movement. The working principle of these gears is explained on the right side of Figure 2.

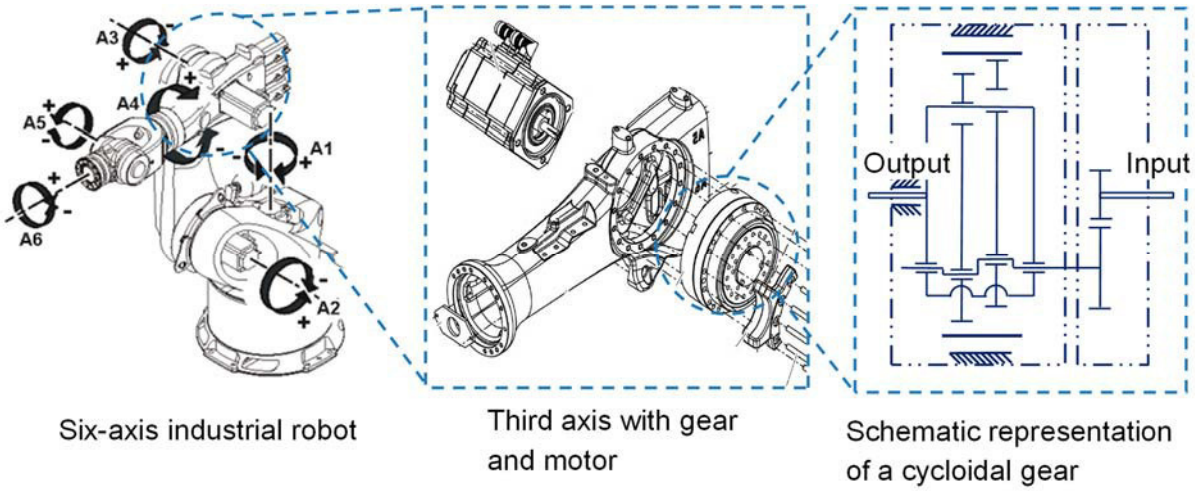

Figure 2: Mechanical structure of an industrial robot following KUKA (2021, p. 38) and NABTESCO (2022, p. 10)

In practice, the gears are exposed to varying temperatures due to the robot's varying utilization. These different temperatures also influence the friction inside the gear (CARVALHO BITTENCOURT 2014) and the damping behavior of the gears (JAGADISH & RAVIKUMAR 2013, SHU ET AL. 2020). Figure 3 exemplifies the changing temperatures of a robot gear operating in a car body plant for over two months. Temperature variations in a range of 30 Kelvin can be observed.

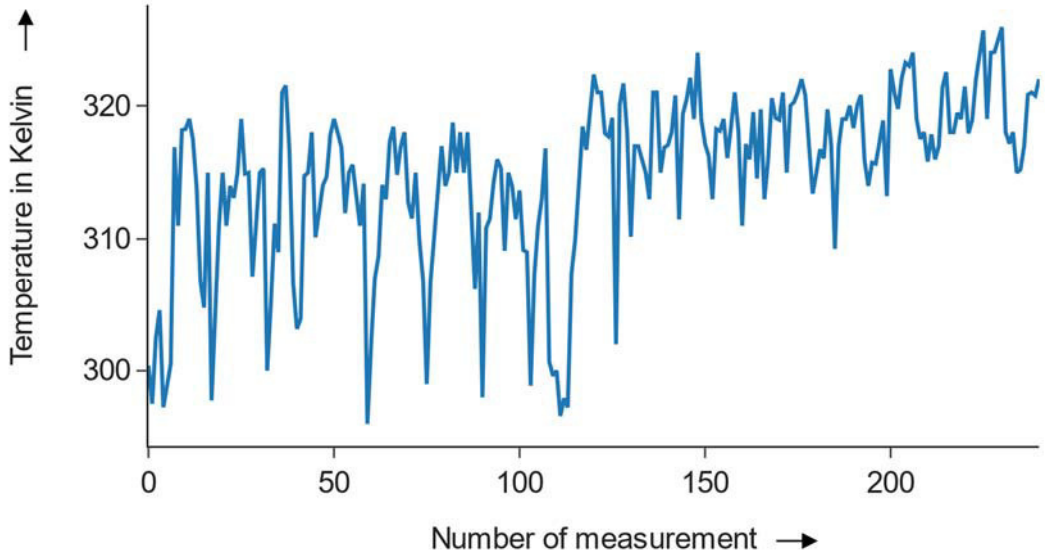

Figure 3: Temperature fluctuations of an industrial robot gear

2.1.2 Faults of Cycloidal Gears

Cycloidal gears can show different defects due to overloading, unsuitable lubrication or aging. Defects can be considered from two points of view. From a maintenance point of view, a robot

has a defect if it cannot fulfill its production task sufficiently. This could be due to the blockage of the gear, broken parts, or an increased number of error messages caused by the robot controller when the torque is not transmitted as expected by the controller (DANIELSON & SCHMUCK 2017, NENTWICH & REINHART 2021a). These error messages stop the automatic working mode of the robot and hence make maintenance necessary. From a tribological point of view, defects can be differentiated by the main cycloidal gear components: shafts, bearings, and gears. In the following, the different defects of these parts are summarized.

The INTERNATIONAL STANDARDIZATION ORGANIZATION (2017) describes different failure modes of bearings that can lead to different defects. Overall, six failure modes can be distinguished.

Rolling contact fatigue is a failure mode caused by periodic stresses between the rolling element and the raceways of a bearing. It can be differentiated into surface and subsurface initiated fatigue. The latter causes microcracks under the components' surface that propagate to the surface and then lead to spalling. The former is based on plastic deformation of the components' surface due to unsuitable lubrication or particles that are pressed between the components' surfaces.

The second failure mode is **wear**, which can be categorized into abrasive wear and adhesive wear. Abrasive wear is the surface removal of components due to sliding between the components in the presence of hard particles. Adhesive wear appears due to frictional heat and describes the transfer of material between component surfaces. The heat first leads to fusing of the surfaces. This bond is then destroyed by the unwinding of the surfaces and material is thereby removed.

Corrosion is another failure mode and is based on chemical reactions on metal surfaces. Corrosion can be caused by contact with moisture that creates rust on the component surface that will eventually lead to pits and spalling. Another cause is friction that leads to the oxidation of the metal surface and creates rust powder on the mating component surfaces.

Currents can also cause bearing defects. This **electrical erosion** can be caused by voltage between the bearing ring and the rolling element that leads to short high-current flows. They cause small pits in the rolling element or the bearing ring runway. Constant current flowing through the bearing causes very small, shallow crates to form close together.

Plastic deformation occurs if the components' material yield strength is exceeded. This can be caused, for example, by high shock loads while the bearing is stationary, which can lead to indentations on the component surfaces. Such indentations can also be caused by particles that are over-rolled.

Cracks and fractures represent the last failure mode. Cracks appear when the tensile strength of the components' materials is locally exceeded. The propagation of a crack through

a component leading to a complete separation of a portion of the component is defined as a fracture. Cracks can be caused by excessive loads. Another cause is fatigue of the material, which is based on repeated excessive bending, tension, or torsional loads. Finally, frictional heating can cause high residual tensile stresses or a re-hardening of steel components, which will eventually lead to cracks. Figure 4 presents examples of different bearing defects.

Figure 4: Bearing defects following INTERNATIONAL STANDARDIZATION ORGANIZATION (2017)

Similar failure modes exist for gear teeth. A detailed description of these failure modes can be found in INTERNATIONAL STANDARDIZATION ORGANIZATION (1995). In this dissertation, faults of IR gears are considered. In the accelerated wear tests that were performed as a part of this work and that are described in NENTWICH & DAUB (2022), combinations of the faults described above could be observed.

2.2 Maintenance

In the following sections, different maintenance strategies and their applicability for different scenarios are explained. Subsequently, a specific strategy – condition-based maintenance – is described in Section 2.2.2.

2.2.1 Maintenance Strategies

To cope with the defects described above, different maintenance strategies can be applied. According to SCHENK (2010, p. 26 - 34), four strategies exist, as presented below.

In a **reactive maintenance strategy**, maintenance is performed after a defect occurs. This minimizes the upfront planning effort but requires the storage of spare parts and leads to unexpected downtimes of the affected production line.

In contrast, in a **preventive maintenance strategy**, maintenance is performed in regular time intervals to avoid defects. In this strategy, the length of downtimes can be reduced compared

to a reactive maintenance scenario, and spare parts can be ordered based on the maintenance intervals. However, it is possible that parts are exchanged that would not have failed soon. Hence, this strategy can incur unnecessary costs of early part exchanges (RYLL & FREUND 2010, p. 28 - 29). Furthermore, planned downtimes occur more frequently compared to a reactive maintenance strategy.

To address these deficiencies, **condition-based maintenance** assesses the condition of components by collecting and analyzing data. Different sensor systems can be used for the data collection. The suitability of the sensor system depends on the components. Vibration, noise, current, temperature, and oil analysis sensors are used for gear-condition monitoring (KOLERUS & WASSERMANN 2017, p. 1). The information from this sensor data can then be used to determine the condition of the system and trigger a maintenance action before a fault occurs. In theory, this would maximize the components' lifetime and avoid unexpected failures. This maintenance strategy, however, incurs additional costs for sensors and data analysis software.

Predictive maintenance advances the principle of CM by using the collected data to predict the future condition of the asset. These predictions can then be used to identify the points of failure of the asset in the future and schedule maintenance action accordingly (TINGA & LOENDERSLOOT 2019). Predictive models can be based on two different principles. Either they are based on a physical model of the asset, which incorporates the wear mechanisms of the asset and models the wear progress correctly, or they are purely data driven (LEI ET AL. 2018). In the latter case, data that correlate with the wear progress must be collected for many similar assets and faults. On the one hand, this maintenance approach would ideally reduce downtimes and allow the integration of maintenance planning in production planning. On the other hand, the implementation of a reliable predictive model requires either deep physical knowledge about the failure modes and wear progress of the asset or large amounts of sensor data related to the observed defects of the asset.

As described above, these maintenance strategies have different benefits and drawbacks. Hence, the question arises which maintenance strategy should be used for which scenario. To make this decision, ideally a cost-benefit analysis of the different strategies is performed. A simpler approach is suggested by LEE ET AL. (2009) and depicted in Figure 5. In this approach, the maintenance strategy for a component is selected by the component's failure probability and the downtime related to the component's failure. Components with low failure probability and low related downtimes should be maintained reactively. Components with a high failure probability and low related downtimes would be maintained with a preventive strategy. A condition-based or predictive maintenance strategy would be applied for components with low failure probability and long downtimes. Components with high failure probability and downtimes should have already been avoided in the product development.

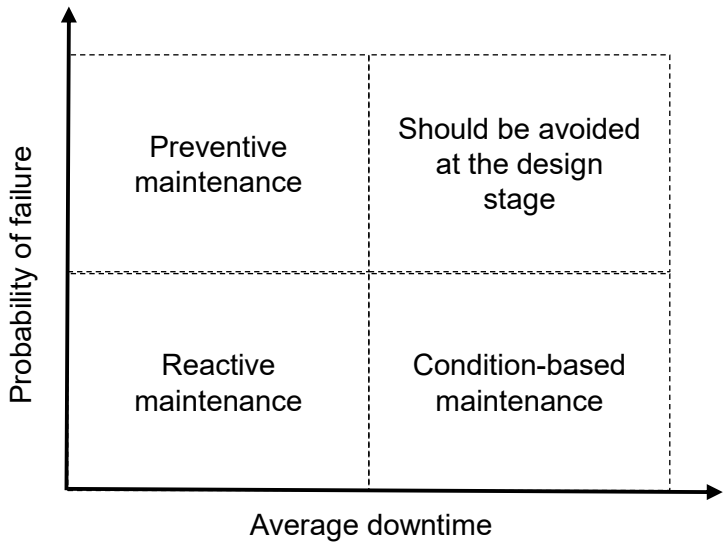

Figure 5: Maintenance strategies according to LEE ET AL. (2009)

In NENTWICH & REINHART (2021c), we found that robot gears have low defect probabilities and long related downtimes based on historic data and expert interviews. This is one reason why a CM approach is pursued in this dissertation. At the core of a condition-monitoring maintenance strategy is the CMS, which observes the wear state of a machine. In the next chapter, the fundamentals of CMSs are explained.

2.2.2 Condition-Monitoring Systems

The implementation of a CM strategy consists of two tasks. A CMS must be designed and integrated into production, and the implications of the CMS must be considered in the production's maintenance processes. A CMS is a system that acquires and processes data that indicate the state of a machine over time (INTERNATIONAL STANDARDIZATION ORGANISATION 2012, p. 1). Designing a CMS is a three-step approach, which is depicted in Figure 6 (DIN DEUTSCHES INSTITUT FÜR NORMUNG E. V 2018).

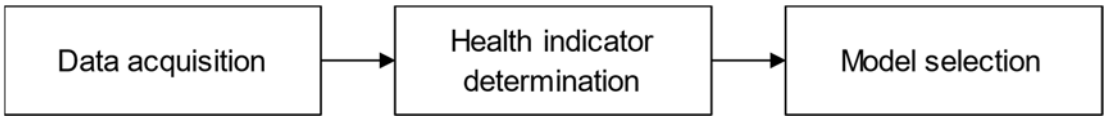

Figure 6: Condition-monitoring system development process following DIN DEUTSCHES INSTITUT FÜR NORMUNG E. V (2018)

First, a suitable data-acquisition system must be designed. This includes the selection of suitable sensors, the definition of measurement routines, and software to collect and store the raw

sensor data for further processing (LEE ET AL. 2014). In the context of this dissertation, a measurement routine describes the state of the asset during the measurement (in the case of an IR, this relates to the trajectory the robot executes) and how often a measurement is performed.

Subsequently, the collected raw data must be further processed. This processing can include different tasks, such as selecting defined time frames of the measurements, filtering of the data to reduce noise, evaluating the quality of the measurement, and deriving one or several health indicators (HIs). An HI is an indicator of the health state of the asset. A change in the health state of the asset ideally also induces a change in the HI value. Numerous approaches exist based on statistics, signal analysis, or machine learning to calculate such HIs (LEI ET AL. 2018).

Finally, these HIs must be monitored for trends and anomalies. These can be evidence for defects and can be used to trigger a maintenance action (PHAM ET AL. 2006, p. 110). These three steps are discussed in detail below.

Data acquisition

In data acquisition, the central question to be answered is that of which sensor to select. Multiple options exist for gear CM. Since different machine faults have different physical effects, different sensor systems can be used to measure these effects and hence detect faults. Figure 7 shows the frequency of different data sources used in publications that were analyzed in the literature review in NENTWICH & REINHART (2021c).

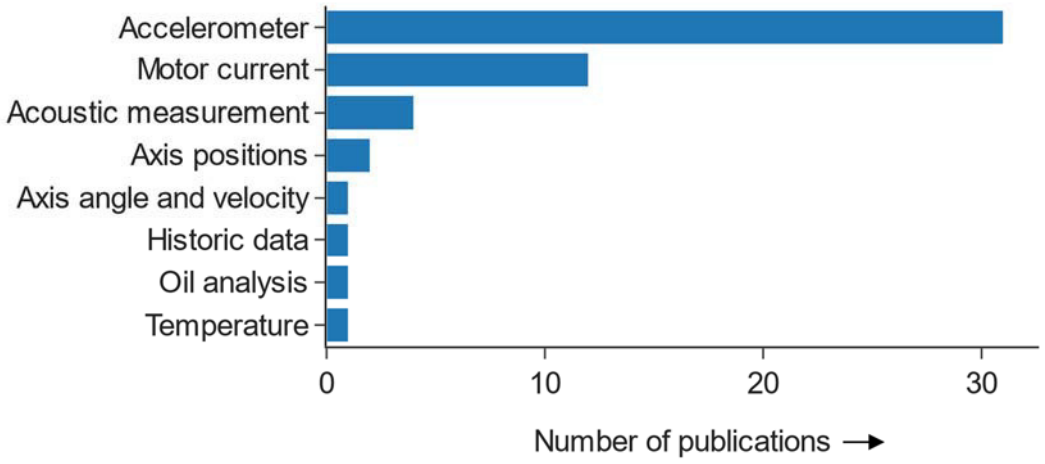

Figure 7: Data sources used for gear condition-based maintenance following NENTWICH & REINHART (2021c)

Acceleration sensors attached to the gear cap are used most frequently. These sensors ideally capture vibrations of the gear that occur at certain frequencies depending on the rotational speed of the gear and the geometry of the faulty component, such as a bearing. In theory, these frequencies can be calculated as shown in Formula 1 for faults at the inner ring of a

bearing (GIRDHAR & SCHEFFER 2004, p. 112). Similar formulas exist for other components, such as pinions.

$$BPFI = \frac{N_b}{2} * S * [1 + \left(\frac{B_d}{D_P} * \cos(\theta)\right)] \quad (1)$$

In Formula 1, $BPFI$ is the ball passing frequency at the inner ring of a bearing with N_b roller elements, a diameter B_d, a pitch diameter D_P, and a contact angle θ that spins at a rotational speed of S.

The calculation of these frequencies requires knowledge about the exact geometries of the gear, which is often not available. Furthermore, these frequencies can deviate in reality because of measurement noise and interferences such as vibrations in the environment (GIRDHAR & SCHEFFER 2004, p. 115).

The same principle can be used with motor current signals. The vibrations induce torques into the system, which can be traced back through the drive train to the motor. These torque changes can lead to motor current changes, which can then be measured (KAR & MOHANTY 2006). Another principle that can be used for CM with motor currents is the change of friction in the gear due to wear. BITTENCOURT ET AL. (2012) showed that the friction in a robot gear increases with wear. These changes can be calculated from measurements of the motor currents during defined robot movements.

These two data sources are also considered in this dissertation. For a more detailed explanation about the fault principles that are used in oil or noise analysis, please refer to MOBLEY (2002a) and MOBLEY (2002b).

The signals acquired from acceleration or current sensors are usually collected for equidistant time steps and can be considered as time series (BROCKWELL & DAVIS 2016, p. 1). Time series can have different characteristics, including a constant or varying mean value. In the latter case, the time series shows a trending behavior. If these trends occur in repeating time intervals, they are called *periodicities*. Furthermore, time series can have random variations, which are referred to as *noise* (BROCKWELL & DAVIS 2016, p. 12).

The time series from acceleration or current sensors of rotatory machinery such as gears can be considered as the superposition of many periodic time series that relate to the characteristic gear component frequencies as described above (GIRDHAR & SCHEFFER 2004). To capture the signals at certain frequencies, the sensor system must have certain characteristics. First, its sampling frequency must be at least twice the maximum frequency of interest (SHANNON 1949). Moreover, the sensor's frequency range must include this maximum frequency (BRANDT 2011, p. 151 - 152).

Health indicator determination

As described above, the overall objective of the data transformation step is to derive meaningful HIs that correlate with the health state of the robot gear. For this, the collected sensor signal can be analyzed in different domains (ALLEN & MILLS 2003, p. 56). The signal is captured in the time domain. This means that its amplitude values are collected at discrete points in time. The left side of Figure 8 shows a synthetically created signal in the time domain. Closer inspection shows that the signal appears to follow a sine function with noise. These data can also be analyzed in the frequency domain, where it becomes clearer that the signal consists of a sine function with a defined amplitude, as shown in the spectrum on the right side of Figure 8.

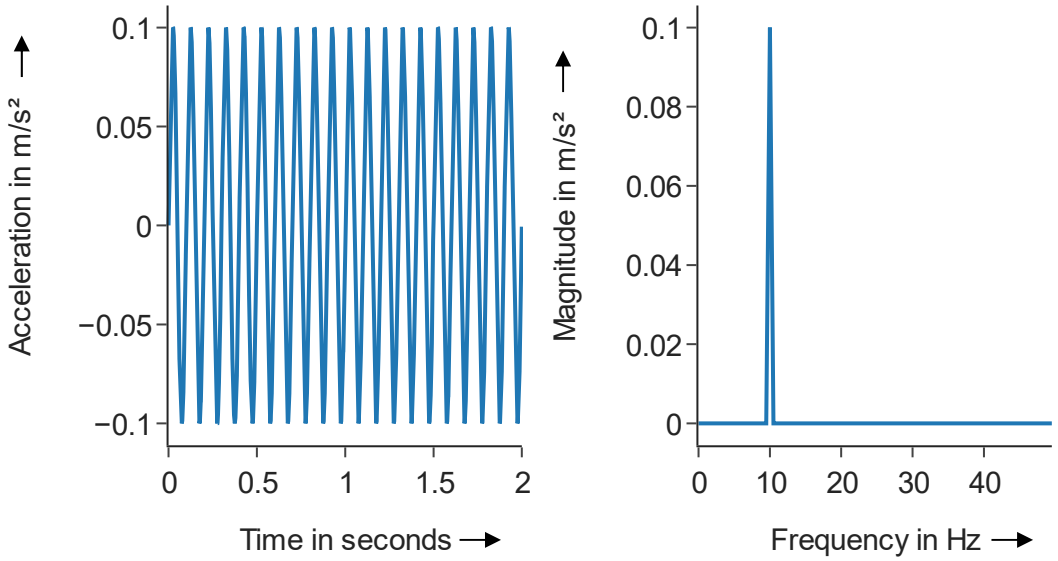

Figure 8: Signal in time and frequency domain

To transform the signal in the frequency domain, the discrete Fourier transform is used, which is described in Formula 2 (COOLEY & TUKEY 1965, BRANDT 2011, p. 180):

$$X_k = \sum_{n=0}^{N-1} x(n) e^{-j2\pi kn/N} \tag{2}$$

where X_k is the Fourier-transformed signal at frequency k; $x(n)$ is the signal at time step n; j is a complex number; and N is the number of samples of the signal.

As X_k is a complex number, the absolute value of X_k is calculated to derive an amplitude spectrum value (TAN & JIANG 2013, p. 97). If a gear operates at a constant, known velocity and the geometries of the gear components are known, the amplitudes of the characteristic gear component frequencies can be monitored for changes, which can then be an indicator of a defect, as described, for example, in Formula 1 (GIRDHAR & SCHEFFER 2004, p. 112). If the gear operates at varying velocities, the frequencies of the gear components and the captured

signal change. This leads to side bands in the spectra, which hinder the analysis of specific frequency amplitudes (BRANDT 2011, p. 269 - 271). This is exemplified for a signal with varying frequencies on the right side of Figure 9.

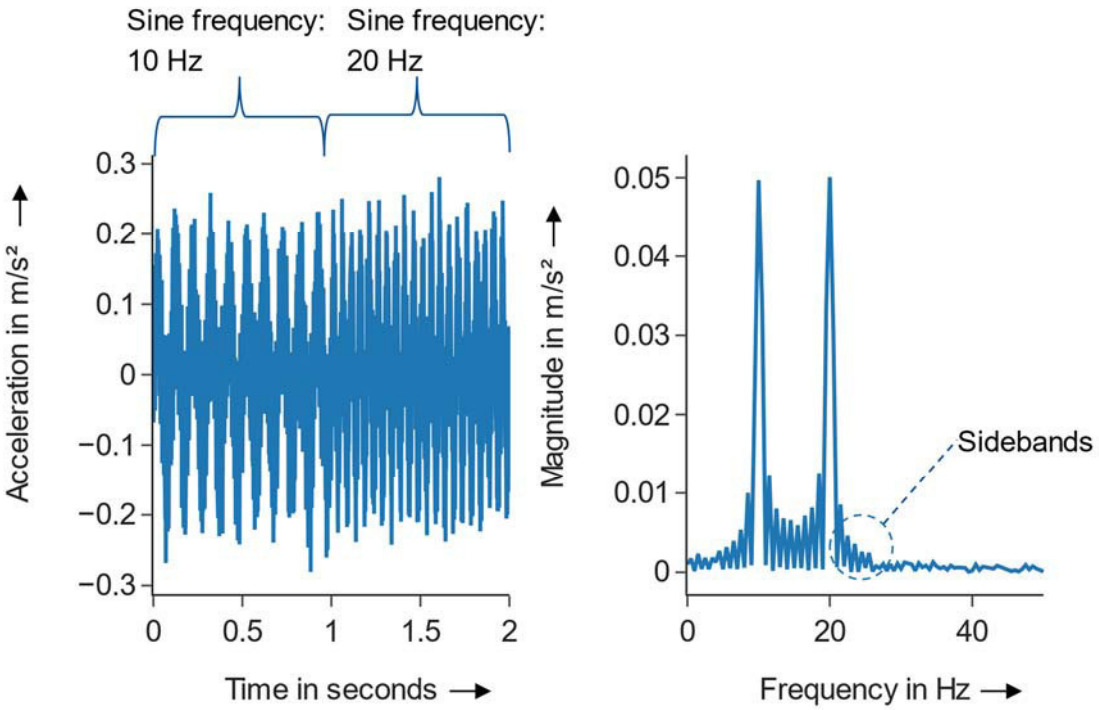

Figure 9: Transient signal in time and frequency domains

To cope with varying velocities or non-stationary signals, the time signal can also be transformed to the time-frequency domain. In this domain, the signal can be observed as a spectrogram. The spectrogram of the non-stationary signal is depicted in Figure 10. Here, magnitudes at different frequencies related to different component vibrations can be monitored.

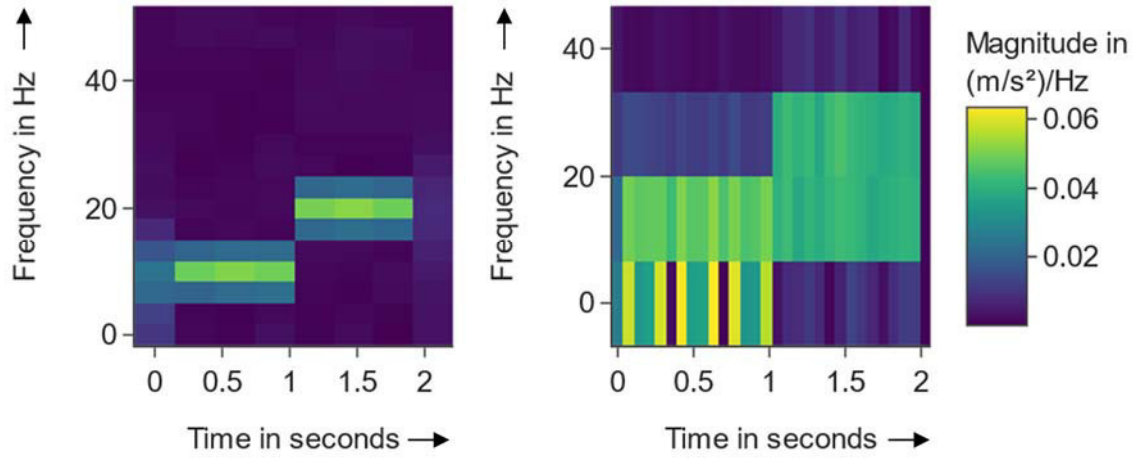

Figure 10: Spectrograms with a large window size (left image) and a small window size (right image)

To derive a spectrogram, the short-time Fourier transform (STFT) $X_m(t,k)$ in Formula 3 must be calculated from the time signal $x(n)$. Here, the discrete Fourier transform is applied to small time windows of the signal, which can then be considered almost stationary (ALLEN 1977).

$$X_m(t,k) = \sum_{n=-\infty}^{\infty} x(n) * w(m-n) * e^{j2\pi kn/N} \tag{3}$$

To extract these small time windows, the signal is multiplied with a window function w at time position m. Again, the absolute values or the squared values of the STFT are calculated to derive an energy or power spectrogram. The choice of the window length influences the time and frequency resolution of the spectrogram. Longer window lengths lead to a higher frequency-resolution and a lower time-resolution, and vice versa (BRANDT 2011, p. 264 - 265). This is illustrated in Figure 10 for the signal from Figure 9, which changes its frequency at a certain point in time. In the left image in Figure 10, it is clearer which frequencies the signal is composed of. Here, a longer time window is used. In the right image in Figure 10, shorter time intervals are shown. In this case, a shorter time window was used. In the use case of CM, longer time windows can be used to detect magnitude changes in frequency ranges of interest, such as the characteristic gear frequencies. If these frequencies are unknown, a medium-sized time window can be used to achieve a compromise between time- and frequency-resolution. The window-size selection process is usually driven by expert knowledge.

As can also be seen in Figure 10, the noise of the time signal blurs the spectrogram image. To reduce this high-frequency noise, low-pass filters can be used. These filters can be applied to the time signal and reduce the frequency content of the signal above a cut-off frequency. Filters exhibit different damping behaviors based on filter type and order. In this context, damping relates to the reduction of magnitudes of the signal content in certain frequency ranges. The filter order describes how often the basic filter is applied to the time signal. For a more detailed description of how these filters are calculated, please refer to BRANDT (2011, p. 42 - 50).

Another measure to reduce noise in a spectrogram is the Z-score (ALTMAN 1968). The Z-score can be calculated for a signal. For this, the mean $\bar{x}$ and the standard deviation σ of the signal or population are calculated. For each signal value or each sample of the population x, the Z-score can be calculated as shown in Formula 4. This principle was originally introduced in statistics and is also a common preprocessing step in machine learning.

$$Z_{score} = \frac{x - \bar{x}}{\sigma} \tag{4}$$

Based on these preprocessed data, HIs can be derived per measurement in the different signal domains. These HIs can describe the energy of the signal (in a certain frequency range) or describe statistical characteristics of the signal. The energy of a signal can refer to the squared

magnitudes of the signal or the integral of the squared magnitudes in a certain frequency range (BOUDRAA & SALZENSTEIN 2016, p. 209). As there exists an enormous number of HIs for different applications, no holistic overview of these HIs can be given in this dissertation. NENTWICH & REINHART (2021b) or VEČEŘ ET AL. (2005) can serve as good entry points for a more detailed analysis of this subject.

Over time, multiple measurements will be made for an asset, and an HI time series can be analyzed to decide whether the asset – in this work, the IR gear – is defective or healthy. In summary, time series on two different time scales are considered in this dissertation. A measurement is a time series that lasts seconds and is sampled at high frequencies (e.g., several kHz). HIs are calculated per measurement time series. HI values from several measurements form another time series, which might include data of several years. One time step in these time series corresponds to hours or days.

Ideally, the time series of these HIs shows a monotonous course over time with a low standard deviation. In this case, higher values of the HIs can be easily related to faults. To assess this behavior, different figures of merit can be used, such as monotonicity or robustness (LEE ET AL. 2014). Another possibility is to fit basic functions, such as a linear or quadratic polynomial or an exponential function, on the time series and calculate the R^2 measure of the fit (NENTWICH & REINHART 2021a). The R^2 measure quantifies the distance of the fitted function to the data points of the time series relative to the time series variance. It can be calculated as shown in Formula 5 (WRIGHT 1921):

$$R^2 = 1 - \frac{\sum_{n=0}^{N}(x_n - \widehat{x_n})^2}{\sum_{n=0}^{N}(x_n - \overline{x_n})^2} \tag{5}$$

where x_n is a value of the HI time series with length N; $\widehat{x_n}$ is the estimated value of the fitted function at position n; and $\overline{x_n}$ is the mean value of the HI time series. The principle of the R^2 measure is exemplified in Figure 11. The orange linear fit of the blue HI time series results in an R^2 value of 0.81. The R^2 measure is defined to be in the value range 0 to 1, where a value of 1 describes a perfect fit. Such a perfect fit would refer to a monotonous time series with low noise, as would be desired for an ideal HI. Since this is often not the case, fault detection models are required to detect patterns in the time series that could be related to faults such as trends or anomalies.

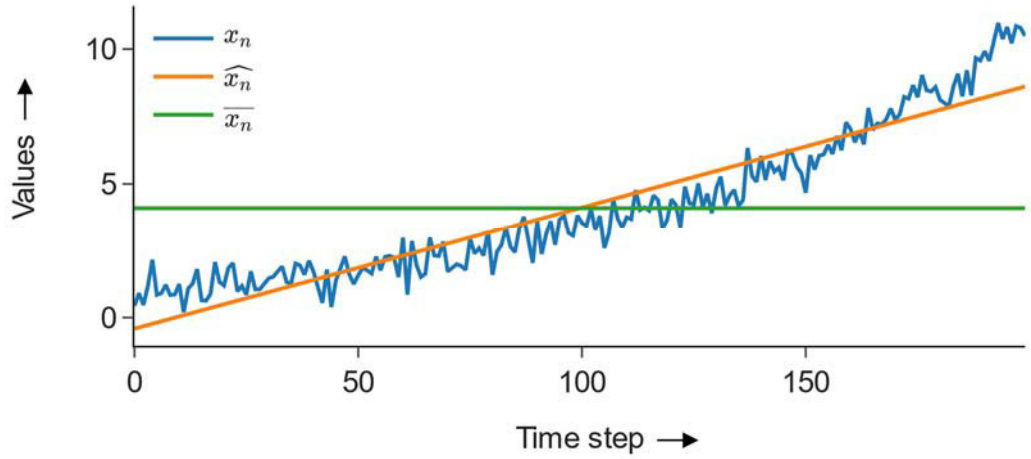

Figure 11: Example time series with linear fitted function (with arbitrary units)

Model selection

LEE ET AL. (2014) distinguish between physics-based and data-driven models. For the former, detailed knowledge about the wear processes must be available (see e.g. THÜMMEL ET AL. (2015)), which is not the case for the application considered in this dissertation. For the latter, anomaly-detection and trend-detection models can be used. With increasing wear, usually trends and anomalies appear in the HI time series (AIVALIOTIS ET AL. 2021, TANDON & PAREY 2006, SKF 2017, p. 10). The detection of trends or anomalies can be used as a decision basis for maintenance actions. As the supervision of the time series for several robot gears is usually costly, trends and anomalies should ideally be detected automatically. Machine learning, or more precisely trend- and anomaly-detection models, are suitable for this task. Hence, these three topics will be presented in the next sections.

2.3 Machine Learning

A machine learning (ML) model can be considered as a system in which features serve as input and the labels are the model's output. Features and labels can be scalars, vectors, matrices, or tensors (HASTIE ET AL. 2009, p. 1 - 2). The combination of both features and labels is referred to as a dataset in this work. In mathematical terms, a machine learning model estimates a function, as presented in Formula 6:

$$y = f(w, x) \tag{6}$$

where y is a label; f is the machine learning model; and x is a set of features. In a training phase, a training dataset is used to estimate the parameters w of f to predict the labels correctly. Then, in a testing phase, the trained model with fixed parameters w is evaluated with

testing data regarding different figures of merit. Some of these figures are described in Section 2.3.2. Furthermore, there are different ways to determine the parameters of this function depending on the model category and specific type (HASTIE ET AL. 2009, p. 2).

2.3.1 Categories of Machine Learning

Different classification schemes for machine learning models exist. One classification scheme differentiates supervised and unsupervised models (BISHOP 2009, p. 3). If a set of features and known labels of these features are used to determine the model's parameters, the model can be classified as a supervised model. In this category, regression and classification models can be distinguished based on the characteristics of the labels. Either the labels are on a continuous scale, in which case the model can be classified as a regression model, or the labels are on a discrete scale (such as two categories), in which case the model can be defined as a classification model (BISHOP 2009, p. 3). In contrast, in unsupervised machine learning, no labels are used to train the model. The model learns only certain characteristics of the features, which can then be used to cluster data or reproduce similar data (BISHOP 2009, p. 3).

Another common problem is the lack of data for certain classes in a classification problem (YANG ET AL. 2021). In the application of CM, it is time-consuming to acquire data from faulty robots because of their long lifetimes. To overcome this challenge, models from the category of one-class classification can be used. In this case, only data from one class are required to train the model. Considering the CM application, this means that only data from functional robots are used. During the training, the model learns the characteristics of these functional data. Afterwards, the model can determine if a sample belongs to the class it was trained with (MOYA & HUSH 1996).

2.3.2 Evaluation of Machine Learning Models

Different possibilities exist for assessing how well the model's parameters were estimated for its specific task. For one-class classification models that distinguish samples from two classes – the positive and negative class – the true positive rate (TPR) and false positive rate (FPR) are important figures of merit to describe the model performance. The TPR can be calculated for a test dataset based on Formula 7 and the FPR based on Formula 8 (YERUSHALMY 1947):

$$TPR = \frac{TP}{TP + FN} \tag{7}$$

$$FPR = \frac{FP}{FP + TP} \tag{8}$$

where TP are positive samples that are classified correctly; FN are the positive samples that are classified as negative samples; and FP are negative samples that are classified as positive. For many one-class classification models, a trade-off exists between the TPR and FPR depending on the model parameters. Either a model is conservative and shows a low FPR at the cost of a decreased TPR or a model is liberal, having a high TPR in combination with an increased FPR(FAWCETT 2006). The principle of the different rates is shown in Figure 12.

	Data from positive class	Data from negative class
Positive classified data	TP	FP
Negative classified data	FN	TN

Figure 12: Relation between different figures of merit and classified data

Receiver operator characteristic (ROC) curves are used to evaluate this trade-off. A ROC curve displays the TPR and FPR for different model parameter combinations. A model parameter is, for instance, a parameter that characterizes the model and influences its training process. Ideally, a model parameter combination shows a TPR of 1 and a FPR of 0, which represents a model that identifies all positive values correctly while not causing any false alarms. In contrast, an entry in the ROC curve on the angle bisector of the diagram refers to a model parameter combination of a “guessing” model. Here, both rates are 0.5, which means that the model randomly decides if an anomaly is present or not (EMMERICH 1967). The principle of a ROC curve is presented in Figure 13 and illustrated in the following example: The ROC curve values could be derived from a model that identifies abnormal vibration measurements of a robot by a simple threshold rule. If the maximum measured vibration exceeds a set threshold, a measurement is classified as abnormal. The threshold defines the model parameter combination. If this threshold is low, it is likely to detect all actual abnormal measurements and obtain a high TPR. However, many normal measurements will also be classified as abnormal leading to a high FPR. This is illustrated in Figure13 in case A. This case would mark one point in the ROC curve. If the threshold is now increased, it is likely that the FPR will decrease and the TPR will decrease slightly leading to a new point in the ROC curve, e.g. as case B in Figure 13. By increasing this threshold in multiple steps, multiple points in the ROC curve can be determined.

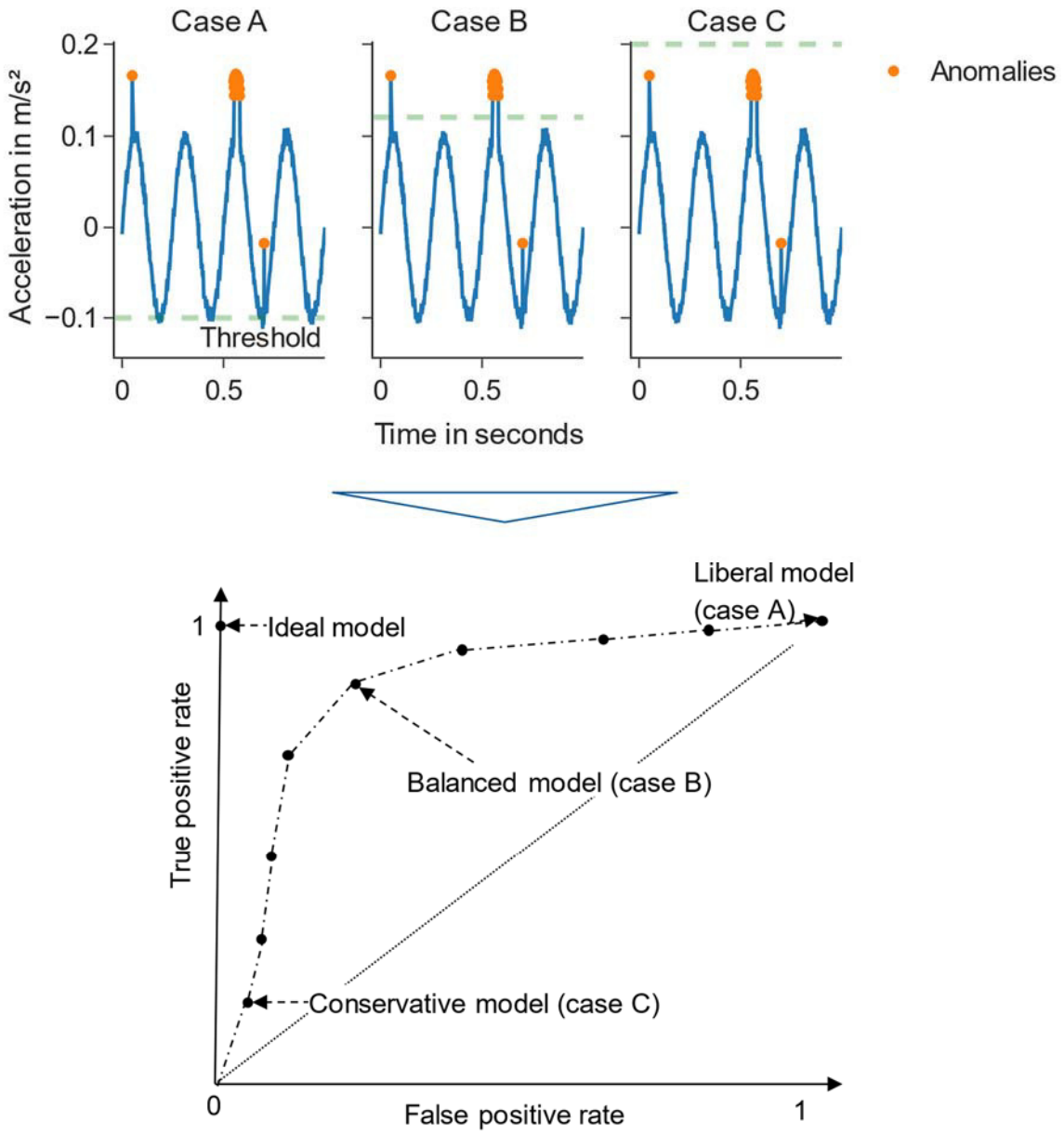

Figure 13: Principle of a receiver operator characteristic curve

To summarize the information of a ROC curve, the area under the curve (AUC) value can be calculated. To do so, the entries of the ROC curve are linearly interpolated, and the integral under this curve is calculated. A higher AUC value usually refers to a model with higher performance (SWETS 1979). However, even models with lower AUC values can show the ideal behavior of a TPR value of 1 and an FPR value of 0. As a model is used in production with only one parameter set (e.g. one threshold for the vibration), always multiple figures of merit such as the AUC and the TPR should be used to evaluate model performance. ROC curves can also be determined for trend-detection models, which are considered in the next section.

2.4 Trend-Detection Models

In this section, the term *trend* is first defined. Subsequently, different trend-detection models are categorized, and the most relevant model for this dissertation – the Cox-Stuart test – is presented in detail. In the context of this work, a trend describes the basic direction of a time series, which is independent from stochastic deviations (SCHNECK 2015, p. 711). A time series with a trend is also called *non-stationary* and has no fixed average value (ALBERS 2009, p. 396).

2.4.1 Trend-Detection Model Categories

There are different trend-detection approaches for different purposes. Some methods detect whether a trend is present in a time series; other approaches focus on the visualization of trends in data. Another purpose is to detect change points. Change points are steps in a time series where an increasing trend changes into a decreasing trend or vice versa (SHARMA ET AL. 2016).

Methods for **trend detection** are based on various principles. Statistical tests determine whether a trend is present in a time series. For this, the Mann-Kendall test, the Cox-Stuart test, or the Wilcoxon-Mann-Whitney test can be used (MANN 1945, COX & STUART 1955, WILCOXON 1945). Trends can also be detected by clustering the data points of a time series and comparing the slope of the cluster centers with defined thresholds (MELEK ET AL. 2005). Alternatively, they can be detected by fitting functions on the data or segments of the data and comparing the fit of these functions on the data quantified by figures of merit such as the R^2 to thresholds (NENTWICH & REINHART 2021a).

These function fits can also be used for **trend visualization**. Filters can be used to reduce noise in a time series and thus also visualize trends (NIEMINEN ET AL. 1989). Finally, methods exist to identify change points.

In IR gear CM, it is necessary to detect whether trends are present in the HI time series, since a trend can indicate a defect (AIVALIOTIS ET AL. 2021, TANDON & PAREY 2006, SKF 2017, p. 10). This means that statistical trend tests are potentially suitable for this application. Methods based on function fitting and comparing these fits' goodness with thresholds could also be applied. Finally, cluster fitting is potentially applicable for trend detection for IR gear CM. In NENTWICH & REINHART (2021a), which will also be presented in Section 4.2.4, it is shown that the Cox-Stuart test is the most suitable test for this purpose. Thus, this test will be presented in more detail below.

2.4.2 The Cox-Stuart Test

The Cox-Stuart test is a non-parametric trend test (COX & STUART 1955). In this context, *non-parametric* means that the distribution of the time series does not have to be known. The test is used to accept or reject the null hypothesis that no trend is present in a dataset. In principle, this test consists of four steps. Firstly, data pairs from data points in the first and last third of the time series are created. Secondly, the differences between these data pairs are calculated, and the occurrence of the signs of these differences, which can be positive, negative, or zero, is counted. Thirdly, a test statistic is calculated based on the largest number of occurrences and the number of data points of the time series. Finally, the *p*-value for the test statistic is derived and compared to a desired confidence level. Formalized, the maximal occurrence value of a sign S_{cs} can be calculated according to Formula 9; the test statistic Z_{cs} is then calculated by Formula 10 and the *p*-value derived by Formula 11.

$$S_{cs} = \max_j \left\{ \sum_{n=1}^{N/3} \delta \left[\mathrm{sgn}\left\{ \mathrm{x}_{\mathrm{N}-\frac{N}{3}+n} - x_n \right\} = j \right], j = -1,0,1 \right\} \tag{9}$$

where δ is the Dirac operator, sgn is the sign function, and x_n is a sample of the time series with the length N at position n.

$$Z_{cs} = \frac{|S_{cs}| - \frac{N}{6}}{\sqrt{\frac{N}{12}}} \tag{10}$$

$$p = P\left(\left|\ddot{X}\right| > |Z_{cs}|\right), \ddot{X} \sim N(0,1) \tag{11}$$

In Formula 11, P describes a probability and $\ddot{X}$ a normal probability distribution N with mean 0 and standard deviation 1. Finally, the calculated *p*-value is compared with a significance level. A significance level expresses the required certainty level of the trend detection as a probability. If the *p*-value is smaller than the significance level, the null hypothesis is rejected and the presence of a trend can be assumed. To apply the test, only the required significance level must be defined. A smaller significance level corresponds to a higher probability that a trend is present. This principle is exemplified in Figure 14. The Cox-Stuart test is applied with different significance intervals. A lower significance level results in a later detection of the trend, when it is clearer that a trend is present in the time series.

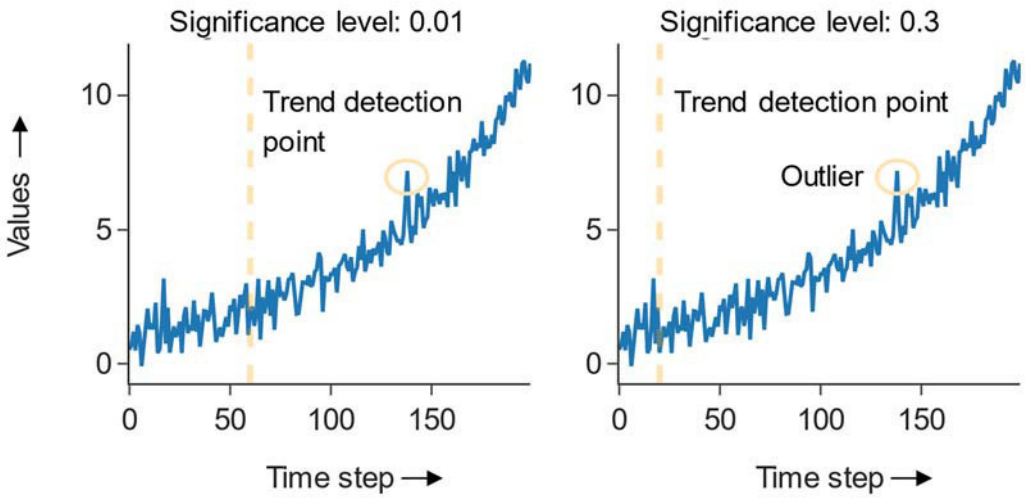

Figure 14: Cox-Stuart test with different significance levels (in arbitrary units)

Figure 14 shows an outlier around time step 135. Such anomalies can be detected by anomaly-detection models, which are discussed in the next section.

2.5 Anomaly-Detection Models

In this section, after anomalies are defined, an overview is given of different types of anomaly-detection models for time series. The most relevant anomaly-detection models for this work – the long short-term memory neural network and the local outlier factor – are then explained. According to HAWKINS (1980, p. 1), an anomaly or outlier is “an observation which deviates so much from other observations as to arouse suspicions that it was generated by a different mechanism.”

Anomalies can be differentiated by type. In the context of a time series, anomalies include point, collective and contextual types (CHANDOLA ET AL. 2009, p. 7 - 8). Point anomalies are individual data points that deviate significantly from the time series. Collective anomalies are multiple data points whose occurrence together form an anomaly. Contextual anomalies are data points whose occurrence is rare in a given context (e.g., high outdoor temperature values measured in winter). In Figure 15, the different types of anomalies are exemplified.

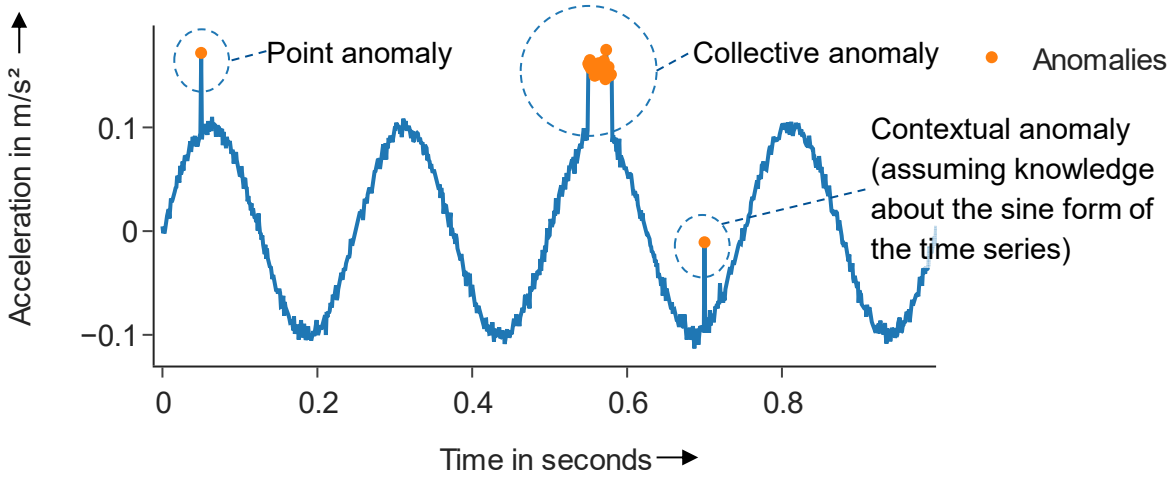

Figure 15: Time series with different types of anomaly

Assuming that the periodic behavior of the time series is known, the rightmost anomaly in Figure 15 can be classified as a contextual anomaly or as a point anomaly. Lower values would usually be expected at this position of the periodicity. The contextual anomaly could also consist of multiple data points. Often, contextual anomalies are more difficult to detect with simple rules. In the example above, the point and collective anomalies could be detected by defining a threshold around 0.1. No false positives would occur. If the same approach would be used for the contextual anomaly, a very small threshold would have to be used leading to a high and undesired false positive rate.

In the context of this thesis, anomalies are defined as the positive class for the data classification scheme presented in Figure 12. Normal data are considered samples of the negative class.

The algorithms used to automatically detect these anomalies in time series are referred to as anomaly-detection models in this dissertation. If a gear defect occurs, such models can be used to detect the anomalies in the HI time series automatically. This reduces the manual monitoring required in the CM system.

2.5.1 Categories of Anomaly-Detection Models

In Section 2.2.2 on page 12, the different characteristics of time series were introduced. In the introduction to Section 2.5, it was shown that there are different types of anomalies. The choice of an anomaly-detection model depends on these characteristics and the anomaly types present. Different types of anomaly-detection models and different classification schemes for these models (PIMENTEL ET AL. 2014, CHANDOLA ET AL. 2009, AGGARWAL 2017, WANG ET AL. 2019) exist. This dissertation follows the classification scheme presented by PIMENTEL ET AL. (2014). It suggests distinguishing between probabilistic, distance-based, reconstruction-

based, domain-based and information-theoretic approaches. An overview of these classes is given below.

Probabilistic approaches evaluate the probability of a data point belonging to a certain data distribution. If this probability is lower than a defined threshold, the data point is an anomaly.

Distance-based approaches calculate the distance of a data point to certain neighbor data points or to clusters of neighbor data points. This distance measure can be the Euclidean distance, for example. If the distance lies above a defined threshold, the data point is marked as an anomaly.

Reconstruction-based approaches are regression models that are fitted on the historic data of the considered time series. The regression model is then used to predict the next steps of the time series. These predictions are then compared with the actual next steps of the time series. If the distance between the prediction and the actual value exceeds a certain threshold, an anomaly is assumed.

Domain-based approaches create borders in higher-dimensional spaces and evaluate whether a data point lies within or without these border lines. If the data point lies outside the border lines, it is an anomaly.

Finally, **information-theoretic approaches** calculate the information content of the time series based on statistical measures for the whole time series and subsets in which certain data points are excluded. If the exclusion leads to a severe drop in information content, the excluded data point is anomalous.

2.5.2 Long Short-Term Memory Neural Networks

In the context of this dissertation, a reconstruction-based anomaly-detection model based on long short-term memory neural networks (LSTMs) (HOCHREITER & SCHMIDHUBER 1997) has shown itself to be particularly suited. It is used to predict the next step of the HI time series of a robot axis. The comparison of these predictions with the actual values of the time series allows the identification of anomalies. For this, the LSTM is used as a regression model, as described in Formula 12, in which s is the maximum step back of the HI time series considered for the prediction.

$$x(n) = f(x_{n-1}, x_{n-2} \dots, x_{n-s}) \tag{12}$$

The regression function is approximated by the neural network, which consists of layers of interconnected neurons. The working principle of a neuron is depicted in Figure 16 and is called *forward pass*.

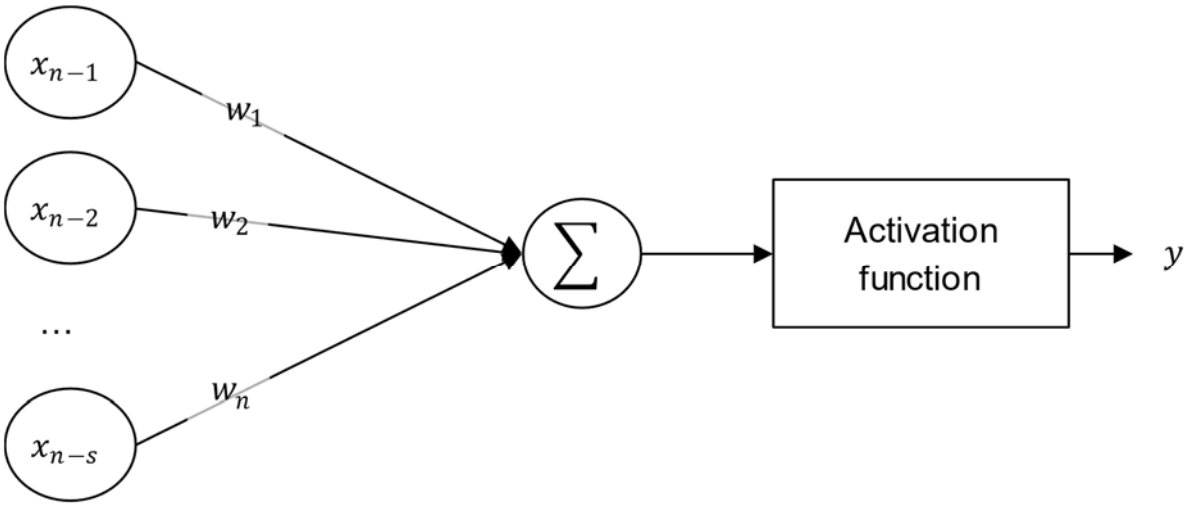

Figure 16: Principle of a neuron according to SKANSI (2018, p. 62)

A neuron sums up weighted input values, which can be, for example, data points of a time series. This sum is used as the argument for an activation function. The function value of this argument is the output of the neuron. The output y depends only on the input vector and the weights.

In an LSTM, neurons are replaced by cells, and the output of a cell depends not only on the input and weights, but also on an internal state of the cell c_t represented by a vector. Furthermore, cells consist of three parts, namely input gates, output gates, and forget gates, which are themselves neuron layers. These allow the networks to relate important data points in time series with large time lags in between. In detail, when an LSTM cell is presented with an input vector, the former cell state c_{t-1} and the input vector $(x_{n-1}, x_{n-2} \dots, x_{n-s})$ are fed into the forget gate layer to determine which part of the cell state should be forgotten. Furthermore, the input vector is fed into the input gate layer to define which new information should be stored in the cell state and which information should be altered in the cell state. Finally, they are also fed into the output gate layer, whose output is used together with the altered cell state to calculate the new output of the LSTM cell. Hereby, the calculation of the output value does not only depend on the current input values but also on the internal state of the cell. That state can store information about data passed through the cell multiple previous time steps ago. The concept of an LSTM cell is shown in Figure 17. To determine the weights of the gates of each cell and layer, training algorithms such as gradient descent can be applied (RUMELHART ET AL. 1986). The required training data are HI time series from time periods where no defects occurred.

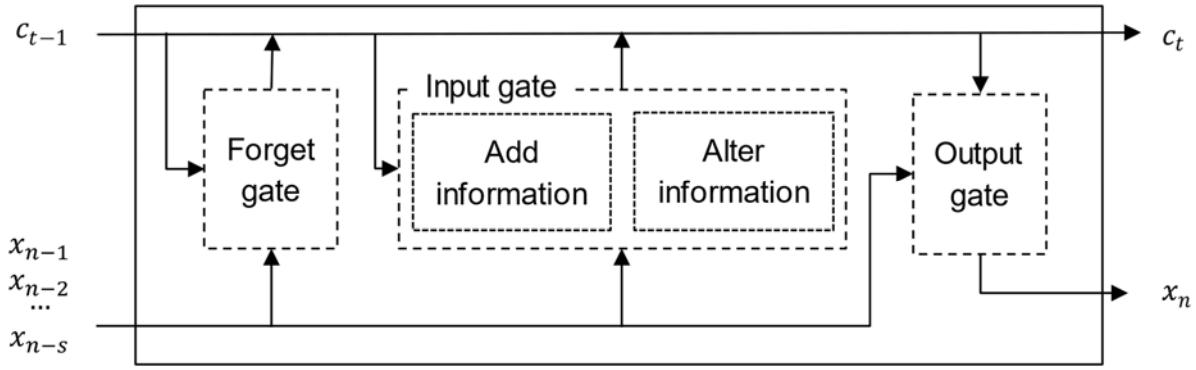

Figure 17: Principle of a long short-term memory cell following HOCHREITER & SCHMIDHUBER (1997)

Ideally, the LSTM would capture the characteristics of these time series and hence would be able to predict time steps for HI data from functional robot gears with low errors, the so-called reconstruction error. In contrast, this error should be large for anomalies, as they deviate from the characteristics of the time series. The distribution of these reconstruction errors can be modeled with a normal distribution. The reconstruction errors of anomalies would have a low likelihood of belonging to this distribution. This concept is depicted for an example time series in Figure 18. The blue time series represents artificial HI data, which is reconstructed by the LSTM model. The error between the reconstruction increases in magnitude if anomalies appear. In this way, the anomalies can be classified. Defining a threshold for this likelihood therefore represents the last step during the setup of the anomaly-detection model (NENTWICH & REINHART 2021a).

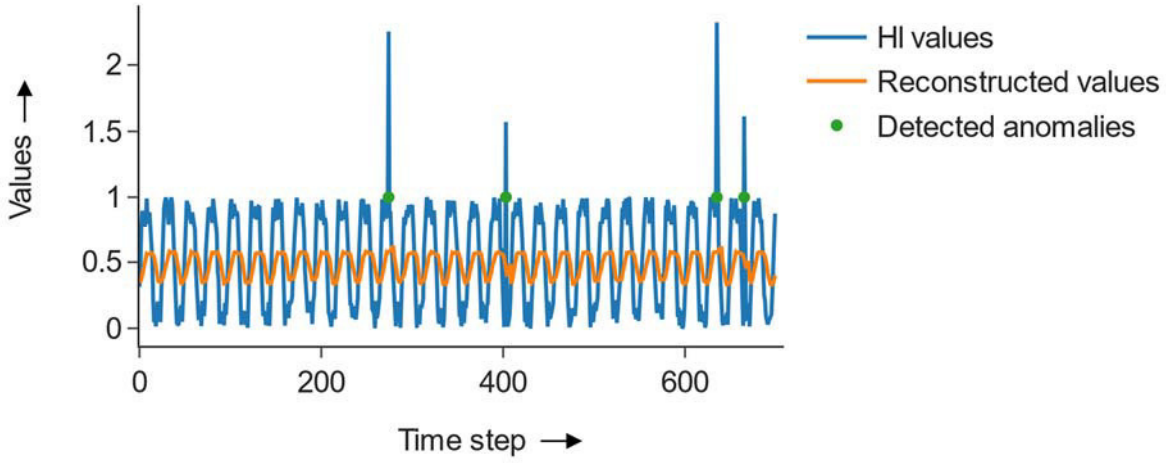

Figure 18: Example time series with reconstructed values and anomalies detected by a long short-term memory model

2.5.3 Local Outlier Factor

The local outlier factor (LOF) is another distance-based anomaly-detection model (BREUNIG ET AL. 2000). The principle of this algorithm is to compare the density of several data points in a certain area. If the density of data points around one specific data point is very low compared to the density around other data points, it is considered an outlier. The algorithm is divided into four steps. First, the $i\text{-distance(A)}$ to the *i*-nearest neighbor of a data point A is calculated, where *i* is an integer number usually smaller 20. Second, the number of data points $|N_i(A)|$ that are within this distance is calculated for each data point. Here, $N_i(A)$ is the set of data points that are within the *i*-distance. Then, the local reachability density $lrd_i(A)$ is calculated for each point according to Formula 13:

$$lrd_i(A) = \frac{1}{\sum_{B \in i(A)} \frac{\text{i-distance(A)}}{|N_i(A)|}} \tag{13}$$

Small values refer to data points that are distant from a cluster of neighbor data points. Finally, this value is compared to the values of neighbor data points by calculating the LOF value $LOF_i(A)$ according to Formula 14:

$$LOF_i(A) = \frac{\sum_{B \in N_i(A)} lrd_i(B)}{|N_i(A)| * lrd_i(A)} \tag{14}$$

A value larger than 1 indicates that the density of data points around the specific data point is lower compared to its neighbors. If this is the case, the data point can be assumed to be an outlier. The principle of the LOF algorithm is shown in Figure 19 for *i* equals 2.

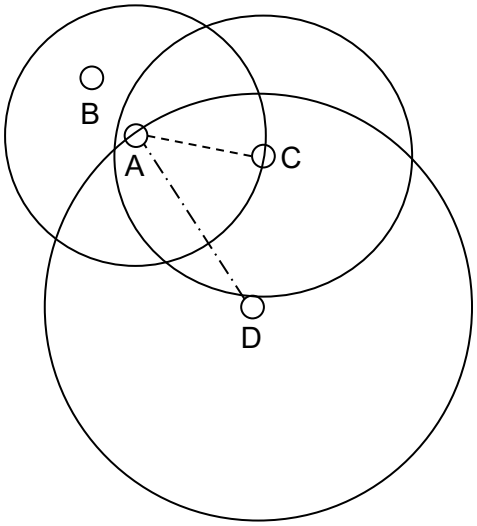

-- i-distance(A)
·– i-distance(D)
$N_i(A)$ = {B,C}
$|N_i(A)|$ = 2

	Data point A	Data point D
i-distance	1,41	2,44
$\|N_i(A)\|$	2,00	2,00
lrd_i	0,71	0,41
LOF_i	0,72	**1,57**

Figure 19: Principle of the local outlier factor algorithm

In Figure 19, the data points A, B, and C are located close to each other, resulting in high lrd_i values and LOF_i values around 1, as the density is lower in the area of these data points. The data point D is further away, which results in a lower lrd_i value and a LOF_i value larger than 1.

2.6 Summary of the Fundamentals

In Section 2.1, IRs and their gear faults were introduced. Multiple types of fault exist for different gear components. These faults can be detected in a CM-based maintenance scenario before they cause unexpected downtimes using sensor data that correlate with the occurrence of the faults. In Section 2.2, it was pointed out that acceleration sensor data and current data are commonly used for gear CM. Time series data from one sensor measurement are transformed to HIs by means of signal analysis and statistical methods. As robots usually exhibit a transient velocity behavior, an analysis of the sensor data in the time-frequency domain offers the potential to obtain information about the vibration of different gear components (compare p. 13 and 14). An HI time series can be created by calculating such HIs for several measurements. This time series can then be examined for trends and anomalies to support a maintenance decision. To automate these analyses, unsupervised machine learning models for trend detection, such as the Cox-Stuart test, and one-class classification models for anomaly detection, such as an LSTM, can be used. These fundamentals also allow the focus of the analysis of the state of the art to be set, as presented in the next chapter.

3 State of the Art

In this chapter, the applied literature review methodology is presented in Section 3.1 The state of the art is then summarized in Section 3.2, and an initial conclusion is drawn. Next, suitable approaches for CM of IR gears are presented in Section 3.3. This summary is limited to approaches focusing on time-frequency analysis or methods based on one-class classification, since time-frequency analysis has the best capabilities to cope with the transient velocity behavior of robots, and one-class classification approaches require no data from faulty robots, which are hard to acquire. Finally, the research gap addressed in this dissertation is defined in Section 3.4.

3.1 Review Method

An initial literature review was performed in 2020 following the methodology of WEBSTER & WATSON (2002) using Google Scholar, which queries various databases such as Scopus and Web of Science. After an initial screening, it was decided to use the following search terms for the structured review:

- industrial robot condition monitoring
- industrial robot health management
- predictive maintenance industrial robot

The screening showed that these search terms also cover publications in related areas such as methods for gear condition monitoring. Subsequently, a Google Scholar search alert was set up with the same search terms. This search alert captured new publications related to the search terms, and the alerts were sent to the user via email. In January 2022, all the received search alerts were analyzed to create a comprehensive literature overview. For this, the titles and abstracts of approximately 6,500 publications were screened. Forty-five publications were included in the final analysis of the state of the art. The literature review in this dissertation is limited to IR applications. For a more comprehensive review of HIs or models for fault classification for gears related to this work, please refer to NENTWICH & REINHART (2021a) or NENTWICH & REINHART (2021b).

3.2 Research Overview

This section gives an overview of the literature found by the method described in Section 3.1. The literature is classified into the following categories: the data-acquisition system considered in the publication, the faults that were investigated, the method used for HI determination, and the type of the applied model.

The final literature review consisted of 45 publications. An overview of these publications is given in Appendix 8.6. Over 75 % of these publications were published between 2019 and 2022. 80 % focus on six-axis articulated robots, and the remainder focuses on parallel and SCARA robots or experiments in gear test beds.

Figure 20 shows the sources used for data acquisition in these publications. It shows a similar distribution of data sources for IR CM compared to gear CM as presented in Figure 6. As stated in Chapter 2, two measurement principles are most prominent. Vibrations are captured using acceleration sensors or acoustic-emission sensors. Alternatively, torques or currents are measured to capture these vibrations or friction changes. Additionally, some approaches combine multiple data sources. None of the publications evaluates the suitability of different data sources for the robot gear CM task.

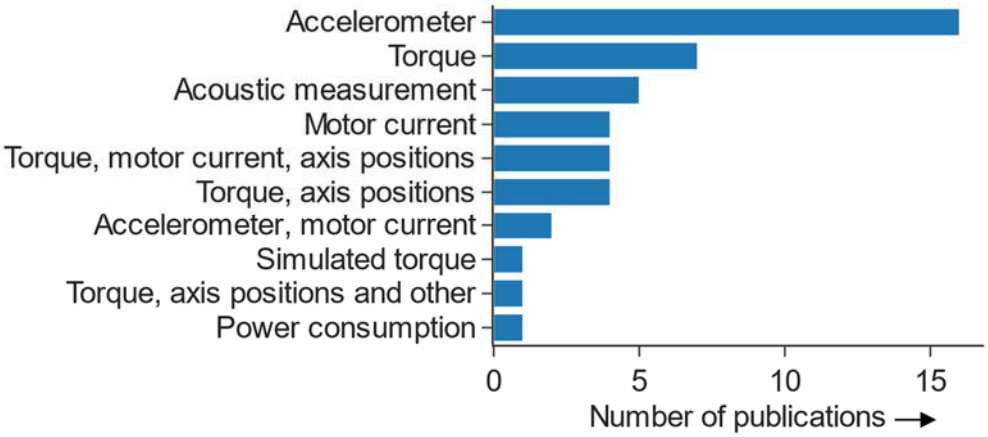

Figure 20: Data sources used for condition monitoring of robots

Figure 21 presents the components that were investigated in the publications. The review shows that many publications do not explore actual faults. For example, GOLIBAGH MAHYARI & LOCHER (2021) present an approach for anomaly detection for IRs based on torque data and validate their approach based on robot data in which an anomaly is present. However, they did not investigate whether the anomaly is related to a component fault. In addition to this category of publication, 13 publications address faults of the RV reducer, which is also the focus of this work. This finding aligns with the issue stated in Section 1.1. Even though the number of publications related to IR CM increases, the transferability of the approaches to

industry is hindered due to a lack of a relevance in practice. Publications that do not consider actual faults are unlikely to contribute to a higher transferability.

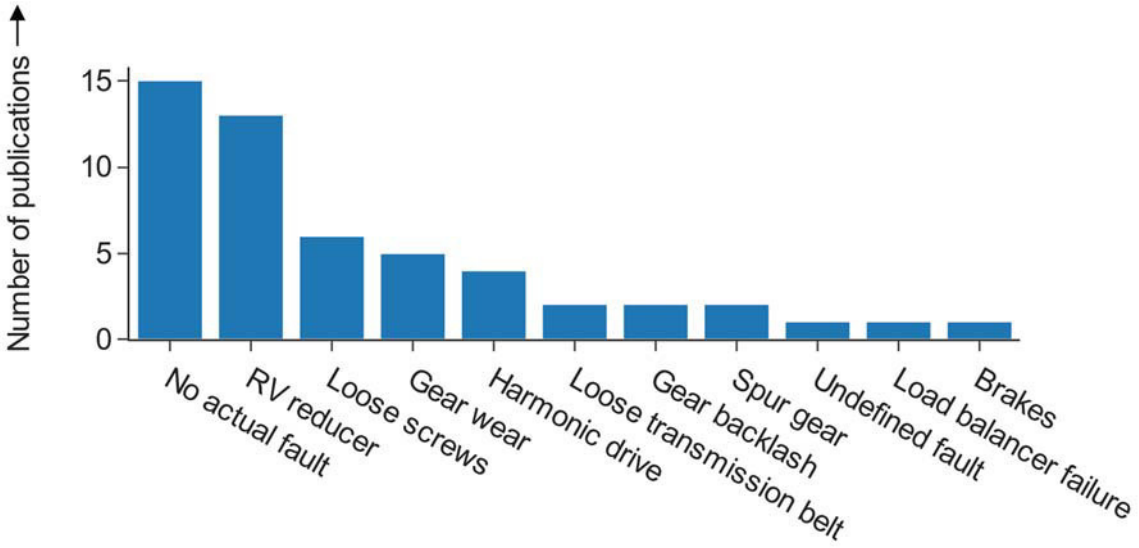

Figure 21: Faults considered in condition monitoring publications

For HI determination, most publications (20) consider HIs from the time domain. The use of raw data or HIs from the frequency domain or the time-frequency domain is less popular than the use of data from the time domain, as shown in Figure 22. Only a small number of publications focus on approaches based on time-frequency analysis. In practice, the transient velocity behavior of IRs in industry can hinder the applicability of non-time-frequency approaches because of sidebands that appear in the frequency domain and limited analysis possibilities in the time domain.

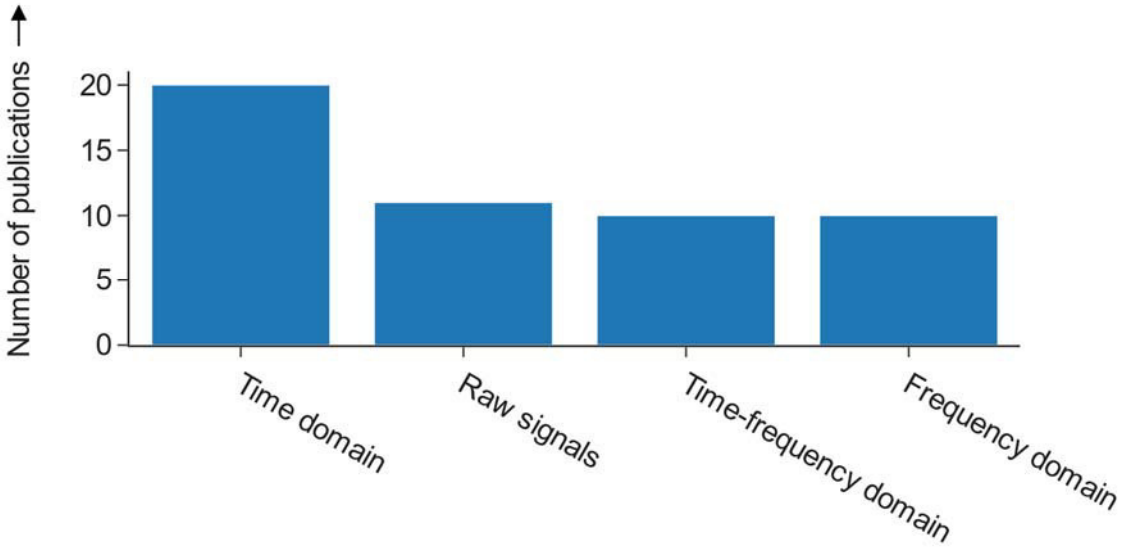

Figure 22: Health indicator types used in publications

In terms of modeling, mostly supervised models are used, as shown in Figure 23. Moreover, some publications use no models or one-class classification models. Publications presenting no models focus, for example, only on a method for HI determination. Again, many of the approaches cannot reasonably be transferred to industrial use. Methods based on supervised machine learning require data from faulty robots, which are hard to acquire in industry and which inherently limits the application in a CM scenario. The publications that do not provide a model require manual supervision of HI data, which is not feasible for large robot fleets.

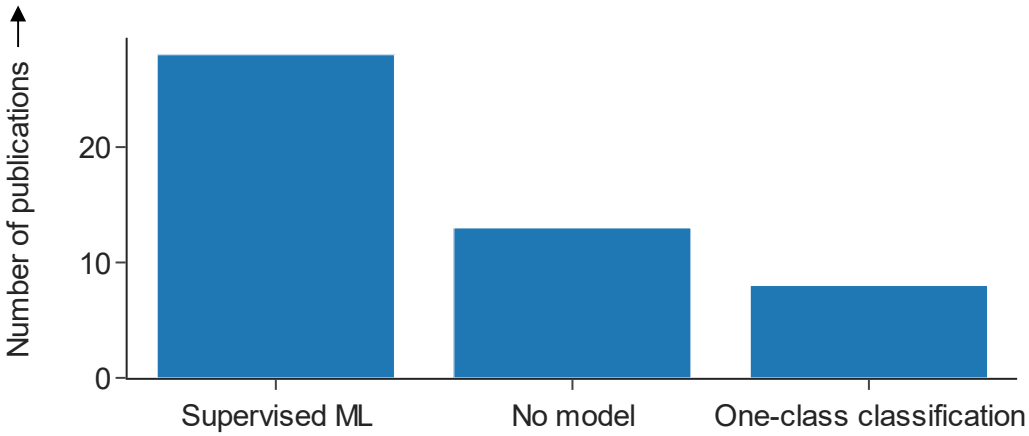

Figure 23: Machine learning model types used in publications

This overview shows that many research approaches are used to solve problems with a limited reference to real-world applications, as they do not consider actual faults, disregard the transient velocity behavior of IRs, or assume the availability of data from faulty robots that is hard to acquire. Furthermore, only a few publications that consider actual faults evaluate their approaches for different type of faults.

3.3 Selected Research Approaches

In this section, the research approaches with a higher potential transferability into practice are considered. These are publications that focus on one-class classification models and HIs in the time-frequency domain. More comprehensive literature reviews that consider the different steps of CM can be found in the state of the art or fundamentals section of the publications in Appendix 8.2 – 8.4.

3.3.1 Approaches Based on Time-Frequency Domain Health Indicators

BYNUM & LATTANZI (2021) use spectrograms based on the STFT in combination with convolutional neural networks to segment the motions of robots based on acoustic sensor data. The

method is exemplified using a SCARA robot. The motions are subsequently clustered by the *k*-means algorithm. However, the spectrograms are not used for fault detection. The motion segmentation represents only one potential data-preprocessing step for CM.

JABER (2017) and JABER & BICKER (2016) present an approach for fault detection based on acceleration sensor data. Time domain HIs such as the standard deviation of the signal are used in combination with statistical control charts. A statistical control chart provides thresholds based on the standard deviation of the considered HI. If these thresholds are exceeded, a fault is assumed. Subsequently, the faults are classified based on a wavelet transform of the signals, which provides good time and frequency resolution by design. Finally, a neural network is used to classify different artificially introduced faults. The approach was validated using a SCARA robot that had screw backlash, partly removed gear teeth, or pits on a bearing ring runway.

LIU ET AL. (2016) present a method in that the STFT spectrogram of acceleration sensors is used to detect the speed of a robot gear. This speed information is then used to calculate an order-tracking spectrum of acoustic sensor data. The fault-related frequencies in this spectrum are monitored. This concept was validated for a six-axis articulated robot that had a fault on an outer race of a bearing of the RV reducer.

Another fault-detection method based on acceleration sensor data is presented in WANG ET AL. (2021). The Hilbert-Huang transform is used to transform the sensor data to the time-frequency domain. The energy of the enveloped signal of each intrinsic mode function – the output of the Hilbert-Huang transform – is then calculated. These energies are used in a decision tree to classify faults. The approach was tested successfully for a SCARA robot with loose screws and one with an unstable base as fault modes.

YUN ET AL. (2021) describe a method for anomaly detection based on autoencoders. STFT spectrograms from acoustic sensors are used as an input for this neural network architecture. The autoencoder is trained to reproduce these spectrograms. For each reproduced spectrogram, a similarity measure to the actual spectrogram is calculated based on a reconstruction error. If this reconstruction error exceeds a defined threshold, an anomaly is assumed. The approach was tested for a six-axis articulated robot. Anomalies were introduced by attaching different weights to the end effector.

ZHANG ET AL. (2019) use the wavelet transform from acoustic sensor data as input for a hidden Markov model. This model is used to derive energy and kurtosis values for the different gear teeth of an RV reducer. These values are subsequently compared to differentiate levels of gear backlash visually. No classification or anomaly-detection model is presented. The method was tested with a RV reducer test bench.

ZHI ET AL. (2021) present an approach for fault classification of harmonic drives. They use filter techniques and the wavelet transform for data preprocessing. A neural network based on convolutional layers and long short-term memory layers is proposed to differentiate the faults. The approach was validated for various faults of the harmonic drive, such as wave generator misalignment and broken parts of a gear bearing. A test bench was used for data acquisition.

In contrast to the publications above, CHENG ET AL. (2019) present a fault-classification approach based on motor current data. The measurement data are first filtered and segmented into the different robot movements and then transformed to the time-frequency domain with the Hilbert-Huang transform and the STFT. Then, the difference between the minimum and the maximum value is calculated for the intrinsic mode functions, and the signal-to-noise ratio is calculated for the STFT spectrograms. These HIs are then used to fit a Gaussian mixture model. This model can then be used to calculate the probability that a measurement is abnormal. The approach was validated with a six-axis articulated robot with a degreased gear.

Finally, GOLIBAGH MAHYARI & LOCHER (2021) present an approach based on torque, position, and speed data. These data are transformed to STFT spectrograms, and a principal component analysis is performed to reduce these matrices to a vector. Subsequently, a transfer learning algorithm is applied to align data from different working conditions. An anomaly score is derived based on the Euclidean distance. The approach was tested on data from a six-axis articulated robot. It was shown that the changes in the anomaly score due to varying working conditions were reduced and that an anomaly was detected in two experiments. However, the anomaly was not further described.

3.3.2 Approaches Based on One-Class Classification

An approach to detect wear in a robot gear based on motor current data is presented by BITTENCOURT ET AL. (2012). The Kullbach-Leibler divergence between the kernel density estimators of the torques from functional robot gears is compared to measurements over a longer period. Increasing wear leads to an increase in the Kullbach-Leibler divergence. Thresholds for this index are used for fault detection. The approach was validated in an accelerated wear test of a six-axis articulated robot.

Gear friction values, estimated inertia, and mass of the axes serve as input for an autoencoder in the method presented by FATHI ET AL. (2021). The reconstruction error of the autoencoder in combination with a defined threshold is used for anomaly detection. Additionally, the progress of the retrieved HI is predicted by a Gaussian process model. Anomalies were introduced by artificial noise in the raw sensor signals. The approach was validated for different movements of a parallel robot.

HSU ET AL. (2021) present a method for fault detection and diagnosis based on current, encoder, and acceleration sensor data. A principal component analysis is applied on the difference between commanded current and measured current, the difference between commanded encoder positions and actual positions, and the raw vibration data to reduce the dimension of the raw data. The principal components – the outcome of the principal component analysis – are subsequently monitored with a statistical control chart. If an anomaly occurs, the reason for the anomaly can be derived by a classification model based on a support vector machine. The models were tested with data from a six-axis articulated robot with increased friction or a loose belt in the drive train.

PANGIONE ET AL. (2021) evaluated an anomaly-detection model based on the raw sensor data of robot position, velocity, currents, and torque. The raw sensor data are used to train a variational autoencoder. Anomalies were introduced artificially by changing signal values or swapping value ranges, and different time window lengths of the input data were tested for seven-axis articulated robots.

In TAHA ET AL.'s (2021) approach, the deviation of the tool center point of a six-axis articulated robot is predicted based on measured position, velocity, current, acceleration and torque data. An LSTM model is used for this task. Subsequently, the difference between the measured and predicted tool center point position is used in a regression adjustment multivariate to detect anomalies.

Furthermore, YUN ET AL. (2021), GOLIBAGH MAHYARI & LOCHER (2021), and JABER (2017) present one-class classification approaches that are described in detail in Section 3.3.1.

3.4 Discussion of the State of the Art

The state of the art presented in the previous sections offers a variety of approaches for detecting faults in IRs. Ideally, such an approach would fulfill various criteria:

- It would handle the **transient velocity behavior** of IRs by observing the sensor data in the time-frequency domain or time domain.
- The desired concept would be based on one-class classification, since **acquiring data from faulty robots is costly**.
- The approach should be evaluated in near real-world conditions. This means
    - that **different faults** should be detectable and
    - the approach copes with the **temperature fluctuations** of the robot gears.

In Section 3.2, however, it was shown that only a few approaches rely on the combination of these desired characteristics. In detail, 35 publications build up on HIs from the time domain, the time-frequency domain, or raw data. These approaches could potentially cope with the transient velocity behavior. Only eight of these methods, however, use a one-class classification approach. Such an approach is required to avoid the data acquisition from defective robots, which is time- and resource-consuming. Furthermore, only three of the eight concepts consider actual faults, which reduces the potential applicability of the approaches in industry. Two of these three publications, BITTENCOURT ET AL. (2012) and HSU ET AL. (2021), consider only anomalies such as increased friction, which might be induced by wear but also by temperature variations. Finally, JABER (2017) validates his anomaly-detection approach only for different levels of backlash. Other faults, such as those presented in Section 2.1.2, are not evaluated. This analysis is summarized in Figure 24.

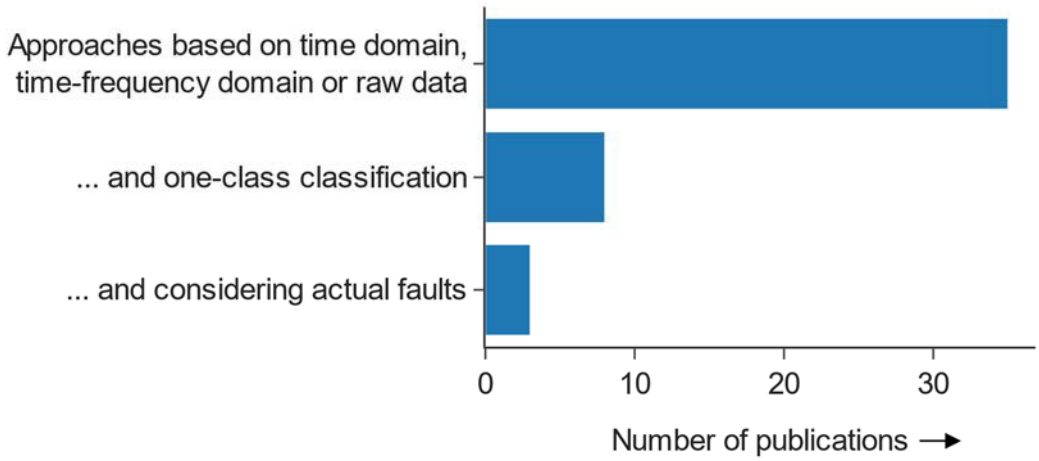

Figure 24: Publications considering relevant aspects of industrial robot gear condition monitoring

This dissertation addresses this research gap. The CM RA for IR gears should be capable of coping with the transient velocity behavior of IRs and gear temperature fluctuations, it should rely on a small amount of data from only functional robots, and it should be evaluated in near real-world conditions.

4 Reference Architecture for Condition Monitoring of Industrial Robot Gears

After the research clarification and the first literature-based descriptive study conducted in Chapters 2 and 3, this chapter focuses on the RA. First, an overview of the architecture is given, and then the publications on which the architecture builds are summarized. In the design research methodology, this chapter presents the prescriptive and second descriptive study.

4.1 Overview of the Reference Architecture

The RA's structure follows the development steps of a CM system as presented in Section 2.2.2. It consists of a data-acquisition module, an HI-determination module, and a model-selection module. These modules provide concrete suggestions for the design of the systems and methodologies to derive such a design.

More precisely, the **data-acquisition module** answers the questions of which measurement trajectory should be used for data collection, which sensor type should be chosen, and how many measurements should be collected to estimate the health state of a robot at a certain confidence level. In detail, it suggests using a robot trajectory with isolated axis movements in large axis angle areas. Acceleration sensors are suggested as the most suitable type of sensor for data acquisition, and a statistical formula is provided that allows the calculation of the number of required measurements in a given time period.

The **HI-determination module** is based on the findings of the data-acquisition module and suggests a new HI for the specific requirements of IR gear CM. These requirements include fluctuating gear temperatures, a variety of related defects, and the mostly transient velocity behavior of IRs. Moreover, the module provides methods for selecting an HI that fulfills these requirements. This HI is based on spectrograms and the principle of Z-scores.

Finally, the **model-selection module** enables the automatic CM of IR gears by identifying a trend- and anomaly-detection model suitable for the characteristics of the HI time series that was defined in the data-transformation module. The Cox-Stuart test is suggested as a trend-detection model and an LSTM or LOF are proposed for anomaly detection. The whole RA is summarized in Figure 25.

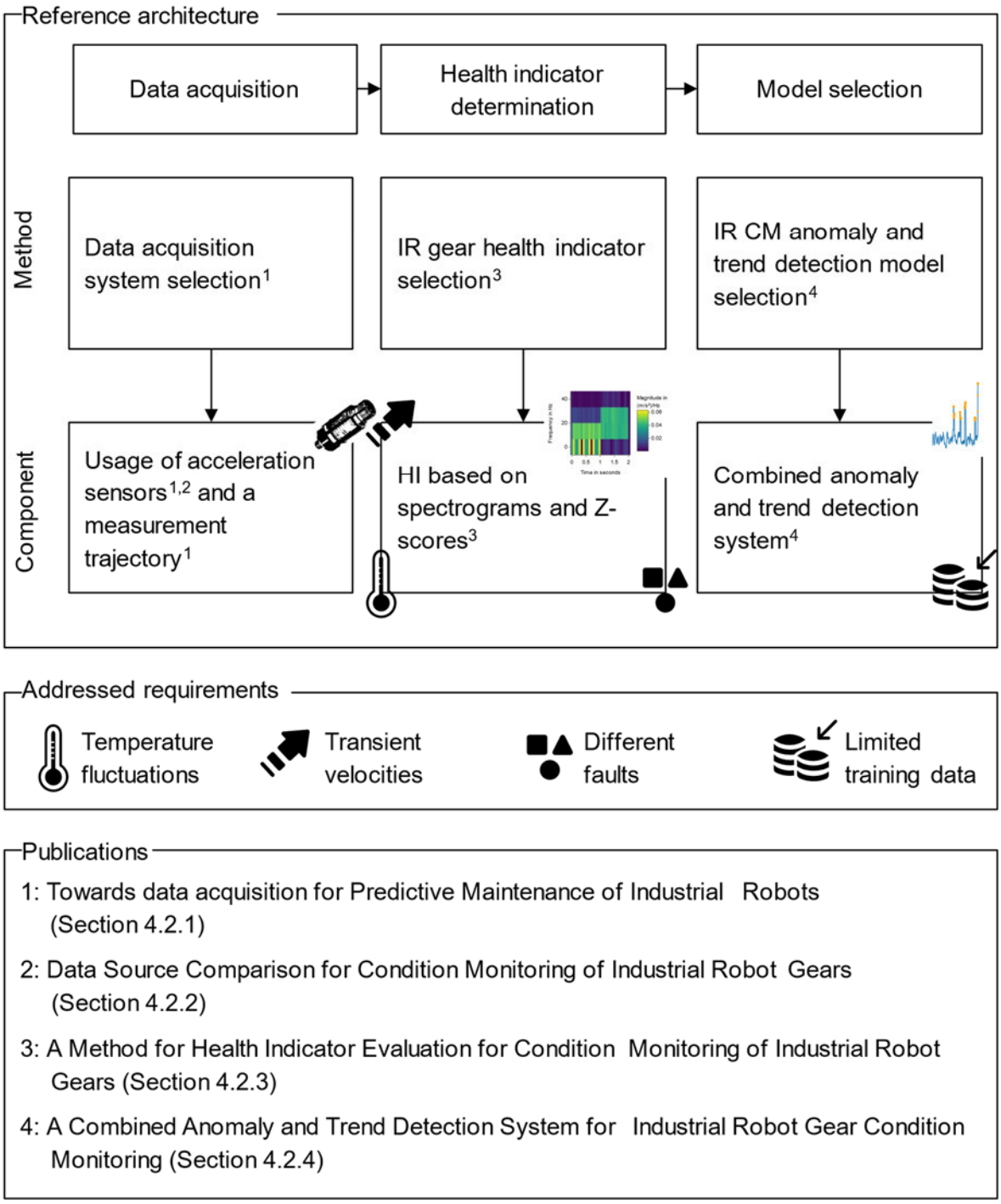

Figure 25: Overview of the reference architecture

4.2 Related Publications

The RA's modules are described in detail in different publications. The publications relating to the data-acquisition module are presented in Sections 4.2.1 and 4.2.2. The data-transformation module is discussed in Section 4.2.3. The modeling module is explained in Section 4.2.4. The whole system is analyzed in a cost-benefit analysis in the publication presented in

Section 4.2.5. The contribution of each author to the regarding publication can be found in Appendix 8.7.

4.2.1 Towards Data Acquisition for Predictive Maintenance of Industrial Robots

Authors	Conference/journal
Corbinian Nentwich, Gunther Reinhart	CIRP Conference on Manufacturing Systems 2021

In this publication, a methodology is suggested for determining how to design a suitable data-acquisition system for IR CM and predictive maintenance. This methodology consists of six steps, as shown in Figure 26.

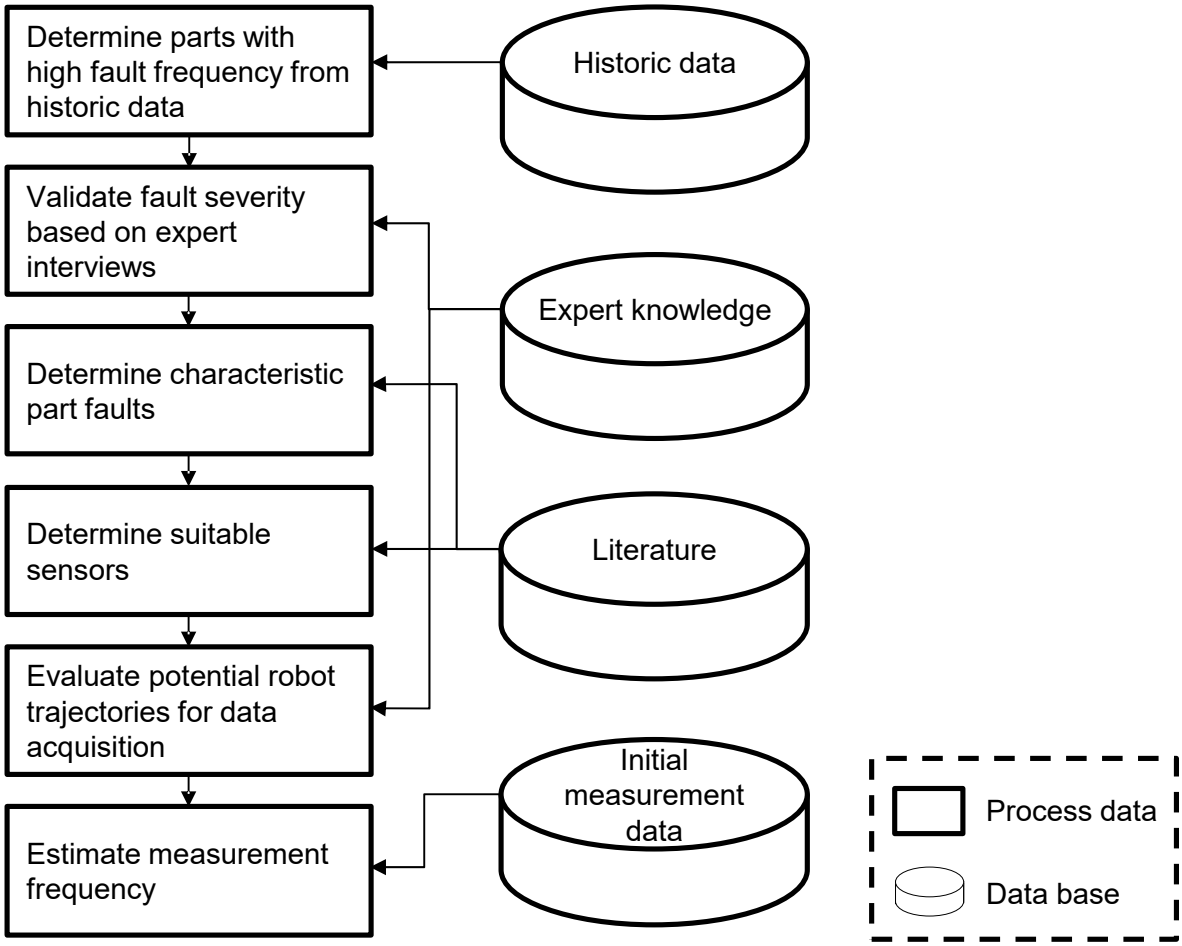

Figure 26: Method for data-acquisition system design

First, historic fault data should be analyzed to determine the fault frequency of the robot components. Such data are often available in the maintenance departments of manufacturing companies or in the spare part retail departments of robot manufacturing companies. Second, the

severity of the faults should be discussed with the maintenance department. The severity is characterized by the fault related downtimes and downtime costs. Components with defects causing long downtimes should be in the focus of a CM approach.

Third, the failure modes of these components and suitable sensor types for the CM task should be identified. For this, we suggest an approach based on a literature review. We suggest using the sensor systems that are used most frequently in the literature for the CM task. In Section 4.2.2, this approach is extended by a method based on accelerated wear tests to identify a suitable sensor system.

Fourth, different robot movements must be compared based on information about the critical components and the sensor system, expert knowledge to select a measurement trajectory. For this, the method of the pairwise comparison can be used. This comparison allows the evaluation of robot trajectories in two categories: their economic efficiency and potential data quality. For each category, a questionnaire was designed and discussed with experts from the maintenance crew of a car body plant, a robot manufacturer, and a CM company. One criterion from the economic efficiency category is the effort required to integrate the measurement into the production operation. One criterion from the potential data quality category is whether the data acquired for one axis are influenced by movements from other robot axes.

Given a suitable sensor system and robot trajectory, the number of required measurements can be determined based on a statistical formula. A measurement corresponds to the recording of data during the execution of the measurement trajectory. To apply this formula, the data-acquisition system must be set up and a set of initial measurements must be taken. Based on these measurements, a suitable HI can be calculated. Such a health indicator is for example described in Section 4.2.3. For the time series of the HI of these reference measurements, a standard deviation σ can be calculated. By defining an allowed error e of the time series of the HI, a desired confidence level α, and the corresponding z-value, the number of required measurements n can be calculated using Formula 15 (HÄRDLE ET AL. 2015, p. 306):

$$n = \left(\frac{z_{1-\frac{\alpha}{2}} * \sigma}{e} \right)^2 \tag{15}$$

We applied the whole methodology presented in Figure 26 to six-axis articulated robots and found that gears are responsible for the longest and thus most critical robot defects. We conducted a literature review of gear components and failure modes and used sensor systems to create a literature graph connecting publications with components, their failures, and the sensors used for CM. Based on this review, we suggest using acceleration sensors and motor current data for CM data acquisition, since they are used most frequently in the literature.

Next, we compared four trajectories for data acquisition that vary in the angle areas of the axes and their velocity profiles. The first trajectory is the production trajectory, which represents the movements that the robot performs during its production task. These are usually characterized by the combined movements of several axes in different angle areas and by different velocities. The second trajectory is defined by isolated movements in large angle areas. It is performed during the robot's idle times. The third trajectory combines movements of several axes in small angle areas. The fourth trajectory consists of a quick deceleration of the robot arm. During or after this procedure, the swing-out behavior of the robot is observed. The evaluation of the trajectories with the method of the pairwise comparison and the survey data lead to two findings. The production trajectory has the highest economic efficiency, and the measurement trajectory with the isolated movements has the highest potential data quality. The trajectories are shown in Figure 27.

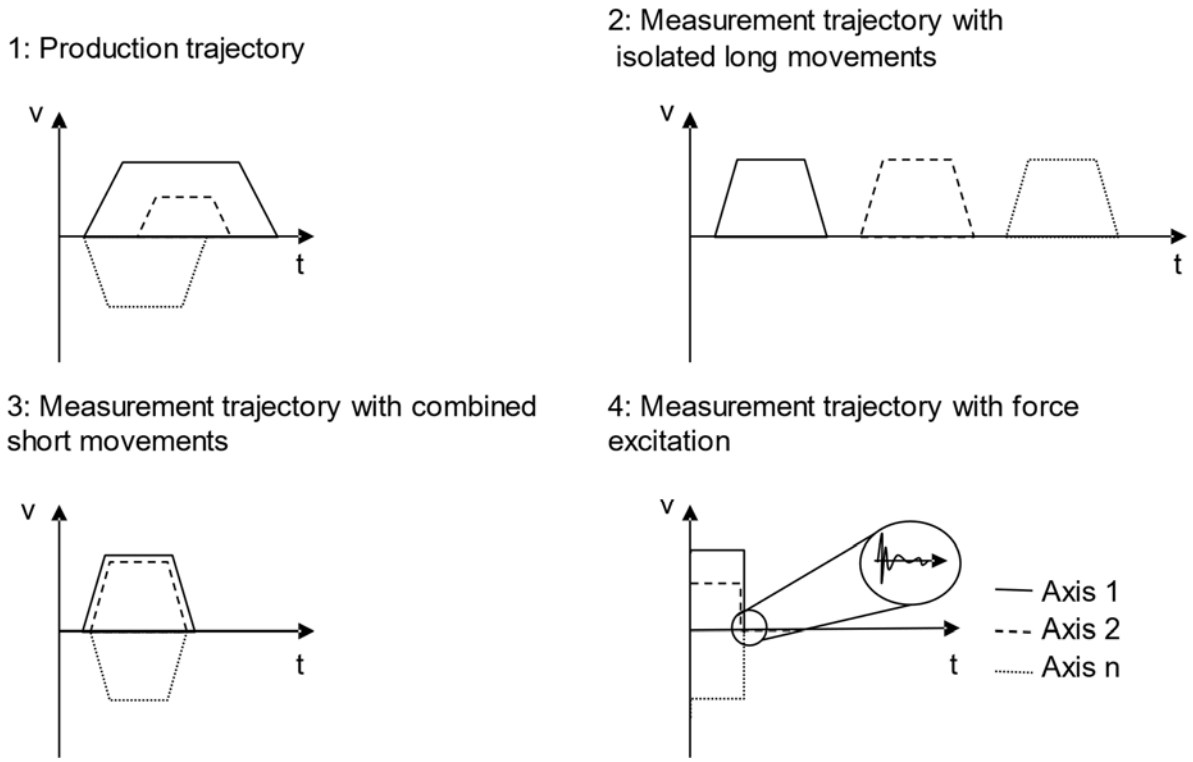

Figure 27: Different conceptional measurement trajectories

Finally, we provided a proof of concept for Formula 15. We applied it to HI data from an accelerated wear test of an IR, where 10 samples in a 24 hour time window were required to reach a 95 % confidence interval at a given error range. In a testing interval, 90 % of the data lay within the defined error range.

In summary, this publication contributes to the RA by suggesting the use of a measurement trajectory in large angle areas, by recommending that data be acquired with acceleration or

current sensors, and by proposing a formula to determine the required number of measurements in a certain time interval. The full manuscript of the publication can be found in Appendix 8.1.

4.2.2 Data Source Comparison for Condition Monitoring of Industrial Robot Gears

Authors	Conference/journal
Corbinian Nentwich, Rüdiger Daub	CIRP Conference on Manufacturing Systems 2022

The publication presented in Section 4.2.1 suggests using acceleration or current sensors for data acquisition of IR gear CM based on the findings of a literature review. In this publication, the suitability of both sensor systems is evaluated based on data from four accelerated wear tests. Furthermore, the sampling frequency required to capture all characteristic component frequencies during one measurement, as discussed in Section 2.2.2, is investigated. The experiments were performed with different robots with a payload larger than 200 kg, a robot trajectory with an isolated movement of one axis, and different sensor systems. The experiments were of different durations, as they were stopped due to the occurrence of defects. The metadata of the experiments (exp.) are summarized in Table 1.

Table 1: Accelerated wear tests of industrial robots (Vibration: Vib., Current: Cur.)

	Sampling frequency in kHz	Number of measurements	Length in months	STFT window length in samples	Reason for failure
Exp. 1	Vib.: 20 Cur.: 2	Vib.: 1726 Cur.: 485	3	256	Worn out motor pinions
Exp. 2	Vib.: 24 Cur.: 1	Vib.: 680 Cur.: 680	3	512	Drastically increased noise level
Exp. 3	Vib.: 10	Vib: 2440	12	256	Increased number of controller errors
Exp. 4	Vib.: 20	Vib: 914	3	256	Blocked gear due to broken roller bearing

Two analyses were carried out to determine a suitable sensor system and its required frequency range. We calculated a suitable HI – called *Z-score* – for the comparison of the suitability of the sensor systems. This HI will be described in detail in the next section. Then, the HI time series were evaluated in terms of existing trends and the occurrence of anomalies. For the analysis of the required sampling range, we additionally applied low-pass filters on the raw sensor data to simulate sensor systems with a lower sampling frequency. Next, the HIs were calculated based on these downsampled raw data, and the HI time series were analyzed for trends and the time points when anomalies become prominent. Furthermore, the fluctuations of the HI time series were characterized with the signal-to-noise ratio. The overall analysis flow is summarized in Figure 28.

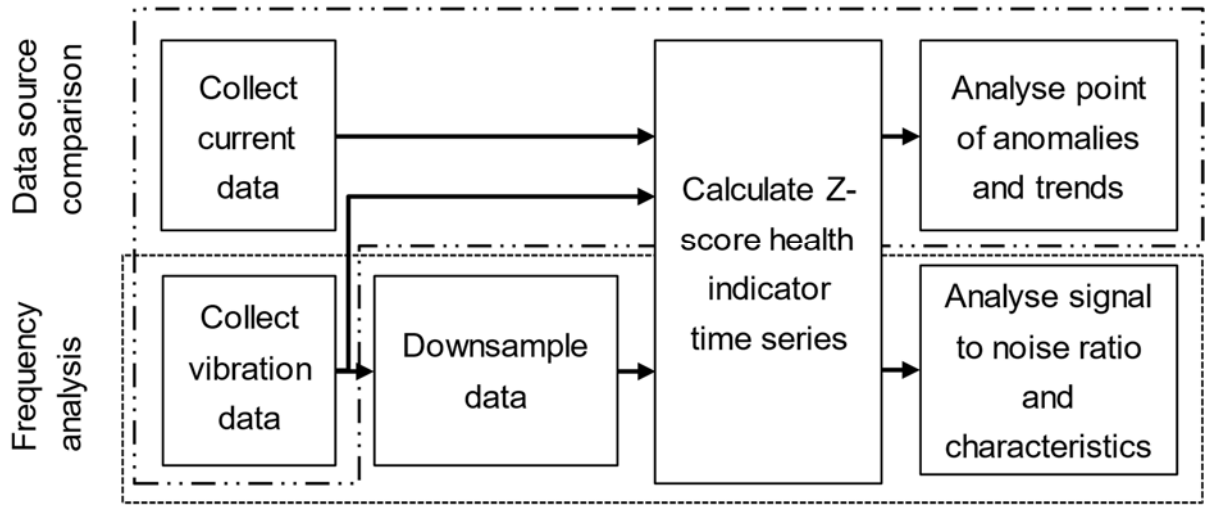

Figure 28: Analysis flow for data source and sampling frequency comparison

The analysis showed that, in both data sources, trends and anomalies are present more than one week before the end of the experiments during two accelerated wear tests. Both experiments were stopped because of defects in the robot gears. The HI time series of Experiment 2 is summarized in Figure 29. A clear increase around measurement 600 is visible. This measurement was taken two weeks before the end of the experiment due to a gear pinion fault.

The analysis of the required sampling rates showed that, even at lower sampling frequencies down to 250 Hz, anomalies and trends can be identified in the HI time series of all four accelerated wear tests. Furthermore, in three of the four experiments, higher sampling frequencies were correlated to a higher signal-to-noise ratio.

Based on these findings, both data sources (acceleration sensors and current sensors) would be potentially suitable for the CM task. However, the collection of current data through the robot controller sensor system is cumbersome due to proprietary software and limited access to sensor data. Hence, we suggest using acceleration sensor data for robust data acquisition that can even be implemented for heterogeneous robot fleets.

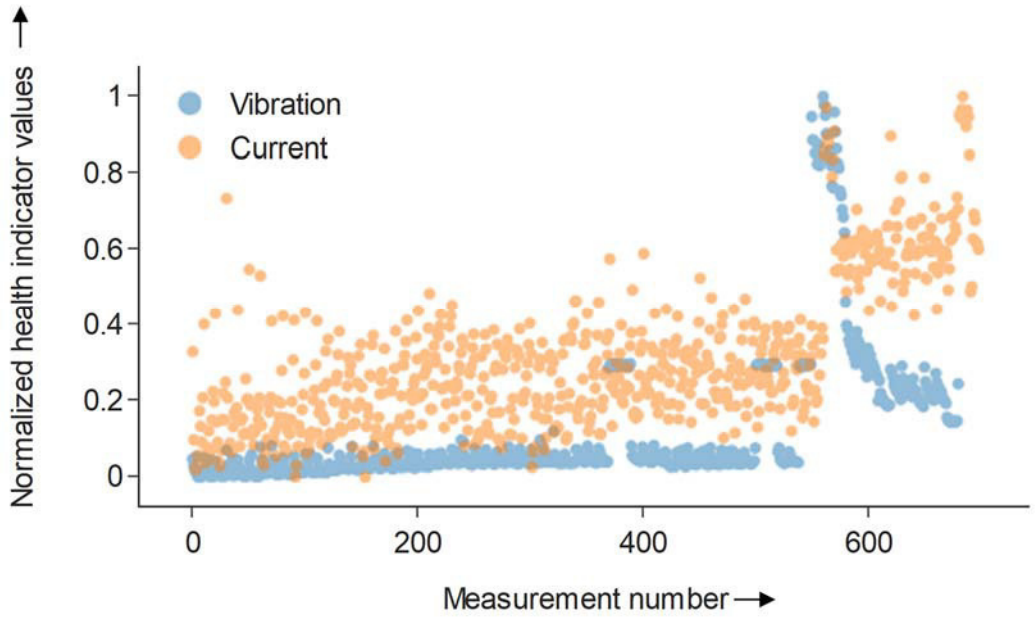

Figure 29: Comparison of data sources for an accelerated wear test

Regarding the required sampling frequency of the sensor system, we suggest using sensors with a sampling frequency that is high enough to capture all characteristic frequencies of the robot gear and as low as possible to reduce the sensor cost. We provide a formula (Formula 16) to calculate the minimum frequency $f_{sampling}$ based on the robot axis speed ω_{robot} and the transmission ratio of the axis' gear $n_{robot\ gear}$.

$$f_{sampling} = \omega_{robot} * n_{robot\ gear} * m_{max} * 2 * n_{harm} \quad (16)$$

This formula takes into account that the sampling frequency must be at least two times the required frequency due to the Nyquist criterion. It considers up to the n_{harm} harmonic (multitude) of this frequency, as faults can also change the amplitudes of vibrations at these harmonics, and it allows the analysis of frequencies at a multiple of m_{max} of the input gear speed. This number relates to the maximum turning speed of robot gear components in relation to the input gear speed, as discussed in DANIELSON & SCHMUCK (2017, p. 50).

The contribution of this publication is the suggestion to use acceleration sensors for data acquisition to handle the CM of heterogeneous robot fleets. The full manuscript of the publication can be found in Appendix 8.2.

4.2.3 A Method for Health Indicator Evaluation for Condition Monitoring of Industrial Robot Gears

Authors	Conference/journal
Corbinian Nentwich, Gunther Reinhart	MDPI *Robotics*

The HI shown in Figure 29 was developed in the course of the work of this publication. The purpose of this research was to identify an HI capable of handling the operating characteristics of IRs. As shown in Table 1, different defects occur within IR gears. Furthermore, the temperatures in the robot gears vary depending on the utilization of the robots. These variations induce fluctuations in HIs. Moreover, for the HI selection, the transient velocity behavior of IRs must be considered. Hence, an ideal HI would be able to detect different defects, exhibit low temperature sensitivity, and be able to deal with the mostly transient velocity behavior of IRs.

The designed HI is based on STFT spectrograms $spec(n,k)_{meas}$ as discussed in Section 2.2.2. This allows a differentiated analysis of a signal collected from a transient system. Defects become prominent in a spectrogram by increased amplitudes in certain characteristic frequency bands or in certain time intervals. Moreover, such changes can also be caused by temperature fluctuations of the gears. To decrease the influence of the temperature fluctuations, a Z-score matrix is calculated for the spectrogram $spec(n,k)_{meas}$ following Formula 17:

$$Z(n,k) = \left| \frac{spec(n,k)_{meas} - spec(n,k)_{avg,ref}}{spec(n,k)_{std,ref}} \right| \tag{17}$$

The mean $spec(n,k)_{avg,ref}$ and the standard deviation $spec(n,k)_{std,ref}$ are calculated based on reference measurements. These measurements must be taken for a range of gear temperatures to capture the typical variance induced by these temperature fluctuations and while the robot is still functional. This would typically be done at the beginning of the operating time of the robot.

To aggregate $Z(n,k)$ to a single HI value Z_{score}, the average of this matrix is calculated as shown in Formula 18:

$$Z_{score} = \frac{1}{0.5TK} \sum_{n=0}^{T} \sum_{k=0}^{0.5K} Z(n,k) \tag{18}$$

where T is the length of the measurement and K is the sampling frequency, which is reduced by a factor of 0.5 because of the Nyquist theorem.

To evaluate the potential of this HI, a four-step approach was followed. First, a literature review was conducted regarding HIs for gears. Second, potentially suitable HIs were evaluated in terms of their capability to detect different faults. Third, the temperature sensitivity of the most

promising HIs was analyzed. Finally, the HIs with low temperature sensitivity were applied to data from two accelerated wear tests of IR gears. The last three steps of this process will be discussed in detail below.

The time series of all HIs identified in the literature review was calculated for the FEMTO dataset (NECTOUX ET AL. 2012). This dataset consists of acceleration sensor measurements from accelerated wear tests from 16 identical bearings. The experiments were run until a defect occurred. Different defects occurred for the 16 bearings. After calculating the HI values, different functions that show a monotonous behavior were fitted on the HI time series. These were exponential or sigmoid functions and second order polynomials. The R^2 measure was calculated for each of the fits and displayed as box plots. HIs with a high mean R^2 measure and a low variance were considered for the next step of the analysis. These HIs' time series show an overall ideal behavior, as they can be modeled with basic functions to a high extent (high mean R^2) and also for different defects (low variance of R^2). Seven HIs showed this behavior. In the measurement time series, the root mean square (RMS), the peak value, the peak-to-peak value, the standard deviation, and the Z-score HI presented in this section showed good performance.

Data from an experiment with an IR were used to analyze the temperature sensitivity of these HIs. Acceleration sensor data were captured for isolated axis movements at different gear temperatures. In total, four acceleration sensors were attached to the gear caps of axes 1 to 4. As the gears of axes 5 and 6 are located closely to the gear of axis 4 in the robot's wrist, no additional sensors were used for these axes. The HIs were calculated for the measurements, and the absolute change in percentage of the HI for measurements at low and high gear temperatures was determined. The proposed Z-score HI and the root mean square HI showed the lowest sensitivity. The result of this analysis is shown in Figure 30. The reason for the low temperature sensitivity of the Z-score HI can be explained by its design. Fluctuations in the measured vibrations due to temperature changes lead to increased standard deviations of the spectrograms at certain positions in time and frequency. In the Z-score matrix, these influences are reduced by dividing the spectrogram values by these standard deviations. As the influences are reduced for all Z-score matrix entries, this influence is also decreased in the averaged value of all Z-score-matrix entries, which is the Z-score HI.

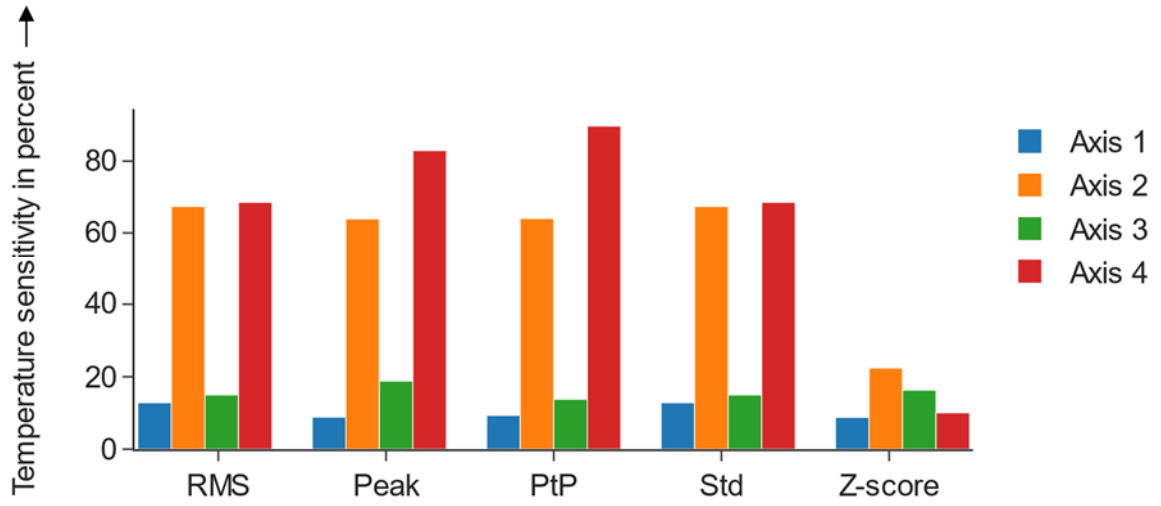

Figure 30: Temperature sensitivity of health indicators

In the last step, these HIs were analyzed using data from two accelerated wear tests. These experiments are Experiments 3 and 4 described in Table 1. At the time of publishing, experiment 1 and 2 were still ongoing and it was not predictable if these experiments would provide any failure data. Therefore, the analysis was only performed for experiment 3 and 4. The Z-score showed a smaller fluctuation and a better trend behavior than the root mean square. The HI time series for Experiment 3 is shown in Figure 31.

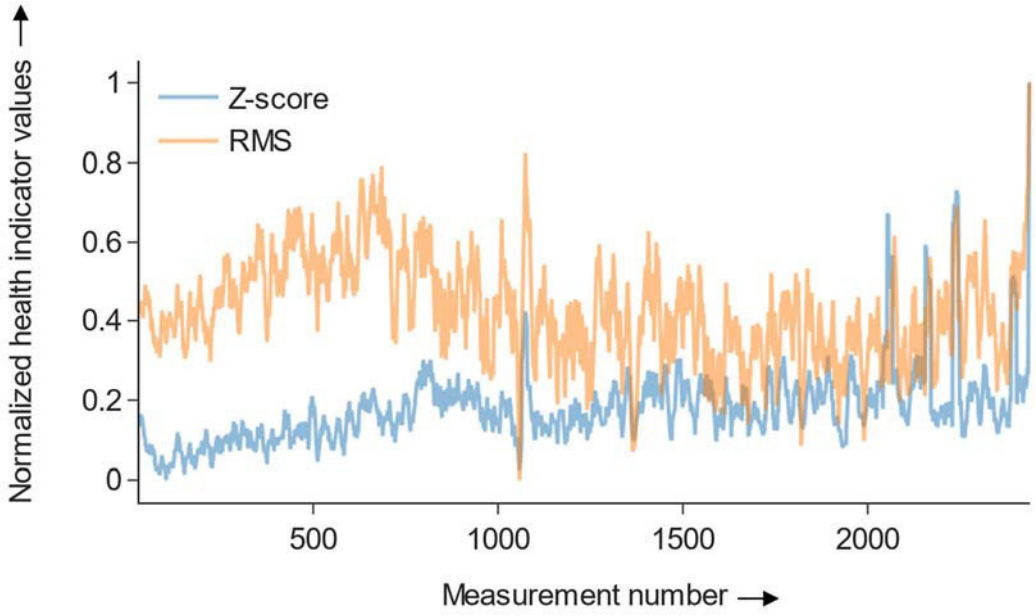

Figure 31: Comparison of health indicator time series

In context of the RA, this publication provides the HI that should be used for IR gear CM. The HI copes with the transient velocity of the robot gears and their temperature fluctuations. Additionally, it is capable of detecting different faults. The full manuscript of the publication can be found in Appendix 8.3.

4.2.4 A Combined Anomaly and Trend Detection System for Industrial Robot Gear Condition Monitoring

Authors	Conference/journal
Corbinian Nentwich, Gunther Reinhart	MDPI *Applied Science*

To implement a CM system for a robot fleet, anomalies and trends such as those presented in Figure 31 must be detected automatically, since manual monitoring cannot be performed for large robot fleets. This automatic detection can be achieved with an appropriate anomaly- and trend-detection model. The purpose of this publication was to identify such models.

Potentially suitable models were identified in a literature review. Different representative probabilistic models, domain-based models, distance-based models, and reconstruction-based models were considered for anomaly detection. Models based on statistical tests and slope-based models were evaluated for the trend-detection task.

The models were first evaluated using synthetic data. These data comprised simulated time series $x(t)$ with the same characteristics as real-world Z-score HI time series. The time series were modeled according to Formula 19:

$$x(t) = x(t)_{periodicity} + x(t)_{noise} + x(t)_{trend} + x(t)_{anomaly} \quad (19)$$

An example for this super positioned time series is given in Figure 32, which shows a sine-shaped periodicity combined with a low noise level, different kinds of anomaly, and a trend starting at measurement 500.

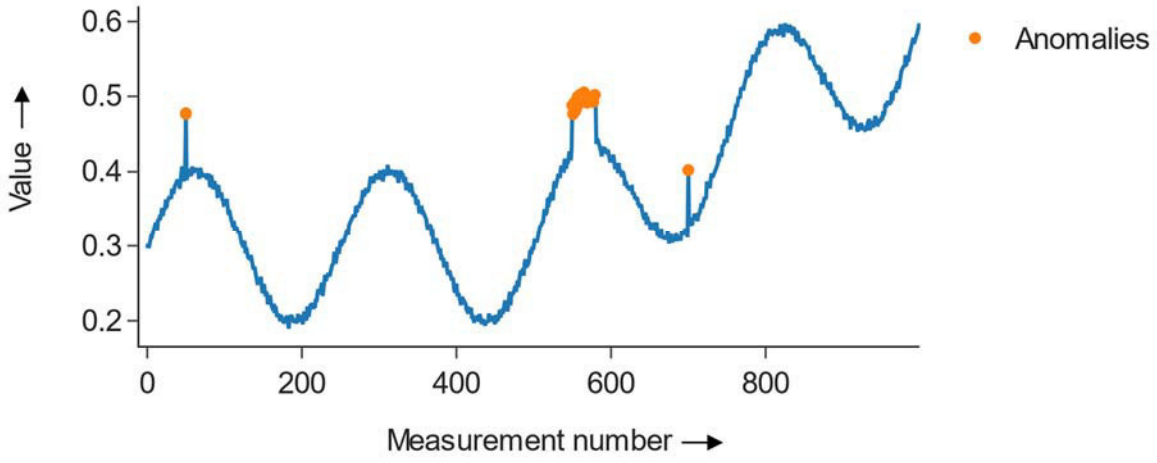

Figure 32: Example of a synthetic time series with periodicities, anomalies, and trend

In general, different methods were used to model noise $x(t)_{noise}$ and periodicities $x(t)_{periodicity}$. For noise modeling, normal-distributed and uniform-distributed noise was applied. Periodicities were introduced on the basis of a sine function and a hand-crafted function

representing temperature fluctuations in a three-shift working production plant with reduced utilization of the robots at night. Anomalies $x(t)_{anomaly}$ with different amplitudes, positions, and lengths were added to the signal. Trends $x(t)_{trend}$ were modeled by linear and quadratic polynomials with varying slope. In total, 32 time series comprising over 8,700 time steps and including at least 40 anomalies were used for model training and evaluation. The time series were split into two datasets. Dataset 1 included 16 of these time series with low noise and low amplitudes of the periodicities; dataset 2 held the other time series with higher noise and periodicities.

The models were evaluated using both datasets. A ROC curve per model per dataset was created for different parameters of the models. The AUC values of the ROC curves per model were then calculated. For anomaly detection, a reconstruction-based LSTM model, a distance-based LOF model, and a distance-based standard deviation model had the highest overall AUC values. For trend detection, two test-based models, the Cox-Stuart test and the Mann-Kendall test, showed the overall highest AUC values.

The models with high average AUC values for both datasets were subsequently applied to the Z-score HI time series of two accelerated wear tests (Experiments 3 and 4 in Table 1). Both trend-detection models were capable of detecting the trends, and the Cox-Stuart test is less sensitive than the Mann-Kendall test to outliers. It is thus suggested to use the Cox-Stuart test in a CM system. Moreover, both the LSTM model and the LOF model could detect the anomalies at low false positive rates. Figure 33 shows the HI time series and the anomalies detected by the LSTM model in Experiment 3.

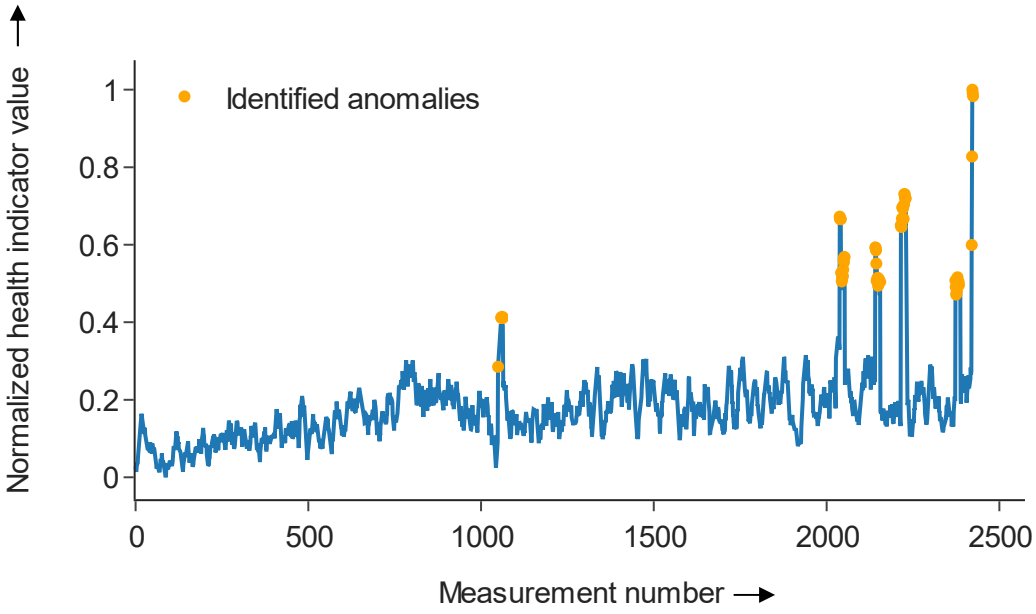

Figure 33: Detected anomalies in a health indicator time series

It is suggested to run both the trend-detection (the Cox-Stuart test) and anomaly-detection (the LSTM or the LOF) models in parallel for CM. If a trend is detected by the model over a defined time frame, a warning is presented to the maintenance crew. If an anomaly is detected over a defined time frame, an alert is presented to the maintenance crew to inspect the affected gear.

In relation to the RA, the suggested combined trend- and anomaly-detection model increases the automation level of the CM system. By using these models, the HI time series of several robot axes of a robot fleet do not have to be monitored manually, and the maintenance departments is alerted only when trends or anomalies occur. Furthermore, these models require little or no training data. The full manuscript of the publication can be found in Appendix 8.4.

4.2.5 Cost-Benefit Analysis of Industrial Robot Gear Condition Monitoring

Authors	Conference/journal
Corbinian Nentwich, Rüdiger Daub	CIRP Conference on Manufacturing Systems 2022

In this publication, the economic efficiency of CM for IR gears is evaluated based on a cost-benefit analysis. A cost model was defined and parameterized, and different scenarios were analyzed. The cost model includes depreciation costs of the robots and the CM equipment, running costs of the CM equipment, downtime costs, and development costs of the system on a yearly basis and per robot. These costs are summed up to give a total yearly cost per maintenance scenario. The total costs for CM scenarios are summarized in Formula 20:

$$C_{CM,Robot} = C_{dep} + C_{dep,CMs} + C_{running} + C_{downtime} \quad (20)$$

The costs for preventive maintenance scenarios do not include depreciation costs for CM equipment and are calculated according to Formula 21:

$$C_{prev,Robot} = C_{dep} + C_{running} + C_{downtime} \quad (21)$$

In these formulas, $C_{running}$ are the running costs of the system, $C_{dep,CMs}$ are the depreciation costs of the CM system, $C_{downtime}$ are the downtime costs, and C_{dep} are the depreciation costs of the robot.

The development costs are based on estimates for the development time of the system without the use of the RA. The model was parameterized based on historic data such as the failure rates of IR gears, market research, costs for sensors systems, and surveys that were used, for example, to determine the development times of the CM system. Model parameters that could not be estimated with confidence were incorporated as sensitivities in the model. The

parameterized model was then used to compare different maintenance scenarios. A CM scenario was compared to a purely preventive maintenance scenario for two different robot runtimes – 7 and 14 years. Preventive maintenance scenarios have no additional running costs and lower depreciation costs, since no CM equipment is used. However, more defects occur that cause downtime costs in comparison to a CM scenario. These costs increase with the runtime of the robots while the depreciation costs decrease.

The analyses show that CM is only economically efficient in the 14-year-runtime scenario. Assuming an increasing failure rate over the runtime of the robot, the break-even point for the CM scenario is reached between year 7 and year 8 of the runtime. Furthermore, the biggest potential for cost savings in the CM scenario is the development costs of the CM system. In the examined cost model, it is assumed that the whole CM system must still be designed. In Figure 34, the cost components of the different scenarios are summarized. The “Ref 7”- and “Ref 14”-scenario represent scenarios where a preventive maintenance strategy is applied for a robot runtime 7 or 14 years. A vibration-sensor-based condition monitoring strategy is used in the “Vib 7”- and “Vib 14”-senario for a robot operating time of 7 or 14 years.

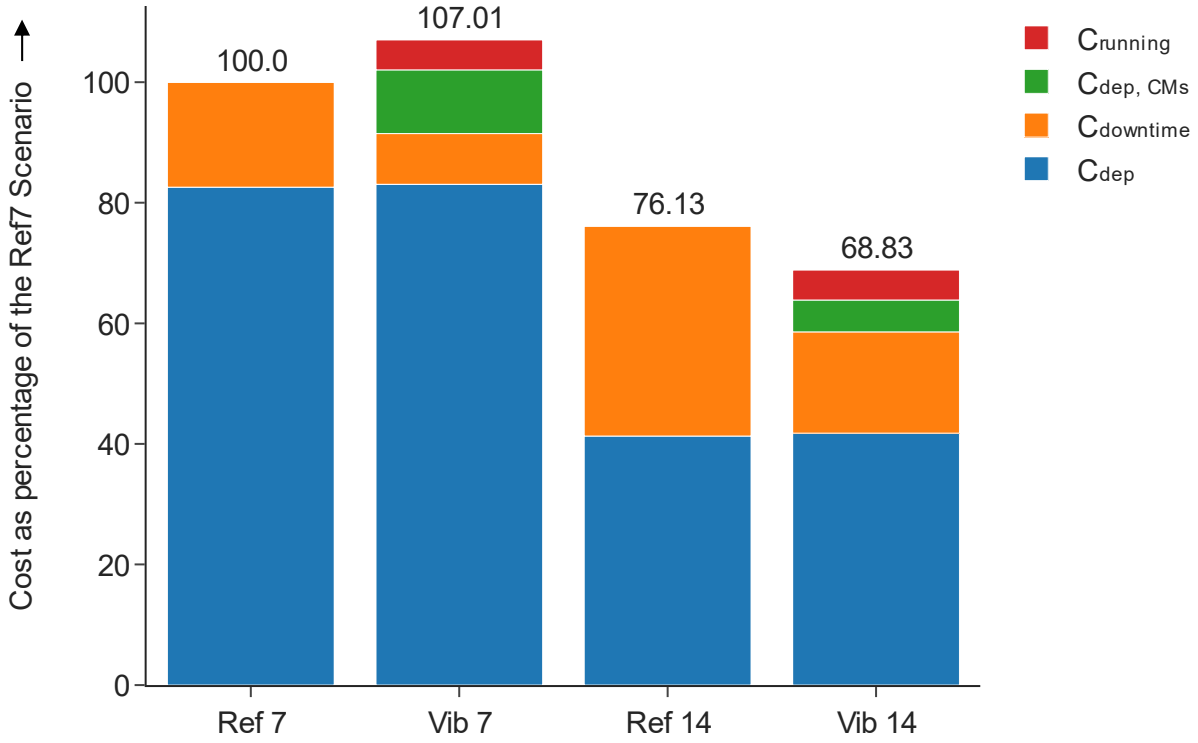

Figure 34: Cost comparison of maintenance scenarios

Investigations beyond this publication showed that if the data-transformation and modeling component of the presented RA were used and the development time for these modules thus saved, the overall development costs could be reduced by approximately 50 %, and hence the overall yearly maintenance cost could be reduced by 6 %. In this way, the efficiency of the

development process of IR gear CM systems could be improved. Furthermore, inventory costs for spare parts could be reduced in a CM scenario. This was not quantified in the publication.

The full manuscript of the publication can be found in Appendix 8.5.

5 Discussion and contribution to the state of the art

As stated in Section 3.4, no approach exists for IR gear CM based on one-class classification and an HI from the time-frequency domain that has low temperature sensitivity and that is evaluated in near real-world conditions. This research gap is addressed in Section 4 of this dissertation by presenting a RA. In this section, we discuss this contribution based on three classification schemes. In Section 5.1, the novelty of the contribution is summarized. Section 5.2 examines the contribution to different research domains. The transferability of the RA to applications beyond six-axis IRs is discussed in Section 5.3.

5.1 Novelty of the Reference Architecture

To describe the novelty of the suggested approach, the different modules of the RA – the data-acquisition module, the HI-determination module, and the model-selection module – must be considered separately.

No clear description exists for a robot gear CM **data-acquisition system** (compare Figure 25 on the left side). Such a description would answer the questions of which sensor system to choose, how many measurements to take, and which robot trajectory to perform during data collection. The data-acquisition module of the RA considers these questions. Based on experiments and expert knowledge, acceleration sensors are suggested for use in combination with long and isolated movements of the robot axes. To determine the number of required measurements, a statistical formula can be used (compare Formula 15). The whole module is presented in Section 4.2.1 and 4.2.2.

For **HI determination** (compare Figure 25 in the middle), no HI has been suggested in the literature that copes with the transient velocity behavior, the temperature fluctuations, and the varying faults of the robot gears. Hence, an HI based on STFT spectrograms and Z-scores is provided in the RA that overcomes these challenges. This HI is presented in Section 4.2.3

Finally, many models for automatic fault detection are built on data from faulty robots that are difficult to acquire. In the context of **model selection** (compare Figure 25 on the right side), the RA offers a combined trend- and anomaly-detection model that operates with little training data and allows the automatic identification of trends and anomalies that can support maintenance decisions. Such a combination of models has so far not been presented in the literature.

5.2 Contribution to Different Research Domains

Another way of thinking about this dissertation's contribution to research is to consider the different research domains this dissertation builds upon. These are the areas of robotics, CM, signal analysis, and machine learning.

In the area of robotics, the RA adds a new – and from the author's perspective, industry oriented – approach to CM of six-axis articulated robot gears. According to the literature review in Chapter 3 and to the best knowledge of the author, no approach exists in this domain that is based on a combination of anomaly and trend detection as well as the HI that was suggested in this dissertation. Similarly, the RA can be considered a new approach to the CM of gears that takes into account transient velocities and temperature fluctuations and requires little data to implement.

For signal analysis, a new approach to detect fault signatures in vibration signals is presented based on the spectrograms and the Z-score. Both spectrograms and Z-scores can be considered fundamentals in this research domain. To the best of the author's knowledge, however, the combination of the two methods to reduce temperature fluctuations in an HI has not been considered previously.

Finally, the application of the LSTM or LOF model for anomaly detection and the use of the Cox-Stuart test for trend detection in the context of IR gear CM provides a new use case for these machine learning models, which can be considered a contribution to the machine learning research domain.

5.3 Transferability of the Reference Architecture

To understand the transferability of the presented approach, the three RA modules must be discussed individually. The **data-acquisition module** (Figure 25 on the left side) suggests using a robot trajectory with isolated axis movements, acceleration sensors for data collection, and a statistical formula to determine the number of required measurements in a given period. A trajectory of isolated axis movements could also be used for other robot types and components to reduce the influence from components that are not to be monitored. To the best of the author's knowledge, acceleration sensors can also be used for other gear types, as they follow the same fault principles and hence also cause vibrations. To detect faults in the electric drives of robots, the use of currents or torques might be more suitable. The statistical formula could be applied in other CM scenarios, not only for other components in robots, but also for other rotatory equipment. Its only boundary condition is a normally distributed HI time series.

The **HI-determination module** (Figure 25 in the middle) provides an HI based on spectrograms and Z-scores. This HI can also be used to detect defects of other gears, as they exhibit the same fault principles. These faults will change the amplitudes in the spectrogram in different frequency or time ranges, which will lead to an increase in the presented HI. Moreover, in NENTWICH & DAUB (2022), a motor fault could be detected based on current data and the HI. The only boundary condition of this HI is that the gear in question must perform the same movements for every measurement. Additionally, isolated movements of axes must be used as described in the data-acquisition module.

Finally, the **model-selection module** (Figure 25 on the right side) suggests models for trend and anomaly detection in HI time series. These could also be used for the CM of other components if the HI time series of these components possess similar noise and periodicities as the data that the anomaly- and trend-detection models were evaluated on.

More generally, the RA can easily be deployed to industry. The source code of the anomaly- and trend-detection model and the code to calculate the spectrogram based Z-score have been published and can easily be integrated into CM systems (NENTWICH 2021). This can reduce the development time of CM systems by up to 50 %, as discussed in Section 4.2.5.

6 Conclusion

The dissertation is first summarized in Section 6.1, and an outlook is given in Section 6.2.

6.1 Summary

The motivation for the condition monitoring of industrial robot gears was set out in Chapter 1 by describing its potential to increase the usage time and availability of industrial robots and thus save costs. As the development of such a system is costly, the objective of this work was to increase the efficiency of the development process of a condition monitoring system by delivering a reference architecture (RA) that can be used for the development of CM-systems. The structure of the dissertation, based on the design research methodology, was then presented.

In Chapter 2, the fundamentals of this work were described. These focus on the structure and faults of industrial robots and maintenance with a focus on condition monitoring. The process for the design of a CM system was introduced. First, a suitable data acquisition system must be selected that captures data correlating with the robot's health state. Second, these data must be transformed in meaningful health indicators. Finally, models must be selected that support the maintenance planning. Furthermore, the topic of machine learning, especially anomaly- and trend-detection models, was explained.

Next, the state of the art of industrial robot condition monitoring was presented and analyzed in Chapter 3. After describing the used literature review methodology, an overview of the state of the art was given and selected approaches based on time-frequency domain health indicators or one-class classification were presented. A research gap was then defined. To the best of the author's knowledge, no approach exists for condition monitoring of industrial robot gears that can cope with varying faults, the transient velocity behavior, and the temperature fluctuations of robot gears and that relies on small amounts of data for parameterization. Developing a suitable condition monitoring system would take a long time and reduce the profitability of such a system.

In Chapter 4, a reference architecture for industrial robot gear condition monitoring was presented that fulfills these requirements. This reference architecture can be used by practitioners to accelerate the development time of such a condition monitoring system. Five publications were presented. Two of the publications describe a **data-acquisition system** (compare Figure 25 on the left side) based on measurements collected with acceleration sensors during isolated and long axis movements. In the field of **health indicator determination** (compare Figure 25

in the middle), one publication describes a health indicator that can be determined based on these measurements. The health indicator can detect multiple faults, copes with the transient velocity behavior by means of spectrograms, and has a low temperature sensitivity. In the area of **model selection** (compare Figure 25 on the right side), another publication suggests a combined anomaly- and trend-detection system based on a long short-term memory neural network or the local outlier factor and the Cox-Stuart test to automate the monitoring of the health indicator time series. These models can be implemented only using data from functional robots. Hence, these models can be set up quickly in operating manufacturing systems.

The last publication considers the economic efficiency of a condition-monitoring system for industrial robot gears. It is pointed out that the benefits of a condition-monitoring system increase with longer robot runtimes and that the most effective way to reduce CM costs is to reduce the development costs of the condition-monitoring system, which is realized by the reference architecture.

Finally, the contribution of the reference architecture to the state of the art is discussed in Chapter 5. The contribution is considered from different point of views. The novelty of the approach, the contribution to different research domains, and the transferability of the RA are analyzed.

6.2 Outlook

The reference architecture partly paves the way to a more sustainable use of industrial robots. CM systems based on the reference architecture could be used to increase the usage time of industrial robots, since faults can be detected before critical downtimes occur. Nevertheless, there are several steps that could be taken to improve the reference architecture and work towards the vision of a more sustainable use of industrial robots on different time scales.

From a short-term perspective, the reference architecture could be used for a CM system that is implemented for a large robot fleet. In this way, larger amounts of data could be gathered to test the robustness of the proposed architecture in an industry setting. The gathered data could also be used to implement models to predict defects of industrial robots. Furthermore, the reference architecture could be extended to other components of industrial robots, such as electric drives.

From a long-term perspective, new business models could be investigated for industrial robots. If a robust CM system for large robot fleets and their components existed, a pay-per-use model could be provided by robot manufacturers instead of a pay-per-product model. In this way, the overall number of manufactured robots could be decreased, which could reduce the cost structure of the robot manufacturers and also increase the sustainability of industrial robots.

7 Bibliography

AGGARWAL 2017
Aggarwal, C. C.: Outlier Analysis. 2nd ed. 2017. Cham: Springer 2017. ISBN: 9783319475783. (Springer eBook Collection Computer Science).

AIVALIOTIS ET AL. 2021
Aivaliotis, P.; Arkouli, Z.; Georgoulias, K.; Makris, S.: Degradation curves integration in physics-based models: Towards the predictive maintenance of industrial robots. Robotics and Computer-Integrated Manufacturing 71 (2021), p. 102177.

ALBERS 2009
Albers, S.: Methodik der empirischen Forschung. 3., überarbeitete und erweiterte Auflage. Wiesbaden: Gabler Verlag 2009. ISBN: 9783322964069. (Springer eBook Collection Business and Economics).

ALLEN 1977
Allen, J.: Short term spectral analysis, synthesis, and modification by discrete Fourier transform. IEEE Transactions on Acoustics, Speech, and Signal Processing 25 (1977) 3, p. 235 – 238.

ALLEN & MILLS 2003
Allen, R. L.; Mills, D. W.: Signal Analysis. Hoboken, NJ, USA: John Wiley & Sons, Inc 2003. ISBN: 0471234419.

ALTMAN 1968
Altman, E. I.: FINANCIAL RATIOS, DISCRIMINANT ANALYSIS AND THE PREDICTION OF CORPORATE BANKRUPTCY. The Journal of Finance 23 (1968) 4, p. 589 – 609.

BISHOP 2009
Bishop, C. M.: Pattern recognition and machine learning. Corrected at 8th printing 2009. New York, NY: Springer 2009. ISBN: 978-0-387-31073-2. (Information science and statistics).

BITTENCOURT ET AL. 2012
Bittencourt, A. C.; Saarinen, K.; Sander-Tavallaey, S.: A Data-driven Method for Monitoring Systems that Operate Repetitively -Applications to Wear Monitoring in an Industrial Robot Joint1. IFAC Proceedings Volumes 45 (2012) 20, p. 198 – 203.

BLESSING & CHAKRABARTI 2009
Blessing, L. T.; Chakrabarti, A.: DRM, a Design Research Methodology. London: Springer London 2009. ISBN: 978-1-84882-586-4.

BOUDRAA & SALZENSTEIN 2016
Boudraa, A.-O.; Salzenstein, F.: Advanced Time-Frequency Signal and System Analysis. (pub.): Time-Frequency Signal Analysis and Processing: Elsevier 2016, p. 141 – 236. ISBN: 9780123984999.

BRANDT 2011
Brandt, A.: Noise and Vibration Analysis. Chichester, UK: John Wiley & Sons, Ltd 2011. ISBN: 9780470978160.

BREUNIG ET AL. 2000
Breunig, M. M.; Kriegel, H.-P.; Ng, R. T.; Sander, J.: LOF: identifying density-based local outliers. ACM SIGMOD Record 29 (2000) 2, p. 93 – 104.

BROCKWELL & DAVIS 2016
Brockwell, P. J.; Davis, R. A.: Introduction. In: Brockwell, P. J. et al. (pub.): Introduction to Time Series and Forecasting. Cham: Springer International Publishing 2016, p. 1 – 37. ISBN: 978-3-319-29852-8. (Springer Texts in Statistics).

BUNDESMINISTERIUM FÜR UMWELT, NATURSCHUTZ UND NUKLEARE SICHERHEI 2019: Klimaschutzprogramm 2030. Maßnahmen zur Erreichung der Klimaschutzziele 2030. https://www.bmuv.de/fileadmin/Daten_BMU/Pools/Broschueren/klimaschutzprogramm_2030_bf.pdf. last accessed — 01.13.2022.

BYNUM & LATTANZI 2021
Bynum, J.; Lattanzi, D.: Combining convolutional neural networks with unsupervised learning for acoustic monitoring of robotic manufacturing facilities. Advances in Mechanical Engineering 13 (2021) 4.

CADEZ & CZERNY 2016
Cadez, S.; Czerny, A.: Climate change mitigation strategies in carbon-intensive firms. Journal of Cleaner Production 112 (2016), p. 4132 – 4143.

CARVALHO BITTENCOURT 2014
Carvalho Bittencourt, A.: Modeling and Diagnosis of Friction and Wear in Industrial Robots. Linköping: Linköping University Electronic Press 2014. ISBN: 9789175192512. (1617).

CHANDOLA ET AL. 2009
Chandola, V.; Banerjee, A.; Kumar, V.: Anomaly detection. ACM Computing Surveys 41 (2009) 3, p. 1 – 58.

CHENG ET AL. 2019
Cheng, F.; Raghavan, A.; Jung, D.; Sasaki, Y.; Tajika, Y.: High-Accuracy Unsupervised Fault Detection of Industrial Robots Using Current Signal Analysis. IEEE International Conference on Prognostics and Health Management (ICPHM) (2019).

COOLEY & TUKEY 1965
Cooley, J. W.; Tukey, J. W.: An algorithm for the machine calculation of complex Fourier series. Mathematics of Computation 19 (1965) 90, p. 297 – 301.

COX & STUART 1955
Cox, D. R.; Stuart, A.: Some Quick Sign Tests for Trend in Location and Dispersion. Biometrika 42 (1955) 1/2, p. 80.

DALENOGARE ET AL. 2018
Dalenogare, L. S.; Benitez, G. B.; Ayala, N. F.; Frank, A. G.: The expected contribution of Industry 4.0 technologies for industrial performance. International Journal of Production Economics 204 (2018), p. 383 – 394.

Danielson, H.; Schmuck, B. von: Robot Condition Monitoring : A first step in Condition Monitoring for robotic applications (2017).

DEUTSCHES INSTITUT FÜR NORMUNG E. V 2012: DIN EN ISO 10218-1:2012-01, Industrieroboter - Sicherheitsanforderungen - Teil 1: Roboter (ISO 10218-1:2011); Deutsche Fassung EN ISO 10218-1:2011. Deutsches Institut für Normung e. V. Berlin: Beuth Verlag GmbH 2012.

DIN DEUTSCHES INSTITUT FÜR NORMUNG E. V 2018
DIN Deutsches Institut für Normung e. V: DIN ISO 17359:2018-05, Zustandsüberwachung und -diagnostik von Maschinen - Allgemeine Anleitungen (ISO 17359:2018). DIN Deutsches Institut für Normung e. V. Berlin: Beuth Verlag GmbH 2018.

EMMERICH 1967
Emmerich, D. S.: Signal Detection Theory and Psychophysics . David M. Green , John A. Swets. The Quarterly Review of Biology 42 (1967) 4, p. 578.

FATHI ET AL. 2021
Fathi, K.; van de Venn, H. W.; Honegger, M.: Predictive Maintenance: An Autoencoder Anomaly-Based Approach for a 3 DoF Delta Robot. Sensors (Basel, Switzerland) 21 (2021) 21.

FAWCETT 2006
Fawcett, T.: An introduction to ROC analysis. Pattern Recognition Letters 27 (2006) 8, p. 861 – 874.

GIRDHAR & SCHEFFER 2004
Girdhar, P.; Scheffer, C.: Machinery fault diagnosis using vibration analysis. (pub.): Practical Machinery Vibration Analysis and Predictive Maintenance: Elsevier 2004, p. 89 – 133. ISBN: 9780750662758.

GOLIBAGH MAHYARI & LOCHER 2021
Golibagh Mahyari, A.; Locher, T.: Robust Predictive Maintenance for Robotics via Unsupervised Transfer Learning. The International FLAIRS Conference Proceedings 34 (2021) 1.

HÄRDLE ET AL. 2015
Härdle, W. K.; Klinke, S.; Röonz, B.: Estimation. In: Härdle, W. K. et al. (pub.): Introduction to Statistics. Cham: Springer International Publishing 2015, p. 251 – 309. ISBN: 978-3-319-17703-8.

HASTIE ET AL. 2009
Hastie, T.; Tibshirani, R.; Friedman, J.: Introduction. In: Hastie, T. et al. (pub.): The elements of statistical learning. Data mining, inference, and prediction. Second edition Aufl. New York: Springer 2009, p. 1 – 8. ISBN: 978-0-387-84857-0. (Springer Series in Statistics).

HAWKINS 1980
Hawkins, D. M.: Identification of Outliers. Dordrecht: Springer Netherlands 1980. ISBN: 978-94-015-3996-8.

HOCHREITER & SCHMIDHUBER 1997
Hochreiter, S.; Schmidhuber, J.: Long short-term memory. Neural computation 9 (1997) 8, p. 1735 – 1780.

HSU ET AL. 2021
HSU, H.-K.; TING, H.-Y.; HUANG, M.-B.; HUANG, H.-P.: Intelligent Fault Detection, Diagnosis and Health Evaluation for Industrial Robots. Mechanics 27 (2021) 1, p. 70 – 79.

INTERNATIONAL STANDARDIZATION ORGANISATION 2012
International Standardization Organisation: ISO 13372:2012-09. Condition monitoring and diagnostics of machines - Vocabulary (2012).

INTERNATIONAL STANDARDIZATION ORGANIZATION 1995: ISO 10825:1995. Gears — Wear and damage to gear teeth — Terminology. International Standardization Organization. 1995.

INTERNATIONAL STANDARDIZATION ORGANIZATION 2017: ISO 15243:2017. Rolling bearings — Damage and failures — Terms, characteristics and causes. International Standardization Organization. Geneva, Switzerland: ISO copyright office 2017.

ISO/IEC 2021
ISO/IEC: Informationstechnik - Internet der Dinge (IoT) - Vokabular. ISO/IEC: Beuth Verlag GmbH 2021.

JABER 2017
Jaber, A. A.: Design of an Intelligent Embedded System for Condition Monitoring of an Industrial Robot. Cham, s.l.: Springer International Publishing 2017. ISBN: 9783319449319. (Springer Theses, Recognizing Outstanding Ph.D. Research).

JABER & BICKER 2016
Jaber, A. A.; Bicker, R.: Industrial Robot Backlash Fault Diagnosis Based on Discrete Wavelet Transform and Artificial Neural Network. American Journal of Mechanical Engineering Vol. 4, No. 1 (2016), p. 21 – 31.

JAGADISH & RAVIKUMAR 2013
Jagadish, H. P.; Ravikumar, L.: Effect of Temperature and Electric Field on the Damping and Stiffness Characteristics of ER Fluid Short Squeeze Film Dampers. Advances in Tribology 2013 (2013), p. 1 – 10.

JUSTIN ROWLATT 2021
Justin Rowlatt: Bill Gates: Solving Covid easy compared with climate. https://www.bbc.com/news/science-environment-56042029. last accessed — 01.13.2022.

KAR & MOHANTY 2006
Kar, C.; Mohanty, A. R.: Monitoring gear vibrations through motor current signature analysis and wavelet transform. Mechanical Systems and Signal Processing 20 (2006) 1, p. 158 – 187.

KOLERUS & WASSERMANN 2017
Kolerus, J.; Wassermann, J.: Zustandsüberwachung von Maschinen. Das Lehr- und Arbeitsbuch für den Praktiker. 7., aktualisierte Auflage. Stuttgart, Konstanz: UTB GmbH; UVK 2017. ISBN: 9783825251819. (utb-studi-e-book 5181).

KUKA 2021
KUKA: KR 600 FORTEC. Montageanleitung. 2021.

LEE ET AL. 2009
Lee, J.; Liao, L.; Lapira, E.; Ni, J.; Li, L.: Informatics Platform for Designing and Deploying e-Manufacturing Systems. In: Wang, L. et al. (pub.): Collaborative Design and Planning for Digital Manufacturing. London: Springer London 2009, p. 1 – 35. ISBN: 978-1-84882-286-3.

LEE ET AL. 2014
Lee, J.; Wu, F.; Zhao, W.; Ghaffari, M.; Liao, L.; Siegel, D.: Prognostics and health management design for rotary machinery systems — Reviews, methodology and applications. Mechanical Systems and Signal Processing 42 (2014) 1-2, p. 314 – 334.

LEI ET AL. 2018
Lei, Y.; Li, N.; Guo, L.; Li, N.; Yan, T.; Lin, J.: Machinery health prognostics: A systematic review from data acquisition to RUL prediction. Mechanical Systems and Signal Processing 104 (2018), p. 799 – 834.

LIU ET AL. 2016
Liu, X.; Wu, X.; Liu, C.; Liu, T.: RESEARCH ON CONDITION MONITORING OF SPEED REDUCER OF INDUSTRIAL ROBOT WITH ACOUSTIC EMISSION. Transactions of the Canadian Society for Mechanical Engineering 40 (2016) 5, p. 1041 – 1049.

MANN 1945
Mann, H. B.: Nonparametric Tests Against Trend. Econometrica 13 (1945) 3, p. 245.

MELEK ET AL. 2005
Melek, W. W.; Lu, Z.; Kapps, A.; Fraser, W. D.: Comparison of trend detection algorithms in the analysis of physiological time-series data. IEEE transactions on bio-medical engineering 52 (2005) 4, p. 639 – 651.

MOBLEY 2002a
Mobley, R. K.: Tribology. (pub.): An Introduction to Predictive Maintenance: Elsevier 2002, p. 202 – 216. ISBN: 9780750675314.

MOBLEY 2002b
Mobley, R. K.: Ultrasonics. (pub.): An Introduction to Predictive Maintenance: Elsevier 2002, p. 256 – 258. ISBN: 9780750675314.

MOYA & HUSH 1996
Moya, M. M.; Hush, D. R.: Network constraints and multi-objective optimization for one-class classification. Neural Networks 9 (1996) 3, p. 463 – 474.

MULDERS & HAARMAN 2018
Mulders, M.; Haarman, M.: Predictive Maintenance 4.0. Beyond the hype. https://www.pwc.de/de/industrielle-produktion/pwc-predictive-maintenance-4-0.pdf. last accessed — 10.14.2021.

NABTESCO 2022
Nabtesco: Vigo Drives RV Series. Technical Data. http://www.motionusa.com.s3-website-us-east-1.amazonaws.com/nabtesco/RV_Series_Full_Catalog.pdf. last accessed — 02.16.2022.

NECTOUX ET AL. 2012
Nectoux, P.; Gouriveau, R.; Medjaher, K.; Ramasso, E.; Chebel-Morello, B.; Zerhouni, N.; Varnier, C.: PRONOSTIA: An experimental platform for bearings accelerated degradation tests. IEEE International Conference on Prognostics and Health Management PHM'12 (2012), p. 1 – 8.

NENTWICH 2021
Nentwich, C.: CATS—A Combined Anomaly Detection and Trend Detection Model. https://github.com/xorbey/CATS_public. last accessed — 03.18.2022.

NENTWICH & DAUB 2022
Nentwich, C.; Daub, R.: Comparison of Data Sources for Robot Gear Condition Monitoring. Procedia CIRP (2022).

NENTWICH & REINHART 2021a
Nentwich, C.; Reinhart, G.: A Combined Anomaly and Trend Detection System for Industrial Robot Gear Condition Monitoring. Applied Sciences 11 (2021) 21, p. 10403.

NENTWICH & REINHART 2021b
Nentwich, C.; Reinhart, G.: A Method for Health Indicator Evaluation for Condition Monitoring of Industrial Robot Gears. Robotics 10 (2021) 2, p. 80.

NENTWICH & REINHART 2021c
Nentwich, C.; Reinhart, G.: Towards Data Acquisition for Predictive Maintenance of Industrial Robots. Procedia CIRP 104 (2021), p. 62 – 67.

NIEMINEN ET AL. 1989
Nieminen, A.; Neuvo, Y.; Värri, A.; Mitra, U.: Algorithms for real-time trend detection. Signal Processing 18 (1989) 1, p. 1 – 15.

PANGIONE ET AL. 2021
Pangione, L.; Burroughes, G.; Skilton, R.: Variational AutoEncoder to Identify Anomalous Data in Robots. Robotics 10 (2021) 3, p. 93.

PHAM ET AL. 2006
Pham, D. T.; Wang, Lihui; Gao, Robert X. (Hrsg.): Condition Monitoring and Control for Intelligent Manufacturing. London: Springer London 2006. ISBN: 978-1-84628-268-3. (Springer Series in Advanced Manufacturing).

PHAM & AHN 2018
Pham, A.-D.; Ahn, H.-J.: High Precision Reducers for Industrial Robots Driving 4th Industrial Revolution: State of Arts, Analysis, Design, Performance Evaluation and Perspective. International Journal of Precision Engineering and Manufacturing-Green Technology 5 (2018) 4, p. 519 – 533.

PIMENTEL ET AL. 2014
Pimentel, M. A.; Clifton, D. A.; Clifton, L.; Tarassenko, L.: A review of novelty detection. Signal Processing 99 (2014) 4, p. 215 – 249.

RUMELHART ET AL. 1986
Rumelhart, D. E.; Hinton, G. E.; Williams, R. J.: Learning representations by back-propagating errors. Nature 323 (1986) 6088, p. 533 – 536.

RYLL & FREUND 2010
Ryll, F.; Freund, C.: Grundlagen der Instandhaltung. In: Schenk, M. (pub.): Instandhaltung technischer Systeme. Berlin, Heidelberg: Springer Berlin Heidelberg 2010, p. 23 – 101. ISBN: 978-3-642-03948-5.

SCHENK 2010
Schenk, M.: Instandhaltung technischer Systeme. Berlin, Heidelberg: Springer Berlin Heidelberg 2010. ISBN: 978-3-642-03948-5.

SCHNECK 2015
Schneck, Ottmar (Hrsg.): Lexikon der Betriebswirtschaft. 3.000 grundlegende und aktuelle Begriffe für Studium und Beruf. 9., vollständig überarbeitete Auflage, Original-Ausgabe. C.H.Beck: Deutscher Taschenbuch Verlag; C.H.Beck 2015. ISBN: 9783406673474. (Beck-Wirtschaftsberater 24).

SHANNON 1949
Shannon, C. E.: Communication in the Presence of Noise. Proceedings of the IRE 37 (1949) 1, p. 10 – 21.

SHARMA ET AL. 2016
Sharma, S.; Swayne, D. A.; Obimbo, C.: Trend analysis and change point techniques: a survey. Energy, Ecology and Environment 1 (2016) 3, p. 123 – 130.

SHU ET AL. 2020
Shu, N.; Gu, H.; Liu, H.: Analysis of temperature effect on damping characteristics of landing gear shock absorber. (pub.): Proceedings of the 2020 International Conference on Aviation Safety and Information Technology, ICASIT 2020: 2020 International Conference on Aviation Safety and Information Technology. New York,NY,United States: Association for Computing Machinery 2020, p. 76 – 81. ISBN: 9781450375764.

SICILIANO & KHATIB 2008
Siciliano, B.; Khatib, O.: Springer Handbook of Robotics. Berlin, Heidelberg: Springer Berlin Heidelberg 2008. ISBN: 978-3-540-23957-4.

SKANSI 2018
Skansi, S.: Introduction to Deep Learning. From Logical Calculus to Artificial Intelligence. Cham: Springer 2018. ISBN: 9783319730042. (Springer eBook Collection Computer Science).

SKF 2017
SKF: Bearing damage and failure analysis. https://www.skf.com/binaries/pub12/Images/0901d1968064c148-Bearing-failures---14219_2-EN_tcm_12-297619.pdf. last accessed — 02.17.2022.

SWETS 1979
Swets, J. A.: ROC analysis applied to the evaluation of medical imaging techniques. Investigative radiology 14 (1979) 2, p. 109 – 121.

TAHA ET AL. 2021
Taha, H. A.; Yacout, S.; Birglen, L.: Detection and Monitoring for Anomalies and Degradation of a Robotic Arm Using Machine Learning. In: Weißgraeber, P. et al. (pub.): Advances in Automotive Production Technology – Theory and Application. Berlin, Heidelberg: Springer Berlin Heidelberg 2021, p. 230 – 237. ISBN: 978-3-662-62961-1. (ARENA2036).

TAN & JIANG 2013
Tan, L.; Jiang, J.: Discrete Fourier Transform and Signal Spectrum. (pub.): Digital Signal Processing: Elsevier 2013, p. 87 – 136. ISBN: 9780124158931.

TANDON & PAREY 2006
Tandon, N.; Parey, A.: Condition Monitoring of Rotary Machines. In: Pham, D. T. et al. (pub.): Condition Monitoring and Control for Intelligent Manufacturing. London: Springer London 2006, p. 109 – 136. ISBN: 978-1-84628-268-3. (Springer Series in Advanced Manufacturing).

THÜMMEL ET AL. 2015
Thümmel, T.; Roßner, M.; Ulbrich, H.; Rixen, D.: Unterscheidung verschiedener Fehlerarten beim modellbasierten Monitoring. (pub.): SIRM 2015 – 11. Internationale Tagung Schwingungen in rotierenden Maschinen. Magedburg 2015.

TINGA & LOENDERSLOOT 2019
Tinga, T.; Loendersloot, R.: Physical Model-Based Prognostics and Health Monitoring to Enable Predictive Maintenance. In: Lughofer, E. et al. (pub.): Predictive maintenance in dynamic systems. Advanced methods, decision support tools and real-world applications. Cham: Springer 2019, p. 313 – 353. ISBN: 978-3-030-05644-5.

VEČEŘ ET AL. 2005
Večeř, P.; Kreidl, M.; Šmíd, R.: Condition Indicators for Gearbox Condition Monitoring Systems. Acta Polytechnica 45 (2005) 6.

WANG ET AL. 2019
Wang, H.; Bah, M. J.; Hammad, M.: Progress in Outlier Detection Techniques: A Survey. IEEE Access 7 (2019), p. 107964 – 108000.

WANG ET AL. 2021
Wang, X.; Sun, L.; Yu, K.; Wang, B.; Li, X.: Research on SCARA Robot Fault Diagnosis Based on Hilbert-Huang Transform and Decision Tree. (pub.): 2021 IEEE 9th International Conference on Computer Science and Network Technology (ICCSNT). Dalian, China, 2021: IEEE 2021, p. 115 – 118. ISBN: 978-1-6654-4364-7.

WEBSTER & WATSON 2002
Webster, J.; Watson, R. T.: Analyzing the Past to Prepare for the Future: Writing a Literature Review. MIS Quarterly 26 (2002) 2, p. xiii – xxiii.

WILCOXON 1945
Wilcoxon, F.: Individual Comparisons by Ranking Methods. Biometrics Bulletin 1 (1945) 6, p. 80.

WRIGHT 1921
Wright, s.: Correlation and causation. Journal of agricultural research 20 (1921) 3.

YANG ET AL. 2021
Yang, G.; Zhong, Y.; Yang, L.; Tao, H.; Li, J.; Du, R.: Fault Diagnosis of Harmonic Drive With Imbalanced Data Using Generative Adversarial Network. IEEE Transactions on Instrumentation and Measurement 70 (2021), p. 1 – 11.

YERUSHALMY 1947
Yerushalmy, J.: Statistical Problems in Assessing Methods of Medical Diagnosis, with Special Reference to X-Ray Techniques. Public Health Reports (1896-1970) 62 (1947) 40, p. 1432.

YUN ET AL. 2021
Yun, H.; Kim, H.; Jeong, Y. H.; Jun, M. B.: Autoencoder-based anomaly detection of industrial robot arm using stethoscope based internal sound sensor. Journal of Intelligent Manufacturing (2021).

ZHANG ET AL. 2019
Zhang, Y.; An, H.; Ding, X.; Liang, W.; Yuan, M.; Ji, C.; Tan, J.: Industrial Robot Rotate Vector Reducer Fault Detection Based on Hidden Markov Models. (pub.): 2019 IEEE International Conference on Robotics and Biomimetics (ROBIO). Dali, China, 2019: IEEE 2019, p. 3013 – 3018. ISBN: 978-1-7281-6321-5.

ZHI ET AL. 2021
Zhi, Z.; Liu, L.; Liu, D.; Hu, C.: Fault detection of the harmonic reducer based on CNN-LSTM with a novel denoising algorithm. IEEE Sensors Journal (2021), p. 1.

Appendix

8.1 Towards data acquisition for Predictive Maintenance of Industrial Robots

Available online at www.sciencedirect.com

ScienceDirect

Procedia CIRP 104 (2021) 62–67

www.elsevier.com/locate/procedia

54th CIRP Conference on Manufacturing Systems

Towards Data Acquisition for Predictive Maintenance of Industrial Robots

Corbinian Nentwich[a,*], Gunther Reinhart[a]

[a]*Technical University Munich, Boltzmannstraße 15, 85748 Garching, Germany*
*Corresponding author. Tel.: +49 89 289 15542; *E-mail address:* corbinian.nentwich@iwb.tum.de

Abstract

Predictive Maintenance of industrial robots offers the potential to increase productivity and cut costs in highly automated production systems. The success of such maintenance strategies is highly dependent on the data acquisition strategy used to monitor the robot's health state. In this publication, we first describe a methodology for deriving a suitable data acquisition strategy. Second, we apply this methodology to shape a data acquisition strategy for articulated robots. This strategy defines the robot components for which data is acquired, the robot trajectories used for the data acquisition and the frequency that measurements are taken. To conclude, we discuss the methodology's limitations.

Keywords: Industrial robot; Predictive Maintenance; Data Acquisition

1. Introduction

Industrial robots are an important component of highly automated production systems due to their versatility, precision and speed [1]. However, the breakdown of a robot leads to increased costs and reduced productivity. To prevent such downtimes, predictive maintenance (PdM) can be used to forecast robot failures and plan maintenance actions within production breaks [2]. This maintenance strategy thereby relies on Prognostics and Health Management Models (PHM-models), which capture the robot's present wear state and extrapolate it into the future [3]. These regression and classification models are either physics-based or mainly data-based [4]. For the latter, data has to be collected for the different wear conditions of the robot and a correlation between this data and the wear state must exist. For this, the data is often transformed into a so-called health indicator (HI), which represents the health state of the monitored machine by means of statistics or signal analysis. A wide range of sensor systems is available for the task of data acquisition such as acceleration sensors, temperature sensors, current sensors and oil analysis sensors [4]. To setup a reliable PHM-model, sensors must be used that can detect the defects occurring in the industrial robot, and robot trajectories have to be used for the measurements that make the defects prominent in the data. However, up to now, it has not been clear what severe faults occur in industrial robots and hence which sensor systems and robot trajectories to use could not be clearly argued. This motivates the contribution of our publication: We present a methodology to define a data acquisition strategy in PHM-approaches for articulated robots. By applying this methodology, we further

- describe the relationships between fault-prone robot parts, their defects and suitable sensor systems as an ontology based on historic and literature data,
- evaluate sensor systems, which are suitable for the described defects based on literature data,
- evaluate different conceptional robot trajectories to capture the current robot's wear state based on technical and economic characteristics, and
- propose a method to calculate the number of measurements that must be taken to estimate the wear state with a certain confidence interval.

Hence, the remainder of the publication is structured in the following sections: In the state of the art section, we summarise existing PHM-frameworks and PHM-approaches for industrial robots. We thereby highlight the remaining research potential that motivates our paper. Afterwards, we

10.1016/j.procir.2021.11.011

propose the new methodology. Subsequently, we apply the methodology to articulated six-axis robots. Then, we evaluate our methodology in the discussion section. Finally, we sum up our results and give an outlook in the conclusion section.

2. State of the art

As the number of specific PHM-approaches has increased drastically in recent years, many authors have suggested PHM-frameworks to give practitioners guidelines to implement their own PHM-models. [5] describes a framework based on ISO 13374, which consists of six steps. These are data acquisition, data manipulation, state detection, health assessment, prognostics assessment and advisory generation. The focus of the framework lies in the description of the health and prognostics assessment with a neural network. Similarly, many frameworks emphasise the step of raw sensor data transformation or model creation, which is used to classify current or predict future asset health states: [6] suggests a framework focusing on a long short term memory neural network. [7] describes a generalised framework focusing on statistical feature extraction and data-driven modelling. [8] proposes a framework focusing on feature extraction using autoencoders and modelling based on feedforward neural networks. [9] presents a more holistic approach considering different machine parts, the process of information collection regarding these parts and a PHM-framework consisting of six steps. Here, data acquisition and pre-processing are followed by feature extraction, fault diagnosis and prognosis, and finally a cost and benefit analysis. However, none of these approaches illuminates the question, which sensors should be used for the data acquisition step.

[10] proposes a PHM-methodology that considers this question employing hazard analysis where the selection of sensors is based on expert knowledge, which is used to identify the machine's fault-sensitive components. Then, they select physical machine parameters that change because of a component's fault propagation. Finally, they choose suitable sensors for these parameters. [11] suggests a sophisticated method for sensor selection, which is also based on expert knowledge. Here, failure modes and effects analysis is used to identify system fault modes and sensible fault signatures. Subsequently, a risk assessment for these faults is conducted and sensor candidates are compiled along with their response characteristics and variance due to environmental noise. By using this sensor information, as well as a physical model of the system and a diagnostic model to determine the health state, a figure of merit can be calculated for each sensor candidate. Using a genetic algorithm, different sensors are combined, and their figures of merit determined to derive an optimal sensor combination. Another concept to address the issue of sensor selection is sensor fusion. Here, multiple sensors are used in parallel and their data is combined within the health assessment model [12]. [13] focuses on the integration of the sensor system design into the mechanical system design for embedded PHM-systems. Nevertheless, these four publications do not offer a tool to decide how many measurements are needed to determine the current system health state with confidence.

The frequency of required measurements is described qualitatively in [14] dependent on the observed signal changes. If the measured signal remains in the same magnitude range, the measurement periods stay constant; if changes in the magnitudes are present, the frequency of measurements should be increased to verify trends or determine outliers. Another approach to determine the measurement periods is presented by [15] based on the probabilistic modelling of wear progress. This model is then used in a cost comparison calculation. Here, they try to find the break-even between costs that appear as a result of faults that were not detected because not enough measurements had been taken, and costs caused by taking too many measurements. The number of measurements that are required for this break-even is recommended for use in the PHM-system.

Besides the determination of suitable sensor systems and the number of measurements for a confident health estimation in a period of time, the robot trajectory used for the data acquisition has to be considered, since the chosen trajectory influences the measured sensor data. An ideal trajectory would provide data that has little noise and a high information content regarding the robot's health state. After considering the recent publications in the field of PHM-models for industrial robots, three literature clusters can be determined. In the first cluster, repetitive trajectories are used for data acquisition, which are not described further [16–19]. In the second cluster, trajectories are used to determine backlash or friction in the robot joints, which set conditions for the dynamics of the trajectory [20, 21]. In the third cluster, the trajectory is not explained at all [22, 23].

In summary, the state of the art relies mostly on expert knowledge to define the sensor system for PHM-models. The period between measurements is described qualitatively or by modelling the wear progress statistically, which can be error-prone, especially in the context of complex systems such as industrial robots. Finally, the robot trajectories used for PHM data acquisition have not been evaluated up to now. This motivates the suggested new integrated methodology for data acquisition, which will be presented in detail in the next section.

3. Methodology

In contrast to the state of the art, we propose a methodology that allows data source selection based on historic and literature data, trajectory selection based on expert knowledge, and measurement period selection based on simple statistics. The methodology is divided into six steps that are illustrated in Figure 1.

First, we determine fault sensitive robot parts based on historic fault data from a production plant. In particular, we use a log of the maintenance department stating every fault that occurred in the factory, the associated timestamp and the taken maintenance action. By clustering this data by robot parts, the fault frequency of each component can be derived.

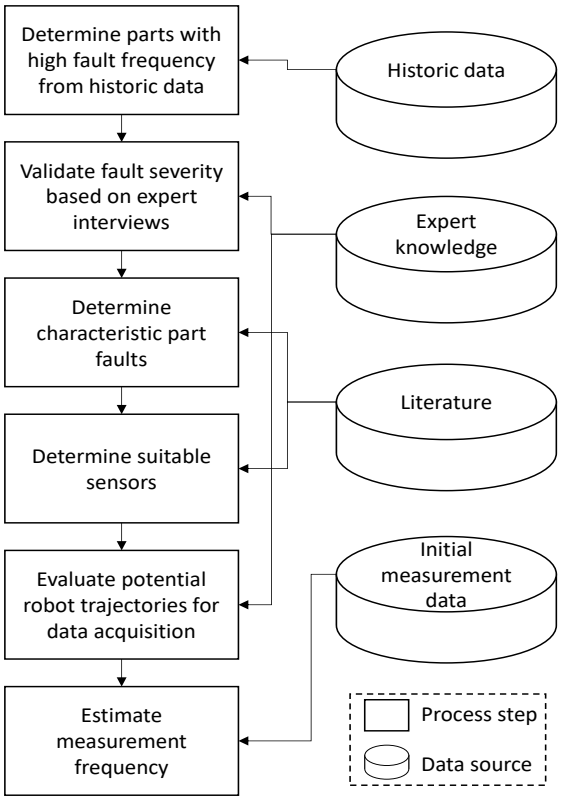

Figure 1. Methodology for the design of a data acquisition system.

Second, we validate this data with expert interviews to verify the economic severity of the faults. The objective in this step is to evaluate the maintenance time needed to replace the error-prone parts. Part faults with high replacement times lead to longer downtimes with higher related maintenance costs. Hence, these parts should be focused on in a predictive maintenance strategy.

Third, we derive typical faults for these parts based on literature data, as well as suitable sensors to trace these faults. For this, we follow the procedure for a literature review proposed by [24]. We summarise the data about parts, faults and sensors in a graph-based ontology. This graph consists of entities of different node classes representing robot components, faults, data sources and publications. They are connected by entities of different edge classes, which are described in Table 1.

Table 1. Node and edge classes

Node Class	Component	Publication	Data source	Fault
Component	is subcomponent		can be monitored with	
Publication	holds information regarding		holds information regarding	holds information regarding
Fault	appears in			

In the fourth step, edges connecting each data source with publications are counted. In this way, the usage frequency for each data source can be determined. We suggest using the sensor systems most frequently used in literature for the considered faults in the data acquisition system.

In the fifth step, we evaluate four different conceptional robot trajectories based on multiple criteria and a pairwise comparison taking into account the selected sensor systems. As this evaluation is based on expert knowledge, the results can vary depending on the persons performing the comparison and the production system under consideration. Thus, it is recommended to complete this evaluation for every production system individually and with several experts to obtain reliable results. The characteristics of these trajectories are explained in Figure 2. The first trajectory is defined by the movements the robot usually performs in production. During the second trajectory, the robot performs an isolated movement with one axis in a large angle range. This movement is executed for all axes. During the third trajectory, the robot makes a combined movement with all axes in a small angle range (less than 10°). For the fourth trajectory, the robot is decelerated abruptly by using the mechanical brakes of each axis. The measurement starts with this deceleration and captures the swing-out behaviour of the robot. These four trajectories are compared using criteria that can be divided into two sections. Section one covers the criteria for the economic efficiency of the trajectory. We consider in detail the required effort to integrate the trajectory into an existing production environment and the loss of production time while performing the measurement trajectory. Moreover, we evaluate the time needed for software and hardware changes to integrate the measurement procedure into the robot control. Section two covers the potential data quality for predictive maintenance. One criterion from this section is, how heavily the movements of the other robot axes influence the measurement data from one specific axis. We also compare the trajectories for their capability to measure data, which can be used to diagnose faults on specific components such as bearings. Finally, we evaluate the influence of changes in the production trajectory on measurement data. Please refer to [25] for the full evaluation.

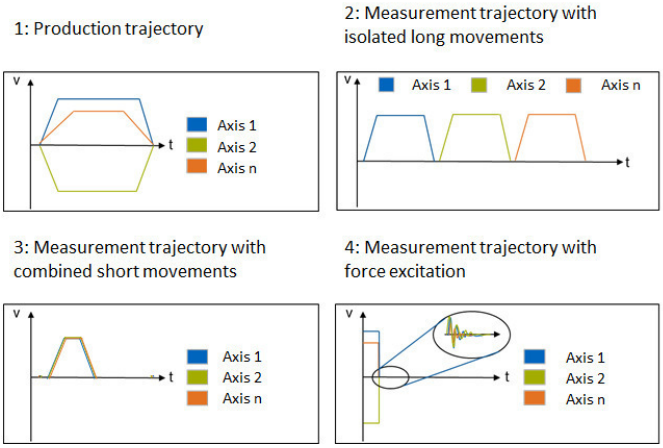

Figure 2. Potential measurement trajectories

After selecting the trajectory with the highest evaluation score, we estimate the number of measurements, which are necessary for estimating the robot's health condition reliably

in the last step. Within this publication, we assume that the HI to monitor the robot's health state has already been chosen as there exist numerous approaches to select HIs for industrial robots [16, 17, 19]. It is calculated from the data of one measurement performed with the chosen trajectory. The HI must be normally distributed in a timeframe, where the health state is unlikely to change. Given these conditions, the number of required measurements n to estimate the average HI with a confidence interval α, an observed variance of the HI σ and an allowed error e can be calculated by formula 1. Here, z describes the z-score for the chosen confidence interval α [26].

$$n = \left(\frac{z*\sigma}{e}\right)^2 \quad (1)$$

To calculate n, the allowed error and the desired confidence interval must be set. The variance in the HI can be sample-based. Therefore, we suggest collecting the HI data during the setup of the PdM-system for one week and one measurement per hour.

4. Results

To evaluate the described methodology, we applied it on articulated six axis robots. The findings of this application are presented in this section. Figure 3 shows the results of the initial data analysis for data collected in a car manufacturing plant over six years. The components with the highest fault frequency are electrical components (e.g. the robot drive controllers and the motors). Discussing these results with the plant's maintenance experts showed that the most severe faults are gear faults as they can lead to the time-intensive exchange of a robot during production, causing high economic losses, while faults induced by the servo controllers and power supplies can be fixed quickly by exchanging the whole robot control. Hence, we focused the literature review on publications related to gear faults.

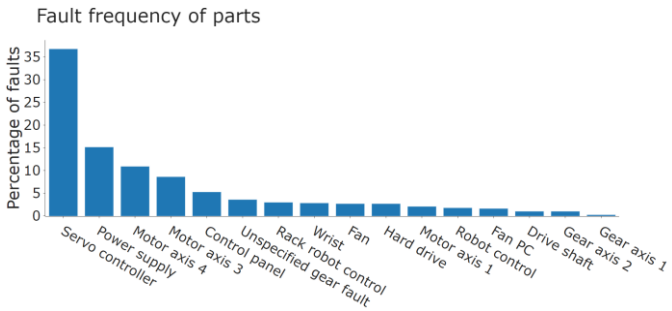

Figure 3. Frequency of faults in industrial robots

The result of this literature review is summarised partly in the graph depicted in Figure 4 for 60 publications, which were relevant for our application. The metadata of the publications are available in [27]. Based on this graph, we analysed the frequency of use for different data sources as shown in Figure 5 by counting the outgoing edges for each data source node. According to these results, we suggest using both accelerometers and motor currents as potential suitable data sources for PdM for industrial robots. In the next step, we evaluated the different trajectories and validated the results with further expert interviews.

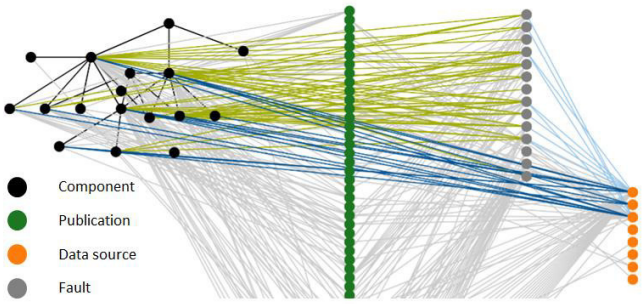

Figure 4. Part of the literature graph

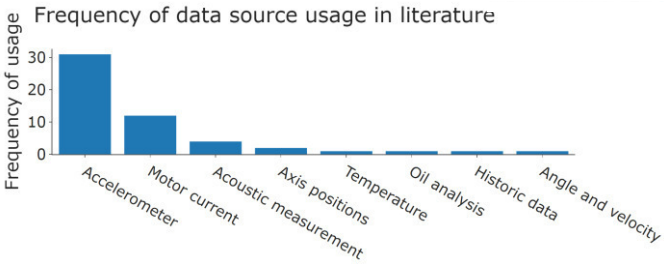

Figure 5. Usage frequency of data sources for PdM

As can be seen in Figure 6, the production trajectory shows the highest economic efficiency. However, it also shows the lowest potential data quality. The criteria from this section are best met by the measurement trajectory with large angle ranges and isolated movements of each axis. We validated this result with 6 experts from the robot development and condition monitoring domain in the form of expert interviews. As no trajectory shows the highest evaluation score in both sections, it must be carefully evaluated, which trajectory will be used. If it is possible from a technical and organisational point of view, we recommend to use the trajectory with long isolated movements. Otherwise, the production trajectory should be used.

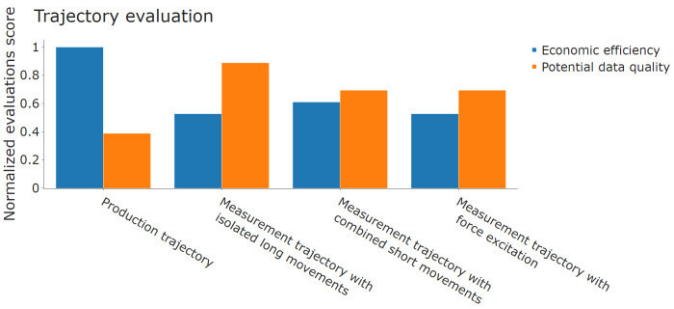

Figure 6. Results of the trajectory evaluation

Finally, we applied the last step of our methodology to determine the number of measurements required for a confident estimation of a robot's health state. For this, we acquired vibration data with an acceleration sensor attached axially to the case of the gear of the second joint of a six-axis articulated robot of type KUKA KR 210. The sensor sampled data with a frequency of 26 kHz. One measurement lasted 2.6 s. The raw data of one measurement is depicted in Figure

7. Measurements were executed every hour for 56 days as part of a long-term test. During the measurement, the robot performed an isolated movement of the second axis in a 90° range of motion. The remaining time, the robot performed a complex trajectory with varying angular speeds to accelerate its wear. We chose the root mean square (RMS) as the feature to track the robot's health state. From the gathered data, we calculated the RMS for each measurement based on N samples per measurement and the measurement value per sample x_i according to formula 2.

$$RMS = \sqrt{\frac{1}{N}\sum_i^N x_i^2} \qquad (2)$$

The RMS was chosen exemplarily as a feature since it is used frequently for condition monitoring of machinery. Based on the averaged variance of these RMS values per day in the first week of the measurements, a confidence interval of 95% and an allowed error of 0.05 m/s², the required number of measurements equalled 10. To validate this result, we considered 58 sets of 10 random measurements in a 24h time window, calculated the mean RMS of these measurements and verified, whether this mean lies within the range of the 24h mean and the allowed error. This approach showed that 90 % of the measurements were inside the defined error range. The used data is also depicted in Figure 8. The data shown in blue are the original RMS values. The data depicted in orange are the estimated data based on three samples in a 24h time window. The green and red line define the 95 % confidence interval of the 24h mean for an error of 0.05. Most of the original data lies in this interval. Only some high value peaks lie outside (around 10% of the measurements). The used data set is available upon request due to confidentiality reasons.

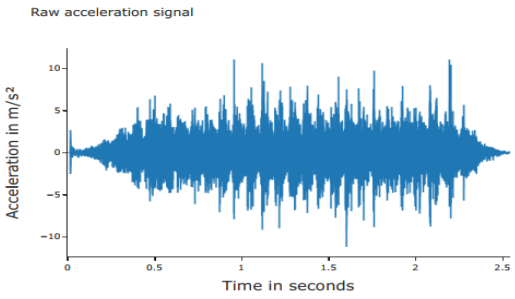

Figure 7: Raw acceleration signal of one measurement

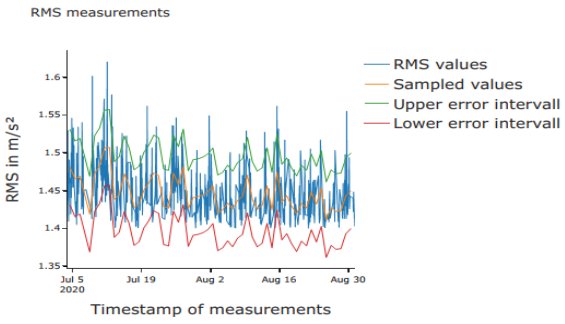

Figure 8. RMS measurements with confidence interval and rolling mean

5. Discussion

The main objective of the presented methodology is to select suitable sensors, trajectories and the number of measurements for the HI determination at an early design stage of a predictive maintenance system for industrial robots. However, some remarks remain considering the step of sensor selection and the methodology as a whole.

Taking a closer look at the step of sensor selection, we point out that the frequency of usage in literature for each sensor system as a decision criterion can mislead. Based on this approach not only the sensor best fitted for the monitoring task could be selected. The reasons why a specific sensor system was chosen in a publication could also be that this sensor system was already present or was more affordable. Hence, sensor systems with a low suitability could have a high frequency of usage in literature.

Regarding the methodology in general, we have to clarify that the generated knowledge is only valid for one considered production system and the experts providing detailed information about this system. Hence, our presented results might not hold true for another production system e.g. in the electronics industry.

Furthermore, the methodology should be applied repeatedly, when the PHM-system operates. While the system is running, data is produced continuously on a large scale. This data can be used to advance the applied sensor setup, trajectories, and the number of measurements. For instance, if a high percentage of faults can be detected with the integrated current sensors, it might be possible to avoid external acceleration sensors. In this way, the overall costs of the PHM-system can be reduced. Furthermore, data could be acquired using not only the measurement trajectory but also the production trajectory. Thus, a parallel PHM-system could be built up based on this trajectory. If it is possible to derive reliable HIs and models for the PHM-system based on the production trajectory, it might be possible to create a system, that reliably classifies and predicts faults and is economically efficient, too. This is of particular importance, as in many production setups it might not be possible to perform non-value-adding measurement trajectories. Regarding the number of required measurements, the variance of the chosen HIs should be reevaluated on a regular basis. If this variance changes, it might be necessary to increase the number of measurements to estimate the HIs mean accurately.

6. Summary and outlook

In this publication, we presented a methodology for the setup of data acquisition for predictive maintenance of industrial robots. This methodology is based on literature, historic data, expert knowledge and statistics. It gives an overview of fault-prone components of six axis articulated robots operating in an automotive plant, which are the electronic components such as the power supply and motors, as well as the robot gears, and the data sources that are suitable to detect such faults. Vibration and motor current analysis is most frequently used for this purpose. To gather the required data, we evaluated different robot trajectories

qualitatively. We suggest using either the production trajectory to achieve a high economic efficiency or a measurement trajectory with isolated axis movements and large angle ranges for the measurements to collect high-quality data. Finally, we suggest using the method proposed in [26] to determine the number of required measurements in a timeframe to estimate the robot's health state with confidence.

In future research, we plan to find out whether a significant difference in the fault detection rate of PHM-models for industrial robot gears can be measured based on either vibration or current data.

Acknowledgements

We express our gratitude to the Bavarian Ministry of Economic Affairs, Regional Development and Energy for the funding of our research. The formulated outlook will be investigated as part of the research project "KIVI" (grant number IUK-1809-0008 IUK597/003) and will be further developed and implemented.

References

[1] Hägele, M., Nilsson, K., Pires, J.N., 2008. Industrial Robotics, in *Springer Handbook of Robotics*, Springer Science+Business Media, Berlin, Heidelberg, p. 963.

[2] Gouriveau, R., Medjaher, K., Zerhouni, N., 2016. *From Prognostics and Health Systems Management to Predictive Maintenance 1*. John Wiley & Sons, Inc, Hoboken, NJ, USA.

[3] Tsui, K.L., Chen, N., Zhou, Q., Hai, Y. *et al.*, 2015. Prognostics and Health Management: A Review on Data Driven Approaches, in *Mathematical Applications to Reliability 2015*, p. 1.

[4] Lei, Y., Li, N., Guo, L., Li, N. *et al.*, 2018. Machinery health prognostics: A systematic review from data acquisition to RUL prediction, in *Mechanical Systems and Signal Processing 104*, p. 799.

[5] Cachada, A., Barbosa, J., Leitno, P., Gcraldcs, C.A.S. *et al.*, 2018. Maintenance 4.0: Intelligent and Predictive Maintenance System Architecture, in *IEEE 23rd International Conference on Emerging Technologies and Factory Automation (ETFA)*, IEEE, Piscataway, NJ, p. 139.

[6] Nguyen, K.T.P., Medjaher, K., 2019. A new dynamic predictive maintenance framework using deep learning for failure prognostics, in *Reliability Engineering & System Safety 188*, p. 251.

[7] Xiang, S., Huang, D., Li, X., 2018. A Generalized Predictive Framework for Data Driven Prognostics and Diagnostics using Machine Logs, in *Proceedings of TECON 2018*, IEEE, Piscataway, New Jersey, p. 695.

[8] Lin, Y., Li, X., Hu, Y., 2018. Deep diagnostics and prognostics: An integrated hierarchical learning framework in PHM applications, in *Applied Soft Computing 72*, p. 555.

[9] Shin, I., Lee, J., Lee, J.Y., Jung, K. *et al.*, 2018. A Framework for Prognostics and Health Management Applications toward Smart Manufacturing Systems, in *International Journal of Precision Engineering 5*, p. 535.

[10] Mosallam, A., Medjaher, K., Zerhouni, N., 2015. Component based data-driven prognostics for complex systems: Methodology and applications, in *First International Conference on Reliability Systems Engineering (ICRSE)*, IEEE, p. 1.

[11] Santi, L., Sowers, T., Aguilar, R., 2005. Optimal Sensor Selection for Health Monitoring Systems, in *41st AIAA/ASME/SAE/ASEE Joint Propulsion Conference*, p.30.

[12] Wu, J., Su, Y., Cheng, Y., Shao, X. *et al.*, 2018. Multi-sensor information fusion for remaining useful life prediction of machining tools by adaptive network based fuzzy inference system, in *Applied Soft Computing 68*, p. 13.

[13] Chen, Z.S., Yang, Y.M., Hu, Z., 2012. A Technical Framework and Roadmap of Embedded Diagnostics and Prognostics for Complex Mechanical Systems in Prognostics and Health Management Systems, in *IEEE Trans. Rel. (IEEE Transactions on Reliability)*, p. 314.

[14] ISO, 2002. *DIN ISO 13373-1:2002-07, Zustandsüberwachung und -diagnostik von Maschinen-Schwingungs-Zustandsüberwachung- Teil 1: Allgemeine Anleitungen (ISO 13373-1:2002)*. Beuth Verlag GmbH, Berlin.

[15] Christer, A.H., Wang, W., 1995. A simple condition monitoring model for a direct monitoring process *European Journal of Operational Research 82*, p. 258.

[16] Bittencourt, A.C., Saarinen, K., Sander-Tavallaey, S., 2012. A Data-driven Method for Monitoring Systems that Operate Repetitively -Applications to Wear Monitoring in an Industrial Robot Joint1, in *IFAC Proceedings Volumes*, p. 198.

[17] Borgi, T., Hidri, A., Neef, B., Naceur, M.S., 2017. Data analytics for predictive maintenance of industrial robots, in *Proceedings 2017 International Conference on Advanced Systems and Electric Technologies (IC_ASET)*, IEEE, Piscataway, NJ, p. 412.

[18] Cheng, F., Raghavan, A., Jung, D., Sasaki, Y. *et al.*, 2019. High-Accuracy Unsupervised Fault Detection of Industrial Robots Using Current Signal Analysis, in *IEEE International Conference on Prognostics and Health Management (ICPHM)*.

[19] Kim, Y., Park, J., Na, K., Yuan, H. *et al.*, 2020. Phase-based time domain averaging (PTDA) for fault detection of a gearbox in an industrial robot using vibration signals, in *Mechanical Systems and Signal Processing 138*, p. 106544.

[20] Carvalho Bittencourt, A., 2014. *Modeling and Diagnosis of Friction and Wear in Industrial Robots*. Linköping University Electronic Press, Linköping.

[21] Slamani, M., Bonev, I.A., 2013. Characterization and experimental evaluation of gear transmission errors in an industrial robot, in *Industrial Robot (Industrial Robot: An International Journal) 40*, p. 441.

[22] Costa, M.A., Wullt, B., Norrlöf, M., Gunnarsson, S., 2019. Failure detection in robotic arms using statistical modeling, machine learning and hybrid gradient boosting, in *Measurement 146*, p. 425.

[23] Hong, Y., Sun, Z., Zou, X., Long, J., 2020. Multi-joint Industrial Robot Fault Identification using Deep Sparse Auto-Encoder Network with Attitude Data, in *2020 Prognostics and Health Management Conference*, IEEE, p. 176.

[24] Webster, J., Watson, R.T., 2002. Analyzing the Past to Prepare for the Future: Writing a Literature Review, in *MIS Quarterly 26*, p. xiii.

[25] Nentwich, C. Evaluation of robot trajectories for Predictive Maintenance of Industrial robots. https://mediatum.ub.tum.de/1577850. Accessed 17 November 2020.

[26] Härdle, W., Klinke, S., Rönz, B., 2015. *Introduction to statistics: Using interactive MM*Stat elements*. Springer, Cham, Heidelberg, New York, Dordrecht, London.

[27] Nentwich, C. Literature review for sensor selection for predictive maintenance of industrial robot gears. https://mediatum.ub.tum.de/1164627?show_id=1611505&style=full_text. Accessed 12 May 2021.

8.2 Data Source Comparison for Condition Monitoring of Industrial Robot Gears

Available online at www.sciencedirect.com

ScienceDirect

Procedia CIRP 107 (2022) 314–319

www.elsevier.com/locate/procedia

55th CIRP Conference on Manufacturing Systems

Comparison of Data Sources for Robot Gear Condition Monitoring

Corbinian Nentwich[a,]*, Rüdiger Daub[a] *

[a]*Technical University Munich, Boltzmannstraße 15, 85748 Garching, Germany*

* Corresponding author. Tel.: +49 89 289 1554. *E-mail address:* corbinian.nentwich@iwb.tum.de

Abstract

Industrial robot gear condition monitoring has the potential to increase the productivity of highly automated production lines. In order to implement an effective condition monitoring system, data must be collected which correlates with the robot gear's state of health. The sensor choice and the characteristics of these sensors are crucial to the success of a condition monitoring system. Hence, we compare current and vibration sensor data from different accelerated robot gear wear tests in different frequency ranges to determine a suitable sensor setup. In the presented experiments, both data sources detect faults at a similar point in time and the variation of the frequency ranges has different effects on the data quality.

Keywords: industrial robot, condition monitoring, data acquisition

1. Introduction

The productivity of industrial robots is reduced by unexpected downtimes, which can be caused by gear defects [1]. To overcome this problem, condition monitoring (CM) can be used to trigger maintenance actions before a failure can occur. A four-step approach can be followed for implementing a CM system. First, data that correlates with the development of defects must be collected. Second, this data must be transformed into meaningful health indicators (HI), which represent the health state of the system. Third, these HI data have to be used to detect anomalies or trends, classify data from damaged robots or predict the occurrence of defects with suitable data or model driven approaches [2]. In earlier publications, we presented a suitable data acquisition system for the CM of industrial robot gears [1]. We suggested a data transformation approach to derive an appropriate HI for each robot axis in [3] and described a robust combined anomaly and trend detection model in [4]. However, in the field of data acquisition some questions remain unanswered for this application. In this publication, we intend to address the questions of,

- which data source, vibration data or current data, should be used for data acquisition and
- which frequency range must be considered during data collection to provide HI time series that display defects sufficiently.

Hence, we present the state of the art regarding these research questions in Section 2 and clarify the research gap that we are addressing. Subsequently, in Section 3 we describe the methodology that was followed to compare data sources and the considered frequency ranges. Afterwards, we present the results of multiple accelerated wear tests of industrial robots in Section 4 that were executed with different data sources and frequency bands. These results are discussed in Section 5 and summarized in Section 6, which also provides an outlook for further research topics.

2. State of the Art

In the following, an overview of publications is given that compare different data sources for robot or gear CM. Additionally, the sampling rates used for data acquisition in

10.1016/j.procir.2022.04.051

these publications will be summarized as higher sampling frequencies allow the analysis of higher frequency ranges.

Vibration and current data were compared for a two-stage gearbox in [5]. Sampling rates of up to 50 kHz were used for measurements lasting up to 36 seconds for different speeds and loads. Twenty-four measurements were performed per unique gear condition. Defects were induced by drilling holes of varying diameters in the outer ring of the shaft bearing. Then 882 features from the time- and frequency-domains were derived for the vibration measurements and used with a support vector machine to classify the measurements. Here, two cases were investigated. In the first experiment, the support vector machine only had to distinguish defective measurements from healthy ones, which was possible with 100% accuracy. In the second experiment, the different drilled diameters should be differentiated. This was possible with recall values above 97%. Additionally, the current data was analyzed based on wavelet analysis. Here, only the defect signals with the two larger diameters could be differentiated from the normal signals.

Different signal processing techniques for current and vibration data for the CM of multi-stage gears were compared in [6]. The authors use characteristic frequencies in the vibration signal spectra and wavelet techniques for the current data for defect detection. Data was acquired at different loads, with a sampling frequency of up to 20 kHz and a measurement length of up to 2 seconds. They conclude that both data sources can be used for the CM task.

A comparison of vibration and current data for the fault detection of a multi-stage gear is conducted in [7]. Defects, such as one or two missing gear teeth, were induced artificially. Measurement data was acquired at different loads, a measurement time of 2 s and measurement frequencies up to 20 kHz. They compare the non-defect signals with the defect signals based on the Kolmogorov-Smirnov test. This test is used to determine whether two data sets have the same probability distribution. Based on this test, it was shown that with motor current data the defect measurements can be distinguished from the healthy measurements at all load levels. Vibration measurements of healthy and faulty gears cannot be distinguished at low loads.

Another multi-stage gear CM approach was investigated in [8]. Here, samples were taken at a sampling rate of 10 kHz and a measurement time of 0.4–0.8 seconds. Different scenarios regarding load and removed teeth were investigated. The data are analyzed in the time-frequency domain with the short-time Fourier transform and the discrete wavelet transform. The analysis shows that the defects alter the spectrograms of the different data sources in different ways, but the effect of the defects is visible for both data sources and data processing methods.

A methodology for current based CM of gears based on the synchronous signal averaging method is presented in [9]. The authors compare their method to vibration data measurements for the case of a defective gear tooth. The defect consisted of artificially introduced pitting at the output gear of a two-stage gear. Data was sampled at 4.44 kHz for the current sensors and 10 kHz for the vibration data. Thirty samples were taken for different load levels and a measurement time of 26.88 s. Results indicate that both data sources show differences between defective and healthy measurements. Variations due to the different loads exist.

Vibration and current data were evaluated based on measurements lasting one second at a sampling rate of 8 kHz for a test rig including an automotive gear in [10]. Different loads and defect conditions were investigated. Simple statistical features were derived for the vibration data and motor current signature specific features were calculated from these measurements. Subsequently, two classifiers – an artificial neural network and a support vector machine – were trained and used to classify the measurements. The classification accuracies are the highest for the current data, followed by slightly lower values for the vibration data, depending on the defect and operating condition of the gear.

The detection of pitting defects with different severities in terms of number and size of pits was investigated in [11]. Data were acquired at a two-stage gear test bed. Current data were collected at 25 kHz, vibration data were sampled at 50 kHz for a time of 10 seconds per measurement. Different load and speed scenarios were considered. Twenty features from the time domain were derived from the raw data, such as the RMS or the log energy entropy. Subsequently, these features were used in a classifier to distinguish defect measurements from healthy measurements. Here, the classifier based on the vibration data showed higher accuracy values compared to the model based on current data.

Vibration data was sampled at 3 kHz and current data at 4 kHz for a two-stage gear box in [12]. Experiments were performed at different speed levels and for different gear wear levels. Additionally, a pitting defect in a bearing was artificially introduced. Clear differences in the spectra of the vibration data could be observed for the different defects. The sidebands of the characteristic frequencies increased with increasing velocity, which makes defect detection more challenging. Similarly, the power spectral density was derived for the current data and differences for the various defects were visible for the higher velocity levels. No visible change was observed at the lowest speed level, which was 5 Hz. We presented a more comprehensive literature review regarding gear CM in [1]. For this publication, we analyzed how often certain sampling frequencies and sensor types are used in the literature network graph presented in [1]. The result of this analysis is presented in the histogram in Figure 1. Sampling frequencies higher than 10 kHz are used most often for vibration-based CM. Sampling frequencies of 10 kHz or lower are most frequently used for current-based approaches. Summarizing the presented publications, two observations can be made. First, the suitability of the different data sources depends on the data transformation steps used and the individual system, which is monitored. Second, various sampling frequencies and mostly high ones are used for the experiments. To the best of our knowledge, neither a comparison of data sources for industrial robot gear

CM exists, nor an analysis of which sampling frequencies and sensor bandwidth are required for this application.

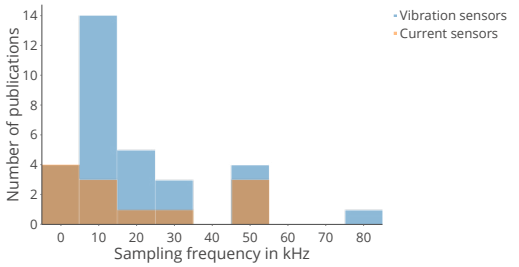

Figure 1: Usage of data sources for presented publications in

3. Methodology

To address the research gap defined above, we analyzed data from different accelerated wear tests of industrial robots. In the following, the experiments will first be presented. Afterwards, we will describe the analysis process applied to the data. The four accelerated wear tests were performed with different six-axis articulated robots with a payload greater than 200 kg and cycloidal gears in the considered axes at their second or third axis. The summary data of all experiments is presented in Table 1. The sampling frequencies of the experiments varied due to restrictions of the measurement systems.

The first experiment was performed with an ABB-6640 235/2.55. Here, the wear was increased by degreasing the robot gear at axis 3 and adding abrasive additives into the gear box. The experiment lasted 3 months and during this time 1726 measurements were collected for isolated movements of the third axis from the vibration sensor and 485 from the current sensor. Vibration sensor data were sampled at 20 kHz and current sensor data at 2 kHz. The experiment stopped when the motor pins were worn out and hence were no longer able to drive the gear. The second experiment was performed with a KUKA KR 510 R3060. Similar to the first experiment, the robot gear at axis 3 was degreased and abrasive additives were added. The 680 current and vibration measurements were recorded in 3 months for isolated movements of the third axis. The experiment was stopped after the noise level increased to a level at which a defect could be clearly assumed acoustically. The third experiment was performed with an ABB 6600-255/2.55. Data were sampled at 10 kHz, captured with a vibration sensor attached to the second axis gear cap while the robot made isolated movements of the second axis. Over 2290 measurements were collected in over 12 months. The experiment was stopped due to the high number of error messages issued by the robot controller. More information regarding this experiment can be found in [13, 14]. The fourth experiment was performed with an ABB 7600-340/2.8. Vibration data were sampled with 20 kHz at a similar position at the gear cap. The robot performed isolated movements with this axis. Over 920 measurements were collected in over 3 months. One measurement contains the information of one movement. The experiment stopped since a broken part of a roller bearing blocked the gear of the second axis and the robot was unable to move this axis anymore. This experiment is described in more detail in [3]. All experiments were performed in isolated test beds to reduce influences that could occur in a production environment.

In total, two analyses were performed regarding the suitability of data sources and the frequency ranges that contain defect-related information. This knowledge can then be used to select suitable sensors regarding type, sampling frequency and frequency range. The sampling frequency must be twice the required defect related frequency [15] and the sensor must have a bandwidth up to this frequency. We performed the latter analysis only for acceleration sensors, since the current sensors are normally built-in features of the robot controllers. The characteristics of these sensors are defined by the robot manufacturers and hence cannot be influenced.

We analyzed only the data from experiment 1 and 2 regarding the suitability of different data sources, since no current data were available for experiment 3 and 4. For this, we calculated a HI, which is described in [3] and further below, for the raw data from both data acquisition systems for both experiments.

Table 1: Overview of experiments (exp.), Abbreviations: Vibration (Vib.), Current (Cur.)

	Sampling frequency in kHz	Number of measure-ments	Length in months	STFT window length	Reason for failure
Exp. 1	Vib.: 20 Cur.: 2	Vib.: 1726 Cur.: 485	3	256	Worn out motor pinions
Exp. 2	Vib.: 24 Cur.: 1	Vib.: 680 Cur.: 680	3	512	Drastically increased noise level
Exp. 3	10	2440	12	256	Increased number of controller errors
Exp. 4	20	914	3	256	Blocked gear due to broken roller bearing

Subsequently, we compared the HI time series of the two data sources regarding different criteria. We analyzed whether anomalies appear earlier in one of the data sources' HI time series and whether trends are more prominent in one data source. For the second analysis, we analyzed the vibration data from all experiments in different frequency ranges. For this, we applied low-pass filters on the measurements' raw data at different cut-off frequencies in

the range of 250 to 2500 Hz to remove the signal content of higher frequencies. A 10th order infinite impulse response Chebyshev Type II filter was used for this because of its good damping behavior. In this way, high frequency range information is blurred. If this information would be fault related no anomalies or trends should be visible in the Z-score time series anymore. Then, we derived the same HI as for the data source analysis from the down-sampled data. This HI represents the raw data of one measurement as a single number. For this, the spectrogram of the short-time Fourier transform (STFT) $spec(\tau,\omega)_{meas}$ for each measurement is first calculated. Here, τ is a time step and ω a frequency step in the STFT-spectrogram. The STFT-window lengths are presented in Table 1. A Hamming window function was used for the STFT transform as this showed good time-frequency resolution in preliminary studies related to [3]. For a reference quantity of measurements, the mean $spec(\tau,\omega)_{avg,ref}$ and standard deviation values $spec(\tau,\omega)_{std,ref}$ for each entry in the STFT matrices over all reference measurements are calculated. Based on the $spec(\tau,\omega)_{avg,ref}$ and the $spec(\tau,\omega)_{std,ref}$ matrix, a Z-score matrix $Z(\tau,\omega)$ can be calculated for each new measurement according to Formula 1.

$$Z(\tau,\omega) = \left| \frac{spec(\tau,\omega)_{meas} - spec(\tau,\omega)_{avg,ref}}{spec(\tau,\omega)_{std,ref}} \right| \quad (1)$$

The HI value is determined by averaging all entries of the Z-score matrix and is called in the following Z-score. Please refer to [3] for more detailed information regarding this HI. Afterwards, we analyzed the Z-score time series visually and using the signal to noise ratio, snr. This common figure of merit used in signal analysis describes the information content of a signal and can be calculated as shown in Formula 2.

$$snr = \frac{mean(x(t))}{std(x(t))} \quad (2)$$

Here, $mean(x(t))$ describes the average value of a time series $x(t)$ and $std(x(t))$ the standard deviation of a time series. For this analysis, we considered the first 30 percent of each data set to avoid influences of trends of the Z-score time series on snr. Finally, we summarized observations that could be found in all data sets. The process of the two analyses is summarized in Figure 6.

4. Results

In the following, we will first evaluate data from experiment 1 and 2 to compare the suitability of different data sources. Afterwards, we will compare vibration data from all experiments with different frequency bands. The Z-score time series from experiment 1 are shown in Figure 2. An initial increase in the Z-score is already visible around measurement 210 for the current data and around measurement 250 for the vibration data. The early increase of the current data was due to a motor defect in the form of a short circuit caused by overheating of the motor. The

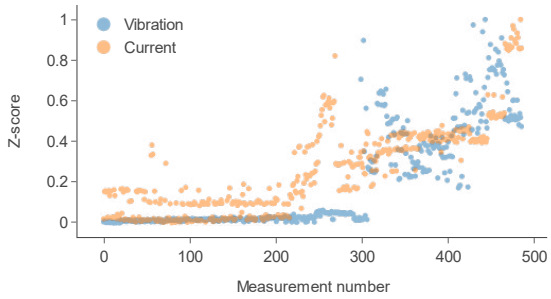

Figure 2: Comparison of data sources in Experiment 1 (data normalized)

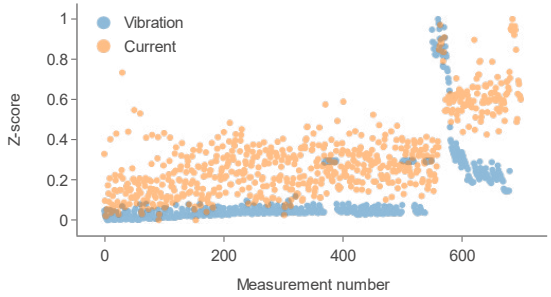

Figure 3: Comparison of data sources in Experiment 2 (data normalized)

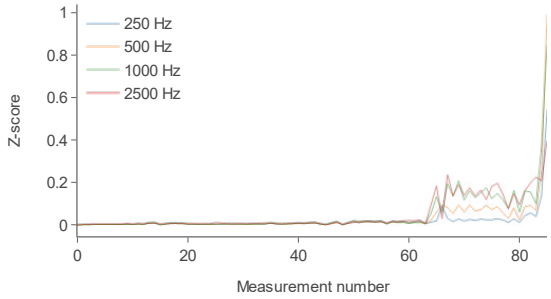

Figure 4: Comparison of normalized vibration-based Z-score time series and different frequency ranges in experiment 1

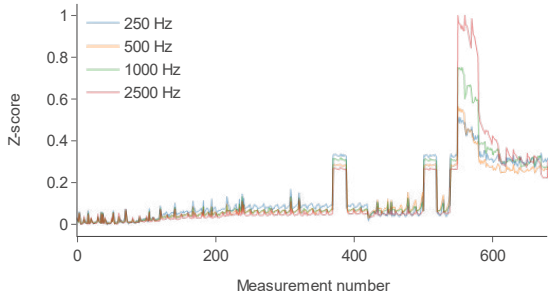

Figure 5: Comparison of normalized vibration-based Z-score time series and different frequency ranges in experiment 2

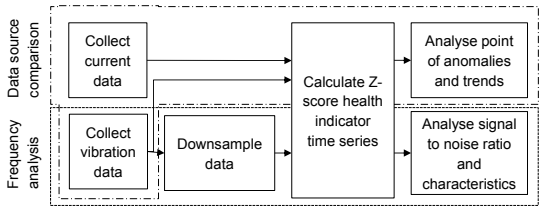

Figure 6: Analysis process

increase of the vibration data or the decrease of the current data around measurement 250 is related to the exchange of the broken motor. This defect was not detected by the

vibration data. Changes in the end of the experiment are visible around measurement 430 in the vibration data and in the current data around measurement 450. This equals a time difference of roughly 24 hours. At this stage, it can be assumed that the gear defect was already present and growing. An accurate analysis of the gear defect state was not possible since it is not possible to disassemble the gear without destroying it.

The Z-score time series of vibration and current data of experiment 2 are shown in Figure 3. Changes in the time series are visible at the end of the experiment before the experiment was ended. These changes are visible around measurement 550 in the vibration data and around measurement 580 in the current data. In this experiment an alarm would have been triggered approximately 24 hours earlier using vibration data compared to using current data. Another characteristic of the vibration data is that it shows a small trend in the beginning of the experiment up to measurement 200. This trend is more prominent in the vibration data compared to the current data. In the end of the experiment, the HI values of the vibration data decrease to a plateau. The values of the current data remain more constantly on a high level.

The results of the frequency range experiments are depicted in Figures 4,5 and 7-9. The various lines in the images represent the time series of the Z-score derived from the differently down-sampled raw vibration data. We compared all time series for one data set with each other to find common patterns between the data sets. Four similar characteristics could be observed for all four experiments. With increasing frequency range, the noise level of the Z-score time series is reduced in experiments 1–3. This is also shown in Figure 9. It indicates the signal to noise ratios for the different experiments and cut-off frequencies. Increased cut-off frequencies lead to an increased signal to noise ratio. Furthermore, depending on the cut-off frequency used, different parts of the Z-score time series become more prominent. This means that they have higher amplitudes within a given time range. This can be observed, for example, in Figure 5 around measurement 380 or in Figure 7 around measurement 1000. An explanation for this observation could be that different parts of the gear, such as the bearings or the gear teeth, stimulate vibrations at different frequencies depending on the gear speed. The third observation is that even at a low cut-off frequency of 250 Hz, clear changes in the HI time series are visible before the gear defect. These changes become more visible with increasing cut-off frequencies. These observations are also summarized in Table 2. An interactive version of Figures 3–8 can be found in [16].

5. Discussion

In this section we will first elaborate on the findings of the data source comparison experiments. Afterwards, we will discuss the indications given by the frequency range analysis. In experiment 1, data from both sources could detect the gear defect in the end of the experiment. The gear defect was detected in the same 24-hour window for both data sources. Furthermore, only in the current HI data a motor defect could be detected. In experiment 2 the gear defect was detected 24 hours earlier by the vibration HI

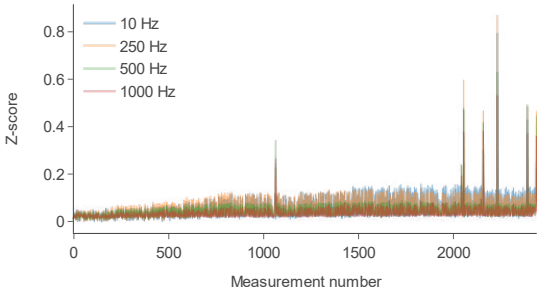

Figure 7: Comparison of normalized vibration-based Z-score time series and different frequency ranges in experiment 3

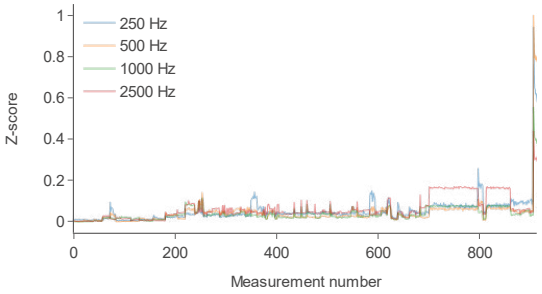

Figure 8: Comparison of normalized vibration-based Z-score time series and different frequency ranges in experiment 4

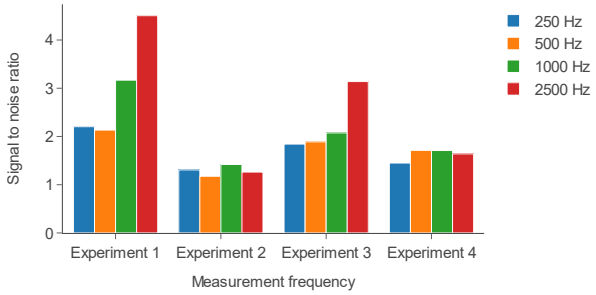

Figure 9: Signal to noise ratios of different experiments and sampling frequencies

Table 2: Observations of the frequency experiment (yes: Y, no: N)

Observation	Experiment			
	1	2	3	4
Higher cut-off frequencies reduce noise.	Y	Y	Y	N
Different cut-off frequencies lead to prominence of different signal parts.	Y	Y	Y	Y
Changes are prominent before the defect occurs above 250 Hz	Y	Y	Y	Y
Higher cut-off frequencies up to 1000 Hz increase the changes in the health indicator due to wear.	Y	N	Y	Y

data compared to the current HI data. Thus, both systems qualify for the CM task. Based on these findings, no clear recommendation can be given on which data source to use from our point of view. However, there are several other criteria that must be considered for the selection. A CM system for robot gears must be scalable to heterogenous robot fleets. Using current data requires the availability of data connectors, which must be provided by the various robot manufacturers. This issue could be overcome by using external vibration sensors attached to the robots. However, in the vibration data scenario, additional costs are created for the sensor purchase. These costs can be reduced by narrowing down the fleet size of robots to be monitored. The CM system should be used only for robots that are either positioned at bottlenecks of the production system or that are highly stressed by their production task. Another argument against a vibration-based system could be the inability of the motor defect detection in experiment 1. Discussions with the maintenance department of a car manufacturing plant showed that these defects do not cause long downtimes, since in most cases motors can be exchanged quickly [1]. Therefore, these faults are not critical and thus are not considered in the proposed CM system. Therefore, we suggest using a vibration-data based CM system as it can detect gear defects and can be implemented faster compared to a current-data based system.

The second analysis regarding the required frequency range showed that changes in the HI time series are already present at low cut-off frequencies in the case of a gear defect. Moreover, the Z-score noise level is reduced at higher cut-off frequencies, and from a theoretical point of view a specific frequency range is necessary to capture the vibrations from the various gear components. These vibration frequencies depend on the components' speed and thus the robot speed and the gear transmission ratios [17]. Summarizing, a sampling frequency and frequency range should be chosen that is as low as possible to reduce sensor cost and as high as necessary to ensure capturing the vibrations of all gear components. A minimum required sampling frequency could be derived based on the electric drive speed which can be calculated with the robot speed ω_{robot} and the gear transmission rate $n_{robot\,gear}$. In the following, an estimation of the required sampling frequency based on robot data sheet information and state of the art knowledge on robot gear transmission rates will be performed according to Formula 3.

$$f_{sampling} = \omega_{robot} * n_{robot\,gear} * m_{max} * n_{harm} * 2 \quad (3)$$

Here, we rely on the calculations that the maximum component speed within a robot gear correlates with a constant m_{max} [13]. To capture a signal at a specific frequency, the sampling frequency must be two times this frequency [15]. Furthermore, defect related information can not only be represented in a component's frequency, but also at its harmonics n_{harm} (multiples) [17]. The required frequency range of the sensor is then half $f_{sampling}$. Assuming a maximum robot speed of 90 °/s and a gear ratio of 268 for the third axis of the robot used in experiment 4, setting m_{max} 22 times the electric drive speed [13] and n_{harm} equal 3, this would require a sampling frequency of 8.844 kHz to capture all component frequencies and harmonics reliably at maximum robot speed. Formula 3 can be used in practice to estimate the minimum required sensor sampling resolution.

6. Conclusion

Experiments for comparing different data sources and required frequency ranges for industrial robot gear condition monitoring were conducted in this work. The raw sensor data was transformed to a HI based on the short-time Fourier transform and the principle of Z-scores. The experiments showed that both vibration and current sensor data, are capable to detect robot gear defects. Based on practical implementation challenges, we suggest using vibration data in a condition monitoring system. The experiments also showed that the defects could be detected considering low cut-off frequencies. However, to be sure to collect potential vibrations of all components, we propose a formula to estimate the minimum required sampling frequency and frequency range. Future research could concentrate on further experiments to validate these findings.

Acknowledgements

We express our gratitude to the Bavarian Ministry of Economic Affairs, Regional Development and Energy for the funding of our research in the grant IUK-1809-0008 IUK597/003).

References

[1] Nentwich, C., Reinhart, G., 2021. Towards Data Acquisition for Predictive Maintenance of Industrial Robots. Procedia CIRP.
[2] ISO, 2002. *DIN ISO 13373-1:2002-07, Zustandsüberwachung und -diagnostik von Maschinen-Schwingungs-Zustandsüberwachung- Teil 1: Allgemeine Anleitungen (ISO 13373-1:2002)*. Beuth Verlag GmbH, Berlin.
[3] Nentwich, C., Reinhart, G., 2021. A Method for Health Indicator Evaluation for Condition Monitoring of Industrial Robot Gears. Robotics *10*, p. 80.
[4] Nentwich, C., Reinhart, G., 2021. A Combined Anomaly and Trend Detection System for Industrial Robot Gear Condition Monitoring. Applied Sciences *11*, p. 10403.
[5] Bravo, I., Leturiondo, U., Arnaiz, A., Salgado, O., 2016. Fault diagnosis of rolling element bearings from current and vibration measurements. PHM Society European Conference, 3(1).
[6] Kar, C., Mohanty, A.R., 2006. Monitoring gear vibrations through motor current signature analysis and wavelet transform. Mechanical Systems and Signal Processing *20*, p. 158.
[7] Kar, C., Mohanty, A.R., 2006. Multistage gearbox condition monitoring using motor current signature analysis and Kolmogorov–Smirnov test. Journal of Sound and Vibration *290*, p. 337.
[8] Kar, C., Mohanty, A.R., 2008. Vibration and current transient monitoring for gearbox fault detection using multiresolution Fourier transform. Journal of Sound and Vibration *311*, p. 109.
[9] Ottewill, J.R., Orkisz, M., 2013. Condition monitoring of gearboxes using synchronously averaged electric motor signals. Mechanical Systems and Signal Processing *38*, p. 482.
[10] Praveenkumar, T., Saimurugan, M., Ramachandran, K.I., 2017. Comparison of Vibration, Sound and Motor Current Signature Analysis for Detection of Gear Box Faults. International Journal of Prognostics and Health Management *8*.
[11] Sánchez, R.-V., Lucero, P., Vásquez, R.E., Cerrada, M. *et al.*, 2018. A comparative feature analysis for gear pitting level classification by using acoustic emission, vibration and current signals. IFAC-PapersOnLine *51*, p. 346.
[12] Saucedo-Dorantes, J.J., Delgado-Prieto, M., Ortega-Redondo, J.A., Osornio-Rios, R.A. *et al.*, 2016. Multiple-Fault Detection Methodology Based on Vibration and Current Analysis Applied to Bearings in Induction Motors and Gearboxes on the Kinematic Chain. Shock and Vibration *2016*, p. 1.
[13] Danielson Hugo, Schmuck Benjamin, 2017. *Robot Condition Monitoring: A first step in Condition Monitoring for robotic applications*, Lulea.
[14] Martin Karlsson, Fredrik Hörnqvist, 2018. *Robot Condition Monitoring and Production Simulation*, Lulea.
[15] Shannon, C.E., 1949. Communication in the Presence of Noise. Proceedings of the IRE *37*, p. 10.
[16] Nentwich, C. Figures for data source and sampling frequency comparison. https://github.com/xorbey/datasourcecomparison. Accessed 1 December 2021.
[17] Pham, D.T., Wang, L., Gao, R.X., 2006. *Condition Monitoring and Control for Intelligent Manufacturing*. Springer London, London.

8.3 A Method for Health Indicator Evaluation for Condition Monitoring of Industrial Robot Gears

robotics

MDPI

Article

A Method for Health Indicator Evaluation for Condition Monitoring of Industrial Robot Gears

Corbinian Nentwich * and Gunther Reinhart

Institute for Machine Tools and Industrial Management, Boltzmannstraße 15, 85747 Garching, Germany; emeritus.reinhart@tum.de

* Correspondence: corbinian.nentwich@iwb.tum.de

Abstract: Condition monitoring of industrial robots has the potential to decrease downtimes in highly automated production systems. In this context, we propose a new method to evaluate health indicators for this application and suggest a new health indicator (HI) based on vibration data measurements, Short-time Fourier transform and Z-scores. By executing the method, we find that the proposed health indicator can detect varying faults better, has lower temperature sensitivity and works better in instationary velocity regimes compared to several state-of-the-art HIs. A discussion of the validity of the results concludes our contribution.

Keywords: industrial robot; condition monitoring; health indicator

Citation: Nentwich, C.; Reinhart, G. A Method for Health Indicator Evaluation for Condition Monitoring of Industrial Robot Gears. *Robotics* **2021**, *10*, 80. https://doi.org/10.3390/robotics10020080

Academic Editor: Marco Ceccarelli

Received: 29 April 2021
Accepted: 7 June 2021
Published: 9 June 2021

1. Introduction

Industrial robots are a fundamental part of highly automated production systems, which can be found in the automotive or electronics industry [1]. Since they operate in complex production cells and as a part of linear production lines, robot malfunctions lead to long downtimes for repair or replacement and, hence, to increased costs. In particular, robot gear faults are responsible for the longest downtimes because they often require the replacement of the whole robot [2]. The condition monitoring (CM) of these gears offers the potential to resolve this issue. CM is the monitoring of an asset's health using sensor data. The health state represents a wear reserve before a failure occurs. This health state is quantified with a health indicator (HI). A significant monitored change in this health indicator can be used as a decision-making aid in the planning of maintenance actions [3].

1.1. State-of-the-Art

In recent years, different HIs based on vibration data for several industrial robot components, such as bearings, gears and motors, and their specific faults have been investigated. Furthermore, several approaches to cope with instationary signals in CM have been presented. The next two sections give a short overview of these topics followed by a section stating the contribution of our publication.

1.1.1. Vibration-Based Robot Condition Monitoring

A fault detection method was developed in [4], which first uses a novel phase-based, time-domain averaging method to remove the deterministic part of the vibration signal. Subsequently, the root mean square (RMS) and power spectrum entropy of the remaining residual signal are calculated as health indicators. A vibration signal based CM system for SCARA robots was implemented in [5], which in the first step uses statistical HIs of the time-domain signal to detect the occurrence of a defect and in the second step uses an artificial neural network to diagnose the fault type. A three-layer architecture for remote fault diagnosis of industrial robot gearboxes was proposed using vibration signals in [6]. In the diagnosis layer, the authors present a performance evaluation approach using a support vector machine (SVM), a remaining useful life prediction by a Markov

model and a fault-type diagnosis based on a Bayesian network. The degenerative behavior of an industrial robot gear was observed with vibration sensors by [7] as well as [8] in accelerated wear tests. After pre-processing the signals using order tracking and spectral auto-correlation, the characteristic fault frequencies were calculated and monitored by root mean square analysis, which revealed a trend correlating with increasing wear. In addition to the installation of accelerometers, other additional data sources were investigated in this context. The acoustic emission technology was used to detect robot gearbox faults based on the ball spinning and ball passing frequency of the bearings in [9]. The changes of the RMS-HI and characteristic frequencies for functional and broken strain gears of industrial robots were investigated in [10]. The classification and regression performance of different data-driven models based on frequency-domain data and principal component analysis for dimensionality reduction was evaluated in [11].

1.1.2. Time–Frequency-Based Health Indicators

In addition to vibration data based CM approaches for industrial robots, there also exist several publications considering HIs from the time–frequency-domain. Here, approaches based on the Short-time Fourier transform (STFT), Wavelet transform (WT) or Hilbert Huang transform (HHT) can be divided. STFT is used to derive two HIs named Prominence and Compliance in [12] to detect bearing faults based on their characteristic fault frequencies. A similarity measure between the STFT spectrograms based on standard deviation and correlation is combined with a simple classifier in [13] to detect bearing faults. The same objective was pursued in [14] by means of the marginal time integration of STFTs. Bearing fault classification by means of non-negative matrix factorization or convolutional neural networks and STFT was evaluated in [15,16].

In the field of WT, several approaches exist for different assets. CM of brushless DC motors is investigated based on energies for characteristic frequencies based on both STFT and WT in [17]. A decomposition rate is used in [18] for CM of electric drives based on WT. RMS and Kurtosis are calculated for the WT coefficients for broken bar fault detection in electric drives and combined with a neural network for fault classification in [19]. Bearing fault classification was performed with an SVM based on WT in combination with singular value decomposition for dimensionality reduction in [20]. The spectra of WT coefficients were the basis for the calculation of statistical HIs and frequency specific energy values for the CM of bearing faults in [21]. The similarities of continuous WT spectra are used as an HI for bearing fault detection [22]. The permutation entropy derived from flexible analytical wavelet transform was used as a feature for an SVM for bearing fault classification [23]. Impulse factor, Kurtosis and RMS based on WT coefficients were used for bearing fault detection of helicopters [24]. Statistical features and Hoelder's exponent were derived from WT coefficients for milling tool health state monitoring. Here, the HIs were the input for an SVM and Decision Tree classifier [25]. HIs were derived by a convolutional neural network for milling tool condition monitoring based on the wavelet decomposition in [26]. Energies of WT coefficients were also used for detecting generator and gear faults in wind turbines [27]. Different entropy-based and statistical features were used in [28] for gearbox health monitoring in combination with an SVM. Energy and entropy values derived from WT for characteristic frequencies are applied for gearbox condition monitoring in [29].

In [30], the Shannon entropy based on HHT was used for the CM of gears. HHT was also used in [31] to derive HIs by an autoencoder based on the Marginal Hilbert Spectrum. A component dependent frequency energy based on HHT was used as a label in [32] for a CNN-based regression model trained on raw vibration time series data for bearing fault detection. Different statistical and entropy-based HIs were calculated from the Intrinsic mode functions (IMFs) derived by HHT in [33].

1.2. Contribution to the State-of-the-Art

However, none of these publications assess vibration data-based HIs' ability to detect faults in an industry-like industrial robot application setting. It is characterized by

changing robot axes' velocities, changing temperatures of the gears due to unbalanced robot utilization and unknown robot gear fault types. This is why we present a new HI for robot gear condition monitoring, which potentially copes with these characteristics. Furthermore, we propose a method to evaluate the suitability of HIs for the task of robot gear condition monitoring. We apply this method on the newly formulated HI and several HIs from the state-of-the-art.

2. Materials and Methods

This section is divided in two parts. First, the newly developed HI is presented. Afterwards, the methodologies to evaluate the HI's performance and data sets used in this context are explained.

2.1. Time–Frequency-Domain-Based Z-Score

The concept of the newly designed HI is based on two cornerstones. To deal with instationary velocity regimes, which are found in robot applications due to the typical movement patterns of a robot, the HI is based on time–frequency-domain data. Simultaneously, the HI must take into account a certain variance of this data due to environmental changes such as temperature fluctuations. This is realized by the concept of Z-scores, a common similarity measure from statistics [34]. The process to calculate the new HI is depicted in Figure 1.

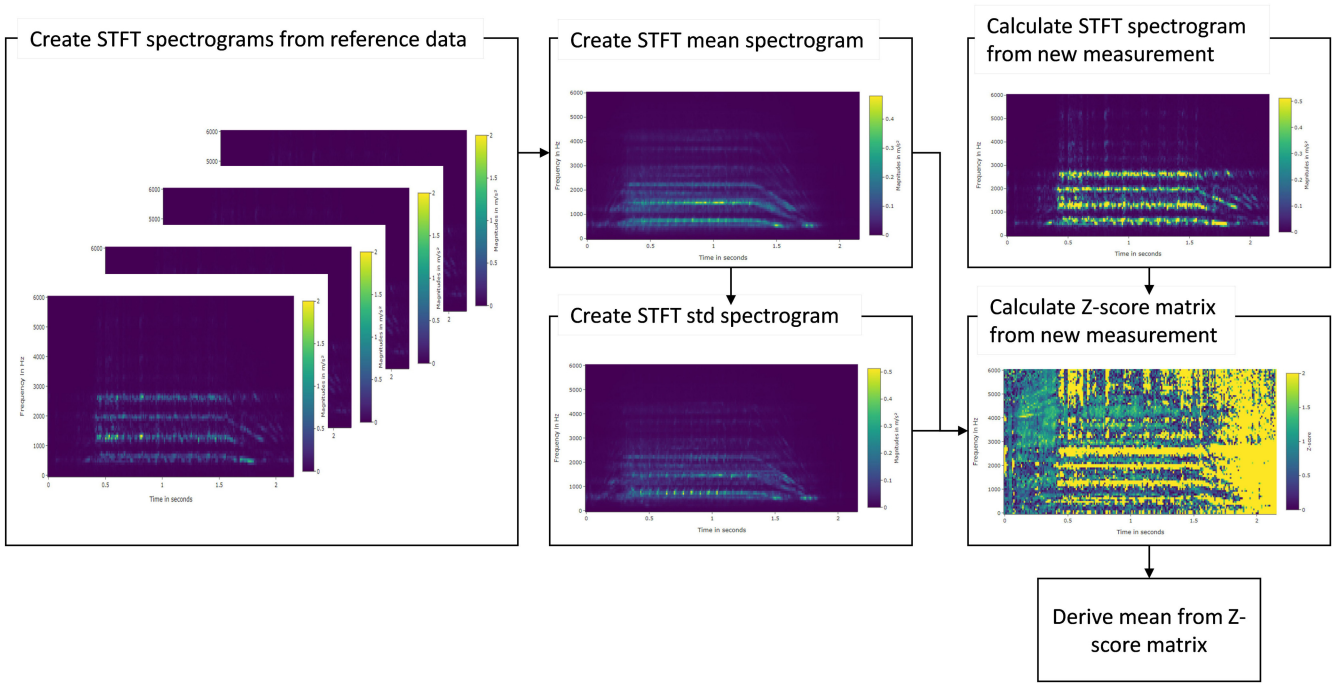

Figure 1. Process to derive the Z-score-based HI.

In detail, the new HI is based on high-frequency sampled acceleration sensor data. Data from one measurement are transformed to a time–frequency-spectrogram by usage of the STFT, which is calculated according to Equation (1). Here, τ and ω are time and frequency indices, $x(n)$ is the time series signal of the vibration signal at timestep n and w is a windowing function with the length R.

$$spec(\tau, \omega) = |\sum_{n=-\infty}^{\infty} x(n)w(n - \tau R)e^{-j\omega n}| \quad (1)$$

To set up the HI, a certain number of vibration signal spectrograms must be collected for the robot to capture its signal signature in a healthy state with its stochastic variations.

This takes place in an initialization phase. For this, initially, two measurements must be collected. In this context, a measurement is defined as the collection of vibration data over one single movement. Based on this data, the two spectrograms are calculated. To determine whether this reference quantity of two spectrograms captures the stochastic variation of the signal, the overall mean (Equation (2)) and standard deviation (Equation (3)) of the spectrograms are calculated.

$$spec(\tau,\omega)_{avg} = \frac{1}{k}\sum_{i=0}^{k} spec(\tau,\omega)_i \tag{2}$$

$$std_{spec,\ overall} = \frac{1}{0.5FT}\sum_{\tau=0}^{T}\sum_{\omega=0}^{0.5F}\sqrt{\frac{\sum_{i=0}^{k}(spec(\tau,\omega)_i - spec(\tau,\omega)_{avg})^2}{k}} \tag{3}$$

In these formulas, k describes the number of measurements in the reference quantity. T is the time length of each measurement, F is the sampling frequency and $spec(\tau,\omega)_{avg}$ is the average value of $spec(\tau,\omega)$ over measurements 0 to k. Afterwards, one measurement is added to the reference quantity at a time, and again $avg_{spec,overall}$ and $std_{spec,overall}$ are calculated. Plotting these standard deviations over the number of measurements in the reference quantity usually first shows an increase in $std_{spec,overall}$ and then a saturation as can be seen in Figure 2. If this saturation is reached, the reference quantity can sufficiently represent the stochastic behavior of the signal signature. In the shown example, this saturation is reached after 5 measurements.

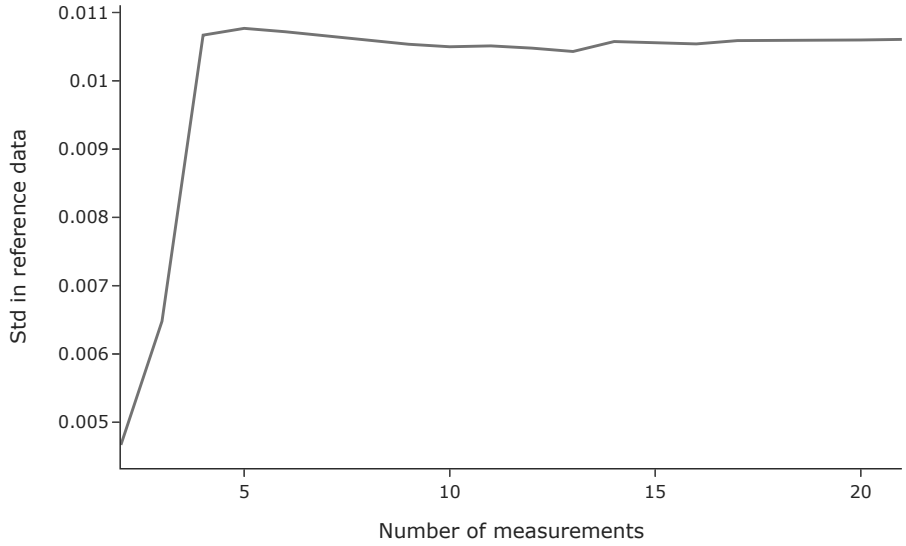

Figure 2. Saturation of the standard deviation in the time–frequency spectrograms.

After the initialization, an HI can be determined based on a newly collected measurement. For this, the measurement's spectrogram overall Z-score is determined according to Equation (4) .

$$HI_{meas} = \frac{1}{0.5FT}\sum_{\tau=0}^{T}\sum_{\omega=0}^{0.5F}\left|\frac{spec(\tau,\omega)_{meas} - spec(\tau,\omega)_{avg,ref}}{spec(\tau,\omega)_{std,ref}}\right| \tag{4}$$

In this context, $spec(\tau,\omega)_{avg,ref}$ and $spec(\tau,\omega)_{std,ref}$ are the mean value and the standard deviation of $spec(\tau,\omega)$ for all measurements in the reference quantity. In Figure 3, the STFT and Z-score spectrograms of exemplary vibration measurements from a healthy and a faulty robot gear are depicted. The Z-score-based spectrogram of the faulty measurement shows more prominent changes compared to the STFT-based spectrogram.

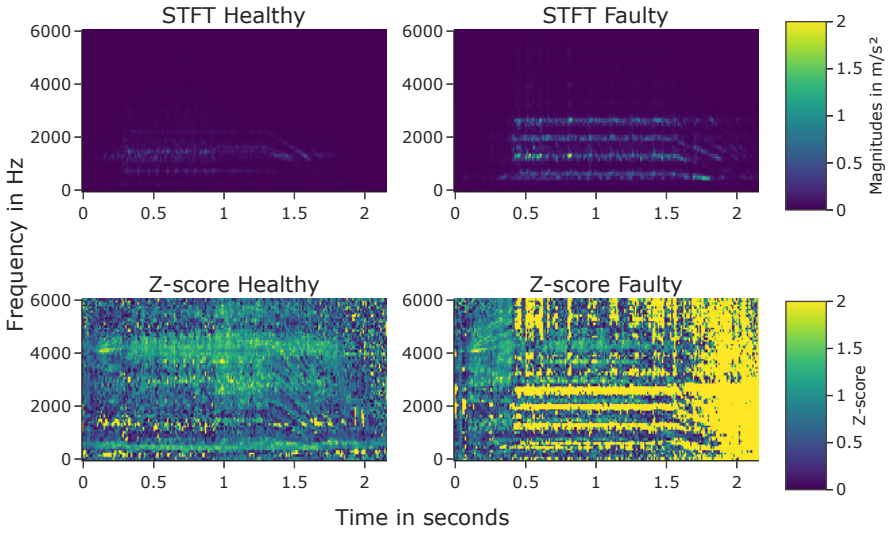

Figure 3. Comparison of STFT and Z-score spectrograms from healthy and faulty robot gear measurements.

2.2. Hi Evaluation Method

To compare the ability of the newly designed HI to cope with industrial robot application characteristics, we followed a three step approach. First of all, we investigated how well the designed HI can detect different kinds of faults in comparison to HIs from the state-of-the-art. Second, we investigated the temperature sensitivity of HIs from the state-of-the-art meeting this criterion and our HI. Third, we investigated the trend behavior of HIs showing a low temperature sensitivity on data from two accelerated wear tests. These three steps are now described more precisely. The overall process of our investigations is also described in Figure 4.

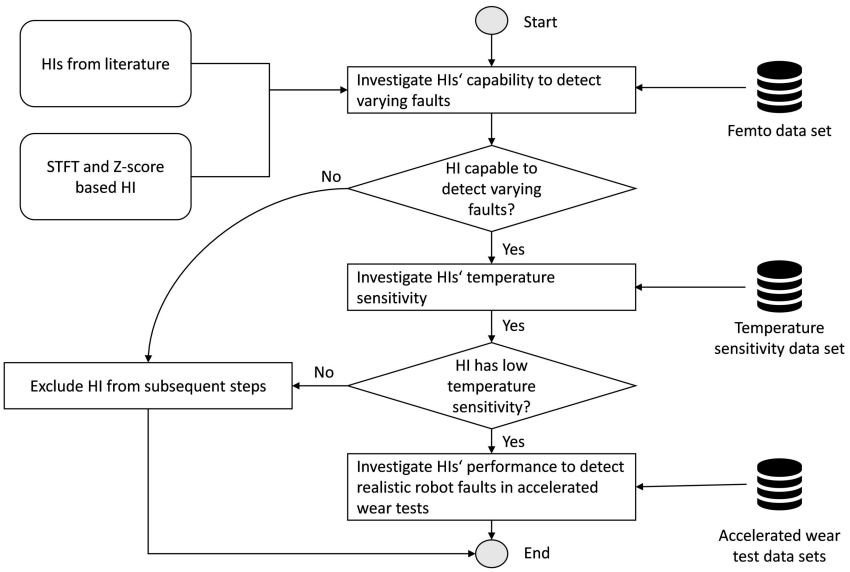

Figure 4. Overall process of the evaluation method.

2.2.1. Varying Fault Detection Analysis

We used the FEMTO data set, which is described in detail in [35], to select HIs capable of detecting different faults. The data set is available in [36]. This data set provides run to failure vibration data from 16 identical bearings and for different faults and working conditions defined by the applied load and the rotational speed. The acceleration sensor sampled data with 25.6 kHz, one measurement has a length of 0.1 s and measurements were

taken in equidistant timesteps of 10 s for all bearings. The test run for one bearing ended when the signal from the acceleration sensor exceeded 20 g. Therefore, different numbers of measurements are available per bearing ranging from 230 to 2803. We calculated the HIs summarized in Table 1 for all measurements of one sensor. These HIs were derived from several review papers regarding gearbox and bearing CM [37–40] and the publications mentioned in Section 1. Therefore, the HI calculation was based either on the raw acceleration signal, an enveloped signal as described in [41] or the residual signal as suggested by [4]. Additionally, the newly designed HI presented in Section 2 was calculated for the measurements based on the raw signals.

Table 1. Calculated HIs.

HI Name	HI Abbreviation	HI Source
Crest Factor	CrF	[40]
Dominant Frequency	DomF	[37]
Impulse Factor	ImpF	[38]
Kurtosis	Kurt	[39]
Margin Factor	MarF	[38]
Mean	Mean	[40]
Median	Med	[40]
Median Frequency	MedF	[37]
Peak	Peak	[39]
Peak to Peak	PtP	[39]
Root Mean Square	RMS	[39]
Skewness	Skew	[40]
Spectral Centroid	SpC	[37]
Spectral Flux	SpF	[37]
Spectral Rollover	SpRO	[37]
Spectral Entropy	SpE	[4]
Standard Deviation	Std	[39]
Discrete Wavelet RMS	DWTRMS	[19]
Discrete Wavelet Impulse Factor	DWTImpF	[19]
Discrete Wavelet Kurtosis	DWTKurt	[19,38]
Discrete Wavelet Entropy	DWTEntr	[4,19]
Discrete Wavelet Decomposition Rate	DecompRate	[18]
Hilbert Huang Entropy	HHTEntr	[30]
Intrinsic Mode Function RMS	IMFRMS	[33]
Intrinsice Mode Function Impulse Factor	IMFImpF	[33]
Intrinsic Mode Function Kurtosis	IMFKurt	[33]
Intrinsic Mode Function Entropy	IMFEntr	[33]
Time Domain Integral	TDI	[14]
Z-score	Z-score	-

To detect whether these HIs are sensitive to multiple faults, different techniques can be applied. In addition to filter techniques, ensemble, wrapper and embedded methods exist [42]. However, the latter three techniques combine classification or regression models with HIs for their evaluation. Hence, this evaluation is always dependent on the used models. Thus, we chose to use filter methods for the evaluation. Here, different figures of merit for regression and classification tasks can be applied, such as trendability, robustness, monotony or discriminance [42]. To combine these different performance indicators, we fitted different basic functions on the HIs calculated for the last 20 percent of measurements per bearing. These functions were first and second degree polynoms, exponential and sigmoid functions. For each of the fits, we calculated the R^2 value. This means that we received four R^2 values per HI and bearing. High R^2 values of these fits correlate with a high trendability, monotony, robustness and discriminance, which are desirable for HIs. To evaluate whether an HI can detect several damages, we considered only the best R^2 value

per HI and bearing. We plotted the statistics of these 16 remaining R^2 values per HI as a boxplot. Suitable HIs should show high R^2 values with low variance.

2.2.2. Temperature Sensitivity Analysis

HIs showing this behavior were analyzed regarding their temperature sensitivity. For this purpose, we acquired vibration data from an industrial robot test rig. This test rig consists of a KUKA KR510 industrial robot with an attached load of 365 kg. We attached acceleration sensors close to the gearboxes as shown in Figure 5 on the right side. These sensors have a sampling rate of 26 kHz. The acceleration direction of the sensors was orthogonal to their contact area. For data acquisition, the robot performed a trajectory where each joint was moved individually at different speeds in an angle area of 10°, as described in Figure 6, and for different gear temperatures in the range of 25 °C and 60 °C and 5 °C steps. One measurement per axis lasted 8 s. The gear temperature was measured at the gearbox cap with an infrared thermometer. For each temperature step, four measurements were made. For each measurement at each temperature step, the remaining HIs were calculated. To determine the temperature sensitivity, we divided the average HI values calculated from measurements at the highest gear temperatures by the values calculated from measurements at the lowest temperature. HIs with a high sensitivity were eliminated for the last step.

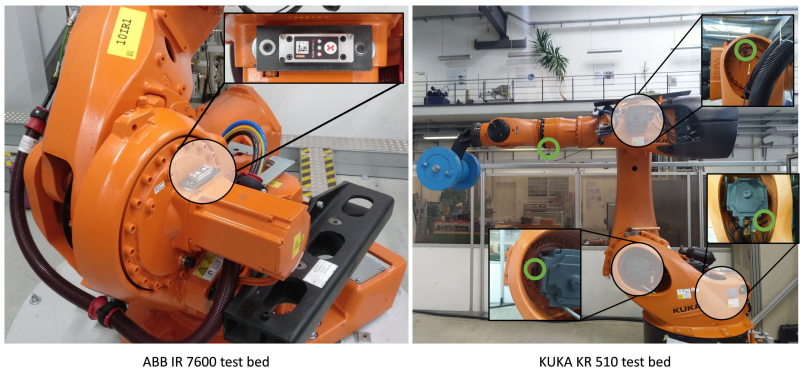

Figure 5. Robot test beds.

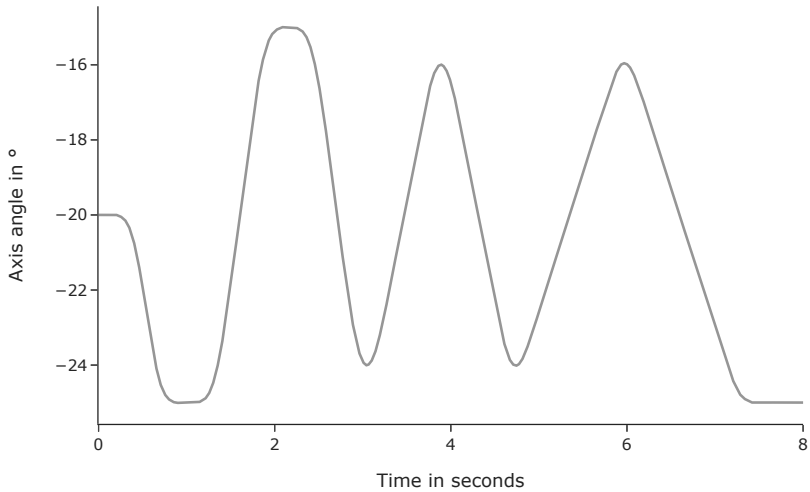

Figure 6. Measurement trajectory for the temperature sensitivity analysis.

2.2.3. Accelerated Wear Test Analysis

Here, we calculated the remaining HIs for measurements from two data sets from accelerated robot wear tests to see how these HIs perform in a more industry like setting

and how they cope with instationary velocity behavior. The first data set was collected during a time range of approximately one year with an ABB robot of type RB 6600-255/2.55. During the data acquisition, the robot performed an isolated movement of the second axis in an angle area of 150° for each measurement. Vibration data were only acquired with a sensor attached axially at the robot axis 2 gearbox. At the end of the experiment, the gearbox was dismantled and faults on the bearings and the shafts of the gear were found. A total of 2290 measurements, equally distributed over time, were taken for our analysis from this data set. One measurement lasted 1.6 s and the sampling rate was 10 kHz. More detailed information about this experiment can be found in [7,8]. The second data set was derived from another experiment. Here, the second axis of an ABB IRB 7600-340/2.8 was moved in an angle area of 80° continuously over the time frame of three months. The vibration sensor attached to the gearbox cap of axis 2 sampled with 20 kHz and one measurement lasted 2.15 s. The measurement setup is presented on the left side in Figure 5. The experiment ended after a roller element of a bearing had cracked and had blocked the gear. In this time range, 920 vibration measurements were taken in total in equidistant time steps. The faults, which occurred in both experiments, can be seen in Figure 7. In both experiments, environmental conditions such as load and trajectory were kept constant. Fluctuations of the temperature were kept at a minimum due to the constant movements of the robots. In this way, signal changes are likely to be correlated to increasing wear.

Figure 7. Faults in the accelerated wear tests, lower image following [7].

3. Results

This section is divided in three parts. First, the results from the varying fault detection experiments are shown. Secondly, the results from the temperature sensitivity analysis are presented. Finally, the application of the HIs on the two accelerated wear tests is described.

3.1. Varying Fault Detection Analysis

From the 16 bearing experiments, the HIs presented in Table 1 were calculated. We used the first 100 measurements per bearing as the reference quantity for the Z-score-HI and set R to 128. Figure 8 shows the R^2 values for a selection of different HIs as a box plot. The R^2 statistics for all HIs can be found in Appendix A. The abbreviations of the HIs are explained in Table 1. The PtP-, Peak-, RMS-, Std- and Z-score-HI show the highest R^2 values on average. They also show the lowest variance between the different bearings. This means that these HIs detect different faults most reliably. Other HIs show also high trend values but only for some of the bearings. HIs derived from the frequency-domain

(DomF, SpC, SpE, SpF, SpRO) perform worse compared to HIs from the time-domain. The preprocessing steps of enveloping the signal or calculating the residual signal do not affect the HI trend behavior significantly, which can be seen in Tables A1–A3. The TDI-, and DWTRMS-HI for specific frequency bands also show high average values with changing variance (see Table A4). If these HIs would be used for robot gear condition monitoring, the progress of all frequency band specific HIs would have to be tracked as different faults stimulate changes in different frequency bands.

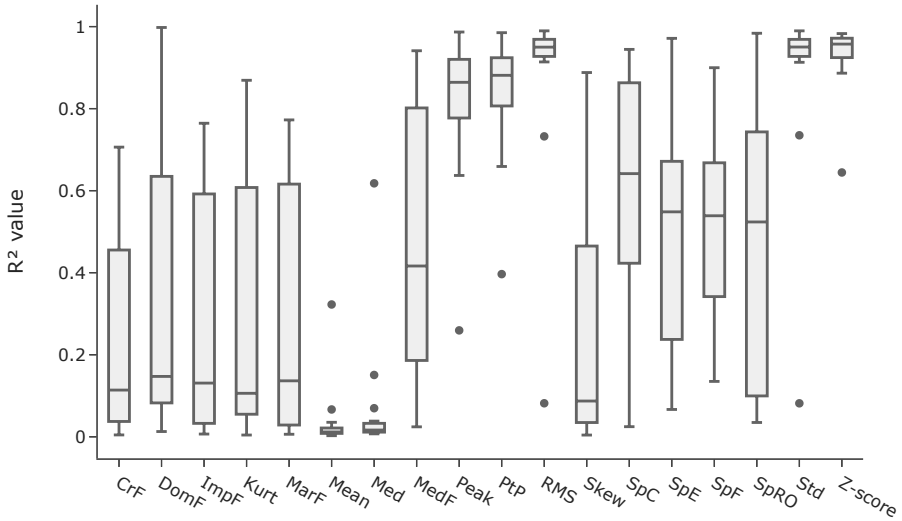

Figure 8. R^2 values for different HIs and bearings from the FEMTO data set based on raw signals.

3.2. Temperature Sensitivity Analysis

Based on this result, we conducted the temperature sensitivity analysis for the PtP-, Peak-, RMS-, Std-, TDI-, DWTRMS- and Z-score-HI. Here, we used one measurement per temperature step as the reference quantity for the Z-score-HI and set R to 128. Figure 9 shows the change of the HIs per axis in percent for the PtP-, Peak-, RMS-, Std- and Z-score-HI. The RMS- and Z-score-HI show the lowest temperature sensitivity overall. Figure 10 shows the results for the DWTRMS-HIs. Here, high sensitivities for different detail coefficient DWTRMS-HIs exist. Figure A1 shows the temperature sensitivity of the TDI-HIs of different frequency bands. Here, a similar result can be seen compared to the DWTRMS-HIs. The data of Figures 10 and A1 can also be found in Tables A5 and A6. In general, the data from axis 4 show the highest temperature sensitivity for all HIs. The comparably higher sensitivity of the HI values derived from data at axis 4 can be related to the robot trajectory. During the trajectory, the robot arm was stretched out, which leads to greater elasticity at the position of the sensor at axis 4. This can cause increased vibrations, which are magnified under changing temperature influences. Given the results of the temperature sensitivity analysis, we analyzed the data sets from the accelerated wear tests with only the RMS- and the Z-score-HI. The other HIs were excluded due to their high temperature sensitivity. Even though some frequency band specific DWTRMS-HIs and TDI-HIs show low sensitivity, they were excluded as robot gear faults do not have to stimulate these frequency bands with low sensitivity.

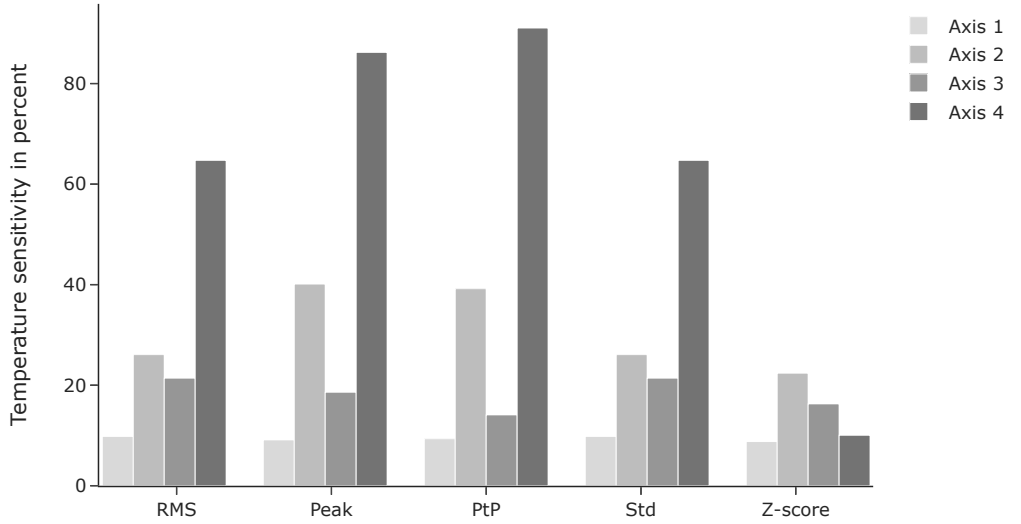

Figure 9. Temperature sensitivity for different HIs and robot axes.

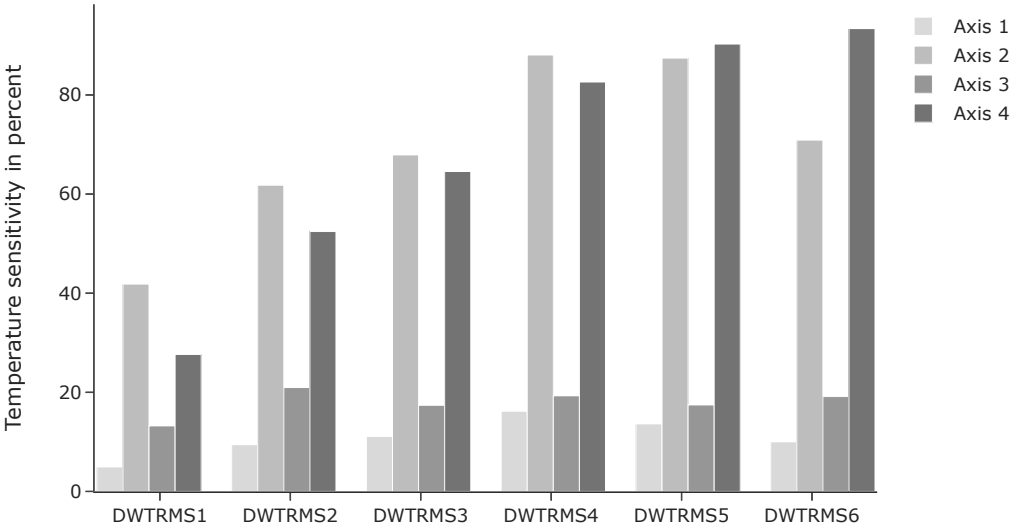

Figure 10. Temperature sensitivity for different DWTRMS-HIs and robot axes.

3.3. Accelerated Wear Tests Analysis

In this analysis, we used the first 100 measurements as the reference quantity for the Z-score-HI and set R to 256. For smoothing, we applied a rolling average with a window length of 15 on both HI series. The progress of the HIs in the accelerated wear test of the ABB IRB 7600 is shown in Figure 11. Both HIs show a plateau with increased values at the end of the experiment. It can be assumed that, at this point in time, faults have already been present. Here, the increased HI values over a longer time period could have been used as a decision criterion for maintenance actions.

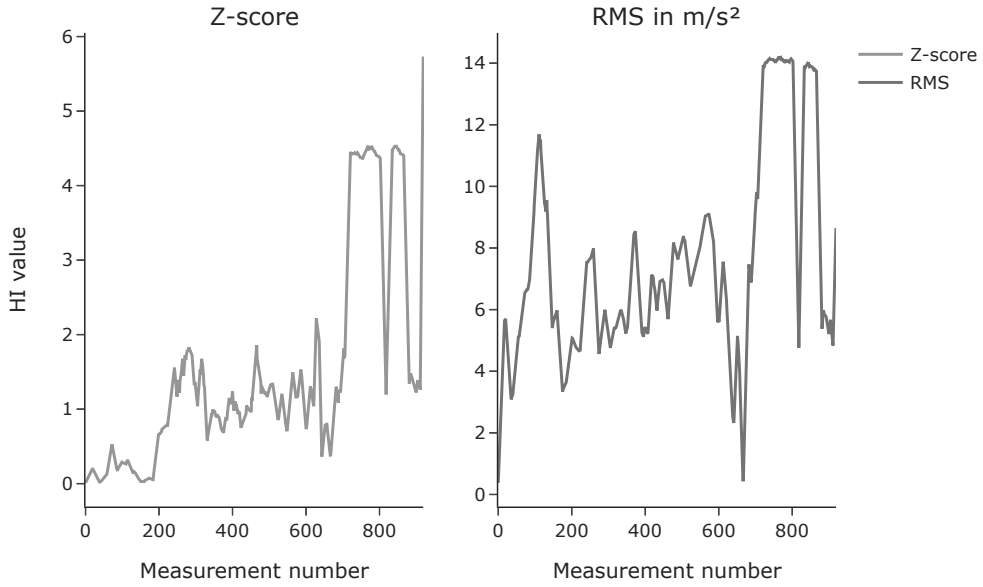

Figure 11. Z-score-HI and RMS-HI for the IRB 7600 experiment.

The measurements at the very end show decreased values again. We assume that this decrease is correlated to a part of the bearing roller. In the end of the experiment, one of the roller elements showed a large pit. During the measurements showing the higher HI values this detached part of the roller element could have been still slightly fixed at the roller element and thus could have caused high vibration. After full detachment, this noise level decreased again. For the measurements before the plateau, the RMS-HI shows higher fluctuations compared to the Z-score-HI. For instance, the RMS-HI shows a first high peak around measurement 100. Such peaks could lead to false alarms in a condition monitoring scenario and should be avoided.

The progress of the HIs in the other accelerated wear test performed with the ABB IRB 6600 is shown in Figure 12. Here, the Z-score-HI shows a trending behavior and the RMS shows a stationary progress. Both HIs show a high increase during the last measurements. In this experiment, the trending behavior of the Z-score could have been a criterion to execute maintenance actions. This information is not present in the RMS-progress. Based on the fact that the Z-score showed a better trend behavior in the ABB IRB 6600 experiment and less noisy behavior in the ABB IRB 7600 experiment, we suggest the use of the Z-score-HI for the condition monitoring of robot gears.

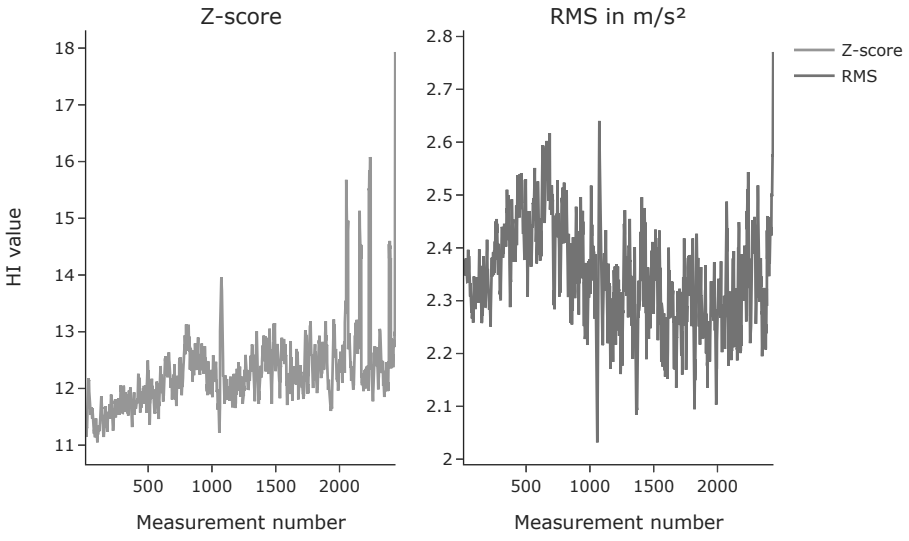

Figure 12. Z-score-HI and RMS-HI for the IRB 6600 experiment.

4. Discussion

The discussion is divided in four parts. First, some remarks regarding our designed HI are given. Afterwards, three parts make up the Results subsections.

To derive the spectrograms required for the Z-score-HI, the length of the window function must be defined. High values for R result in a high frequency resolution and low values in a high time resolution. For the individual experiments, we chose window lengths that lead to a good compromise between time and frequency resolution by inspecting spectrograms created with different window lengths. We chose window lengths that lead to spectrograms appearing the least noisy in a visual inspection. In an industrial setting, an automated approach should be developed for this dependent on the robot's trajectory and the used sensor.

The motivation to use the FEMTO data set to investigate HI performance was to assess HIs' capability to detect multiple faults. Within a robot gearbox, which are mostly RV reducers, not only bearings but also the gear teeth can have faults. Such faults are not taken into account by our analysis explicitly. However, the bearing faults present in the FEMTO data set, e.g., pitting, are similar to typical gear teeth or shaft damage from a signal analysis point of view. Damage from all components modulate the acceleration signals at a specific frequency and its sidebands. Exactly this capability to track such changes in the signal was investigated in our analysis. There also exist HIs that track energy changes at the specific component fault frequencies. Such HIs were excluded from our analysis because expert knowledge about the geometric characteristics of the gears, e.g., the bearing diameters or the number of roller elements, is required to calculate these HIs. This expert knowledge is usually not available to industrial robot users. We also excluded HIs that could be derived automatically from machine learning models, such as autoencoders, as the physical interpretation of these HIs is difficult and hence a transferability between different robot systems is questionable from our point of view.

Regarding the results of the temperature sensitivity analysis, it must be pointed out that the results are valid only for the chosen robot trajectory. As the dynamic behavior of the robot changes within its working space, this analysis should be performed individually for trajectories and robot systems. However, from a theoretical point of view, the Z-score-HI possesses the ability to cope with these temperature fluctuations independently of the trajectory. Temperature variations lead to variance in the STFT spectrograms. This variance is taken into account in the $spec(\tau, \omega)_{avg,ref}$ and $spec(\tau, \omega)_{std,ref}$ during the initialization phase. Hence, Z-score-HIs derived from measurements from functional robot gears and different temperatures will show only little differences in the Z-score-HI value. This becomes more clear considering Figure 13. Here, the STFT and Z-score spectrograms from two vibration measurements of the temperature sensitivity experiment are shown. On the left side, the spectrograms from a cold gear measurement are depicted. On the right side, the spectrograms from a warm gear measurement are shown. Differences are visible in the STFT spectrograms around seconds 1 and 2. No differences are visible in the Z-score spectrograms. The scales of the STFT spectrograms reach from -5 to 0 and the scales of the Z-score spectrograms from 0 to 1.5. Hence, the relative changes of the STFT spectrograms are bigger compared to the Z-score spectrograms. In this example, the total relative change in energy in the STFT spectrogram is 9.15 percent, whereas the total relative change in the Z-score spectrogram is just 1.63 percent.

Finally, the results from the accelerated wear tests show noisy progress over time. This hinders a simple or automated detection of faults in a condition monitoring behavior. To establish an automated CM system, a suitable trend detection in combination with an outlier detection system must be set up. A trend detection system could identify HI progress shown as in Figure 12, whereas an outlier detection system could detect progress as depicted in Figure 11. The development of such a system also marks the outlook of our future work.

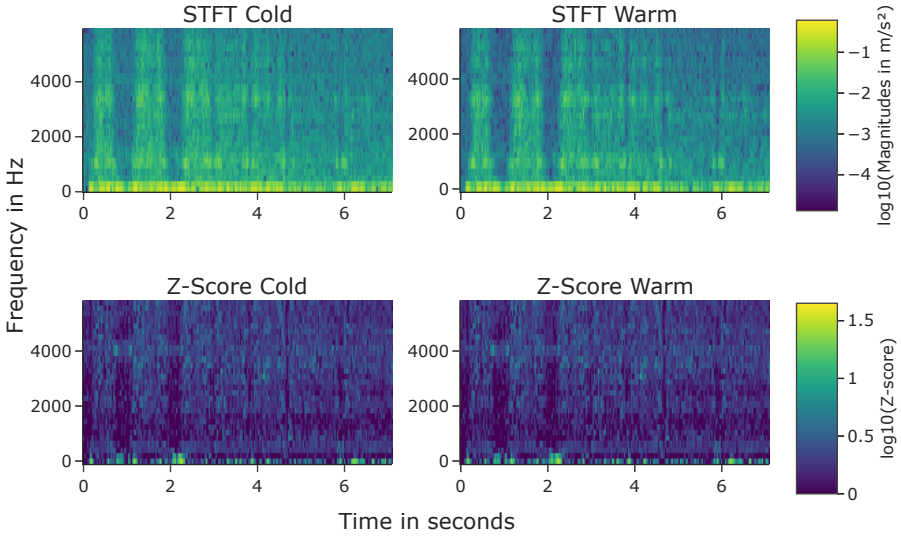

Figure 13. Spectrograms from cold and warm gear measurements.

5. Conclusions

Condition monitoring of robot gears has the potential to decrease production system downtimes. The state-of-the-art provides many health indicators to track the health state of gears. We analyzed these health indicators regarding specific requirements rising from typical industrial robot applications. These requirements are the ability to detect different faults, low temperature sensitivity and the capability to deal with instationary velocity behavior. Additionally, we suggested a new health indicator based on STFT spectrograms and Z-scores that can cope with these requirements. Our analysis showed that the RMS health indicator and our suggested health indicator meet the defined requirements the best. Data from accelerated wear tests show that for an automatic condition monitoring system a combination of a trend detection and an outlier detection system that can deal with a noisy signal is required.

Author Contributions: Conceptualization, C.N. and G.R.; methodology, C.N.; software, C.N.; validation, C.N.; formal analysis, C.N.; investigation, C.N.; resources, G.R.; data curation, C.N.; writing—original draft preparation, C.N.; writing—review and editing, G.R.; visualization, C.N.; supervision, G.R.; project administration, C.N.; funding acquisition, G.R. All authors have read and agreed to the published version of the manuscript.

Funding: We express our gratitude to the Bavarian Ministry of Economic Affairs, Regional Development, and Energy for the funding of our research. The formulated outlook will be investigated as part of the research project "KIVI" (grant number IUK-1809-0008 IUK597/003) and will be further developed and implemented.

Institutional Review Board Statement: Not applicable.

Informed Consent Statement: Not applicable.

Data Availability Statement: The data presented in this study are available on request from the corresponding author. The data are not publicly available due to confidentiality reasons.

Conflicts of Interest: The authors declare no conflict of interest. The funders had no role in the design of the study; in the collection, analyses, or interpretation of data; in the writing of the manuscript, or in the decision to publish the results.

Appendix A

Table A1. R^2 statistics for HIs derived from the normal signal.

	CrF	DomF	ImpF	Kurt	MarF	Mean	Med	MedF	Peak	PtP	RMS	Skew	SpC	SpE	SpF	SpRO	Std	Z-Score
Mean	0.231	0.354	0.287	0.336	0.296	0.034	0.063	0.467	0.822	0.844	0.887	0.242	0.599	0.488	0.514	0.491	0.887	0.934
Std	0.246	0.351	0.289	0.334	0.298	0.076	0.147	0.311	0.173	0.145	0.215	0.289	0.298	0.281	0.225	0.322	0.215	0.080
Min	0.005	0.013	0.007	0.004	0.006	0.003	0.007	0.024	0.259	0.397	0.082	0.004	0.025	0.067	0.135	0.035	0.082	0.644
Max	0.706	0.998	0.764	0.869	0.773	0.323	0.618	0.941	0.987	0.985	0.990	0.888	0.944	0.971	0.900	0.984	0.990	0.983

Table A2. R^2 statistics for HIs derived from the enveloped signal.

	CrF	DomF	ImpF	Kurt	MarF	Mean	Med	MedF	Peak	PtP	RMS	Skew	SpC	SpE	SpF	SpRO	Std
Mean	0.215	0.139	0.284	0.299	0.296	0.776	0.819	0.496	0.816	0.816	0.872	0.275	0.605	0.464	0.462	0.514	0.898
Std	0.229	0.248	0.283	0.328	0.291	0.296	0.248	0.318	0.178	0.178	0.227	0.303	0.286	0.298	0.276	0.309	0.131
Min	0.005	0.001	0.006	0.001	0.005	0.010	0.014	0.023	0.246	0.246	0.074	0.008	0.046	0.013	0.012	0.007	0.427
Max	0.635	0.997	0.741	0.919	0.766	0.977	0.983	0.981	0.988	0.988	0.989	0.905	0.939	0.978	0.901	0.987	0.987

Table A3. R^2 statistics for HIs derived from the residual signal as suggestet by [4].

	CrF	DomF	ImpF	Kurt	MarF	Mean	Med	MedF	Peak	PtP	RMS	Skew	SpC	SpF	SpRO	Std	SpE
Mean	0.329	0.423	0.348	0.365	0.355	0.032	0.088	0.608	0.847	0.859	0.884	0.237	0.701	0.609	0.605	0.884	0.534
Std	0.270	0.348	0.303	0.337	0.312	0.089	0.187	0.292	0.178	0.153	0.221	0.319	0.196	0.202	0.213	0.221	0.316
Min	0.010	0.021	0.003	0.007	0.018	0.001	0.001	0.016	0.211	0.328	0.082	0.003	0.425	0.147	0.132	0.083	0.023
Max	0.802	0.992	0.828	0.858	0.830	0.374	0.671	0.988	0.987	0.987	0.990	0.943	0.959	0.930	0.977	0.990	0.969

Table A4. R^2 statistics for HIs derived from the time–frequency-domain. DWT-, IMF-, and TDI-based HIs were calculated for different frequency bands. The frequency bands are encoded in the abbreviation of the HI name. Large numbers correspond to high frequency bands for TDI-HIs and low frequency bands for DWT- and IMF-HIs.

	Mean	Std	Min	Max
DWTRMS5	0.891	0.207	0.099	0.990
DWTRMS4	0.889	0.223	0.032	0.988
TDI33	0.882	0.087	0.583	0.965
DWTRMS6	0.882	0.216	0.117	0.991
TDI43	0.871	0.156	0.296	0.983
IMFRMS2	0.869	0.227	0.014	0.991
TDI36	0.867	0.203	0.095	0.976
TDI14	0.865	0.154	0.327	0.970
TDI35	0.864	0.202	0.096	0.981
TDI22	0.862	0.196	0.135	0.963
TDI34	0.861	0.197	0.114	0.974
TDI23	0.860	0.181	0.200	0.961
TDI21	0.859	0.197	0.147	0.971
DWTRMS3	0.859	0.245	0.019	0.998
TDI37	0.857	0.208	0.072	0.969
TDI39	0.853	0.221	0.017	0.975
TDI15	0.847	0.218	0.035	0.982
IMFRMS1	0.845	0.210	0.091	0.978
TDI44	0.844	0.223	0.004	0.984
TDI13	0.842	0.224	0.015	0.975
TDI12	0.841	0.218	0.022	0.969
TDI40	0.840	0.215	0.072	0.969
TDI24	0.837	0.223	0.027	0.954
TDI41	0.836	0.221	0.061	0.970
TDI16	0.833	0.228	0.022	0.969
TDI42	0.830	0.221	0.072	0.964
TDI18	0.830	0.237	0.044	0.976
TDI10	0.830	0.214	0.025	0.966
TDI5	0.827	0.273	0.032	0.995
TDI6	0.825	0.263	0.015	0.983
TDI8	0.825	0.206	0.051	0.948
TDI9	0.824	0.209	0.047	0.954
TDI4	0.823	0.273	0.151	0.995
TDI45	0.820	0.220	0.013	0.986
TDI20	0.818	0.277	0.066	0.963
TDI38	0.816	0.259	0.038	0.972
TDI32	0.815	0.272	0.090	0.968
TDI46	0.813	0.218	0.023	0.987
TDI7	0.813	0.264	0.008	0.973
TDI47	0.812	0.217	0.013	0.988
TDI11	0.812	0.251	0.017	0.966
TDI17	0.808	0.293	0.005	0.967
DWTRMS2	0.804	0.297	0.101	0.981
IMFRMS3	0.803	0.243	0.025	0.961
TDI3	0.803	0.290	0.148	0.987
TDI49	0.792	0.215	0.018	0.990
TDI19	0.782	0.304	0.026	0.959
TDI28	0.782	0.270	0.014	0.960
TDI50	0.780	0.216	0.026	0.989
TDI52	0.770	0.216	0.025	0.989
TDI30	0.769	0.293	0.049	0.964
TDI25	0.769	0.290	0.025	0.966
TDI53	0.767	0.215	0.025	0.989
TDI54	0.766	0.215	0.025	0.990

Table A4. *Cont.*

	Mean	Std	Min	Max
TDI48	0.765	0.252	0.024	0.988
TDI55	0.765	0.215	0.028	0.989
TDI58	0.762	0.215	0.026	0.990
TDI57	0.761	0.216	0.028	0.989
TDI60	0.756	0.222	0.028	0.989
TDI31	0.747	0.312	0.073	0.971
TDI51	0.747	0.253	0.022	0.989
TDI29	0.744	0.297	0.032	0.961
TDI2	0.744	0.319	0.069	0.977
DWTRMS1	0.740	0.306	0.026	0.978
TDI27	0.739	0.292	0.027	0.954
TDI63	0.736	0.253	0.028	0.989
TDI62	0.736	0.254	0.026	0.990
TDI59	0.735	0.254	0.024	0.990
TDI56	0.735	0.254	0.023	0.989
TDI61	0.734	0.254	0.024	0.989
TDI64	0.732	0.254	0.024	0.989
TDI26	0.712	0.342	0.043	0.964
IMFRMS4	0.665	0.335	0.035	0.985
HHTentr	0.646	0.317	0.021	0.982
TDI1	0.588	0.313	0.011	0.937
IMFRMS5	0.567	0.313	0.016	0.934
IMFRMS6	0.460	0.223	0.110	0.829
DecompRate	0.458	0.292	0.075	0.974
DWTKurt5	0.383	0.296	0.014	0.821
DWTKurt2	0.381	0.318	0.007	0.815
DWTEntr6	0.380	0.319	0.017	0.991
DWTImpF2	0.377	0.308	0.005	0.806
DWTKurt4	0.361	0.315	0.007	0.851
DWTKurt6	0.353	0.330	0.003	0.860
DWTImpF6	0.327	0.280	0.001	0.796
DWTImpF5	0.326	0.274	0.001	0.766
IMFRMS7	0.326	0.271	0.026	0.863
TDI0	0.325	0.246	0.037	0.906
DWTImpF3	0.325	0.260	0.017	0.701
IMFKurt1	0.320	0.314	0.009	0.816
DWTKurt3	0.319	0.296	0.007	0.827
DWTImpF4	0.302	0.273	0.004	0.748
IMFImpF1	0.288	0.280	0.009	0.838
IMFKurt3	0.287	0.288	0.017	0.843
IMFKurt4	0.286	0.222	0.024	0.677
DWTKurt1	0.282	0.217	0.012	0.722
IMFImpF4	0.277	0.202	0.014	0.601
IMFKurt2	0.263	0.274	0.010	0.689
IMFEntr2	0.254	0.265	0.012	0.867
DWTEntr5	0.254	0.291	0.001	0.989
DWTImpF1	0.251	0.213	0.006	0.660
IMFImpF3	0.242	0.253	0.016	0.761
IMFEntr1	0.232	0.280	0.009	0.944
IMFImpF2	0.224	0.185	0.011	0.602
IMFEntr3	0.207	0.269	0.013	0.888
IMFKurt5	0.184	0.215	0.007	0.822
IMFRMS8	0.181	0.238	0.000	0.682
IMFImpF5	0.164	0.187	0.007	0.693
IMFEntr4	0.153	0.138	0.005	0.524
DWTEntr4	0.136	0.235	0.005	0.969
IMFImpF6	0.121	0.118	0.010	0.377
IMFKurt6	0.121	0.125	0.010	0.428

Table A4. *Cont.*

	Mean	Std	Min	Max
IMFEntr6	0.105	0.102	0.009	0.393
DWTEntr3	0.101	0.187	0.003	0.783
IMFEntr5	0.095	0.095	0.002	0.367
IMFEntr7	0.089	0.092	0.003	0.276
DWTEntr2	0.062	0.111	0.001	0.417
IMFImpF7	0.048	0.039	0.002	0.134
IMFKurt7	0.042	0.033	0.002	0.106
IMFEntr8	0.032	0.111	0.000	0.461
DWTEntr1	0.031	0.034	0.003	0.141
IMFImpF8	0.026	0.028	0.000	0.078
IMFKurt8	0.021	0.031	0.000	0.114
IMFRMS9	0.000	0.000	0.000	0.000
IMFKurt9	0.000	0.000	0.000	0.000
IMFImpF9	0.000	0.000	0.000	0.000
IMFEntr9	0.000	0.000	0.000	0.000
IMFRMS10	0.000	0.000	0.000	0.000
IMFImpF10	0.000	0.000	0.000	0.000
IMFKurt10	0.000	0.000	0.000	0.000
IMFEntr10	0.000	0.000	0.000	0.000
IMFRMS11	0.000	NaN	0.000	0.000
IMFImpF11	0.000	NaN	0.000	0.000
IMFKurt11	0.000	NaN	0.000	0.000
IMFEntr11	0.000	NaN	0.000	0.000

Table A5. Temperature sensitivity of the different DWTRMS-HIs.

	1	2	3	4
DWTRMS1	4.944734	41.833250	13.225817	27.640727
DWTRMS2	9.431779	61.784386	20.966405	52.444752
DWTRMS3	11.100870	67.906341	17.372290	64.555873
DWTRMS4	16.176322	88.064015	19.294715	82.614996
DWTRMS5	13.631686	87.439763	17.451681	90.271799
DWTRMS6	10.015797	70.887870	19.141733	93.391435

Table A6. Temperature sensitivity of the different TDI-HIs.

	Axis 1	Axis 2	Axis 3	Axis 4
TDI0	7.887680	3.623626	4.032428	9.856386
TDI1	7.345230	13.780192	1.419329	15.104011
TDI2	5.702217	46.387687	23.876372	24.639909
TDI3	6.721355	47.590460	22.691756	42.390072
TDI4	10.873829	59.621503	24.158641	38.671919
TDI5	13.127752	74.783219	17.398075	54.988992
TDI6	14.670516	59.576255	12.953424	75.739203
TDI7	18.161779	57.596831	17.545132	65.254182
TDI8	15.090433	70.501830	11.004508	68.946535
TDI9	19.130819	94.756567	10.267873	63.083458
TDI10	19.817337	140.434648	22.212611	48.494003
TDI11	31.037879	152.473705	28.134321	75.366125
TDI12	33.675873	93.057559	18.953184	98.385403
TDI13	26.250892	79.866002	17.152706	92.669107
TDI14	11.635896	58.286933	24.510069	86.809206
TDI15	23.377379	46.907903	16.496553	72.502066
TDI16	30.064213	55.243855	11.119799	59.119520
TDI17	21.268743	64.332588	7.938803	79.776374

Table A6. *Cont.*

	Axis 1	Axis 2	Axis 3	Axis 4
TDI18	9.808639	52.933143	4.197856	87.106639
TDI19	3.420408	57.102301	3.507140	94.175140
TDI20	0.062629	58.697728	5.538016	107.584154
TDI21	17.433815	60.093605	12.872000	112.916761
TDI22	23.980438	65.038102	9.486835	164.461250
TDI23	23.749318	91.055389	11.379480	152.353906
TDI24	11.483126	109.842746	21.619409	121.442989
TDI25	6.596706	85.653753	23.250270	111.067700
TDI26	16.057350	68.794132	20.724566	88.922105
TDI27	16.557670	68.373539	18.973086	114.047417
TDI28	19.372075	65.937430	13.256130	140.639806
TDI29	22.613427	68.081118	27.002980	129.175849
TDI30	15.441241	68.255349	31.219217	111.829705
TDI31	4.729546	68.353458	28.824115	116.071704
TDI32	1.112630	69.440683	18.666493	104.393062
TDI33	3.010018	66.107354	13.594603	104.544706
TDI34	6.223136	49.771212	14.597765	135.411471
TDI35	10.119042	33.536590	4.257545	167.094574
TDI36	0.777079	33.963467	0.393118	158.518025
TDI37	0.893584	47.211867	18.367647	110.996278
TDI38	8.789406	39.550853	33.938136	55.254421
TDI39	18.286551	4.903817	23.615781	35.301715
TDI40	28.767525	34.224059	6.485524	47.061077
TDI41	21.670495	39.728416	9.696093	33.227046
TDI42	4.437817	59.765908	18.549288	79.919517
TDI43	0.147523	52.939389	19.848252	83.294446
TDI44	0.446057	53.539446	19.351326	79.595920
TDI45	0.657082	52.356513	19.032092	77.824663
TDI46	0.199947	55.873800	19.528656	75.827413
TDI47	1.388775	57.010168	19.014225	76.394986
TDI48	2.097117	57.774286	18.889822	76.077127
TDI49	3.164926	58.959065	18.696796	75.814731
TDI50	3.851514	59.592621	18.410404	75.719379
TDI51	4.577587	60.339446	18.308180	75.543086
TDI52	5.160258	60.877095	18.211340	75.458546
TDI53	5.659315	61.365144	18.069126	75.348426
TDI54	6.077128	61.761218	17.976632	75.218693
TDI55	6.436426	62.077612	17.945549	75.121278
TDI56	6.763257	62.361230	17.851473	75.050770
TDI57	7.080730	62.591447	17.781367	74.975471
TDI58	7.369667	62.781646	17.783673	74.880725
TDI59	7.622924	62.946830	17.710259	74.853578
TDI60	7.828532	63.078384	17.670637	74.815067
TDI61	7.974544	63.177746	17.693925	74.733074
TDI62	8.072173	63.259698	17.636933	74.758740
TDI63	8.128858	63.308959	17.623715	74.750804
TDI64	8.147158	63.322210	17.664456	74.689287

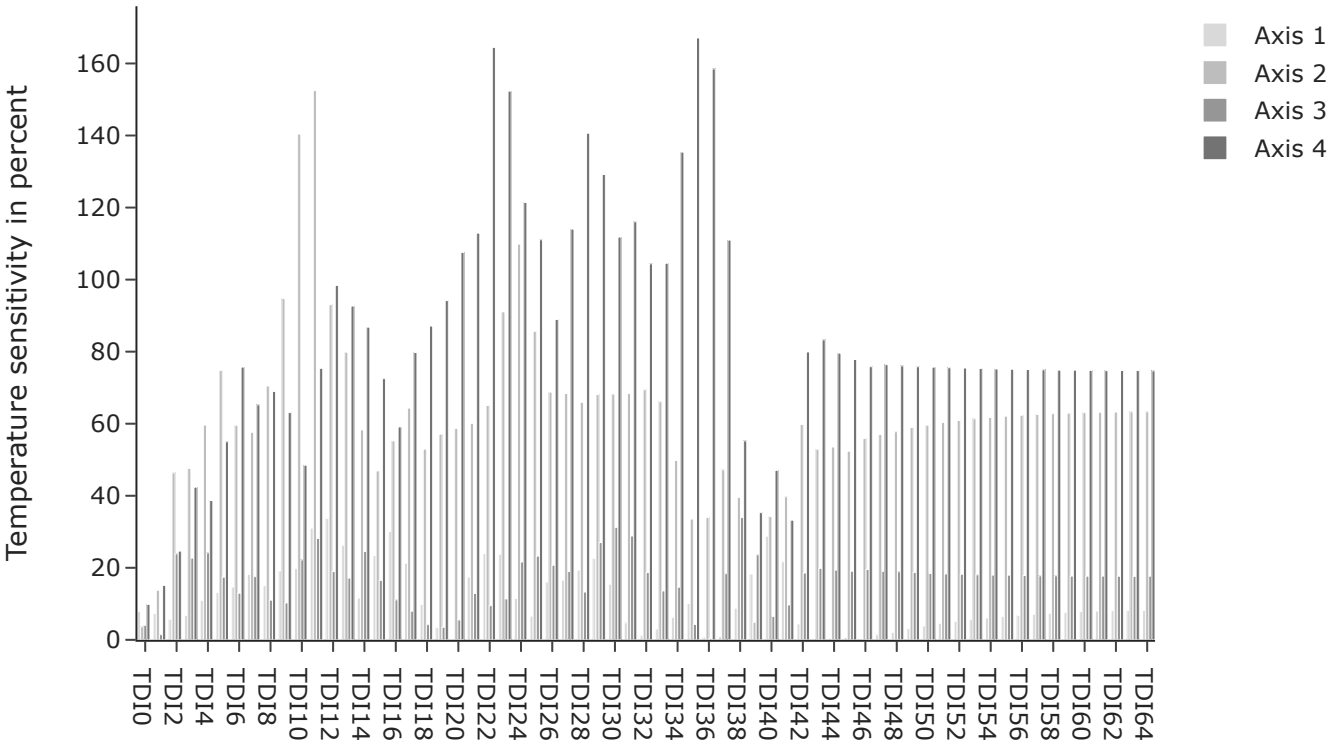

Figure A1. Temperature sensitivity for the different TDI-HIs and robot axes.

References

1. Krockenberger, O. Industrial Robots for the Automotive Industry. *Sae Tech. Pap. Ser.* **1996**. [CrossRef]
2. Lee, J.; Wu, F.; Zhao, W.; Ghaffari, M.; Liao, L.; Siegel, D. Prognostics and health management design for rotary machinery systems—Reviews, methodology and applications. *Mech. Syst. Signal Process.* **2014**, *42*, 314–334. [CrossRef]
3. ISO. *DIN ISO 17359:2018-05, Zustandsüberwachung und -Diagnostik von Maschinen—Allgemeine Anleitungen (ISO_17359:2018)*; Beuth Verlag GmbH: Berlin, Germany, 2018. [CrossRef]
4. Kim, Y.; Park, J.; Na, K.; Yuan, H.; Youn, B.D.; Kang, C.S. Phase-based time domain averaging (PTDA) for fault detection of a gearbox in an industrial robot using vibration signals. *Mech. Syst. Signal Process.* **2020**, *138*, 106544. [CrossRef]
5. Jaber, A.A. *Design of an Intelligent Embedded System for Condition Monitoring of an Industrial Robot*; Springer Theses, Recognizing Outstanding Ph.D. Research; Springer International Publishing: Cham, Switzerland, 2017. [CrossRef]
6. Zhi, H.; Yangi-Shang . Remote performance evaluation, life prediction and fault diagnosis of RV reducer for industrial robot. *J. Physics: Conf. Ser.* **2020**, *1676*, 012212. [CrossRef]
7. Hugo, D.; Benjamin, S. Robot Condition Monitoring: A first Step in Condition Monitoring for Robotic Applications. Master's Thesis, Lulea University of Technology, Lulea, Sweden, 2017.
8. Karlsson, M.; Hörnqvist, F. Robot Condition Monitoring and Production Simulation. Master's Thesis, Lulea University of Technology, Lulea, Sweden, 2018.
9. Liu, X.; Wu, X.; Liu, C.; Liu, T. Research on condition monitoring of speed reducer of industrial robot with acoustic emission. *Trans. Can. Soc. Mech. Eng.* **2016**, *40*, 1041–1049. [CrossRef]
10. Sun, H.; Zhang, J. Health Monitoring of Strain Wave Gear on Industrial Robots. In Proceedings of the 2019 IEEE 8th Data Driven Control and Learning Systems Conference (DDCLS), Dali, China, 24–27 May 2019.
11. Nentwich, C.; Junker, S.; Reinhart, G. Data-driven Models for Fault Classification and Prediction of Industrial Robots. *Procedia CIRP* **2020**, *93*, 1055–1060. [CrossRef]
12. Jahagirdar, A.C.; Gupta, K.K. Cumulative Distribution Sharpness Profiling Based Bearing Fault Diagnosis Framework Under Variable Speed Conditions. *IEEE Sensors J.* **2021**. [CrossRef]
13. Attoui, I.; Boutasseta, N.; Fergani, N. Novel Machinery Monitoring Strategy Based on Time–Frequency Domain Similarity Measurement With Limited Labeled Data. *IEEE Trans. Instrum. Meas.* **2021**, *70*, 1–8. [CrossRef]
14. Cocconcelli, M.; Zimroz, R.; Rubini, R.; Bartelmus, W. STFT Based Approach for Ball Bearing Fault Detection in a Varying Speed Motor. In *Condition Monitoring of Machinery in Non-Stationary Operations*; Fakhfakh, T., Bartelmus, W., Chaari, F., Zimroz, R., Haddar, M., Eds.; Springer: Berlin/Heidelberg, Germany, 2012; Volume 34, pp. 41–50. [CrossRef]
15. Gao, H.; Liang, L.; Chen, X.; Xu, G. Feature extraction and recognition for rolling element bearing fault utilizing short-time Fourier transform and non-negative matrix factorization. *Chin. J. Mech. Eng.* **2015**, *28*, 96–105. [CrossRef]

16. Jian, B.L.; Su, X.Y.; Yau, H.T. Bearing Fault Diagnosis Based on Chaotic Dynamic Errors in Key Components. *IEEE Access* **2021**, *9*, 53509–53517. [CrossRef]
17. Vippala, S.R.; Bhat, S.; Reddy, A.A. Condition Monitoring of BLDC Motor Using Short Time Fourier Transform. In Proceedings of the 2021 IEEE Second International Conference on Control, Measurement and Instrumentation (CMI), Kolkata, India, 8–10 January 2021, pp. 110–115. [CrossRef]
18. Veerendra, A.S.; Mohamed, M.R.; Punya Sekhar, C. A novel fault—Detection methodology of proposed reduced switch MLI fed induction motor drive using discrete wavelet transforms. *Int. Trans. Electr. Energy Syst.* **2021**, *31*. [CrossRef]
19. Defdaf, M.; Berrabah, F.; Chebabhi, A.; Cherif, B.D.E. A new transform discrete wavelet technique based on artificial neural network for induction motor broken rotor bar faults diagnosis. *Int. Trans. Electr. Energy Syst.* **2021**, *31*. [CrossRef]
20. Zhu, H.; He, Z.; Wei, J.; Wang, J.; Zhou, H. Bearing Fault Feature Extraction and Fault Diagnosis Method Based on Feature Fusion. *Sensors* **2021**, *21*, 2524. [CrossRef]
21. Kotsanidis, K.; Benardos, P. Rolling element bearings fault classification based on feature extraction from acceleration data and artificial neural networks. *Iop Conf. Ser. Mater. Sci. Eng.* **2021**, *1037*, 012008. [CrossRef]
22. Skariah, A.; Pradeep, R.; Rejith, R.; Bijudas, C.R. Health monitoring of rolling element bearings using improved wavelet cross spectrum technique and support vector machines. *Tribol. Int.* **2021**, *154*, 106650. [CrossRef]
23. Sharma, S.; Tiwari, S.K.; Singh, S. Integrated approach based on flexible analytical wavelet transform and permutation entropy for fault detection in rotary machines. *Measurement* **2021**, *169*, 108389. [CrossRef]
24. Elasha, F.; Li, X.; Mba, D.; Ogundare, A.; Ojolo, S. A Novel Condition Indicator for Bearing Fault Detection Within Helicopter Transmission. *J. Vib. Eng. Technol.* **2021**, *9*, 215–224. [CrossRef]
25. Mohanraj, T.; Yerchuru, J.; Krishnan, H.; Nithin Aravind, R.S.; Yameni, R. Development of tool condition monitoring system in end milling process using wavelet features and Hoelder's exponent with machine learning algorithms. *Measurement* **2021**, *173*, 108671. [CrossRef]
26. Duan, J.; Duan, J.; Zhou, H.; Zhan, X.; Li, T.; Shi, T. Multi-frequency-band deep CNN model for tool wear prediction. *Meas. Sci. Technol.* **2021**, *32*, 065009. [CrossRef]
27. Gómez, M.J.; Marklund, P.; Strombergsson, D.; Castejón, C.; García-Prada, J.C. Analysis of Vibration Signals of Drivetrain Failures in Wind Turbines for Condition Monitoring. *Exp. Tech.* **2021**, *45*, 1–12. [CrossRef]
28. Suresh, S.; Naidu, V.P.S. Gearbox Health Condition Monitoring Using DWT Features. In Proceedings of the 6th National Symposium on Rotor Dynamics, Bangalore, India, 2–3 July 2019; Rao, J.S., Arun Kumar, V., Jana, S., Eds.; Springer: Singapore, 2021; Volume 329, pp. 361–374.
29. de Sena, A.P.C.; de Freitas, I.S.; Filho, A.C.L.; Sobrinho, C.A.N. Fuzzy diagnostics for gearbox failures based on induction motor current and wavelet entropy. *J. Braz. Soc. Mech. Sci. Eng.* **2021**, *43*. [CrossRef]
30. Yu, D.; Yang, Y.; Cheng, J. Application of time—Frequency entropy method based on Hilbert-Huang transform to gear fault diagnosis. *Measurement* **2007**, *40*, 823–830. [CrossRef]
31. Mao, W.; He, J.; Zuo, M.J. Predicting Remaining Useful Life of Rolling Bearings Based on Deep Feature Representation and Transfer Learning. *IEEE Trans. Instrum. Meas.* **2020**, *69*, 1594–1608. [CrossRef]
32. Cheng, C.; Ma, G.; Zhang, Y.; Sun, M.; Teng, F.; Ding, H.; Yuan, Y. A Deep Learning-Based Remaining Useful Life Prediction Approach for Bearings. *IEEE/ASME Trans. Mechatron.* **2020**, *25*, 1243–1254. [CrossRef]
33. Thakker, H.T.; Dave, V.; Vakharia, V.; Singh, S. Fault Diagnosis of Ball Bearing Using Hilbert Huang Transform and LASSO Feature Ranking Technique. *Iop Conf. Ser. Mater. Sci. Eng.* **2020**, *841*, 012006. [CrossRef]
34. Larsen, R.J.; Marx, M.L. *An Introduction to Mathematical Statistics and Its Applications*, 3rd ed.; Prentice Hall: Upper Saddle River, NJ, USA, 2001.
35. Nectoux, P.; Gouriveau, R.; Medjaher, K.; Ramasso, E.; Chebel-Morello, B.; Zerhouni, N.; Varnier, C. PRONOSTIA: An experimental platform for bearings accelerated degradation tests. In Proceedings of the IEEE International Conference on Prognostics and Health Management, PHM'12, Denver, CO, USA, 23–27 September 2012.
36. Nectoux, P.; Gouriveau, R.; Medjaher, K.; Ramasso, E.; Chebel-Morello, B.; Zerhouni, N.; Varnier, C. PHM IEEE 2012 Data Challenge Data Set. Available online: https://github.com/wkzs111/phm-ieee-2012-data-challenge-dataset (accessed on 19 May 2021).
37. Arun, P.; Lincon, S.A.; Prabhakaran, N. Detection and Characterization of Bearing Faults from the Frequency Domain Features of Vibration. *IETE J. Res.* **2018**, *64*, 634–647. [CrossRef]
38. Caesarendra, W.; Tjahjowidodo, T. A Review of Feature Extraction Methods in Vibration-Based Condition Monitoring and Its Application for Degradation Trend Estimation of Low-Speed Slew Bearing. *Machines* **2017**, *5*, 21. [CrossRef]
39. Vecer, P.; Kreidl, M.; Smid, R. Condition Indicators for Gearbox Condition Monitoring Systems. *Acta Polytech.* **2005**, *45*, 35–42. [CrossRef]
40. Zhu, J.; Nostrand, T.; Spiegel, C.; Morton, B. Survey of condition indicators for condition monitoring systems. In Proceedings of the Annual Conference of the Prognostics and Health Management Society 2014, Fort Worth, TX, USA, 27 September–3 October 2014.
41. Geropp, B. Envelope Analysis—A Signal Analysis Technique for Early Detection and Isolation of Machine Faults. *IFAC Proc. Vol.* **1997**, *30*, 977–981. [CrossRef]
42. Lei, Y.; Li, N.; Guo, L.; Li, N.; Yan, T.; Lin, J. Machinery health prognostics: A systematic review from data acquisition to RUL prediction. *Mech. Syst. Signal Process.* **2018**, *104*, 799–834. [CrossRef]

8.4 A Combined Anomaly and Trend Detection System for Industrial Robot Gear Condition Monitoring

applied sciences

MDPI

Article

A Combined Anomaly and Trend Detection System for Industrial Robot Gear Condition Monitoring

Corbinian Nentwich * and Gunther Reinhart

Institute for Machine Tools and Industrial Management, Technical University Munich, 85747 Garching, Germany; emeritus.reinhart@tum.de

* Correspondence: corbinian.nentwich@iwb.tum.de

Abstract: Conditions monitoring of industrial robot gears has the potential to increase the productivity of highly automated production systems. The huge amount of health indicators needed to monitor multiple gears of multiple robots requires an automated system for anomaly and trend detection. In this publication, such a system is presented and suitable anomaly detection and trend detection methods for the system are selected based on synthetic and real world industrial application data. A statistical test, namely the Cox-Stuart test, appears to be the most suitable approach for trend detection and the local outlier factor algorithm or the long short-term neural network performs best for anomaly detection in the application of industrial robot gear condition monitoring in the presented experiments.

Keywords: condition monitoring; industrial robots; anomaly detection; trend detection

Citation: Nentwich, C.; Reinhart, G. A Combined Anomaly and Trend Detection System for Industrial Robot Gear Condition Monitoring. *Appl. Sci.* **2021**, *11*, 10403. https://doi.org/10.3390/app112110403

Academic Editor: Jasiulewicz-Kaczmarek Małgorzata

Received: 27 September 2021
Accepted: 3 November 2021
Published: 5 November 2021

1. Introduction

Currently, industrial robots are the workhorses of highly automated production systems [1]. A challenge to the productivity of such systems remain faults of industrial robot gears as they can cause extended downtimes. Condition monitoring (CM) of the gears can be a measure for countering this issue. CM describes a maintenance strategy in which sensor data is used to determine the health state of a robot gear. For this, sensor data is transformed into health indicators that correlate with the gear's health state. Critical monitored values within the time series of the health indicators form the decision criterion for a maintenance action [2]. Usually, there are many industrial robots operating in a production system and the health state of each of the axes must be monitored. Hence, manual monitoring is not feasible and an automated system is required. Such a system must be able to detect anomalies and trends in the health indicator data reliably. Anomalies in the data can be related to faults that occur abruptly (e.g., breaking of a gear tooth) and trends can be an indicator for increasing wear [3]. The occurrence of such events should be presented to the maintenance crew while showing only few false alarms. To the best of our knowledge, such a combined system does not yet exist for industrial robot gear condition monitoring. Hence, the contribution of our publication is threefold. Firstly, a combined anomaly and trend detection system (CATS) for industrial robot gear CM and secondly a method for selecting suitable anomaly detection (AD) and trend detection (TD) models for this defined application are presented. Thirdly, the suitability of different AD and TD models for the defined use case is evaluated by applying the method. Thus, the remainder of this publication is structured as follows: in Sections 1.1 and 1.2 an overview of industrial robot CM systems, AD and TD models is given and the addressed research gap is refined. In Section 2, CATS and the AD and TD model evaluation method is described. In Section 3, the method is applied to state-of-the-art AD and TD models and suitable models for CATS are selected. In Section 4, the limitations of the presented approach are discussed. In doing so, the outlook discussed in Section 5 is derived, which also includes a summary of our

contribution. Through the remainder of this publication the term application refers to the condition monitoring of industrial robot gears.

1.1. State of the Art

In this section, first supervised and unsupervised approaches for robot condition monitoring are presented. As this research area does not present the fields of anomaly detection and trend detection models completely, a broader overview of these research fields is given subsequently. Finally, the state of the art is summarised and the research gap is presented that we are addressing.

1.1.1. Industrial Robot Condition Monitoring

Different approaches for the CM of industrial robots exist in the literature. These can be classified by the type of model used, i.e., supervised or unsupervised machine learning models or the raw data used, which are mainly acceleration sensor data or robot controller data.

In the field of supervised models and robot controller data, several models such as XGBoost and different neural networks based on both joint specific data such as speed and torque and operational specific data (e.g., number of emergency stops) were compared from a fleet of 6000 robots. A maximum AUC value (area under the curve) of 0.87 could be achieved for a neural network model for fault detection in axis 2 [4]. A similar model comparison for logistic regression, support vector machines, random forests and ensemble stacking was performed in [5]. Here, angle, angle speed, acceleration and torque data were used from 26 robots to classify gear faults. The best AUC value of 0.77 was reached by the random forest classifier. Fault detection for loose gear belts was performed with a decision tree, a gradient booster and a random forest and statistical features derived from current data. Here, the random forest performed best with F1-scores around 0.9 [6].

In the section of unsupervised models and robot controller data, a kernel density estimator was used to detect faults based on motor angle, angle velocity and torque in combination with the Kullbach-Leibler divergence. Data from accelerated wear tests show a clear increase in the health indicator [7]. In another publication, the transferability of models was investigated for a combination of principle component analysis and Q-residuals. Anomalies were assumed if the distance measure was above a set threshold. The study shows that the use of the differences between measured and set quantities such as torques as raw data perform best in terms of transferability. In this context, transferability describes the training of the model based on the data of only one robot and then also using this model for other robots [8]. A model based on the deviations of a dynamic equation of a robot relative to actual measurements of the robot is combined with Hotelling's T^2 test statistic to determine robot faults [9]. A sliding-window convolutional variational autoencoder was used to detect anomalies in pick-and-place operations of a robot simulated by little strikes on the robot. The method outperforms benchmark models with an F1-score of 0.89 [10]. A long short-term memory neural network was successfully used to detect anomalies within the grinding process of an industrial robot based on speed, position and torque data. Anomalies were generated by applying a force to the robot hand during the process [11].

Turning to supervised learning approaches based on acceleration sensor data, multiple methods are worthy of note. A sparse autoencoder was trained with data from an attitude sensor (collecting acceleration and velocity signals at 100 Hz) attached to the tool centre point of the robot. The sensor collected data from normal behaviour and different fault conditions such as pitting and broken teeth of a gear. The classification results showed accuracy values of 90 percent [12]. Wavelet-based features in combination with a neural network were used to classify backlash faults for a six axis industrial robot [13]. Multiple supervised models such as a support vector machine, neural networks, gaussian processes and random forests were combined with different dimensionality reduction methods based

on data from acceleration sensors attached to the gear caps for gear fault classification. The SVM and GP showed the best performance with accuracy values over 91 percent [14].

In the area of unsupervised models and acceleration sensor data, a gaussian mixture model was used based on health indicators derived from time and the time-frequency domain to differentiate measurements from a degreased robot from normal measurements of the robot. Classification performances over 94 percent for recall and precision values were achieved [15]. Time domain and frequency domain features derived from a residual signal were used in combination with thresholding for gear fault detection for different test trajectories [16]. A one-class generative adversarial autoencoder was used for the detection of artificially introduced faults in a robot gear in [17]. Classification accuracies of 97 percent were achieved for the identification of different faults.

1.1.2. Anomaly Detection Models

The state of the art provides various anomaly detection models for point, collective and contextual anomalies of uni- and multivariate time series and spatial data. One possibility for clustering such models is presented in [18]. Here, anomaly or novelty detection methods are structured in probabilistic, distance-based, reconstruction-based, domain-based and information theoretic approaches. For a detailed review of anomaly detection methods, refer to [18] or more recently to [19]. Below, only those approaches that are considered in the method evaluation of our publication are presented. Different approaches from the above mentioned classification scheme are compared. From the field of probabilistic models, a kernel density estimator (KDE) based on the values of the time series [20] is used. This model fits a non-parametric probability density function on the data. By calculating the probability that a sample (one step of a time series) belongs to this density and by comparing this value with a threshold, anomalies can be determined. Furthermore, a gaussian process (GP) for one-class classification is used, which works based on a similar principle [21]. From the field of distance based approaches, the local outlier factor (LOF) [22], the isolation forest (IF) [23] and the DBSCAN algorithm [24] are used. LOF is based on determining the density of data points and detects anomalies as data points with few close neighbors. IF is based on multiple tree classifiers for one-class classifcation. DBSCAN is a clustering algorithm that determines anomalies based on their distance to reachable points from cluster core points. Multiple representatives from the reconstruction-based model class are used. An autoregressive (AR) [25] and autoregressive moving average model (ARMA) [26] are applied and compared with a convolutional and a long short-term neural network [27,28]. All four models are used as regression models between the past time steps of the signals and a time step of the signal in the future. The deviations between these predictions and the actual progress of the signal are then compared with a threshold. If the deviation exceeds the threshold, an anomaly can be assumed. Furthermore, the one class support vector machines (OCSVM) [29] as a domain-based model is included for the comparison. This model builds a domain of inliers based on support vectors and the border data points of this domain. Data points outside this border line are classified as anomalies. As a simplistic baseline model, an approach is considered where a data point is compared to a multiple of the standard deviation of the reference data (abbreviated STD). If this distance exceeds a defined threshold, an anomaly is assumed.

1.1.3. Trend Detection Models

In the context of this publication a trend is defined as the gradual change in future events from past data in a time series [30]. Trend detection can be differentiated from remaining useful life (RUL) estimation by several aspects. In contrast to RUL estimation, trend detection methods do not extrapolate existing time series into the future. Furthermore, no thresholds for the extrapolated time series are defined which describe the end of lifetime of an asset. Trend detection methods have different purposes. It is possible to differentiate between models for change point detection, trend description and identification of trend

presence in a time series. For the considered application, a model is required that answers the question of whether a trend is present. This is why the remainder of this subsection focuses on the field of trend presence identification. Here, various statistical tests exist. The Mann-Kendall test (MK) is a sign test based on pairs of all samples of a time series and their predecessors [31] to detect trends. The Cox-Stuart (CS) test uses a reduced amount of data pairs for a sign test [32] to achieve the same objective. The Wilcoxon-Mann-Whitney trend test builds a test statistic based on the signs of the slopes between samples and the rank sums of the samples with an increasing and decreasing slope [33] for this purpose. The Durbin-Watson test checks for auto-correlation in the residuals of a regression fit. If the residuals do not show autocorrelation, a trend can be assumed [34]. Furthermore, slope based approaches in combination with thresholds exist. The most simple approach from this field is to fit a linear or quadratic function to the time series data, calculate the slope of this function and compare it with a threshold. This model will be named linear regression model, short LR, for the rest of the publication. If the slope exceeds the threshold value, a trend can be assumed. A more complex approach for trend detection is based on the clustering of a time series. In a first step, a clustering algorithm (e.g., Fuzzy-K-Means) is used to detect clusters within the time series. Then, the slope between the cluster centres is determined. Finally, the slope values of the cluster centres are compared with a threshold to decide, whether a trend exists [35]. The last approach for trend detection presented in this section is based on the comparison of the time series' moving average with its overall mean (moving average model, short MA). In a first step, these two quantities are calculated. Afterwards, the time series' standard deviation multiplied by a factor is added to the overall mean to determine a threshold. Then, it is determined, whether the moving average of the signal rises above this threshold for a defined time window. If this is the case, it can be assumed that a trend is present in the signal. The principle behind this method is also illustrated in Figure 1.

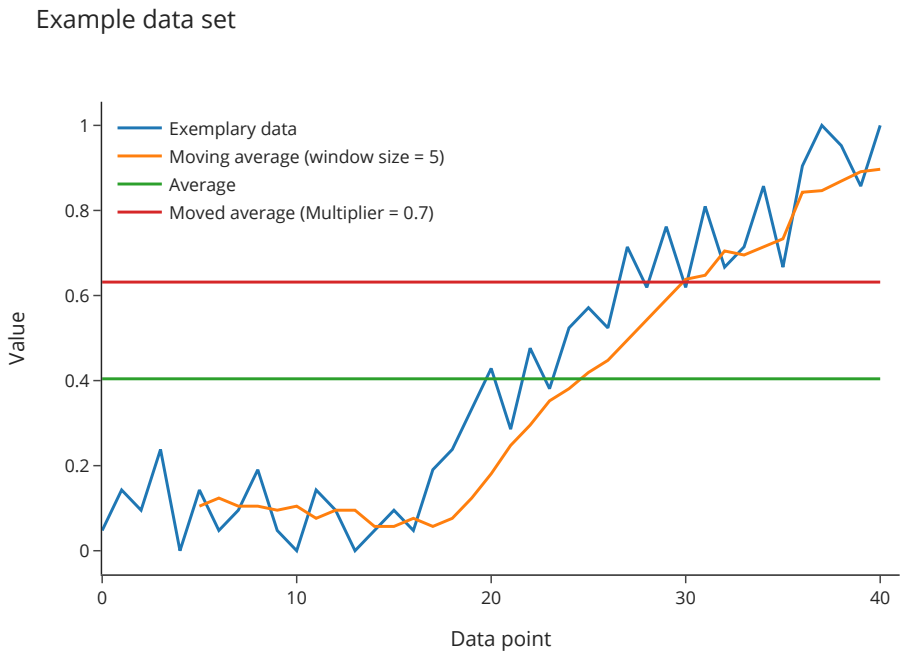

Figure 1. Example for the trend detection method using moving averages.

1.2. Considered Research Gap

In the field of industrial robot gear condition monitoring no combined AD and TD model has been presented up to now to the best of our knowledge. Therefore, the research objective of this publication is to present such a system. For the detailed design of this system, a suitable AD and TD model must be chosen. As no comparison of AD and TD models for univariate time series of HIs derived from acceleration sensors has been

performed up to date, a method to select suitable AD and TD models for the application of industrial robot gear condition monitoring is formulated. Afterwards, it is applied to choose models for the presented combined system. In the context of the framework presented in [36], we address the question of algorithm selection for the inference task. By doing so, we support the transfer of state of the art AI models into practice and reduce the effort of model selection for practitioners. The identification of suitable data acquisition systems or the selection of features is not considered in this publication. This is e.g., considered in [3]. Therefore, the presented work builds up on assumptions derived from this publication. These assumptions are summarized in Section 2.1.1. Furthermore, we limit our research frame to the field of six-axis articulated robots as we can not provide comprehensive experiments for other asset classes and hence validate our approach for such assets.

2. Materials and Methods

In this section, firstly CATS is described. Subsequently, the method for selecting suitable AD and TD models for CATS is described.

2.1. Combined Anomaly and Trend Detection Model

The objective of CATS is the reliable detection of trends and anomalies in industrial robot gear health indicator data. In the following, the assumptions that the system is based on, are defined. Then, the system itself is presented.

2.1.1. System Assumptions

The presented model builds upon certain assumptions. Data ingested in the system must be collected from a setup with a constant robot trajectory and load. The system analyses only univariate time series data of one health indicator per axis derived from acceleration sensor data. A suitable HI is described for example in [3]. The HI exhibits stationary behaviour when the robot axis is in a healthy state. The considered time series can be subject to trends $x_{trend}(t)$, seasonality $x_{seasonality}(t)$, noise $x_{noise}(t)$ and anomalies $x_{anomaly}(t)$. Noise can be caused by changing environmental conditions or sensor effects. Trends can occur due to wear. Trends due to sensor drifts are prevented by the sensor setup or suitable data preprocessing (e.g., high pass filtering of the raw data). Seasonality can occur due to changing temperatures of the gears. These temperature changes lead to variations in the HI (for example, see [37]). These temperature changes result from varying utilisation in the production system. They could be caused for instance by a three shift working model with reduced utilisation during night shift. Summarising, this time series can be expressed as in Equation (1).

$$x(t) = x_{trend}(t) + x_{seasonality}(t) + x_{noise}(t) + x_{anomaly}(t) \quad (1)$$

2.1.2. System Design

The objective of the presented system is to evaluate whether $x_{anomaly}(t) \neq 0$ or $x_{trend}(t) \neq 0$. For this, an anomaly detection model and a trend detection model are deployed in parallel. The detection of an anomaly in a defined number of sequential measurements leads to the recommendation of immediate maintenance actions. The detection of trends in the data of a defined number of a sequential measurements leads to the proposal of maintenance actions in the near future. The working principle of the system is summarized in Figure 2. The design of the system addresses different aspects of the industrial robot gear condition monitoring use case. Faults, whose manifestation but not the underlying fault mechanism progress (e.g., tracking of the growth of a crack in a gear tooth) can be tracked with HIs, will cause point or collective anomalies. The AD model will be used for the detection of such faults. Other faults, whose progress can be tracked (e.g., increasing wear), will cause trends in the HI. These trends will be detected by the trend detection model.

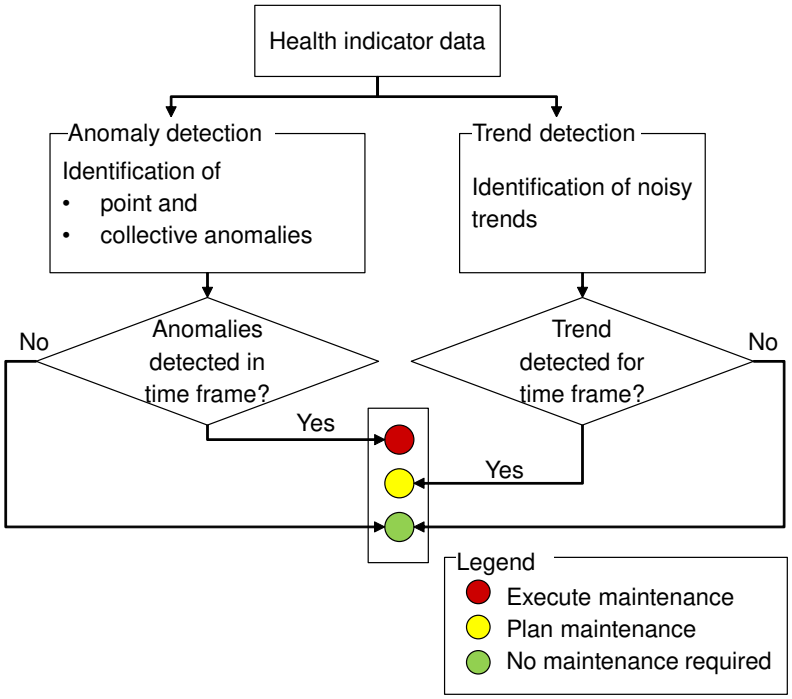

Figure 2. Overview of the condition monitoring system.

2.2. Method for Anomaly and Trend Detection Model Selection

In this section, the overall model evaluation method is proposed. Then, more detailed information is given about the generation of synthetic data and the model evaluation criteria.

2.2.1. Overall Method and Selected Models

To select suitable AD and TD models for the presented system a three step approach was followed to ensure that the most suitable models are chosen. Firstly, potential models were identified in the literature. Secondly, these models were applied on synthetic data meeting defined characteristics of the considered application and evaluated in respect of different quality criteria to reduce the solution space. Thirdly, the best performing models were evaluated using real world data taken from accelerated wear tests of industrial robots. The overall selection process is summarised in Figure 3. In the following, these steps are explained in detail.

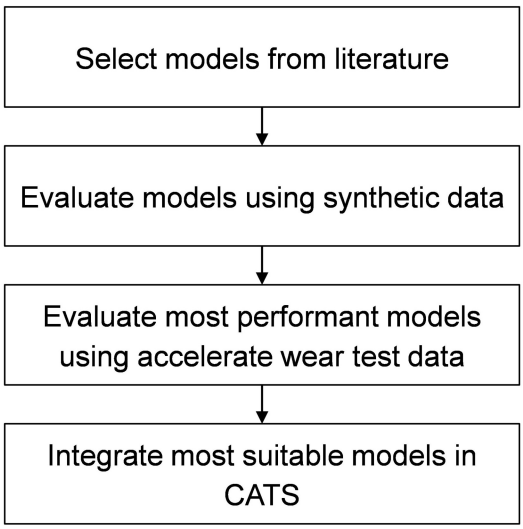

Figure 3. Overview of the model evaluation method.

As described in Section 1.1, a large number of AD and TD models exist. Hence, a holistic comparison of existing approaches is not feasible. Therefore, models from the classes as described in [18] were chosen for the AD model comparison. In detail, the models listed in Table 1 were used. The models are explained in detail above in Section 1.1.2. For TD model comparison, the MK test, the CS test as well as the LR and MA based approaches described in Section 1.1.3 were chosen. The implementation of the models is described in an open source repository [38].

Table 1. Models considered.

Anomaly Detection Model	Anomaly Detection Model Type	Reference
CNN	Reconstruction based	[28]
LSTM	Reconstruction based	[27]
AR	Reconstruction based	[25]
ARMA	Reconstruction based	[26]
KDE	Probabilistic	[20]
GP	Probabilistic	[21]
OCSVM	Domain based	[29]
IF	Distance based	[23]
DBSCAN	Distance based	[24]
LOF	Distance based	[22]
STD	Distance based	[-]
Trend detection model	**Trend detection model type**	**Reference**
MK	Statistical test	[31]
CS	Statistical test	[32]
LR	Slope based	[-]
MA	Slope based	[-]

2.2.2. Synthetic Data Generation

For the model comparison based on synthetic data, a data generator was implemented to create time series as described in Equation (1). Different trend, noise, seasonality and anomaly functions were considered. In detail, linear and quadratic trend functions were implemented. White noise and uniform noise with different variances or ranges were used as noise functions. Sine functions and a hand crafted function as described in Equation (2) were applied for seasonality. Here, t is the current time step, which would relate to the length of one hour of the time series and a is the magnifier factor, which is further described in Table 2. An example of this function is depicted in Figure 4 on the upper right side.

$$f(x) = \begin{cases} (t\%24) \times a/4 & \text{if } (t\%24) \leq 4 \\ 1, & \text{if } 4 < (t\%24) \leq 20 \\ \frac{24-(t\%24)}{4} \times a & \text{otherwise} \end{cases} \quad (2)$$

For the anomaly function, a uniform distribution was used to define the anomaly positions. Different lengths for collective and different amplitudes for both collective and point anomalies were applied. To derive reasonable parameter ranges, certain realistic assumptions were made. A time series consists of 8736 samples representing 24 measurements per day for one year. The range of the trend functions' slopes should allow a doubling of the HI value in no less than one week and no more than half a year. Noise and seasonality should as a minimum result in a deviation of the time series by the factor 0.3 and as a maximum by the factor 9 from the mean of the signal. These assumptions were based on collected HI data from industrial robots in a car manufacturing plant. Due to confidentiality reasons, this data can not be published. The different functions, their parameters, the range of the parameters used and underlying assumptions for the parameter range choice are specified in Table 2. In the first three months of the time series no anomaly or trend occurs. In the last nine months anomalies may occur. Figure 4 shows a typical synthetic time series.

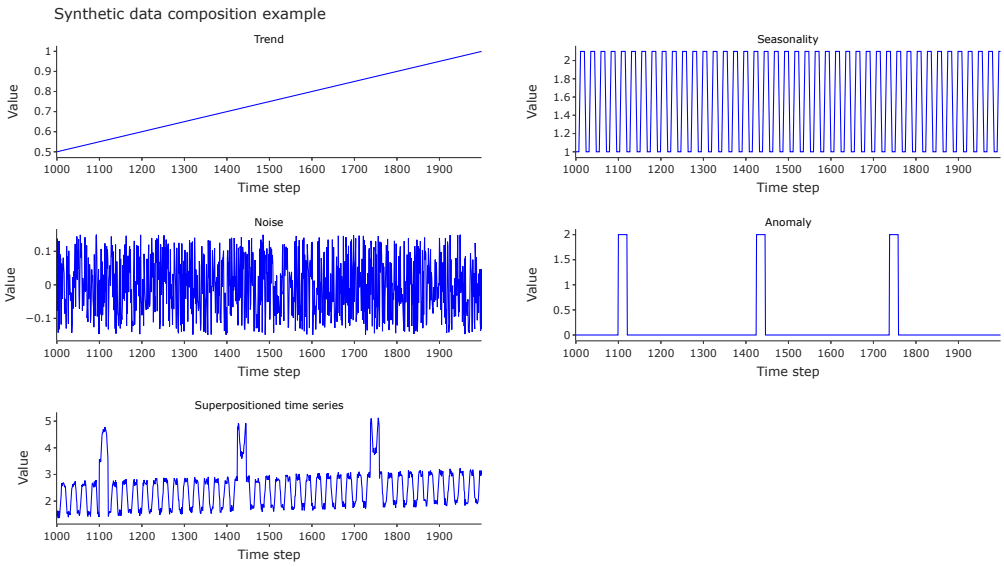

Figure 4. Example of a synthetic time series.

Table 2. Overview of used parameter ranges for the synthetic time series.

Signal	Parameter Type	Parameter Values	
		Synthetic Data Set 1	**Synthetic Data Set 2**
$x_{trend}(t)$	Trend type	Linear	
		Quadratic	
	Trend slope	Linear: 0.012	Linear: 4.58×10^{-4}
		Quadratic: 7.09×10^{-5}	Quadratic: 1.05×10^{-7}
$x_{seasonality}(t)$	Seasonality type	Sine	
		Production cycle (Formula 2)	
	Amplitudes a	Sine: 0.15	Sine: 3
		Production cycle: 1.1	Production cycle: 2
$x_{noise}(t)$	Noise type	Uniform noise	
		White noise	
	Noise parameters	Uniform noise range: 0.15	Uniform noise range: 1
		White noise mean: 0 White noise standard deviation: 0.03	White noise mean: 0 White noise standard deviation: 0.8
$x_{anomaly}(t)$	Anomaly types	Point anomaly	
		Collective anomaly	
	Anomaly parameters	Amplitude: 2	Amplitude: 1.1
		Collective anomaly lengths: 20 measurements	Collective anomaly lengths: 5 measurements

Based on this parameter range, over 26 million unique time series could be modeled. To reduce the computational effort, two reduced data sets were created. The first data set (synthetic data set 1) was used for an initial screening of the models' performance.

It consisted of time series with low noise, trends with a high slope, and large anomaly magnitude values and lengths. Furthermore, a second data set (synthetic data set 2) with more difficult conditions for the detection of trends and anomalies was generated. Here, time series with high noise, low trend slopes, and low anomaly magnitudes and lengths were calculated. In each time series 40 anomalies were present. Each created time series was analysed by each model to detect trends and anomalies. In total, 16 unique time series were analysed per data set.

2.2.3. Model Evaluation

To measure the models' performance, the ROC curves (receiver operating characteristic curves) for different parameter choices of the models were determined. This means that different model parameters were varied and the True Positive Rate (TPR) and False Positive Rates (FPR) of the models for the synthetic data were determined. More precisely, the models were presented with slices of the time series and had to determine, whether trends or anomalies were present in the time series. For the trend detection task, these slices were increased in size per time series with a window size of 1008 samples and an initial size of 2016 samples. This is equivalent to 24 measurements per day for a length of 12 weeks for the initial window. For the anomaly detection, the first 168 values were used to train the models. This is equivalent to 24 measurements per day for one week. The models were then tested on time series with a length of 6720 samples. The parameters that were varied for the different models are summarized in Table A1. The most robust models with high TPR and low FPR and high average AUC values (area under the curve) were then applied to data sets from accelerated robot gear wear tests. A data set, which is based on an accelerated wear test with an ABB IRB 6600-255/2.55, was used to test the trend detection models (Accelerated wear test 1). The experiment caused different faults in the robot gear of the second axis. In total, 2425 measurements over a time span of roughly one year were used from the experiment; these were acquired with an acceleration sensor at the robot gear cap. From this data the HI described in [3] was derived. For more information regarding the experiment, see [39,40]. The same data set and another data set, which was acquired during another accelerated wear test with an ABB IRB 7600-340/2.8, to test the anomaly detection models (Accelerated wear test 2). Here, 920 measurements were acquired over three months at the second axis gear cap with an acceleration sensor, and the same HI was calculated and various gear faults were subsequently detected in the second axis gear. As no obvious trend could be seen in this data set, it was just used for the AD model evaluation.

More information regarding this experiment is given in [3]. Figure 5 presents the various faults of both accelerated wear tests. For analyzing these data sets, the models' parameters were chosen that yielded the best compromise in TPR and FPR during the experiments with the synthetic data. In a real world setup, other parameter sets could be more reasonable in respect of the trade-off between false alarms and undetected faults. A method of how to choose the best parameters given the maintenance circumstances of an individual robot is discussed in Section 4. Based on the results of the accelerated wear test experiments, a suggestion of which models to use for trend and anomaly detection in the CM system is made. The detailed model evaluation method based on synthetic data is depicted in Figure 6.

Figure 5. Overview of the faults of the accelerated wear tests following [3,39].

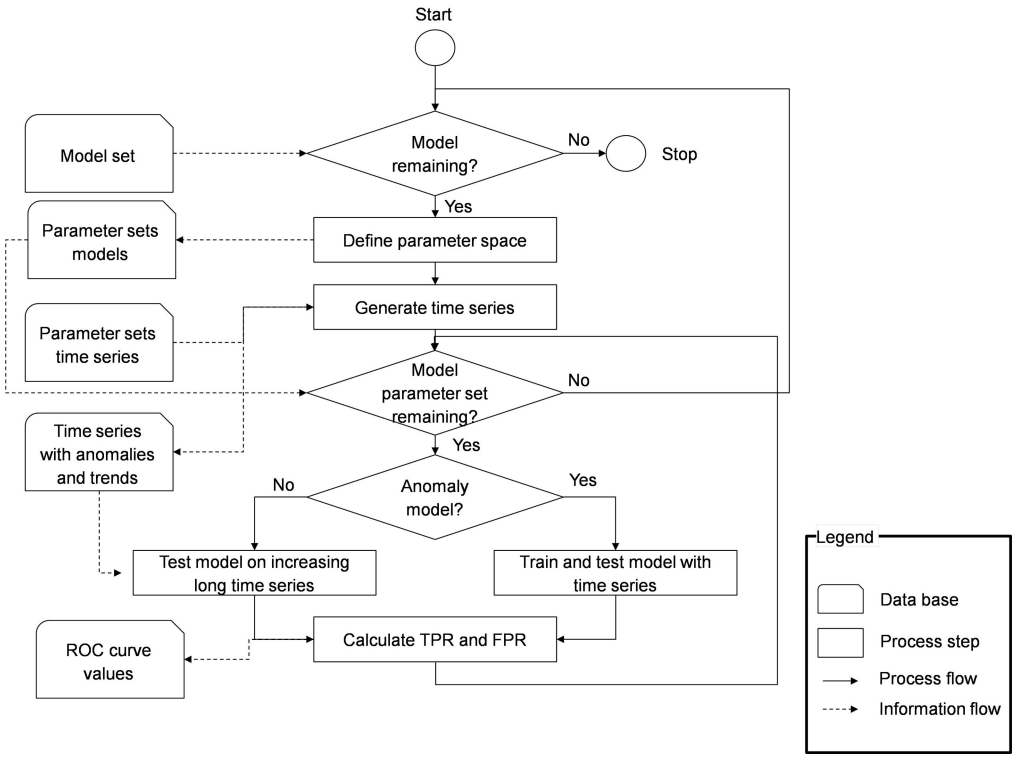

Figure 6. Overview of the model evaluation method.

3. Results

In the following, the presented method from the last section is applied to the AD and TD models listed in Table 1. First, the results for the TD models are shown, then the results of the AD models.

3.1. Trend Detection Model Comparison

Here, first the evaluation of the TD models based on synthetic data are presented. Subsequently, the results based on the accelerated wear test are analysed.

3.1.1. Evaluation Based on Synthetic Data

Figure 7 shows the ROC curve derived from the synthetic data set 1 and the model parameters described in Table A1. Ideally, the plots would show a dot in the upper left corner for a model. Such a dot would refer to a perfect classifier. This means that the model has a TPR of 1 and FPR of 0. Such a model would detect all trends and trigger no false alarms. The LR model and the MA model achieve these perfect classification results. The variation of parameters of the CS model does not influence the model performance and the MK model shows high TPR values only at the expense of an increased false positive rate. The results of synthetic data set 2 with the same model parameters are shown in Figure 8. Here, the CS model shows the best performance as a parameter combination exists where no false alarms are triggered and all trends are detected. It is followed by the MK model, which also yields a performance where all trends are detected and the FPR is small. The LR and the MA models achieve high TPR values only at the expense of increased FPR. The AUC values of the models for both data sets are presented in Table A2. Based on these results, it was decided to apply the CS and the MK model to the accelerated wear tests as they performed best on the more difficult data (synthetic data set 2) and based on their average AUC values.

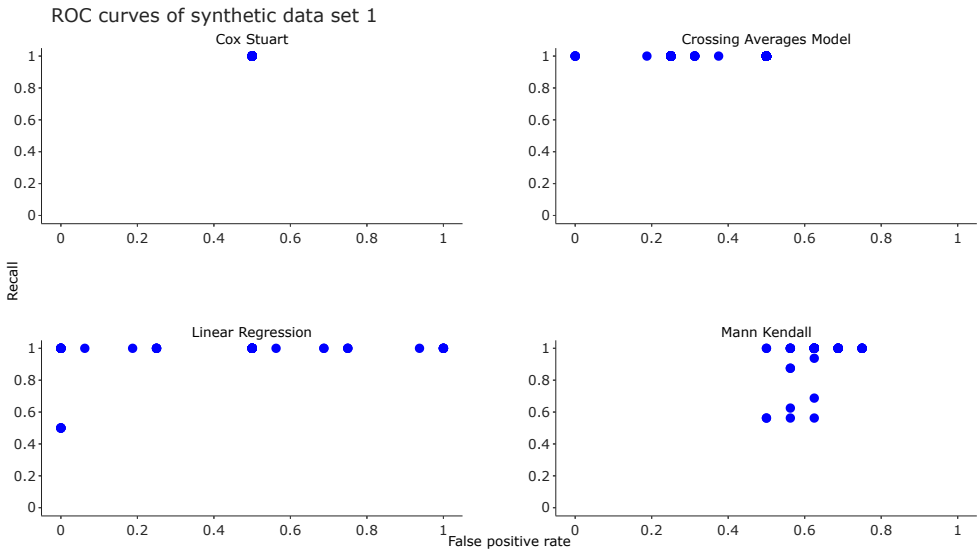

Figure 7. Trend detection model comparison based on the synthetic data set 1.

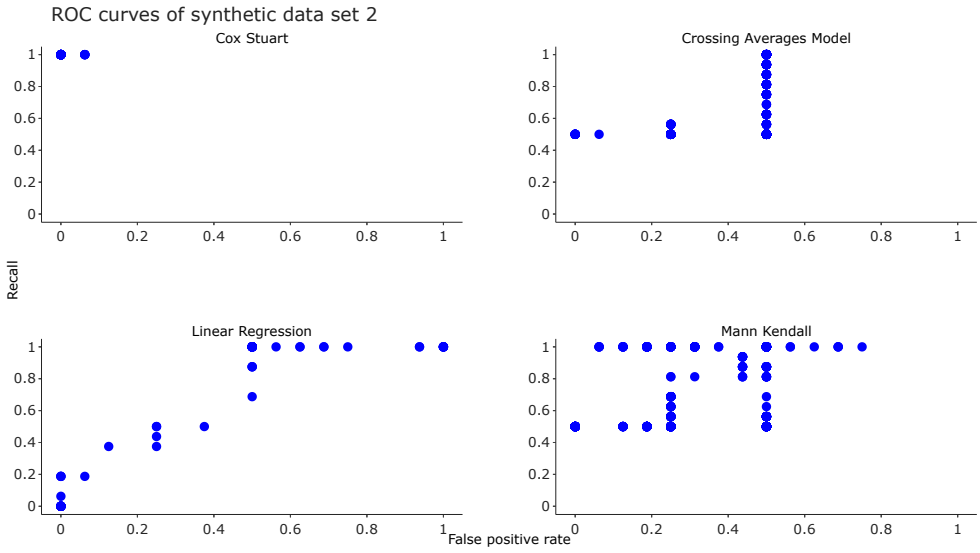

Figure 8. Trend detection model comparison based on the synthetic data set 2.

3.1.2. Evaluation on Accelerated Wear Test Data

The data from the accelerated wear test was analysed using the two chosen models. The results are depicted in Figure 9. The blue line shows the health indicator values, the dots indicate the models' decision of whether a trend is present in the time window of the last 504 samples (which equals a time frame of 2.5 months) while the horizontal yellow line shows, when more then 50 percent of the last 504 decisions were positive.

In such a case, a maintenance action should be planned. It can be seen that both models show similar behaviour for the beginning of the data set where they both detect a trend in the data after the initialisation phase of the first 504 measurements. The outlier at measurement 1000 leads to the rejection of the hypothesis that a trend is present for the following measurements in the MK model. It can be assumed that the CS model interprets the outlier correctly so that even for the following measurements a trend is detected. Both models detect the more stationary behaviour of the time series at its end. As the CS model handles the outlier around measurement 1000 better compared to the MK model, it is suggested to use the CS model in CATS. In this experiment, the confidence level parameters from the ROC curve of synthetic data set 2 were chosen for the models that yielded the highest TPR values with the lowest FPR at the same time.

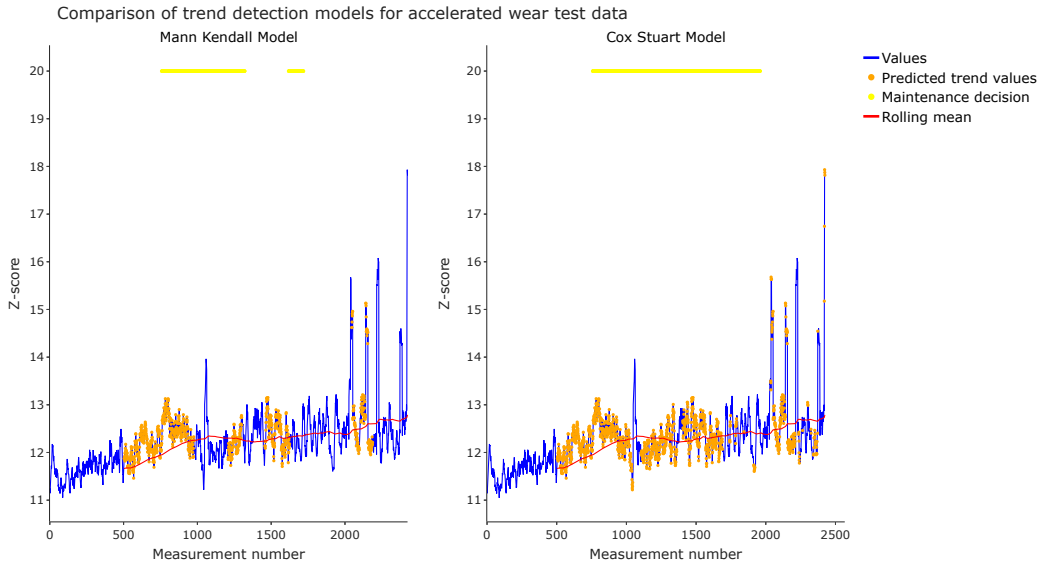

Figure 9. Results of the trend detection models based on accelerated wear test data.

3.2. Anomaly Detection Model Comparison

The presentation of the results of the AD model comparison follows the same scheme as Section 3.1.

3.2.1. Evaluation Based on Synthetic Data

The ROC curves of different models for the synthetic data set 1 are shown in Figure 10. Again, as described in Section 3.1.1 the plot would ideally show dots for the models at the upper left corner. Most of the models show good results except the OCSVM for which parameter combinations exist that yield poor classification performance. This means that all models are capable of identifying anomalies reliably and with a low false alarm rate in the case of high anomaly amplitudes and low noise level. In contrast, the models' overall performance regarding the synthetic data set 2 is rather poor. Figure 11 summarises the ROC curves for this data set. No perfect classifier was found for all models and the distance of the models' ROC curves to the upper left corner is large. Here, it can be concluded that the models struggle to detect anomalies at high noise levels and low anomaly amplitudes. This fact will also be discussed in Section 4. The AUC values for all models and both data sets are provided in Table A3. The individual ROC curves of all models for bothd data sets

are presented in Figures A1 and A2. The best overall performance show the LSTM, STD and LOF models based on their average AUC values. Hence, it was decided to use the LSTM, STD and the LOF model on the accelerated wear test data.

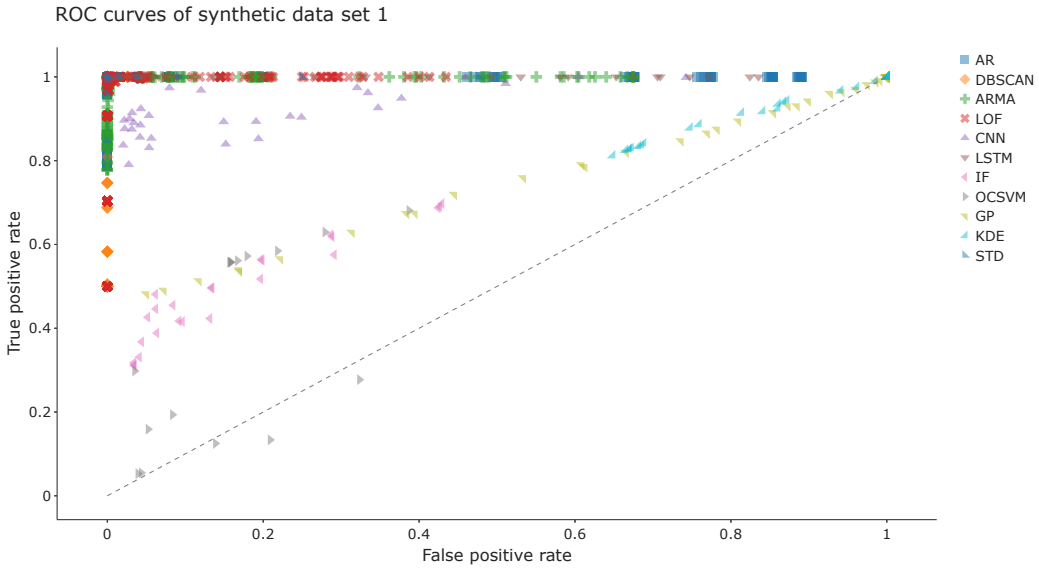

Figure 10. Results of the anomaly detection models based on synthetic data set 1.

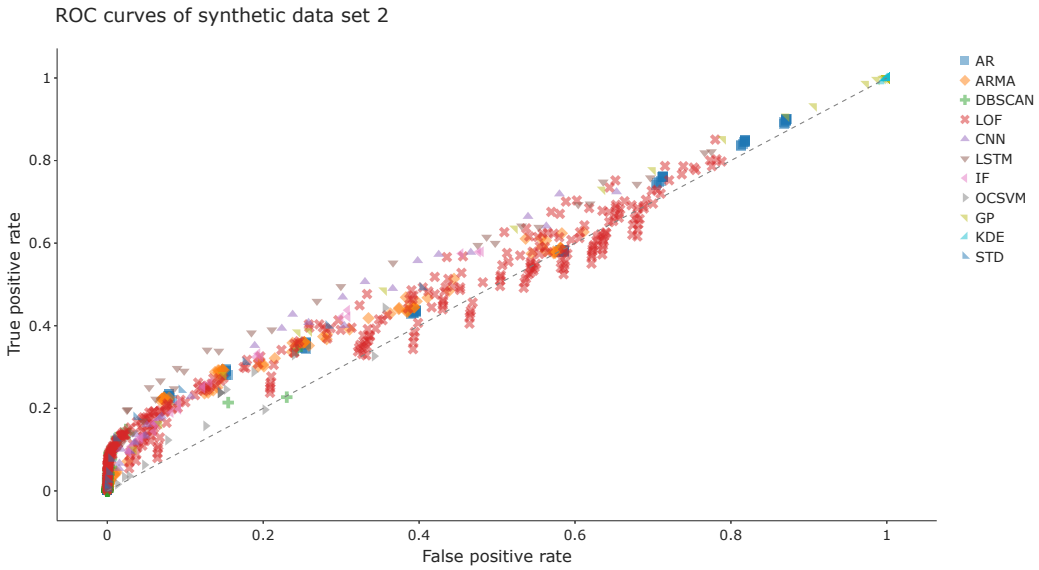

Figure 11. Results of the anomaly detection models based on synthetic data set 2.

3.2.2. Evaluation on Accelerated Wear Test Data

The results of applying the LSTM, STD and LOF models to the data from the accelerated wear test 1 are depicted in Figure 12. For this, all models were trained based on the first 500 measurements with model parameters of the ROC curves that yielded the best compromise between high TPR and low FPR values. It can be seen that all models correctly identify the anomalies at the end of the time series. The LOF model detects the outlier around measurement 1000 as an anomaly. Given a maintenance action decision criterion of 10 detected anomalies in the last 24 measurements, maintenance actions would have been triggered at the end of the data set for all models and a false alarm would have been triggered around measurement 1000 for the LOF model and for many more time ranges for the STD model. The AD models' behaviour on the second data set are summarized in a similar manner in Figure 13. In this scenario, the models were trained

using the first 200 measurements with the same model parameters. It can be seen that the LSTM model and the STD model detect more anomalies than the LOF model along the time series. The apparent anomaly at the end of the time series is detected by all models.The LSTM triggers two false alarms around measurement 300. The STD model triggers many false alarms. Summarising, the STD shows more false alarms compared to other models. The LOF and LSTM model detect only the apparent anomalies with a low false alarm rate. Hence, it is suggested that either the LOF model or LSTM model is used in CATS as the AD model.

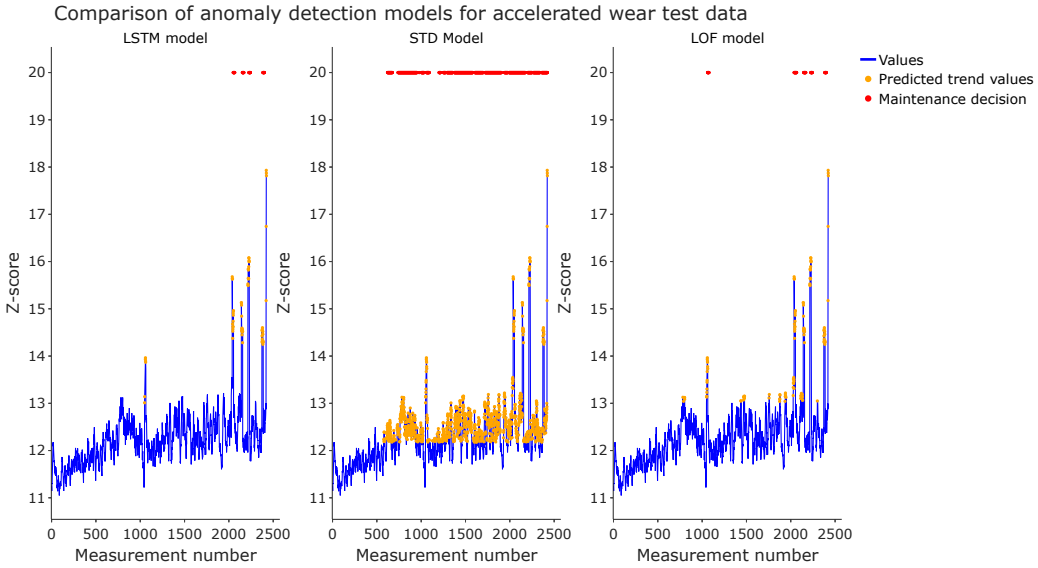

Figure 12. Results of selected anomaly detection models for accelerated wear test 1.

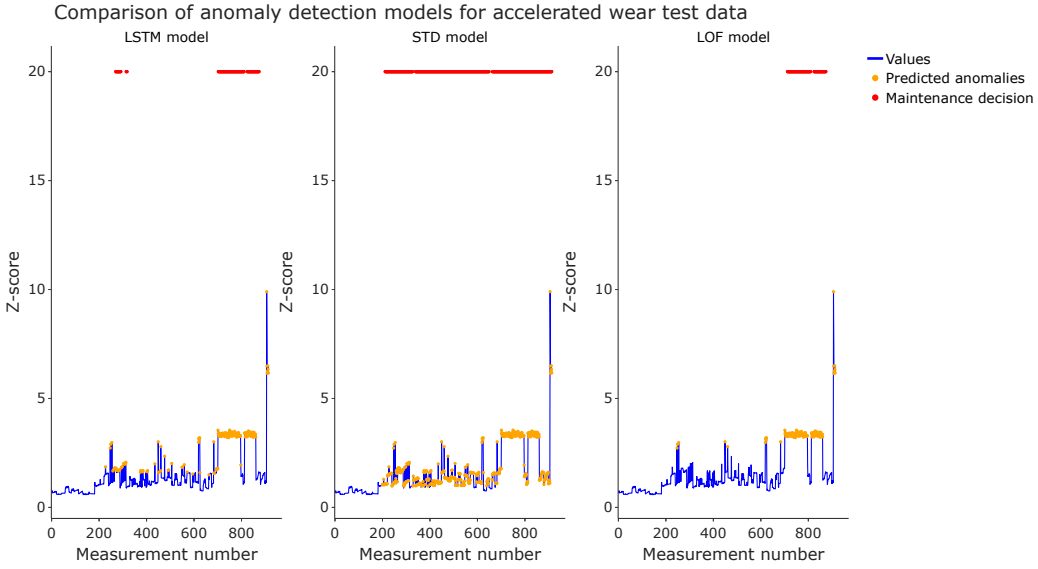

Figure 13. Results of selected anomaly detection models for accelerated wear test 2.

4. Discussion

The presented results highlight some interesting aspects that will be discussed in this section. We will justify our initial choice of models and highlight some aspects of the models' performance on the synthetic data. Then, we will explain the models' parameter choice and end with organisational thoughts regarding the integration of CATS in a real world production site.

As emphasised in Section 1.1.2, a comprehensive comparison of AD and TD models is not feasible due to the high variety of existing models. Our motivation for selecting models from different categories as presented in [18] was to test how their underlying detection mechanisms cope with the different characteristics of time series. The fact that AD and TD models were found that detect the trends and anomalies in the accelerated wear test data reliably, strengthens the argument that the comparison of the selected models is sufficient for the application. From our point of view, the results of the AD model comparison based on synthetic data set 2 clearly highlights the limitations of anomaly detection models in general. High noise levels in the data make it difficult for such models to detect anomalies. Figure 14 shows a typical time series of this data set. Even as a human operator, it is difficult to identify the anomalies. However, from our experience, such extreme noise does not appear in the HI time series as shown in Figure 9 or Figure 13 for the accelerated wear tests. When deploying AD or TD models in real world applications, suitable model parameters must be chosen. For this, from our point of view, the parameters have to be configured for the individual robot considering the common trade-off between false alarms (higher FPR) and undetected faults (lower TPR). If no ideal anomaly or trend detection model can be used considering the ROC curves, this trade-off can be tackled by considering a maintenance score for an individual robot. This maintenance score can be influenced for example by the position of the robot in the production systems in respect of the distance to buffers or the effort required to exchange the robot. Other criteria could be the required calibration effort after the replacement or the response time of the maintenance team if a replacement is required. For robots with a higher maintenance score, model parameters with high TPR and higher FPR should be chosen. For robots with a lower maintenance score, model parameters with lower TPR and low FPR should be selected. This principle is also depicted in Figure 15. The reconfiguration of such models might also be required if the FPR or TPR do not meet the expected behaviour over time. Finally, the implications that the formulated assumptions in Section 2.1.1 yield must be discussed. To meet these assumptions, two aspects must be considered in a real world application. First of all, a measurement trajectory must be used for data acquisition so that the HI data is comparable and has a low noise level. Secondly, CATS must be extended by mechanisms to ensure that anomalies or trends in the HI data are only due to wear and not changing environmental conditions, new robot programs or faulty data acquisition systems.

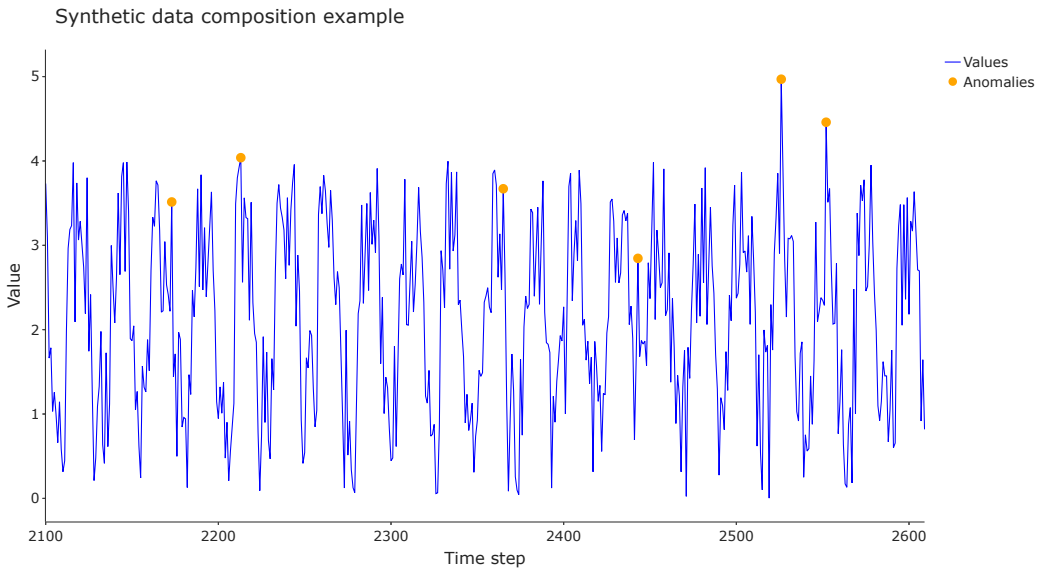

Figure 14. Example of a noisy time series from synthetic data set 2.

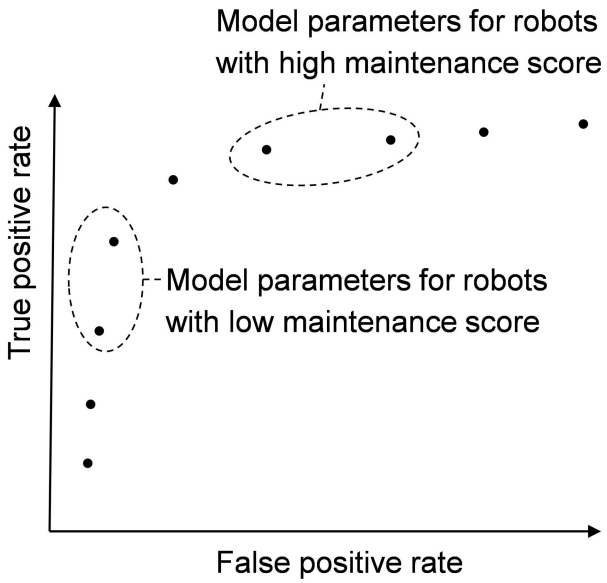

Figure 15. Selection of model parameters based on a maintenance score.

5. Conclusions

A combined anomaly detection and trend detection system for the condition monitoring of industrial robot gears has been presented. To select suitable models for these tasks, a method in which models are evaluated based on synthetic and accelerated wear test data was formulated. The synthetic data consists of time series with noise, cyclic behaviour, trends and anomalies based on realistic assumptions that were gathered from industry data. The accelerated wear test data was collected during two experiments with six-axis industrial robots, which provoked multiple gear faults and exhibited both trends and anomalies. By applying the presented method, it was found that the Cox-Stuart test is most suitable for trend detection and the local outlier factor algorithm or the long short-term neural network are capable of detecting the anomalies in the accelerated wear test data. For future research, we believe that the considerations in Section 4 regarding the extensions of CATS with functionalities to detect reasons for false alarms such as robot program changes or the change of the robot tool and the automatic reconfiguration of models in case of too many false alarms are the most important topics for enabling the automated condition monitoring of industrial robot gears in industry.

Author Contributions: Conceptualization, C.N.; methodology, C.N.; software, C.N.; validation, C.N.; formal analysis, C.N.; investigation, C.N.; resources, G.R.; data curation, C.N.; writing—original draft preparation, C.N.; writing—review and editing, G.R.; visualization, C.N.; supervision, G.R.; project administration, C.N.; funding acquisition, G.R. All authors have read and agreed to the published version of the manuscript.

Funding: We express our gratitude to the Bavarian Ministry of Economic Affairs, Regional Development, and Energy for the funding of our research. The formulated outlook will be investigated as part of the research project "KIVI" (grant number IUK-1809-0008 IUK597/003) and will be further developed and implemented.

Data Availability Statement: The data presented in this study are available on request from the corresponding author. The data are not publicly available due to confidentiality reasons.

Conflicts of Interest: The authors declare no conflict of interest. The funders had no role in the design of the study; in the collection, analyses, or interpretation of data; in the writing of the manuscript, or in the decision to publish the results.

Acknowledgments: We express our gratitude to our project partners BMW, Fluke and KUKA, who participate in the KIVI project for the fruitful discussions and creative ideas.

Appendix A. Model Parameters for ROC Curves

Table A1. Considered Models.

Model	Parameter	Range
MK	Confidence interval	0.9–0.999 in variablestep sizes
CS	Confidence interval	0.9–0.999 in variable step sizes
LR	Slope threshold	0–1 in variable step sizes
MA	Amplifier	min: 0.5, max: 0.8, step: 0.1
	Length above threshold	min: 24, max: 72, step: 2
	Moving Average Window	0.04×(dataset length)–0.18×(dataset length)
ARMA	Autoregression lags	min: 1, max: 9, step: 2
	Moving average lags	min: 0.2, max: 1, step: 0.2
	Anomaly threshold	min: 0.01, max: 0.1, step: 0.02
AR	Autoregression lags	min: 0.2, max: 1, step: 0.2
	Anomaly threshold	min: 0.01, max: 0.1, step: 0.02
CNN	Training epochs	10, 20, 50
	Anomaly threshold	0.1, 0.2, 0.3, 0.4, 0.5, 0.9, 0.95, 0.98, 0.99, 0.999
LSTM	Training epochs	10, 20, 50
	Anomaly threshold	0.1, 0.2, 0.3, 0.4, 0.5, 0.9, 0.95, 0.98, 0.99, 0.999
DBSCAN	Epsilon	min: 0.1, max: 1.3, step: 0.2
	Minimal number of samples	13, 21, 34, 55, 89, 144, 233, 377
GP	Anomaly threshold	0.7, 0.8, 0.9, 0.95
	Kernel upper bound	0.0001, 0.0005, 0.001, 0.002, 0.003, 0.005, 0.008, 0.013, 0.021, 0.034, 0.055, 0.089, 0.144, 0.233, 0.377, 0.61, 0.987
IF	Number of estimators	50, 100, 200
	Contamination	0.01, 0.02, 0.03, 0.05, 0.08, 0.13, 0.21, 0.34
LOF	Number of neighbors	5, 10, 20, 30, 50, 80
	Contamination	0.001, 0.01, 0.02, 0.03, 0.05, 0.08, 0.13, 0.21, 0.34, 0.5
OCSVM	Kernel	'rbf, sigmoid
	Nu	0.01, 0.02, 0.03, 0.05, 0.08, 0.13, 0.21, 0.34
KDE	Bandwidth	0.2, 0.3, 0.5, 0.8, 1.3, 2.1, 3.4, 5.5
	Anomaly threshold	0.75, 0.9, 0.95, 0.99

Appendix B. AUC Tables

Table A2. Overview of the AUC values of the trend detection models.

	Synthetic Data Set 1	Synthetic Data Set 2
Cox Stuart	0.750000	0.968750
Crossing Averages Model	1.000000	0.679688
Linear Regression	0.984375	0.707031
Mann Kendall	0.732422	0.861328

Table A3. Overview of the AUC values of the anomaly detection models.

	Synthetic Data Set 1	Synthetic Data Set 2
AR	0.998641	0.550152
ARMA	0.999713	0.553447
CNN	0.955253	0.596032
DBSCAN	1.000000	0.553332
GP	0.716030	0.591000
IF	0.706679	0.580334
KDE	0.584487	0.499234
LOF	0.999880	0.550426
LSTM	0.995874	0.612189
OCSVM	0.656618	0.542888
STD	0.999951	0.576333

Appendix C. Individual ROC Curves

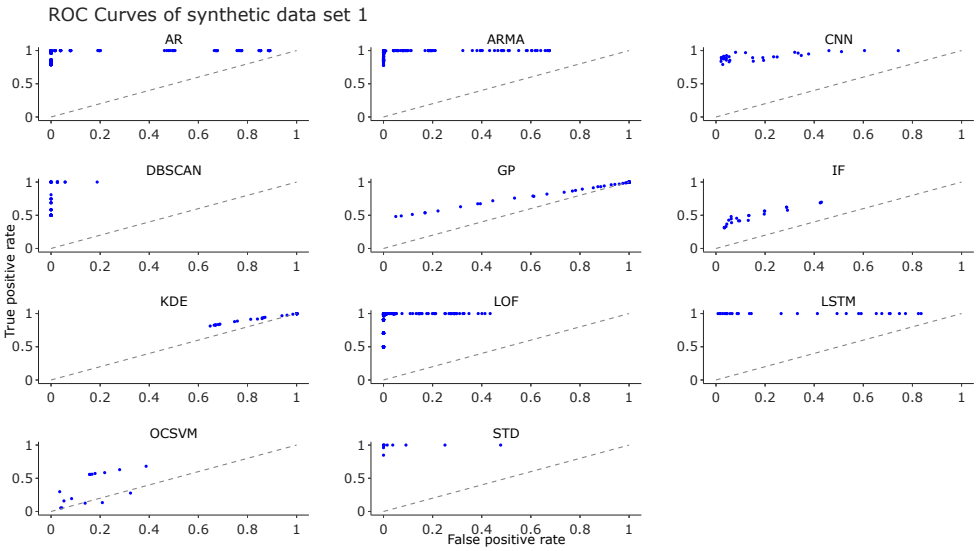

Figure A1. Results of the anomaly detection models based on synthetic data set 1.

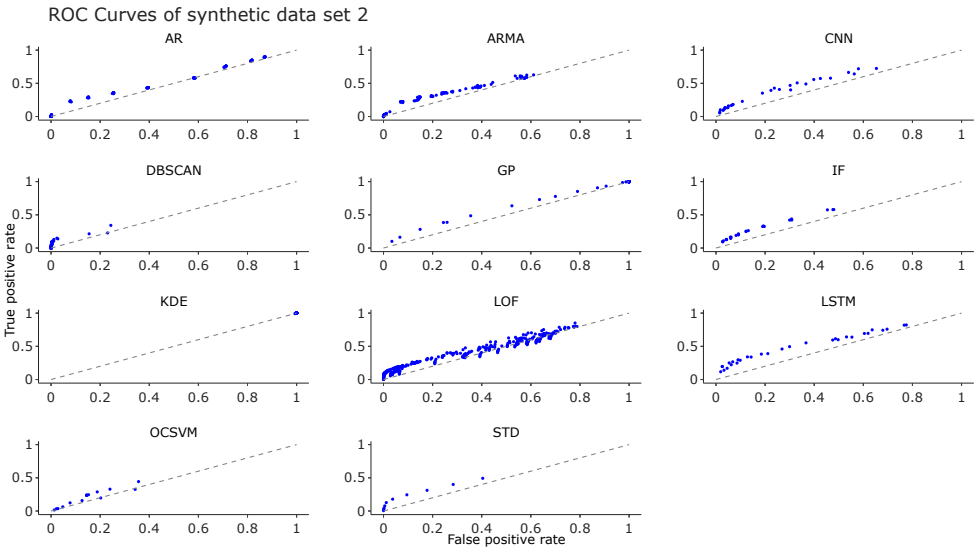

Figure A2. Results of the anomaly detection models based on synthetic data set 2.

References

1. Krockenberger, O. Industrial Robots for the Automotive Industry. In *SAE Technical Paper Series*; SAE International: Warrendale, PA, USA, 1996. [CrossRef]
2. 17359: 2018-05, Zustandsüberwachung und-Diagnostik von Maschinen—Allgemeine Anleitungen (ISO_17359: 2018). 2018. Available online: https://www.iso.org/standard/71194.html (accessed on 4 November 2021).
3. Nentwich, C.; Reinhart, G. A Method for Health Indicator Evaluation for Condition Monitoring of Industrial Robot Gears. *Robotics* **2021**, *10*, 80. [CrossRef]
4. Costa, M.A.; Wullt, B.; Norrlöf, M.; Gunnarsson, S. Failure detection in robotic arms using statistical modeling, machine learning and hybrid gradient boosting. *Measurement* **2019**, *146*, 425–436. [CrossRef]
5. Sathish, V.; Orkisz, M.; Norrlof, M.; Butail, S. Data-driven gearbox failure detection in industrial robots. *IEEE Trans. Ind. Inform.* **2019**, *16*, 193–201. [CrossRef]
6. Cerquitelli, T.; Nikolakis, N.; O'Mahony, N.; Macii, E.; Ippolito, M.; Makris, S. (Eds.) *Predictive Maintenance in Smart Factories*; Information Fusion and Data Science; Springer: Singapore, 2021. [CrossRef]
7. Bittencourt, A.C.; Saarinen, K.; Sander-Tavallaey, S. A Data-driven Method for Monitoring Systems that Operate Repetitively-Applications to Wear Monitoring in an Industrial Robot Joint1. *IFAC Proc. Vol.* **2012**, *45*, 198–203. [CrossRef]
8. Sathish, V.; Ramaswamy, S.; Butail, S. Training data selection criteria for detecting failures in industrial robots. *IFAC-PapersOnLine* **2016**, *49*, 385–390. [CrossRef]
9. Trung, C.T.; Son, H.M.; Nam, D.P.; Long, T.N.; Toi, D.T.; Viet, P.A. Fault detection and isolation for robot manipulator using statistics. In Proceedings of the 2017 International Conference on System Science and Engineering, Ho Chi Minh City, Vietnam, 21–23 July 2017; IEEE: Piscataway, NJ, USA, 2017; pp. 340–343. [CrossRef]
10. Chen, T.; Liu, X.; Xia, B.; Wang, W.; Lai, Y. Unsupervised Anomaly Detection of Industrial Robots Using Sliding-Window Convolutional Variational Autoencoder. *IEEE Access* **2020**, *8*, 47072–47081. [CrossRef]
11. Wen, X.; Chen, H. Heterogeneous Connection and Process Anomaly Detection of Industrial Robot in Intelligent Factory. *Int. J. Pattern Recognit. Artif. Intell.* **2020**, *34*, 2059041. [CrossRef]
12. Hong, Y.; Sun, Z.; Zou, X.; Long, J. Multi-joint Industrial Robot Fault Identification using Deep Sparse Auto-Encoder Network with Attitude Data. In Proceedings of the 2020 Prognostics and Health Management Conference (PHM-Besançon), Besancon, France, 4–7 May 2020; IEEE: Piscataway, NJ, USA, 2020; pp. 176–179. [CrossRef]
13. Jaber, A.A.; Bicker, R. Industrial Robot Backlash Fault Diagnosis Based on Discrete Wavelet Transform and Artificial Neural Network. *Am. J. Mech. Eng.* **2016**, *4*, 21–31.
14. Nentwich, C.; Junker, S.; Reinhart, G. Data-driven Models for Fault Classification and Prediction of Industrial Robots. *Procedia CIRP* **2020**, *93*, 1055–1060. [CrossRef]
15. Cheng, F.; Raghavan, A.; Jung, D.; Sasaki, Y.; Tajika, Y. High-Accuracy Unsupervised Fault Detection of Industrial Robots Using Current Signal Analysis. In Proceedings of the IEEE International Conference on Prognostics and Health Management (ICPHM), San Francisco, CA, USA, 17–20 June 2019.
16. Kim, Y.; Park, J.; Na, K.; Yuan, H.; Youn, B.D.; Kang, C.S. Phase-based time domain averaging (PTDA) for fault detection of a gearbox in an industrial robot using vibration signals. *Mech. Syst. Signal Process.* **2020**, *138*, 106544. [CrossRef]
17. Pu, Z.; Cabrera, D.; Bai, Y.; Li, C. A one-class generative adversarial detection framework for multifunctional fault diagnoses. *IEEE Trans. Ind. Electron.* **2021**. [CrossRef]
18. Pimentel, M.A.; Clifton, D.A.; Clifton, L.; Tarassenko, L. A review of novelty detection. *Signal Process* **2014**, *99*, 215–249. [CrossRef]
19. Braei, M.; Wagner, S. Anomaly Detection in Univariate Time-series: A Survey on the State-of-the-Art. *arXiv* **2020**, arXiv:2004.00433.
20. Bishop, C.M. *Pattern Recognition and Machine Learning*, corrected at 8th printing 2009 ed.; Springer: New York, NY, USA, 2009.
21. Kemmler, M.; Rodner, E.; Wacker, E.S.; Denzler, J. One-class classification with Gaussian processes. *Pattern Recognit.* **2013**, *46*, 3507–3518. [CrossRef]
22. Breunig, M.M.; Kriegel, H.P.; Ng, R.T.; Sander, J. LOF. *ACM SIGMOD Rec.* **2000**, *29*, 93–104. [CrossRef]
23. Liu, F.T.; Ting, K.M.; Zhou, Z.H. Isolation Forest. In Proceedings of the 2008 Eighth IEEE International Conference on Data Mining, Pisa, Italy, 15–19 December 2008; IEEE: Piscataway, NJ, USA, 2008; pp. 413–422. [CrossRef]
24. Ester, M.; Kriegel, H.P.; Sander, J.; Xu, X. A Density-Based Algorithm for Discovering Clusters in Large Spatial Databases with Noise. In Proceedings of the Second International Conference on Knowledge Discovery and Data Mining, KDD'96, Portland, OR, USA, 2–4 August 1996; AAAI Press: Palo Alto, CA, USA 1996; pp. 226–231.
25. Kumar, V.; Banerjee, A.; Chandola, V. Anomaly Detection for Symbolic Sequences and Time Series Data. 2009. Available online: https://conservancy.umn.edu/bitstream/handle/11299/56597/Chandola_umn_0130E_10747.pdf;jsessionid=A026AFB0208E56D91DD811BA4A134056?sequence=1 (accessed on 4 November 2021).
26. Aggarwal, C.C. *Outlier Analysis*, 2nd ed.; Springer International Publishing: Cham, Switzerland, 2017. [CrossRef]
27. Chauhan, S.; Vig, L. Anomaly detection in ECG time signals via deep long short-term memory networks. In Proceedings of the 2015 IEEE International Conference on Data Science and Advanced Analytics (DSAA), Paris, France, 19–21 October 2015; IEEE: Piscataway, NJ, USA, 2015; pp. 1–7. [CrossRef]
28. Munir, M.; Siddiqui, S.A.; Dengel, A.; Ahmed, S. DeepAnT: A Deep Learning Approach for Unsupervised Anomaly Detection in Time Series. *IEEE Access* **2019**, *7*, 1991–2005. [CrossRef]

29. Zhang, R.; Zhang, S.; Muthuraman, S.; Jiang, J. One Class Support Vector Machine for Anomaly Detection in the Communication Network Performance Data. 2007. Available online: http://www.wseas.us/e-library/conferences/2007tenerife/papers/572-618.pdf (accessed on 4 November 2021).
30. Sharma, S.; Swayne, D.A.; Obimbo, C. Trend analysis and change point techniques: A survey. *Energy Ecol. Environ.* **2016**, *1*, 123–130. [CrossRef]
31. Kendall, M.G.; Gibbons, J.D. *Rank Correlation Methods*, 5th ed.; Arnold: London, UK, 1990.
32. Cox, D.R.; Stuart, A. Some Quick Sign Tests for Trend in Location and Dispersion. *Biometrika* **1955**, *42*, 80. [CrossRef]
33. Crawford, C.G.; Slack, J.R.; Hirsch, R.M. *Nonparametric Tests for Trends in Water-Quality Data Using the Statistical Analysis System*; USGS Numbered Series; U.S. Geological Survey: Reston, VA, USA, 1983. [CrossRef]
34. DURBIN, J.; WATSON, G.S. Testing for Serial Correlation in Least Squares Regression. I. *Biometrika* **1950**, *37*, 409–428. [CrossRef]
35. Melek, W.W.; Lu, Z.; Kapps, A.; Fraser, W.D. Comparison of trend detection algorithms in the analysis of physiological time-series data. *IEEE Trans. Bio-Med Eng.* **2005**, *52*, 639–651. [CrossRef]
36. Modi, S.; Lin, Y.; Cheng, L.; Yang, G.; Liu, L.; Zhang, W.J. A Socially Inspired Framework for Human State Inference Using Expert Opinion Integration. *IEEE/ASME Trans. Mechatron.* **2011**, *16*, 874–878. [CrossRef]
37. Carvalho Bittencourt, A. *Modeling and Diagnosis of Friction and Wear in Industrial Robots*; Linköping University Electronic Press: Linköping, Sweden, 2014; Volume 1617. [CrossRef]
38. Nentwich, C. CATS—A Combined Anomaly Detection and Trend Detection Model. Available online: https://github.com/xorbey/CATS_public (accessed on 4 November 2021).
39. Danielson, H.; Schmuck, B. Robot Condition Monitoring: A First Step in Condition Monitoring for Robotic Applications. Master's Thesis, Lulea University of Technology, Lulea, Sweden, 2017.
40. Karlsson, M.; Hörnqvist, F. Robot Condition Monitoring and Production Simulation. Master's Thesis, Lulea University of Technology, Lulea, Sweden, 2018.

8.5 Cost-Benefit Analysis of Industrial Robot Gear Condition Monitoring

Available online at www.sciencedirect.com

ScienceDirect

Procedia CIRP 107 (2022) 143–148

www.elsevier.com/locate/procedia

55th CIRP Conference on Manufacturing Systems

Cost-Benefit Analysis of Industrial Robot Gear Condition Monitoring

Corbinian Nentwich[a,*], Rüdiger Daub[a]

[a]*Technical University Munich, Boltzmannstraße 15, 85748 Garching, Germany*

*Corresponding author. Tel.: +49 89 289 15542; E-mail address: corbinian.nentwich@iwb.tum.de

Abstract

On the one hand, condition monitoring of industrial robot gears can reduce unexpected downtimes of highly automated production lines and thus save related costs. On the other hand, the implementation and operation of such systems is costly itself. In this context, we present a cost model to compare condition monitoring scenarios with preventive maintenance scenarios for the application of industrial robot gear maintenance. We parameterize this model with data from various sources and use the parameterized model to identify scenarios in which condition monitoring is economically efficient.

Keywords: industrial robot, condition monitoring, cost-benefit analysis

1. Introduction

Highly automated production lines are the backbone of many industries such as the automotive or electronics production sector [1]. Industrial robots (IR) are an integral part of such lines, and any downtimes cause a productivity loss that needs to be minimized. Condition monitoring (CM) of robots' gears is one measure to achieve this objective [2–5]. This maintenance strategy uses sensor data to determine a robot's health state and to trigger maintenance decisions before failures occur. A condition monitoring system consists of a data acquisition, a data transformation and a modeling module that provides decision support for determining the time of a maintenance action [6]. A data acquisition system based on vibration sensor data and measurement trajectories was proposed in [7]. The transformation of measurements acquired with this system into meaningful health indicators by means of short-time Fourier transform and Z-scores was presented in [8]. Finally, a system for supporting automated maintenance decisions based on anomaly and trend detection was described in [9] as a suitable modeling module. To deploy such a system in a production environment, it must be ensured that the system adds value to the company's venture. This is why we present a customized cost model to compare the economic efficiency of CM with preventive maintenance in the context of IR gears. We parameterize this model with historic data as well as data taken from surveys and market research. Finally, we use the parameterized model to conduct a sensitivity analysis for various cost parameters and thus determine scenarios in which CM for IR gears is economically efficient. In the remainder of this publication, we first present the state of the art regarding cost-benefit analysis (CBA) of CM and refine the addressed research gap in Section 2. In Section 3, we present our cost model, as well as the method for the parameterization of the model and the approach for the sensitivity analysis. In Section 4, we present the results of the sensitivity analysis. A discussion of these results is given in Section 5. We conclude our work in Section 6, where we also give an outlook to future initiatives in this research field.

2. State of the art

Quantifying the potential benefits of a CM system and justifying the investment in the required technologies is a considerable challenge [10]. Therefore, various approaches

10.1016/j.procir.2022.04.024

and cost models have been proposed in the literature, which differ in the cost factors they consider, the evaluation metrics used, and the ways in which they handle uncertainty. Besides, some publications aim to provide more general concepts, while other approaches are tailored to specific use cases.

A comprehensive overview of cost factors, cost calculation approaches and decision making relating to the investment in a CM system is presented in [10].

[11] suggests a general holistic four-step framework for conducting a CBA of CM systems, which starts by identifying the most critical components in terms of availability and reliability of the monitored manufacturing system. In the second step, different types of failure and applicable monitoring concepts are specified, and development and implementation costs are calculated. Subsequently, the benefits of different scenarios are estimated, and the knowledge gained is iteratively incorporated into the design of the CM system in step three. Finally, the concepts are evaluated using suitable metrics, such as the return on investment (ROI). Since making assumptions for cost parameters is a significant challenge and, at the same time, the quality of the result depends on the quality of the assumptions made, the use of a multivariate trade space analysis was proposed by [12]. A mathematical cost model was introduced in [13] for comparing the net revenue of machines using different maintenance strategies by considering fundamental cost factors such as initial investments, labor costs and breakdown costs. Aiming for a more appropriate cost equation, the approach was extended by considering the specific failure rates of individual components along with a proportional repair rate [14]. Another generally applicable approach for a CBA of CM systems is developed in [15]. Uncertainties and non-monetary benefits are modelled using fuzzy logic concepts. The fuzzy systems enable the investigation of different sensitivities regarding the benefit and risk associated with a CM investment, and they can also be used for optimizing the technical design of the CM system as shown in the case study.

Similar cost models have also been proposed in [16, 17], including use-case relevant cost parameters such as energy tax, energy consumption and secondary quality losses. A specific cost model is presented that takes into account the trade-off between detection rates and false alarm rates of anomaly detection models and considers different costs for these scenarios [18]. A decision-support system is provided to enable practitioners to determine the level of model performance they require for their application. Finally, a case study is presented from the process industry.

A model that considers such cost factors as safety and environmental costs is presented in [19] in the context of the maintenance systems of a fusion reactor and evaluated for different failure rates of the system. It was emphasized that CM not only offers economic benefits but can also be of value with regard to safety and regulatory issues.

[20] determined the break-even point between life cycle cost savings from CM and the required level of failure detection effectiveness. To do this, they modelled system-wide failure probabilities as a time-variant non-homogeneous Poisson process. Using this failure distribution, the detectability level required for the economical use of a CM system is derived by comparing the necessary investments and savings. Additionally, an extension of the model to multiple CM systems and failure modes is introduced, resulting in multidimensional break-even surfaces. Similarly, [21] uses a life cycle cost model supplemented by a maintenance planning model to determine the optimum prognostic distance and a Monte Carlo simulation for analyzing the ROI of CM systems. A model for deriving the optimal maintenance cost based on a linear and stochastically distributed wear model is described in [22]. The impact of fleet data refinement on maintenance costs is analyzed based on a specific cost model in [23] and applied in a case study focusing on pulp dryers.

Industry-specific models were presented, for instance for wind turbines or milling machines as well as in the context of industrial robots. To investigate the economic benefits of CM systems in wind power systems, [24] uses a life cycle cost model, in which the replacement densities of individual components are estimated as Weibull distributions. The sensitivity to different Weibull parameters is analyzed by averaging the resulting life cycle cost distribution. In addition, a stochastic risk analysis was conducted by building sets of failure scenarios using Monte Carlo simulation. The net present value of CM for wind turbines was calculated under consideration of different cost factors, such as logistical costs, failure costs and monitoring system costs. A simulation model based on Monte Carlo Markov chains was used to evaluate various sensitivity scenarios for wind turbine CM. Altered parameters were the distance to shore or the number of wind turbines per farm [25].

A cost model for milling machine CM based on survey data is presented in [26].

In the context of industrial robots, [27] analyze the cost structures of on-site and remote maintenance and provide a model for calculating the cost-effectiveness of the maintenance strategy, which can be used as a decision-making support for practitioners.

The literature review shows that there are already a variety of mathematical cost models, which can be used for the economic evaluation and justification of CM systems. Generalized cost models make it possible to estimate the economic benefit of CM systems [15] but often neglect application-specific factors or the possible technical solution space. In [17], for example, the analysis of CM of energy-intensive induction motors is supplemented with domain-specific cost parameters. The field of industrial robots is characterized by their integration into interlinked and clocked production lines. No CBA for different maintenance scenarios for industrial robots could be identified in the existing research, which considers either these aspects or the technical solution approaches for CM. The case studies in the literature also reveal that CBA is usually limited by insufficient information as well as uncertainties regarding individual cost factors. When conducting a CBA, application-specific risks and uncertainties need to be identified and outlined using a suitable method such as a

sensitivity analysis. In the following sections, we therefore present an application specific cost model for industrial robot gear CM and parameterize it with realistic data taken from different sources.

3. Methodology

In the following, we first present the assumptions on which the model is based before presenting the cost model itself. Then, the model parameterization and analysis processes are described. The overall objective of the presented work is the cost comparison of preventive and condition based maintenance for different robot runtimes. The overall method flow is depicted in Figure 1.

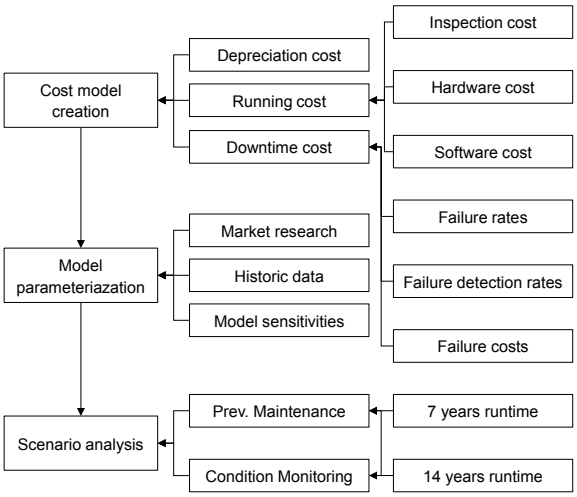

Figure 1: Overall method flow

3.1. Model assumptions

The model is based on certain assumptions, which are presented in this section. We assume that CM is economically efficient if it is the maintenance strategy that yields the lowest costs per robot per year. In addition to the CM strategy, in which inspections and maintenance are executed periodically as well as on the basis of detected anomalies, we consider a preventive maintenance strategy, in which inspections and maintenance are executed only periodically. We assume that acceleration sensors are used for data acquisition in the CM scenario as suggested in [7]. We also assume that the sensors are portable and can thus be used for multiple robots, since the robots' health state does usually not change abruptly. Furthermore, a condition monitoring system is implemented as presented in [8] and [9]. Finally, we assume that the usage of CM can extend the useful lifetime of an industrial robot. In the following, we describe the cost models for the two strategies.

3.2. Model design

The cost model for the CM maintenance strategy is based on the yearly costs per robot $C_{CM,Robot}$ as calculated by Formula 1.

$$C_{CM,Robot} = C_{dep} + C_{running} + C_{downtime} \quad (1)$$

They are based on depreciation costs C_{dep}, running costs $C_{running}$ of the CM system and robot downtime costs $C_{downtime}$. The depreciation cost C_{dep} is the sum of the depreciation costs of the robot investment, the condition monitoring system hardware and installation, and the development of the CM software (Formula 2). These costs are calculated by Formulae $3-5$. They are based on the investment costs per robot $C_{invest,\ r}$, the CM system $C_{invest,\ CM}$ and the CM software $C_{invest,\ CMs}$. The latter is calculated by estimating the development time of the CM software and the associated personnel costs of the development. The depreciation costs depend on the usage times $t_{usage,\ k}$of the system k in years and the number of robots $n_{r,\ usable,\ k}$ for which one system can be used.

$$C_{dep} = C_{dep,r} + C_{dep,\ CM} + C_{dep,\ CMs} \quad (2)$$

$$C_{dep,\ r} = \frac{C_{invest,\ r}}{t_{usage,\ r}} \quad (3)$$

$$C_{dep,\ CM} = \frac{C_{invest,\ CM}}{t_{usage,\ CM} * n_{r,usable\ CM}} \quad (4)$$

$$C_{dep,\ \mathrm{CMs}} = \frac{C_{invest,\ \mathrm{CMs}}}{t_{usage,\ CMs} * n_r} \quad (5)$$

The ongoing costs $C_{running}$ are the operating costs of the CM hardware and software. They are based on personnel costs $C_{p,CM}, C_{p,\ \mathrm{CMs}}$ and inspection times $t_{i,\ CM}, t_{i,\ \mathrm{CMs}}$ needed for both systems and the operating costs of the CM software $C_{r,\ \mathrm{CMs}}$ (Formula 6).

$$C_{running} = C_{p,CM} * t_{i,\ CM} + C_{p,\ \mathrm{CMs}} * t_{i,\ CMs} + C_{r,\ \mathrm{CMs}} \quad (6)$$

Finally, the downtime costs $C_{downtime}$ are calculated using Formula 7.

$$C_{downtime} = (1 - d_g) * f_g * C_{f,g} + f_M * C_{f,M} \quad (7)$$

In this formula, we consider the costs caused by gear faults and motor faults. Gear faults are the most critical faults as they cause long downtimes, motor faults are the most frequent faults that appear. The CM system will only detect gear faults, hence, the costs caused by gear faults are reduced depending on the failure detection rate of the CM system. The detection rate of gear faults d_g is estimated by testing the CM model. The fault frequencies per year f_g for gears and f_M for motors can be derived from historical data such as maintenance protocols. The downtime costs $C_{f,g}$ and $C_{f,M}$ per incident depend on the average duration of the downtime and the structure of the production system. This is expert knowledge which we assume is available in the maintenance department.

Formula 8 can be used to calculate the costs $C_{Ref,Robot}$ of the preventive maintenance strategy.

$$C_{Ref,Robot} = \frac{C_{invest,\ robot}}{t_{usage,\ robot}} + f_g * C_{f,g} + f_M * C_{f,M} \quad (8)$$

If $C_{Ref,Robot}$ is bigger than $C_{CM,Robot}$, it is economically beneficial to introduce a CM system.

3.3. Parameterization Process

Table 1: Parameters of the cost model

Parameter Name	Source	Value / Value range
Price of data acquisition system $C_{invest,\ CM}$ per scenario	Market research	2500 €
Sensor depreciation time $t_{usage,\ CM}$	Interview manufacturer	20 years
Number of robots n_r	Model sensitivity	200
Number of robots per data acquisition system $n_{r,usable\ CM}$	Assumption	10
Yearly time for data acquisition system inspection $t_{insp,\ CM}$	Survey	24 h
Yearly time for CM software inspection $t_{insp,\ CMs}$	Survey	160 h
Personnel cost $C_{p,CM}$ or $C_{p,\ CMs}$	Market research	62,5 €/h
Running cost of software per scenario $C_{r,\ CMs}$	Market research	2000 €
Software development time	Survey	4800 h
Software development cost $C_{invest,\ CMs}$	Survey * developer costs	384,000 €
Software depreciation time $t_{usage,\ CMs}$	Assumption	Scenario runtime
Failure rate of motors f_M	Historic data for 7 years, assumption for 14 years	0.1 for 7 years, 0.15 for 14 years
Failure cost of motor $C_{f,M}$	Historic data	2000 €
Failure rate of gears f_g	Historic data for 7 years, assumption for 14 years	0.003 for 7 years, 0.006 for 14 years
Failure detection rate of gears d_g	Sensitivity	0.95
Failure cost of gear $C_{f,g}$	Historic data	120,000 €
Investment cost of robot $C_{invest,\ r}$		Confidential
Depreciation time of robot $t_{usage,\ r}$	Interview manufacturer	7 or 14
Shape parameter of Weibull distribution	Assumption	9.428
Form parameter of Weibull distribution	Assumption	11.72

Various methods were used to estimate the parameters of the cost model. We conducted market research to derive the running costs of the software, the initial robot investment, the spare part costs and the personnel costs for both the data acquisition system and the CM software inspection. We used information from an interview conducted with experts from Fluke to determine the sensor depreciation time and the maintenance time for the CM system. We used a survey to determine the development time for the CM model, the depreciation time of this model and the maintenance time required for the CM model. In this survey, we gave 24 experts information regarding the different software modules required for data acquisition, data transformation and modeling of the CM system. The experts' task was then to estimate the time required to develop the described software modules. We derived the total development time by totaling the average answer values for these questions. We consider the number of robots in the production system and the failure detection rate as sensitivities in our model. We used historic data to model the failure rates and costs of the gear and motor faults. In a second scenario, we model the gear failure rates with a Weibull distribution for a cost analysis over time. This is a common approach to model the time-dependent fault probability of assets [24]. In this two-parameter Weibull distribution, we assumed that 90 percent of a robot fleet has a gear failure after an operating time of 10 to 14 years. The failure time is evenly distributed over this time frame. The scale parameter α and shape parameter β were derived according to the methodology presented in [28]. Formula 9 describes the cumulative probability density function used. This formula describes the probability whether a robots will have a failure until the year t [29].

$$F(t) = 1 - e^{-\left(\frac{t}{\alpha}\right)^{\beta}}, t \geq 0 \quad (9)$$

All parameters, their sources and their values or value ranges are presented in Table 1.

3.4. Analysis process

We used the parameterized model to calculate the overall cost per year per robot for a baseline scenario and for different values of the sensitivities of our model for a runtime of seven years. The baseline scenario is modeled by the parameters in Table 1, the two different maintenance strategies and two robot runtimes of seven and 14 years. This allowed the identification of parameter sets in which CM is economically efficient. Additionally, we analyzed the costs using a failure rate following an exponential Weibull distribution to simulate increasing failure rates over the

Table 2: Analysed scenarios

Scenario name	Scenario maintenance type	Scenario time span
Ref 7	Preventive maintenance	7
Ref 14	Preventive maintenance	14
Vib 7	CBM	7
Vib 14	CBM	14

increasing lifetime of the robots. The results are presented in the next section. The scenario names are presented in Table 2.

4. Results

Figure 2 shows the average yearly costs for the different scenarios. As the depreciation time increases, the yearly depreciation costs decrease. Likewise, the downtime costs increase as the failure rates increase. This increase in downtime costs makes the condition monitoring scenario more cost efficient over a lifetime of 14 years. The CM system engineering costs in the seven-year scenario would be the biggest lever to render the maintenance scenario cost efficient in the seven-year scenario. In this case, the software development time would have to be reduced by 70 %.

Figure 3 summarizes the sensitivity analysis in terms of the number of robots in the scenario and the failure rate of the robots. The heatmap shows the relative costs of scenario Vib 7 to scenario Ref 7. The borderline in the heatmap separates economically efficient scenarios from inefficient ones. The variation of the number of robots considered by 80 results in a cost difference of 5%. The variation of the failure rates in the range from 0 to 0.006 leads to a cost change of 19%. An increasing failure rate or an increasing number of robots has a positive effect on the economic viability of the scenario.

Figure 4 presents the sensitivity analysis of the number of robots and the failure detection rate. By varying the failure detection rate in the range of 0.85 to 1 a cost change of 1 % can be observed. Even assuming a perfect classification model that can detect all faults, no economically efficient scenario could be found for this range of robots and the remaining parameter values of scenarios Ref 7 and Vib 7. Increasing failure detection rates and increasing numbers of robots decrease the overall yearly cost per robot.

As the failure rate shows the highest sensitivity, we analyzed one more scenario in which it is not assumed to be constant but follows a Weibull distribution. The yearly costs per robot assuming changing failure rates per year are shown in Figure 5. Here, increasing costs can be seen with the rising failure rates modeled by the Weibull distribution. These cost developments are dampened by the CM system in scenarios Vib 7 and Vib 14. Furthermore, the break-even points of the scenarios are visible. The break-even point is reached after seven years. This validates the results shown in Figure 2, where both scenarios are approximately equally efficient for the seven-years scenario and the CM scenario is more efficient for the 14-year scenario.

5. Discussion

In our analysis, we chose to exclude certain costs that could be used in more sophisticated future models. In the following, we will discuss these cost parameters and why we decided to exclude them. We will then elaborate on the implications that the CM scenarios' cost structure yield.
One factor that was not included in the model are the costs induced by false alarms of the CM model. These false alarms would trigger a maintenance action (e.g., exchange of a gear), even though the component is still functional and thus causing unnecessary costs. To include this cost factor, expert knowledge about the number of anomalies detected by the CM system would be required, along with the number of premature gear exchanges in a preventive maintenance

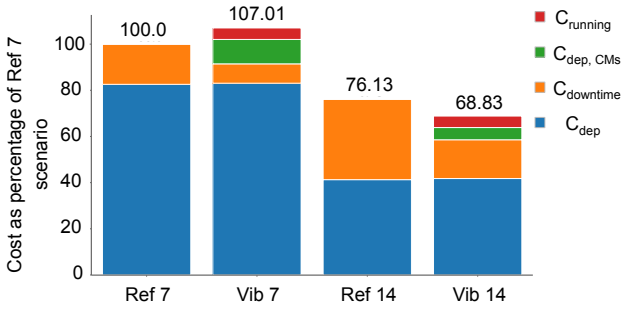

Figure 2: Average yearly costs for maintenance scenarios

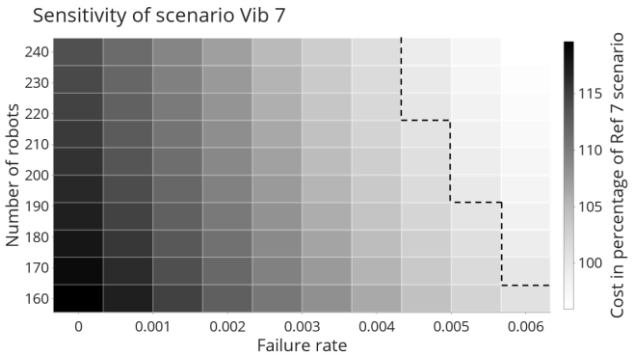

Figure 3: Sensitivity analysis of failure rate and fleet size

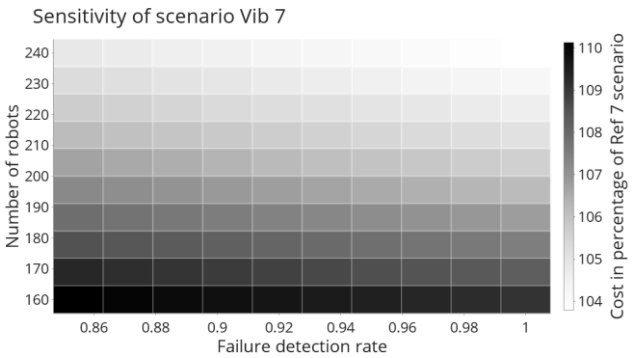

Figure 4: Sensitivity analysis of failure detection rate and fleet size

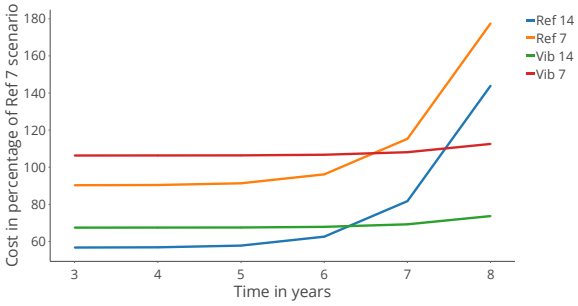

Figure 5: Yearly costs per maintenance scenario assuming a Weibull distributed failure rate

scenario to obtain a fair comparison. As neither of these numbers were available to us, we assumed that the costs due to premature gear exchanges are equal in all scenarios. Hence, this cost factor can be neglected, as we are comparing different scenarios with each other. If this cost factor would be included, the costs for the CM scenario would increase. Furthermore, we did not include spare part costs savings due to the smaller number of exchanges and the reduced storage time due to unavailable data regarding spare parts and storage cost. These factors would reduce the cost of the CM scenario. Finally, we did not include potential personnel savings within the CM scenario, based on more efficient usage of the maintenance department's personnel capacity. This would also reduce the cost of the CM scenario.
This could be possible because of the improved planning security. However, such capacity usage improvements are hard to model, as the maintenance personnel have many different tasks in addition to the alert-triggered maintenance actions. The cost model presented has two levers for reducing the cost of a CM-based maintenance scenario. Firstly, the development costs represent the largest factor that may be reduced. To do this, either the system could be used for more robots, to distribute the costs over a larger fleet or the reference system and open-source code as presented in [7], [8] and [9] could be used to reduce the development time. The second lever are the hardware costs related to the CM system. These costs could be reduced by sharing sensor systems between robots and collecting data for each specific robot periodically rather than continuously.

6. Conclusion

This work presented a cost model for evaluating the cost efficiency of industrial robot gear condition monitoring. The cost model considers depreciation costs of the robot and the condition monitoring system, running cost of the condition monitoring system and downtime costs. The model was parameterized based on historic, survey and market research data. It was then used to compare different maintenance scenarios, namely preventive and condition-based maintenance over a seven-year and a 14-year time horizon. In this analysis, condition-based maintenance was cost efficient in a 14-year time horizon. The failure rate represents the highest sensitivity in the parameterized model described and the break-even point is reached after eight years. Future work could include the integration of further cost factors, such as the costs of false alarms in the model.

Acknowledgements

We express our gratitude to the Bavarian Ministry of Economic Affairs, Regional Development and Energy for the funding of our research investigated as part of the research project "KIVI" (grant number IUK-1809-0008 IUK597/003) and will be further developed and implemented. Furthermore, we thank our project partners BMW, Fluke and KUKA for the fruitful discussions and collaboration.

References

[1] International Federation of Robotics. Executive Summary World Robotics 2020 Industrial Robots. https://ifr.org/img/worldrobotics/Executive_Summary_WR_2020_Industrial_Robots_1.pdf. Accessed 27 October 2021.
[2] Mourtzis, D., Vlachou, E., 2018. A cloud-based cyber-physical system for adaptive shop-floor scheduling and condition-based maintenance *47*, p. 179.
[3] Cao, Q., Giustozzi, F., Zanni-Merk, C., Bertrand Beuvron, F. de *et al.*, 2019. Smart Condition Monitoring for Industry 4.0 Manufacturing Processes: An Ontology-Based Approach *50*, p. 82.
[4] Gouriveau, R., Medjaher, K., Zerhouni, N., 2016. *From Prognostics and Health Systems Management to Predictive Maintenance 1*. John Wiley & Sons, Inc, Hoboken, NJ, USA.
[5] Wang, J., Gao, R.X., 2022. Innovative smart scheduling and predictive maintenance techniques, in *Design and Operation of Production Networks for Mass Personalization in the Era of Cloud Technology*, Elsevier, San Diego, p. 181.
[6] ISO, 2002. *DIN ISO 13373-1:2002-07, Zustandsüberwachung und -diagnostik von Maschinen- Schwingungs-Zustandsüberwachung- Teil 1: Allgemeine Anleitungen (ISO 13373-1:2002)*. Beuth Verlag GmbH, Berlin.
[7] Nentwich, C., Reinhart, G., 2021. Towards Data Acquisition for Predictive Maintenance of Industrial Robots.
[8] Nentwich, C., Reinhart, G., 2021. A Method for Health Indicator Evaluation for Condition Monitoring of Industrial Robot Gears *10*, p. 80.
[9] Nentwich, C., Reinhart, G., 2021. A Combined Anomaly and Trend Detection System for Industrial Robot Gear Condition Monitoring *11*, p. 10403.
[10] Vogl, G.W., Weiss, B.A., Helu, M., 2019. A review of diagnostic and prognostic capabilities and best practices for manufacturing. J Intell Manuf *30*, p. 79.
[11] Banks, J., Reichard, K., Crow, E., Nickell, E., 2005 - 2005. How engineers can conduct cost-benefit analysis for PHM systems, in *2005 IEEE Aerospace Conference*, IEEE, p. 3958.
[12] Banks, J., Merenich, J., 2007 - 2007. Cost Benefit Analysis for Asset Health Management Technology, in *2007 Proceedings - Annual Reliability and Maintainability Sympsoium*, IEEE, p. 95.
[13] Verma, N.K., Subramanian, T., 2012 - 2012. Cost benefit analysis of intelligent condition based maintenance of rotating machinery, in *2012 7th IEEE Conference on Industrial Electronics and Applications (ICIEA)*, IEEE, p. 1390.
[14] Verma, N.K., Khatravath, S., Salour, A., 2013 - 2013. Cost Benefit Analysis for condition based maintenance, in *2013 IEEE Conference on Prognostics and Health Management (PHM)*, IEEE, p. 1.
[15] Verma, N.K., Ghosh, A., Dixit, S., Salour, A., 2015 - 2015. Cost-benefit and reliability analysis of prognostic health management systems using fuzzy rules, in *2015 IEEE Workshop on Computational Intelligence: Theories, Applications and Future Directions (WCI)*, IEEE, p. 1.
[16] Khatravath, S., Verma, N.K., Salour, A., 2015 - 2015. Cost benefit analysis for maintenance of rotating machines, in *2015 IEEE Conference on Prognostics and Health Management (PHM)*, IEEE, p. 1.
[17] Gugaliya, A., Naikan, V., 2020. A model for financial viability of implementation of condition based maintenance for induction motors *26*, p. 213.
[18] Florian, E., Sgarbossa, F., Zennaro, I., 2021. Machine learning-based predictive maintenance: A cost-oriented model for implementation *236*, p. 108114.
[19] Petkov, N., Wu, H., Powell, R., 2020. Cost-benefit analysis of condition monitoring on DEMO remote maintenance system *160*, p. 112022.
[20] Wang, Y., Wang, P., 2013. Cost Benefit Analysis of Condition Monitoring Systems for Optimal Maintenance Decision Making, in *54th AIAA/ASME/ASCE/AHS/ASC Structures, Structural Dynamics, and Materials Conference*, American Institute of Aeronautics and Astronautics, Reston, Virginia.
[21] Feldman, K., Jazouli, T., Sandborn, P.A., 2009. A Methodology for Determining the Return on Investment Associated With Prognostics and Health Management *58*, p. 305.
[22] Curcurù, G., Galante, G., Lombardo, A., 2010. A predictive maintenance policy with imperfect monitoring *95*, p. 989.
[23] Kinnunen, S.K., Arola, S.M., Kärri, T., 2020. The value of fleet information: a cost-benefit model *34*, p. 321.
[24] Besnard, F., Nilsson, J., Bertling, L., 2010 - 2010. On the economic benefits of using Condition Monitoring Systems for maintenance management of wind power systems, in *2010 IEEE 11th International Conference on Probabilistic Methods Applied to Power Systems*, IEEE, p. 160.
[25] Rastegari, A., Bengtsson, M., 2015 - 2015. Cost effectiveness of condition based maintenance in manufacturing, in *2015 Annual Reliability and Maintainability Symposium (RAMS)*, IEEE, p. 1.
[26] Adu-Amankwa, K., Attia, A.K., Janardhanan, M.N., Patel, I., 2019. A predictive maintenance cost model for CNC SMEs in the era of industry 4.0 *104*, p. 3567.
[27] Zhi, H., Nai-Yong, S., 2020. Cost-benefit analysis on remote maintenance for industrial robot *1676*, p. 12210.
[28] Soman, K.P., Misra, K.B., 1992. A least square estimation of three parameters of a Weibull distribution *32*, p. 303.
[29] Johnson, N.L., Kotz, S., Balakrishnan, n., 1994. *Continuous univariate distributions,* 2nd edn. Wiley, New York, Chichester, …

8.6 Literature overview

Title	Year	Sensor	Component	Robot type	Time series	Time domain	Frequency domain	Time frequency domain	Raw signals	Supervised learning	One-class classification	No model
Robot Condition Monitoring 2017	2017	Acceleration sensor	RV reducer	Six axis	Yes		x					x
A study on rotate vector reducer performance degradation based on Acoustic sensor emission techniques	2019	Acoustic sensor	RV reducer	Test bed	no	x						x
Combining convolutional neural networks with unsupervised learning for Acoustic sensor monitoring of robotic manufacturing facilities	2021	Acoustic sensor		Scara	No			x		x		
Fault Diagnosis Method for Industrial Robots based on Dimension Reduction and Random Forest	2021	Acceleration sensor	Loose screws, tight synchronous belt	Parallel	No	x	x			x		

Multi-joint Industrial Robot Fault Identification using Deep Sparse Auto-Encoder Network with Attitude Data	2020	Acceleration sensor	RV reducer	Six axis	No				x	x		
Design of an Intelligent Embedded System for Condition Monitoring of an Industrial Robot	2017	Acceleration sensor	Spur gear	Six axis	No	x		x		x	x	
Industrial Robot Backlash Fault Diagnosis Based on Discrete Wavelet Transform and Artificial Neural Network	2017	Acceleration sensor	Spur gear	Six axis	No			x		x		
Study of the Usage Life for a Robotic Arm Based on Reducer Diagnosis	2020	Acceleration sensor	Harmonic drive	Six axis	No	x	x			x		
Phase-based time domain averaging (PTDA) for fault detection of a gearbox in an industrial robot using vibration signals	2020	Acceleration sensor	RV reducer	Six axis	No	x	x					x

Research on condition monitoring of speed reducer of industrial robot with acoustic emission	2016	Acoustic sensor	RV reducer	Six axis	No		x	x			x
Attitude data-based deep hybrid learning architecture for intelligent fault diagnosis of multi-joint industrial robots	2021	Acceleration sensor	RV reducer	Six axis	No				x	x	
Robot Condition Monitoring and Production Simulation	2018	Acceleration sensor	RV reducer	Six axis	Yes		x				x
Health Monitoring of Strain Wave Gear on Industrial Robots	2019	Acceleration sensor, current	Harmonic drive	Six axis	No	x	x				x
Methodology for the vibration measurement and evaluation on the industrial robot Kuka	2014	Acceleration sensor	Base plate	Six axis	No		x				x
Research on SCARA Robot Fault Diagnosis Based on Hilbert-Huang Transform and Decision Tree	2021	Acceleration sensor	Loose screws, unstable base	Scara	No			x		x	

Fault diagnosis for industrial robots based on a combined approach of manifold learning, treelet transform and Naive Bayes	2020	Acceleration sensor	Overload, backlash	Parallel			x	x		
Fault Detection of Harmonic Drive Using Multiscale Convolutional Neural Network	2021	Acceleration sensor	Harmonic drive	Six axis			x	x		
Fault Diagnosis of Harmonic Drive With Imbalanced Data Using Generative Adversarial Network	2021	Acceleration sensor	No actual fault	Six axis	x			x		
Fault Diagnosis of Rotation Vector Reducer for Industrial Robot Based on a Convolutional Neural Network	2021	Acceleration sensor	RV reducer	Six axis	x			x		
Autoencoder-based anomaly detection of industrial robot arm using stethoscope based internal sound sensor	2021	Acoustic sensor	No actual fault	Six axis		x			x	

Industrial Robot Rotate Vector Reducer Fault Detection Based on Hidden Markov Models	2019	Acoustic sensor	Different level of backlash	Test bed				x			x
Fault detection of the harmonic reducer based on CNN-LSTM with a novel denoising algorithm	2021	Accelera-tion sensor	Harmonic drive	Test bed				x		x	
Neural Network-Based Model for Classification of Faults During Operation of a Robotic Manipulator	2021	Torque	No actual fault	Scara	No				x	x	
Degradation curves integration in physics-based models: Towards the predictive maintenance of industrial robots	2021	Torque	Wear	Six axis	Yes	x				x	
A Data-driven Method for Monitoring Systems that Operate Repetitively - Applications to Wear Monitoring in an Industrial Robot Joint1	2012	Torque	Wear	Six axis	yes	x					x

Data analytics for predictive maintenance of industrial robots	2017	Current	No actual fault	Six axis	No	x			x	
Modeling and Diagnosis of Friction and Wear in Industrial Robots	2014	Torque	Wear	Six axis	yes	x				x
High-Accuracy Unsupervised Fault Detection of Industrial Robots Using Current Signal Analysis	2019	Current	RV reducer	Six axis	no		x		x	
Failure detection in robotic arms using statistical modeling, machine learning and hybrid gradient boosting	2019	Torque, dynamics and other	No actual fault	Six axis	no	x			x	
Wireless monitoring of power consumption for industrial robot during a pick and place task for predictive maintenance	2021	Power consumption	No actual fault	Six axis	no	x				x

Predictive Maintenance: An Autoencoder Anomaly-Based Approach for a 3 DoF Delta Robot	2021	Torque, dynamics	No actual fault	Parallel					x	x	x	
Robust Predictive Maintenance for Robotics via Unsupervised Transfer Learning	2021	Torque, dynamics	No actual fault	Six axis	yes			x			x	
Robot Predictive Maintenance Method Based on Program-Position Cycle	2021	Current	Load balancer failure, shaft break	Six axis	yes	x						x
Intelligent Fault Detection, Diagnosis and Health Evaluation for Industrial Robots	2021	Acceleration sensor, current	Increased friction, loos belt	Six axis	no	x				x	x	
Compound Fault Diagnosis of Industrial Robot Based on Improved Multi-label One-Dimensional Convolutional Neural Network	2021	Torque, current, dynamics	Different faults of modules (Drive, control, etc)	Six axis	no				x	x		
GAN-based Data Augmentation Strategy for Sensor Anomaly Detection in Industrial Robots	2021	Current	No actual fault	Six axis	yes				x	x		

Multi-axis Industrial Robot Fault Diagnosis Model Based on Improved One-Dimensional Convolutional Neural Network	2021	Torque, current, dynamics	No actual fault	Six axis	no			x	x		
A deep transferable motion-adaptive fault detection method for industrial robots using a residual-convolutional neural network	2021	Torque	No actual fault	Six axis	no	x			x		
Variational AutoEncoder to Identify Anomalous Data in Robots	2021	Torque, current, dynamics	No actual fault	Six axis	no			x		x	
Data-driven gearbox failure detection in industrial robots	2019	Torque, dynamics	RV reducer	Six axis	no	x			x		
A simulation based approach to detect wear in industrial robots	2015	Simulated torque	Wear	Six axis	yes	x					x
Training data selection criteria for detecting failures in industrial robots	2016	Torque	Rv reducer, brakes	Six axis	no	x					x

Detection and Monitoring for Anomalies and Degradation of a Robotic Arm Using Machine Learning	2021	Torque, current, dynamics	No actual fault	Six axis	yes			x	x	x
Motion-Adaptive Few-Shot Fault Detection Method of Industrial Robot Gearboxes via Residual Convolutional Neural Network	2020	Torque	RV reducer	Six axis	no	x			x	
Health Index Construction and Remaining Useful Life Prediction of Mechanical Axis Based on Action Cycle Similarity	2021	Torque, dynamics	No actual fault	Six axis	Yes	x			x	

8.7 Contribution of authors to publications

Erklärung der*des Promovierenden zum Eigenanteil an den im Rahmen von publikationsbasierten Dissertationen eingebundenen Publikationen und Bestätigung der Mitautor*innen gem. § 7 Abs. 3 Satz 2 PromO

Name des Promovierenden:

Corbinian Nentwich

Nentwich, C.; Reinhart, G.: Towards Data Acquisition for Predictive Maintenance of Industrial Robots. Procedia CIRP 104 (2021), S. 62-67.

z.B.	Auflistung des Eigenanteils mit Prozentangabe
Entwicklung und Konzeption des Forschungsvorhabens	100%
Erarbeitung, Erhebung, Beschaffung, Bereitstellung der Daten, der Software, der Quellen	100%
Analyse/Auswertung oder Interpretation der Daten, Quellen und an den aus diesen folgenden Schlussfolgerungen	100%
Verfassen des Manuskripts	100%
Review des Manuskripts	50 %

Nentwich, C.; Reinhart, G.: A Method for Health Indicator Evaluation for Condition Monitoring of Industrial Robot Gears. Robotics 2021, 10(2), 80. (20 Seiten)

z.B.	Auflistung des Eigenanteils mit Prozentangabe
Entwicklung und Konzeption des Forschungsvorhabens	100%
Erarbeitung, Erhebung, Beschaffung, Bereitstellung der Daten, der Software, der Quellen	100%
Analyse/Auswertung oder Interpretation der Daten, Quellen und an den aus diesen folgenden Schlussfolgerungen	100%
Verfassen des Manuskripts	100%
Review des Manuskripts	50 %

Nentwich, C.; Reinhart, G. A Combined Anomaly and Trend Detection System for Industrial Robot Gear Condition Monitoring. Appl. Sci. 2021, 11, 10403. (20 Seiten)

z.B.	Auflistung des Eigenanteils mit Prozentangabe
Entwicklung und Konzeption des Forschungsvorhabens	100%

Erarbeitung, Erhebung, Beschaffung, Bereitstellung der Daten, der Software, der Quellen	100%
Analyse/Auswertung oder Interpretation der Daten, Quellen und an den aus diesen folgenden Schlussfolgerungen	100%
Verfassen des Manuskripts	100%
Review des Manuskripts	50 %

Nentwich, C.; Daub, R.: Comparison of Data Sources for Robot Gear Condition Monitoring. Procedia CIRP 107 (2022), S. 314-319.

z.B.	Auflistung des Eigenanteils mit Prozentangabe
Entwicklung und Konzeption des Forschungsvorhabens	100%
Erarbeitung, Erhebung, Beschaffung, Bereitstellung der Daten, der Software, der Quellen	100%
Analyse/Auswertung oder Interpretation der Daten, Quellen und an den aus diesen folgenden Schlussfolgerungen	100%
Verfassen des Manuskripts	100%
Review des Manuskripts	50 %

Nentwich, C.; Daub, R.: Cost-Benefit Analysis of Industrial Robot Gear Condition Monitoring. Procedia CIRP 107 (2022), S. 143-148.

z.B.	Auflistung des Eigenanteils mit Prozentangabe
Entwicklung und Konzeption des Forschungsvorhabens	100%
Erarbeitung, Erhebung, Beschaffung, Bereitstellung der Daten, der Software, der Quellen	100%
Analyse/Auswertung oder Interpretation der Daten, Quellen und an den aus diesen folgenden Schlussfolgerungen	100%
Verfassen des Manuskripts	100%
Review des Manuskripts	50 %

Ort, Datum, Unterschrift der*des Promovierenden

Cambridge, 21.06.2022 [redacted]

Erklärung Mitautor*in:

Als Mitautor*in bestätige ich die oben genannte Erklärung zum Eigenanteil. Ich bin damit einverstanden, dass die Publikation im oben genannten Promotionsverfahren im Rahmen einer publikationsbasierten Dissertation verwendet wird.

Name Mitautor*in	Datum / Unterschrift
Prof. Dr.-Ing. Gunther Reinhart	[redacted]
Prof. Dr.-Ing. Rüdiger Daub	[redacted]

Hinweis: Statt der Unterzeichnung der Erklärung im Original ist alternativ auch eine entsprechende Bestätigung in eingescannter Form möglich.

8.8 Table of student theses

In the context of this dissertation, the student work listed below was carried out at the Institute for Machine Tools and Industrial Management (iwb) of the Technical University of Munich (TUM) in the years 2019 to 2022 under the essential scientific, technical and content-related guidance of the author. In these papers, various issues around the topic of predictive maintenance for industrial robots were investigated. Some of the results have been incorporated into this document. The author would like to thank all students for their commitment in supporting this scientific work.

Title	**Name**
Automatisierte Parametrisierung von 3D-Kinematik-Simulationsmodellen	Maria Guerra
Automatisierte Erkennung von Betriebsmitteln in Montageanlagen	Suzan San
Abschätzung der Anwendbarkeit von künstlicher Intelligenz zur Prädikation der Restlebensdauer verschließbeanspruchter Komponenten bei Industrierobotern	Sebastian Junker
Aufbau eines Predictive Maintenance Prüfstands für Industrieroboter	Timon Schulze
Entwicklung eines Software-Tools zur Feature-Bewertung für Predictive Maintenance bei Industrierobotern	Julius Deyle
Entwicklung eines Transfer-Machine-Learning-Modells für Condition Monitoring bei Industrierobotern	Jonas Joachimmeyer
Entwicklung von Prognosemodellen basierend auf Methoden des maschinellen Lernens für die prädiktive Instandhaltung von Industrierobotern	Deborah Görl
Entwicklung von Machine Learning Modellen zur Klassifizierung des Verschleißzustandes bei Industrierobotern	Simon Botz
Datenakquise und –haltung in cyber-physischen-Produktionssystemen am Beispiel eines Fabrikmodells	Manuel Koch
Aufbau eines Softwareframeworks für Prognostics-and-Health-Management-Modelle von Industrierobotern	Leopold Beck
Literaturrecherche für Predictive Maintenance bei Industrierobotern	Lukas Jünger
Skalierbares Condition Monitoring von Industrierobotern basierend auf datengestützten Verfahren	Simon Veitl
Bayessche neuronale Netze und Gauß-Prozesse im Anwendungsfall der zustandsorientierten Instandhaltung	Ansgar Schäfftlein

Benchmark von Machine-Learning-Modellen für das Clustering von Schäden an Getrieben	Lucas Ribeiro
Transfer Learning für Predictive Maintenance von Industrierobotern beim Betrieb unter variierenden Umweltbedingungen	Katharina Meyer
KI für die Ressourcenallokation in selbst-organisierenden, dezentralen Produktionssystemen	Yevheniya Vytruchenko
Skalierbares Predictive Maintenance für Industrieroboter	Katharina Schneeweiss
Featurebestimmung und –visualisierung für die Zustandsüberwachung von Industrierobotergetrieben	André Braumandl
Anomaliedetektion zur frühzeitigen Erkennung von Getriebeschäden an Industrierobotern	Tobias Vogt
Performance Monitoring von Edge-Connectoren in der Produktion	Florian Gessler
Bewertung der Eignung von Datenquellen für Predictive Maintenance bei Industrierobotern	Julian Mehn
Wirtschaftlichkeitsbewertung von Condition Monitoring für Industrierobotergetriebe	Jacobo Torrens

Eidesstattliche Erklärung

Ich, Corbinian Nentwich, (Vor- und Nachname) erkläre an Eides statt, dass ich die bei der promotionsführenden Einrichtung

TUM School for Engineering and Design

der TUM zur Promotionsprüfung vorgelegte Arbeit mit dem Titel:

Automated Condition Monitoring for Industrial Robot Gears

unter der Anleitung und Betreuung durch: Professor Dr.-Ing. Rüdiger Daub

ohne sonstige Hilfe erstellt und bei der Abfassung nur die gemäß § 7 Abs. 6 und 7 angegebenen Hilfsmittel benutzt habe.

x Ich habe keine Organisation eingeschaltet, die gegen Entgelt Betreuer*innen für die Anfertigung von Dissertationen sucht, oder die mir obliegenden Pflichten hinsichtlich der Prüfungsleistungen für mich ganz oder teilweise erledigt.

x Ich habe die Dissertation in dieser oder ähnlicher Form in keinem anderen Prüfungsverfahren als Prüfungsleistung vorgelegt.

x Teile der Dissertation wurden in Procedia CIRP, MDPI Applied Science und MDPI Robotics veröffentlicht.

x Ich habe den angestrebten Doktorgrad noch nicht erworben und bin nicht in einem früheren Promotionsverfahren für den angestrebten Doktorgrad endgültig gescheitert.

☐ Ich habe bereits am _____ bei der promotionsführenden Einrichtung _____ der Hochschule _____ unter Vorlage einer Dissertation mit dem Thema _____

die Zulassung zur Promotion beantragt mit dem Ergebnis:

_____

x Ich habe keine Kenntnis über ein strafrechtliches Ermittlungsverfahren in Bezug auf wissenschaftsbezogene Straftaten gegen mich oder eine rechtskräftige strafrechtliche Verurteilung mit Wissenschaftsbezug.

Die öffentlich zugängliche Promotionsordnung sowie die Richtlinien zur Sicherung guter wissenschaftlicher Praxis und für den Umgang mit wissenschaftlichem Fehlverhalten der TUM sind mir bekannt, insbesondere habe ich die Bedeutung von § 27 PromO (Nichtigkeit der Promotion) und § 28 PromO (Entzug des Doktorgrades) zur Kenntnis genommen. Ich bin mir der Konsequenzen einer falschen Eidesstattlichen Erklärung bewusst.

Mit der Aufnahme meiner personenbezogenen Daten in die Alumni-Datei bei der TUM bin ich

x einverstanden, ☐ nicht einverstanden.

München, 06.09.2022

Ort, Datum, Unterschrift